



**TECHNISCHE
UNIVERSITÄT
WIEN**

DISSERTATION

Optimal Resource Utilization for Improved Voltage Regulation in Distribution Networks with High Distributed Generation Penetration

Submitted at the
Faculty of Electrical Engineering and Information Technology
Technische Universität Wien
In partial fulfillment of the requirements for the degree of
Doktor der technischen Wissenschaften

under supervision of
Prof. Dr. Peter Palensky
Institute number: 370
Institute of Energy Systems and Electrical Drives

By

Aadil Latif
Matr.Nr. e1329781
Deublergasse 18/34
1210 Vienna, Austria

This dissertation is dedicated to:

My parents; who have raised me to be the person I am today. Your lifelong support, encouragement and love brought this work into realization.

My wife and my two children, Daud and Daniya; you were my constant motivation. Thank you for all your love and support along the way.

Acknowledgements

Foremost, I would like to express sincere gratitude to my advisor at the Complex Energy Systems group of AIT, Prof. Peter Palensky for giving me a chance to be part of his amazing team. I had the opportunity to choose and work on a topic that would be of great interest to me and for that, I am highly indebted. His guidance, encouragement, and support have been a great contribution in this study's success. It has been a pleasure working for him.

I sincerely thank Prof. Wolfgang Gawlik for his patience, enthusiasm, continuous motivation and unwavering support throughout the course of my work. His expert guidance has helped in the research and writing of this thesis. I could not have imagined a better advisor and mentor for my PhD study.

In addition, a thank you to Mr. Matthias Stifter for his endless support, providing me invaluable insight and sharing his knowledge during our time spent working together. I am grateful to all my fellow lab mates in the Complex Energy Systems group for their special company and peer support.

Finally, and most importantly, I would like to thank my family— My father, Izhar ul Haq, whose unimpeachable work ethic has been an inspiration my whole life. My mother, Lubna Izhar, who is not only my biggest supporter, but her undying faith in my abilities and constant push to strive to be a better version of myself has always directed me to the right path. Mom, I have finally fulfilled the dream you had for me as a child. My wife, Madiha Latif, has stood by me through thick and thin and has raised our children virtually single handedly during this journey.

Abstract

Ensuring voltage limits are not violated in the distribution network is the responsibility of the distribution network operator. Ever increasing penetration of non-dispatchable distributed energy resources in the distribution network has led to deterioration of the voltage profile. In recent years, a number of local autonomous voltage control methods for DERs have been employed to support voltage regulation. Local autonomous voltage control methods rely solely on local information and can thus result in inefficient use of resources.

This thesis presents a comparative analysis of the state-of art voltage control schemes proposed for voltage regulation in distribution networks. It further highlights the limitations of local voltage control methods. Finally, three coordination based voltage support algorithms have been proposed based on reactive power compensation, active power curtailment and demand side management.

Coordinating the control action of the controllable resources available within the distribution network can potentially improve the system efficiency, resulting in lower operational cost. The first method proposed is based on coordinated reactive power dispatch from DERs connected with the network. The formulated objective function is a weighted sum to voltage regulation objective and network power loss objective. Modified Bat Algorithm, a population based meta-heuristic algorithm, has been used to minimize the constructed objective function. The proposed method has been implemented in centralized and decentralized manner on the chosen test case. For the purpose of decentralized implementation, Hierarchical Agglomerative Clustering has been used to automate the process of defining zones with strong voltage interdependencies. The decentralized implementation results in reduction in the dimension of the optimization problem and facilitates efficient utilization of local reactive power resources. Although this method has been showcased using DERs, it can be easily extended to work with other technologies such as electric vehicles or battery storages.

Active power curtailment is another method of voltage regulation in distribution networks. In Low Voltage networks the R/X ratio is typically high. This results in reduced voltage control capabilities of reactive power based schemes. Additionally, several countries do not permit reactive power compensation. In such a scenario active power curtailment is one method of regulating network voltage. Local autonomous active power curtailment schemes are inherently unfair as PV owners connected near the end of the LV feeder get their power curtailed the most. The second method proposed in this work aims at mitigating this inherent unfairness. The coordination based method uses an estimation of the sensitivity matrix to ensure that each PV system participates fairly in the voltage support scheme. The scheme has been compared to two schemes from literature, one based on local control and the other on coordinated control. The proposed method is a plug and play solution and should only be used on feeders with high curtailment unfairness index; a KPI formulated in this work.

Thermostatically controlled load are loads that operate within a fixed temperature band and are usually controlled via thermostat. The principal of thermal inertia allows the operational status of the load to be changed for a limited period of time without having an impact on consumer comfort. This makes them an ideal resource for demand response based schemes. The third method proposed in this work aims at combined frequency and voltage regulation. The coordination based scheme uses priority stack to change the operational status of the TCLs. A method of indirect voltage regulation have been tested and the advantages and limitations of the method have been discussed in detail. The results show that it is indeed possible to regulate both frequency and voltage using the proposed DSM scheme.

Table of Contents

Acknowledgements	I
Abstract	II
Table of Figures	VIII
List of Tables	XII
List of Algorithms	XIII
List of Abbreviations.....	XIV
List of Symbols	XVI
List of Author’s Publications	XIX
1. Introduction.....	1
1.1 Recent developments in power systems.....	1
1.1.1 Deregulation of the energy market.....	1
1.1.2 Renewables and distributed generation.....	2
1.1.3 Smart grids	3
1.2 Evolution of distribution network.....	4
1.3 Impact of DERs on distribution networks.....	5
1.3.1 Flicker	6
1.3.2 Harmonics	7
1.3.3 Increase in number of tap changes for OLTC.....	7
1.3.4 Reverse power flows.....	7
1.3.5 Reconfiguration of protection scheme settings.....	8
1.3.6 Increased probability on unintentional islanding	9
1.3.7 Increased error in state estimation	9
1.3.8 Voltage imbalance.....	9
1.3.9 Over voltage.....	10
1.4 Research objective	10
1.5 Summary of methodology.....	11
1.6 Thesis Outline	12
2. State of the Art	13
2.1 Review of concepts.....	13
2.1.1 Active and reactive power.....	13
2.1.2 Voltage drop in radial feeders.....	14

2.1.3	Reactive power compensation	15
2.1.4	Active power curtailment.....	16
2.2	Voltage regulation methods in distribution networks	17
2.2.1	Grid reinforcement.....	17
2.2.2	Alternate routing	18
2.2.3	MV/LV on-load tap changing transformer	18
2.2.4	Capacitor/ Reactor Banks.....	19
2.2.5	Inverter based voltage regulation	20
2.2.6	FACTS Devices	30
2.2.7	Energy Storage.....	32
2.2.8	Demand Side Management	32
2.2.9	Power electronic voltage regulator.....	33
2.3	A visual comparison of the state-of-art.....	34
3.	Methodology	35
4.	Optimal reactive power in distribution networks	39
4.1	Introduction.....	39
4.2	The optimization algorithm.....	40
4.2.1	The Bat Algorithm	40
4.2.2	Modifications	41
4.2.3	Comparison using benchmark equation	43
4.3	Problem formulation	45
4.3.1	Assumptions.....	45
4.3.2	Formulation of objectives and constraints	46
4.4	Study case 1: Optimal reactive power compensation	50
4.4.1	Test case over view	50
4.4.2	Control Implementation	52
4.4.3	Zone creation using visual approximation	54
4.4.4	Flowchart for the proposed method	60
4.5	Results and discussion	61
4.5.1	Constant power factor	61
4.5.2	Variable power factor.....	62
4.5.3	Volt/VAR control.....	63
4.5.4	Centralized implementation	65

4.5.5	Decentralized implementation	66
4.5.6	Comparison of results	69
4.6	Conclusion	70
5.	Coordinated Active Power Curtailment in LVN	72
5.1	Introduction.....	72
5.2	Problem Formulation	73
5.3	Controller modeling.....	74
5.3.1	Implementation of local voltage controller	74
5.3.2	Implementation of the coordinating controller	79
5.4	Formulation of key performance indices (KPIs).....	81
5.4.1	Total Curtailed Energy.....	81
5.4.2	Unfairness in active power curtailment.....	82
5.5	Simulation setup and study case implementation details	83
5.5.1	Simulation setup.....	83
5.5.2	Study case 1: Impact of assumptions on sensitivity matrix estimation.....	83
5.5.3	Study case 2: Implementation of the proposed method on a real LV network	87
5.6	Results and discussion	90
5.6.1	Estimation of the sensitivity matrix	90
5.6.2	Results for voltage control schemes.....	91
5.6.3	A comparison of results	99
5.6.4	Impact of control parameters	101
5.6.5	Impact of communication delay and failure on the proposed scheme	102
5.7	Conclusion	104
6.	Combined frequency and voltage regulation using DSM	106
6.1	Introduction.....	106
6.2	Control modeling	107
6.2.1	TCL controller modeling	107
6.2.2	Coordinating controller	110
6.3	Simulation setup.....	112
6.3.1	Network model.....	112
6.3.2	Co-simulation setup	113
6.4	Results and discussion	113
6.4.1	Base case: no voltage consideration.....	113

6.4.2	Study case 1: Penalizing voltage violation by forced switching.....	116
6.5	Conclision	119
7.	Conclusion and outlook	120
7.1	An overview of the contributions of this thesis	120
7.2	Evaluation from a stakeholder’s perspective	122
7.3	Outlook	123
	References.....	125

Table of Figures

Figure 1-1 Timeline of the deregulation process in US and EU	2
Figure 1-2 Growth in number of installed PV systems	3
Figure 1-3 Increase in the installed PV capacity in Europe.....	4
Figure 1-4 European PV market segmentation in 2013	5
Figure 2-1 Active and reactive power components of apparent AC power	13
Figure 2-2 Single line and phasor diagram for voltage drop along a DL.....	14
Figure 2-3 Impact of power factor on voltage drop.....	15
Figure 2-4 Typical characteristics for droop based active power curtailment	16
Figure 2-5 Voltage regulation methods in distribution networks.....	17
Figure 2-6 Typical voltage trends along feeders with and without PV systems	19
Figure 2-7 Typical characteristics for closed loop voltage control.....	20
Figure 2-8 Constant power factor control	21
Figure 2-9 Variable power factor control	21
Figure 2-10 Typical characteristics for voltage feedback control	22
Figure 2-11 Typical centralized coordinated control implementation.....	24
Figure 2-12 Distributed voltage control implementation	26
Figure 2-13 Combined RPC and APC control	28
Figure 2-14 Curtailment typically increases as the electrical distance from the transformer increases ...	29
Figure 3-1 Methodology flowchart	38
Figure 4-1 Effect of tuning parameters G and H.....	42
Figure 4-2 Benchmark equations used for testing the optimization algorithms	44
Figure 4-3 Voltage drop phasor diagram for 2 bus system	46
Figure 4-4 Phasor diagrams explaining the impact of reactive power in voltage.....	47
Figure 4-5 Capability curve for third generation inverters.....	49
Figure 4-6 The modified IEEE 37 node test feeder.....	50
Figure 4-7 Graphical illustration of PowerFactory and Python coupling scheme.....	51
Figure 4-8 Color plot of the reactive power sensitivity matrix for the IEEE 37 node test feeder	55
Figure 4-9 Color plot of the normalized electrical distance matrix for the IEEE 37 node test feeder	56
Figure 4-10 Dendrogram for clusters produced using ward linkage based agglomerative hierarchical clustering	58

Figure 4-11 Scree plot for the dendrogram	58
Figure 4-12 Graphical illustration of the zones created using agglomerative hierarchical clustering	59
Figure 4-13 Flow chart for the proposed coordinated RPC method	60
Figure 4-14 Dispatched reactive power set points for PV 741; and net reactive power flow from the external grid	61
Figure 4-15 Minimum and maximum voltage seen in the network; and active power losses profiles	61
Figure 4-16 Transformer loading profiles; and saved energy profile	62
Figure 4-17 Dispatched reactive power for PV 741; and net reactive power flow from the external grid	62
Figure 4-18 Minimum and maximum voltage seen in the network; and active power losses profiles	63
Figure 4-19 Transformer loading profiles; and saved energy profile	63
Figure 4-20 Dispatched reactive power for PV 741; and net reactive power flow from the external grid	64
Figure 4-21 Minimum and maximum voltage seen in the network; and active power losses profiles	64
Figure 4-22 Transformer loading profiles; and saved energy profile	65
Figure 4-23 Dispatched reactive power for PV 741; and net reactive power flow from the external grid	65
Figure 4-24 Minimum and maximum voltage seen in the network; and active power losses profiles	66
Figure 4-25 Transformer loading profiles; and saved energy profile	66
Figure 4-26 Dispatched reactive power for PV 704 and PV 741	67
Figure 4-27 Net reactive power flow from the external grid	67
Figure 4-28 Minimum and maximum voltage seen in the network; and active power losses profiles	68
Figure 4-29 Energy saved compared to base case	68
Figure 4-30 Comparison of maximum voltage seen in the network	69
Figure 4-31 Comparison of energy saved compared to base case	69
Figure 5-1 Phasor diagram explaining the voltage drop phenomenon in radial networks using a 2 bus system	73
Figure 5-2 Graphical illustration of the method for calculating electrical distance	77
Figure 5-3 Droop based APC controller with du/dp estimation logic	78
Figure 5-4 PowerFactory and Python coupling via sockets using external DLL	83
Figure 5-5 A simplistic hypothetical LV network	84
Figure 5-6 Impact of branch length on estimation error	85
Figure 5-7 Impact of the branch position in estimation error	86
Figure 5-8 Impact of the increasing the number of branches on estimation error	87
Figure 5-9 Modified Cigre low voltage distribution network	89

Figure 5-10 Calc control signal from the coordinating controller; Voltage at PV connected nodes; du/dp estimation results for PV I2-1	90
Figure 5-11 du/dp estimation error for Feeder 1 and Feeder 2	91
Figure 5-12 Voltage profiles at PCC of each inverter with no voltage control function	92
Figure 5-13 Voltage profiles at PCC of each inverter with local voltage controller	92
Figure 5-14 Curtailed power form each inverter using local droop based voltage curtailment	93
Figure 5-15 Curtailed energy form each inverter using local droop based voltage curtailment.....	93
Figure 5-16 Node currently experiencing the maximum voltage within the network; Signal for starting active power curtailment.....	94
Figure 5-17 Critical voltage set points calculated for each inverter connect to feeder 2	95
Figure 5-18 Maximum expected voltage in the network; reduction in voltage required to ensure no voltage violation occurs.....	95
Figure 5-19 Power curtailment signal before and after the use of the S function	96
Figure 5-20 Voltage profiles at PCC of each inverter with CC1 control scheme.....	96
Figure 5-21 Curtailed power form each inverter using CC1 control scheme	97
Figure 5-22 Curtailed energy form each inverter using CC1 control scheme.....	97
Figure 5-23 Power curtailment signals calculated for each inverter	98
Figure 5-24 Voltage profiles at PCC of each inverter with CC2 control scheme.....	98
Figure 5-25 Curtailed power form each inverter using CC2 control scheme	99
Figure 5-26 Curtailed energy form each inverter using CC2 control scheme.....	99
Figure 5-27 Energy curtailed from each inverter for the three APC control schemes implemented	100
Figure 5-28 Impact of control variable G on energy curtailed and over voltage duration.....	101
Figure 5-29 Impact of control varying the lower voltage bound on energy curtailed, over voltage duration and the peak voltage experiences by the network.....	102
Figure 5-30 Impact of a high value of lower voltage bound on voltage fluctuations	102
Figure 5-31 Impact of communication delay on over voltage duration and peak network voltage on a sunny day.....	103
Figure 5-32 Impact of communication delay on over voltage duration and peak network voltage on a cloudy day.....	103
Figure 5-33 Impact of communication failure on peak voltage.....	104
Figure 6-1 Illustration explaining the dynamics of a TCL and the proposed local control scheme	107
Figure 6-2 Current and reference temperature profiles for the TCL connect at node 118.....	108

Figure 6-3 Time profile for the switch status and the availability of the TCL connect at node 118	108
Figure 6-4 Time profile for the switch status and normalized distance from the temperature boundary for the TCL connect at node 118	109
Figure 6-5 Graphical overview of the simulation setup	111
Figure 6-6 The 119 node test feeder	112
Figure 6-7 Base case reference signal tracking performance	113
Figure 6-8 Time profile for the number of TCLs on at any given time	114
Figure 6-9 Time profile for the number of TCLs available to be turned off.....	114
Figure 6-10 Time profile for the number of TCLs available to be turned on.....	115
Figure 6-11 Base case voltage profile; box plot for the voltage profile	115
Figure 6-12 Impact of forced switching on reference signal tracking	116
Figure 6-13 Impact of forced switching on the availability of TCLs that can be turned off	116
Figure 6-14 Impact of forced switching on the availability of TCLs that can be turned on.....	117
Figure 6-15 Impact of forced switching on temperature regulation	117
Figure 6-16 Impact of forced switching on voltage profile; box plot for the voltage profile	118
Figure 6-17 Comparison of base case and study case 1 tacking error	118

List of Tables

Table 2-1 Comparison of the state-of-art voltage regulation techniques in distribution network	34
Table 4-1 Values of parameters used for benchmarking test	44
Table 4-2 Results of optimization benchmark equations with multiple local minima	45
Table 4-3 Rated power, Node ID and type of the distributed generator	51
Table 4-4 Values of parameters used for the simulations.....	51
Table 4-5 List of nodes grouped in a cluster using hierarchical clustering.....	59
Table 5-1 Line Parameters.....	87
Table 5-2 Line Lengths.....	88
Table 5-3 Transformer data	88
Table 5-4 Generator operational limits	88
Table 5-5 Calculated KPI for the implemented control schemes.....	100

List of Algorithms

Algorithm 4-1 Pseudo code for modified bat algorithm	43
Algorithm 4-2 Pseudo code for hierarchical agglomerative clustering with ward linkage.....	57
Algorithm 5-1 Pseudo code for the coordinating controller	81
Algorithm 6-1 Algorithm for local TCL controller	110
Algorithm 6-2 Algorithm for the coordinating controller.....	111

List of Abbreviations

AC	-	Alternating Current
APC	-	Active Power Curtailment
API	-	Application Programming Interface
AVC	-	Automatic Voltage Control
BA	-	Bat Algorithm
CCx	-	Coordinating Control x
CDF	-	Cumulative Density Function
CUIx	-	Curtailment Unfairness Index x
DC	-	Direct Current
DER	-	Distributed Energy Resources
DL	-	Distribution Line
DPL	-	DIgSILENT Programming Language
DSL	-	DIgSILENT Simulation Language
DSM	-	Demand Side Management
DSO	-	Distribution System Operator
DT	-	Distribution Transformer
EPS	-	Electrical Power System
FACTS	-	Flexible Alternating Current
FPF	-	Fixed Power Factor
HBA	-	Hybrid Bat Algorithm
HVN	-	High Voltage Network
KPIs	-	Key Performance Indices
LDC	-	Line Drop Compensation
LVN	-	Low Voltage Network
MBA	-	Modified Bat Algorithm
MHBA	-	Modified Hybrid Bat Algorithm
MPPT	-	Maximum Power Point Tracking
MVN	-	Medium Voltage Network
NSGA	-	Non-dominant Sorting Genetic Algorithm
OLTC	-	On-load Tap Changing Transformer
p.u.	-	Per Unit
PCC	-	Point of Common Coupling

PDF	-	Probability Density Function
PEVR	-	Power Electronic Voltage Regulator
PI	-	Proportional Integral
PV	-	Photo Voltaic
RC	-	Resistor Capacitor
RPC	-	Reactive Power Compensation
STATCOM	-	Static Synchronous Compensator
SVC	-	Static VAR Compensator
TCE	-	Total Curtailed Energy
TCL	-	Thermostatically Controlled Load
TL	-	Transmission Line
TSO	-	Transmission System Operator
UPFC	-	Unified Power Flow Controller
VAR	-	Volt-Ampere Reactive
VD	-	Voltage Drop
VPF	-	Variable Power Factor
VVC	-	Volt / VAR Control
XML	-	Extensible Markup Language

List of Symbols

S	-	Apparent power
P	-	Active power
Q	-	Reactive power
I	-	Current
U	-	Voltage
u	-	Voltage [p.u.]
R	-	Resistance
X	-	Reactance
δ_{ij}	-	Voltage angle between the i^{th} and j^{th} node
P_L, P_G	-	Active power demand and generation at a node respectively
Q_L, Q_G	-	Reactive power demand and generation at a node respectively
R_l, X_l	-	Line resistance and reactance respectively
θ	-	Angle between voltage and current
U_p, U_s	-	Voltage at the primary and secondary side of the transformer respectively
I_p, I_s	-	Current at the primary and secondary side of the transformer respectively
N_p, N_s	-	Number of turns on the primary and secondary side of the transformer respectively
U^n	-	Nominal voltage
u^{\cdot}, l^{\cdot}	-	Super scripts denote upper and lower bound on the variable respectively
f_i^t	-	Emission frequency of the i^{th} bat at the t^{th} iteration
$u(x, y)$	-	A uniform random number sampled between the lower bound x and the upper bound y .
v_i^t	-	Velocity of the i^{th} bat at the t^{th} iteration
x_i^t	-	Position of the i^{th} bat at the t^{th} iteration
$x_b^t, x_{b_i}^t$	-	Global best solution at the t^{th} iteration and personal best solutions of the i^{th} bat at the t^{th} iteration respectively
$x_w^t, x_{w_i}^t$	-	Global worst solution at the t^{th} iteration and personal worst solutions of the i^{th} bat at the t^{th} iteration respectively
φ	-	scaling factor that determines the step size of the random walk
A_i^t	-	Emission amplitude of the i^{th} bat at the t^{th} iteration
α, γ	-	Constants that control the rate of convergence of the bat algorithm
r_i^t	-	Emission rate of the i^{th} bat at the t^{th} iteration
F	-	Differential weight for the differential evolution algorithm
m_i^t	-	Potential new solution
N	-	Population size for the Bat Algorithm
D	-	Number of dimensions to the problem
β	-	A scaler parameter that determines the probability of crossover
c_x	-	Acceleration constants for the velocity update equation

t_{max}	-	Maximum number of iterations permissible
W^t	-	Value of the inertia weight at the t^{th} iteration
G	-	Parameter controls the shape of the S function
H	-	Parameters controls the position of the S function
P_{loss}	-	Active power loss
$ x $	-	Magnitude of the variable x
$Re\{x\}$	-	Real part of the variable x
$Im\{x\}$	-	Imaginary part of the variable x
g_k	-	Conductance of the i^{th} branch
u^{max}, u^{min}	-	Minimum and maximum voltage in a network at any given instance
u^{uv}, u^{lv}	-	Magnitude of voltage violation at the upper and lower bound respectively
pf	-	Power factor
$S_{tr.}$	-	Rated power of the distribution transformer
B	-	Voltage / reactive power sensitivity matrix
α	-	Sensitivity attenuation matrix
D	-	Electrical distance matrix
D^{norm}	-	Normalized electrical distance matrix
C_x, C_y	-	Denote predefined clusters
k	-	Sequence number of a defined cluster
$L(k)$	-	Level of clustering
Δx	-	Change in variable x
p^{mppt}	-	Active power at maximum power point tracking
p^{cal}	-	Active power output after curtailment by the local controller
p^{rated}	-	Matrix containing rated active power values of the PV systems
p^{min}	-	Denotes the value to which active power can be curtailed
p^{cur}	-	PV system active power output after curtailment
E^{cur}	-	Curtailed Energy
m	-	Proportional gain parameter for the controller
u^{cri}	-	Critical voltage after which curtailment begins
R_{ij}	-	Resistance between the i^{th} and j^{th} node
r	-	Parameter dependent on resistivity and cross sectional area
L_{ij}	-	Electrical distance between the i^{th} and j^{th} node
A	-	Cross sectional area of a conductor
ρ	-	Resistivity of a conductor
Δu^{tap}	-	Change in per unit voltage per tap change
x^{tap}	-	Current tap position
m_i	-	number of non-zero elements in the i^{th} row of P^{rated} matrix
N^{pv}	-	Number of PV systems connected to a feeder
\bar{x}	-	Denotes the average value of a vector

z	- Percentage reduction in active power required from each inverter
S_{ij}	- Denotes element on the i^{th} row and j^{th} column of the sensitivity matrix
ε_{ij}	- Denotes the error in estimation
k	- Time index, where $k \in [1, T]$
θ^i	- Temperature of i^{th} TCL
Δ^i	- Temperature dead-band width of i^{th} TCL
ψ	- Aggregate power deviation from the base value
π^i	- Normalized temperature distance to the switching boundary of i^{th} TCL
β^i	- Control signal from central controller for i^{th} TCL, where $\beta^i \in [1, T]$
ρ^i	- Time duration after status change of i^{th} TCL
$\overline{\rho^i}$	- Short cycling duration of i^{th} TCL
P^i, p^i	- Rated and nominal power of i^{th} TCL

List of Author's Publications

- 1) **Aadil Latif**, Ishtiaq Ahmed, Peter Palensky, and Wolfgang Gawlik, 2016, “Multi-Objective Reactive Power Dispatch in Distribution Networks using Modified Bat Algorithm” *In IEEE Green Energy and Systems Conference, IGESC 2016* (Accepted)
- 2) **Aadil Latif**, Peter Palensky, and Wolfgang Gawlik, 2016, “Quantification and Mitigation of Unfairness in Active Power Curtailment of Rooftop Photovoltaic Systems Using Sensitivity Based Coordinated Control” *Energies* 9, no. 6 (2016): 436-
- 3) **Aadil Latif**, Sohail Khan, Peter Palensky, and Wolfgang Gawlik, 2016, “Co-simulation Based Platform for Thermostatically Controlled Loads as a Frequency Reserve” *In Workshop on Modeling and Simulation of Cyber-Physical Energy Systems, MSCPES 2016*
- 4) Jawad H. Kazmi, **Aadil Latif**, Ishtiaq Ahmed, Peter Palensky, and Wolfgang Gawlik, 2016, “A Flexible Smart Grid Co-Simulation Environment for Cyber Physical Interdependence Analysis” *In Workshop on Modeling and Simulation of Cyber-Physical Energy Systems, MSCPES 2016*
- 5) **Aadil Latif**, Mohsin Shahzad, Peter Palensky, and Wolfgang Gawlik, 2015, “An alternate PowerFactory Matlab coupling approach” *In Smart Electric Distribution Systems and Technologies (EDST), 2015 International Symposium*, pp. 486-491. IEEE, 2015.
- 6) **Aadil Latif** and Peter Palensky, 2014, “Economic dispatch using modified bat algorithm” *Algorithms* 7, no. 3 (2014): 328-338.

1. Introduction

The electrical power system (EPS) is essentially a combination of generating units, transmission lines (TL), distribution lines (DL) and loads. Before the deregulation of the energy markets in the 1980's and the drive towards renewable energy in the early 2000's, the EPS was run in a centralized and unidirectional manner [1]. The energy was generated in bulk generally away from the load centers. This energy was transmitted in bulk at high voltages using TLs. The individual loads would then be connected to the EPS via the distribution network at lower voltage levels. In this traditional power system operation the electric utility was vertically integrated with one entity responsible for generation, transmission and distribution.

The first photo voltaic (PV) systems were developed in the 1970's but very low efficiency and high cost resulted in very little commercial success [2]. In the early 2000's several driving factors such as energy security in Europe, grid reliability in the United States and surge in energy demand in China led to policy driven growth of the grid connected PV systems. Due to increase in PV cell efficiency, lower PV system production cost and government subsidies this time round they were a commercial success. As a result in the last decade there was a phenomenal growth in the number of installed PV systems [3]. Similar trends have been witnessed with other technologies such as wind turbines, micro combined heat and power (CHP) and small hydro [4, 5]. This trend towards more grid connected distributed energy resources (DERs) has led to new engineering challenges.

A high concentration of DERs has led to a number of technical issues such as voltage rise, reverse power flow, phase imbalance and harmonics in many reported instances [6] [7]. Simultaneous under and overvoltage is one of the phenomenon caused by high penetration of DERs in the distribution system. Initially PV systems worked independently but developments in the communication technology created the opportunities to tackle these problems in a coordinated manner. In recent years several pilot projects have used a variety of techniques to overcome these problems. These developments will be reviewed in the next chapter.

1.1 Recent developments in power systems

1.1.1 Deregulation of the energy market

From 1970's through to the 80's Europe went through a period of very high inflation. This resulted in discontent and a public perception of the government's inability to manage public sector entities efficiently. In 1990 United Kingdom became the leader in energy market liberalization when Margret Thatcher privatized the UK electricity supply industry. In 1996 the "The European Directive for the electricity market" was introduced. Defining the rules for every player participating in the market took several years, but by 2007 all European Union member countries had fully liberalized energy markets [8].

In the US, congress passed the “Public Utility Regulatory Policies Act” in 1978 for deregulation of the energy market by opening the market to nonutility producers of electricity. In 1992 congress passed the “Energy Policy Act” which aimed at promoting competition and reducing monopolies in the electricity market [9].

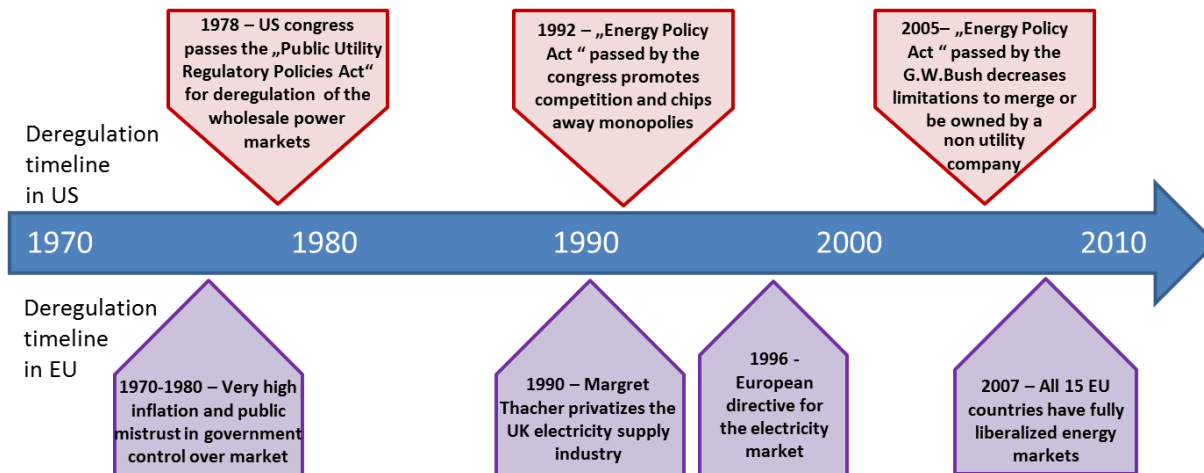


Figure 1-1 Timeline of the deregulation process in US and EU

Deregulation of the energy market made it possible for the consumers to install roof top PV systems and participate in the energy market. It was thus one of the driving factors of the green revolution that followed a decade later. Figure 1-1 presents a graphical overview of the chronological evolution of the deregulation of EU and US energy markets.

1.1.2 Renewables and distributed generation

The wind, sun, water and biomass are the four sources of renewable energy. Renewable generators such as PV panels and wind turbines make use of these sources to produce electricity. Distributed energy resources such as PV systems are small generation technologies that are distributed throughout the distribution network of the power system. Many of these technologies have unique characteristics that need to be taken into account if they are to have a major share in the energy market. PV systems for example have intermittent power output due to the nature of its primary source of energy the sun. High concentration of PV systems in the distribution network can therefore lead to a number of problems if these characteristics are not taken into account.

In the last decade renewable generation technologies have foreseen rapid growth and as a result are now technologically mature. A number of factors have contributed to this phenomenal increase. In Europe reduction of carbon footprint and security of supply were the major driving factors. In November 2010, the European commission adopted the ‘Energy 2020 initiative’ also known as the European Union 20 20 20 strategy. The aim of this strategy was three fold. Firstly, reduce greenhouse gases by 20%. Secondly, reduce the energy consumption by 20% and finally increase the share of renewable energy resources by 20%. All these targets were set for the year

2020 [10]. To reach these goals, many countries like Spain and Germany provided subsidies for both commercial and residential roof top PV systems. This led to a rapid increase in the number of installed PV systems [11].

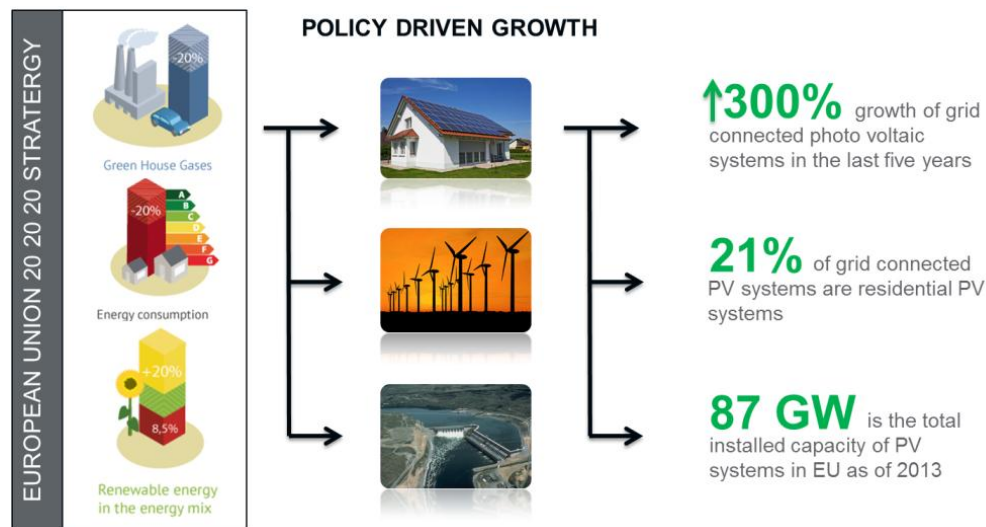


Figure 1-2 Growth in number of installed PV systems in EU

Since the initial boom, Germany and Spain, the largest PV markets, have stopped subsidizing PV systems due to financial constraints. According to the report "Global market outlook for photo voltaic 2013-2017" even without government friendly policies the number of installed PV systems in Europe will increase steadily at an estimated rate of 10000 units / year [3].

1.1.3 Smart grids

The term smart grid was first coined after the North East blackout of 2003. It was a combination of human error and system alarm failure that led to a cascaded failure that left 55 million people without electricity [12]. The smart grid is the next step in the electric grid's evolution. Electric Power Research Institute in 2009 presented one of the most complete definitions of the term 'smart grid' [13].

'The term "Smart Grid" refers to a modernization of the electricity delivery system so it monitors, protects and automatically optimizes the operation of its interconnected elements – from the central and distributed generator through the high-voltage transmission network and the distribution system, to industrial users and building automation systems, to energy storage installations and to end-use consumers and their thermostats, electric vehicles, appliances and other household devices.'

As the number of DERs increase in the distribution system, there is a need to control them for security of supply and to maintain quality of service. Advances in the communication systems enable more monitoring, control and optimization of all elements of the electrical network.

1.2 Evolution of distribution network

The distribution network (DN) consists of networks operating at various voltage levels. DNs is broad term which includes both medium voltage networks (MVNs) and low voltage networks (LVNs), which are the final step in the transportation of electrical energy to individual consumers. In Europe low voltage network follows the IEC standard 230/400V voltages with 3-phase 4-wire distribution. The DNs commonly have radial topology. The main purpose of LVN is to provide consumers given dedicated connections to consumers along the feeder. Before the ‘green revolution’ in Europe the DN was considered the uncontrolled part of the system. In power flow calculations, the DN was considered a lumped load over which, the distribution system operator (DSO) had little or no control. In a typical distribution feeder the voltage drops as the electrical distance from the substation increases. The DNs were originally designed ensuring that the voltage drop (VD) would not exceed threshold prescribed by international standards at the end of the any feeder. The DN therefore was originally not deigned to cater to distributed generation.

In the last decade there has been an enormous increase in the number of installed PV systems. In the year 2007 all EU energy markets were completely deregulated. Also the same year EU 2020 targets were set. This resulted in a period (from 2008 till 2011) of rapid expansion of the PV market. After the year 2011 the growth of PV market started slowing down. The two main reasons were market saturation and the inability to continue subsidies (Spain).

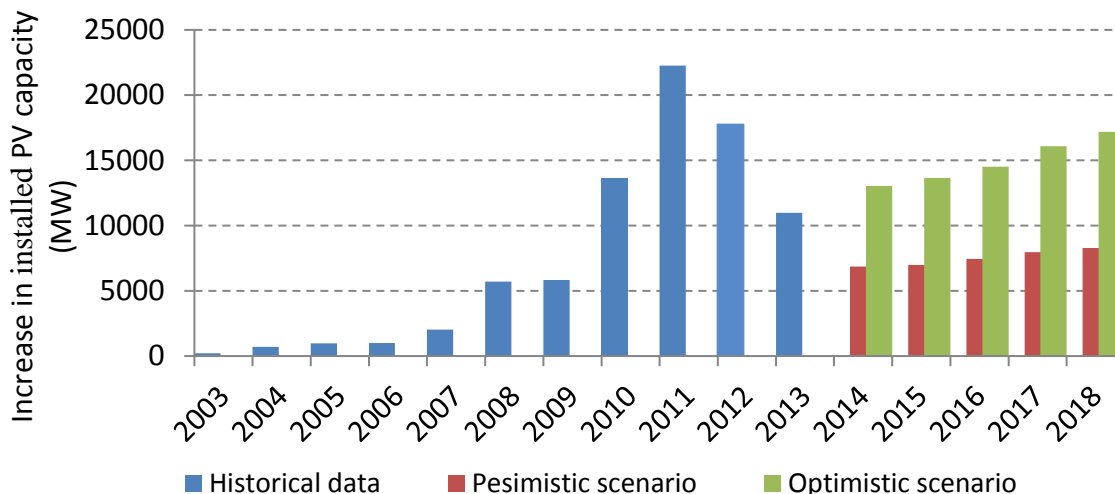


Figure 1-3 Increase in the installed PV capacity in Europe

Studies still predict a steady positive growth rate even in the most pessimistic scenarios, meaning that the grid of tomorrow will have even higher levels of PV systems penetration [3].

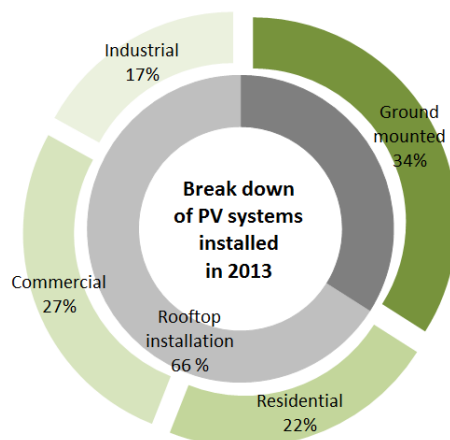


Figure 1-4 European PV market segmentation in 2013

Rooftop installations following the trend from previous year saw the biggest increase. As most of the rooftop installations were at the LVN [3, 14] this ever increasing PV penetration can cause numerous problems relating to grid reliability, power quality and system security that will be discussed briefly in the next section. These challenges have to be met within the constraints of already existing distribution networks.

1.3 Impact of DERs on distribution networks

Generation capacity of individual DERs installed in DN ranges from a few kilowatts to a few megawatts depending on the voltage level at which it is connected. Installation of DERs in the DN provides a number of benefits for both DSO and DER owners.

- It provides an additional source of income for DER owners
- Distributed generation can potentially reduce line losses thereby increasing system efficiency
- It reduces central reserves required to cater for dynamic load demand
- Many DER technologies are clean and therefore reduce carbon footprint
- Local generation and consumption relieves congestion on transmission and distribution networks
- DN with high penetration of DERs can operate in islanded mode in case of a contingency
- With intelligent planning DERs can be used to improve voltage profiles of feeders experiencing under voltages
- It defers investments for network reinforcement needed to keep up with load growths over long periods of time
- Distributed generation can potentially reduce costs associated with import of power from the HVN that are passed on to consumer by the DSO

Although distributed generation brings with it a lot of benefits it also brings with it a number of engineering challenges that need to be overcome. Integration of DERs incur a number of additional costs. DSO bear the brunt of these costs.

Ensuring adequate protection and power quality e.g. need for an additional voltage regulation method might require installation of additional measurement devices or relays. Transformers currently in operation might not be equipped to handle reverse power flows and might need to be replaced. Additionally, for low DER penetration energy losses tend to decrease however, for high penetration levels losses increase. According to [15] network reinforcement cost for low levels of DER penetration is zero but tend to increase as penetration level increases. Finally, DSOs are usually charged by TSOs for providing ancillary services. High numbers of DERs installed in the DN can potentially reduce power quality thereby increasing charges associated with purchase of ancillary services from the TSO [16].

In [17] the authors have detailed UK's experience with distributed generation in LVNs. Ever increasing DER penetration can cause numerous problems relating to grid reliability, power quality and system security that will be discussed briefly in this section. These challenges have to be met within the constraints of already existing DN to ensure power quality and security of supply.

1.3.1 Flicker

IEEE standard 1453-2015 defines flicker as a noticeable change in illumination caused by sudden voltage change in the power system [18]. Flicker results from a sudden increase or decrease of load e.g. switching on a load. Due to the stochastic nature of weather, rapidly changing wind speed and cloud cover, input power of renewable energy resources like solar panels and wind turbines fluctuates. This in turn results in fluctuating output power of the DERs installed in the distribution networks and as the voltage at the point of common coupling (PCC) is a function of the injected power, it also fluctuates rapidly. High levels of flicker can lead to customer complaints limiting the DER hosting capacity of a network [19].

Research shows that flickering illumination is dependent on not only the voltage fluctuation at PCC but also the type of lamp being used for illumination. Human eyes are more sensitive to illumination changes resulting from filament bulbs and are a lot less sensitive to illumination changes resulting from fluorescent lamps [20].

In [21] authors have concluded that flicker is the limiting factor of DER penetration on a weak Brazilian distribution network. It is important to understand that R/X ratio at the PCC has a big impact on flicker emission. High R/X ratio results in higher levels of voltage flicker as voltage becomes more sensitive to active power infeed.

1.3.2 Harmonics

Harmonics are waveforms whose frequency are integer multiple of the fundamental frequency. PV inverters use pulse width modulation switching to convert direct current (DC) power from the PV panels to alternating current (AC) power. High frequency switching results in harmonics and noise. Increase in number and size of inverter based DERs in DNs have resulted in increasing noise and harmonic distortion.

Harmonic distortion is responsible for reduced inverter efficiency and increased converter losses. High level of harmonic emission can result in distortion of the sine wave and reduction in power quality [22] [23]. IEEE standard 1547-2003 specifies allowable limits of harmonics generated by grid connected inverter systems. Both active and passive filter are used in the new generation of inverter to reduce harmonic content from an inverter [24]. Technical advances in inverter technology have mitigated this problem and the third generation inverters provide pure sine wave output [6].

1.3.3 Increase in number of tap changes for OLTC

Tap changers regulate voltage by changing the turn ratio of primary side to the secondary side in a transformer. Unlike manual tap changers on load tap changers (OLTCs) are capable to changing taps on live electrical systems. Traditionally, voltage in the distribution network has been regulated by on-load tap changing transformers controller via automatic voltage controllers using only local voltage information. Typically, in a distribution network, a transformer services multiple feeders and non-uniform connection of DERs among these feeders reduces the control capability of the OLTC transformer. In a scenario where one feeder hosts a high number of DERs and another feeder has little or no generation from DER, an OLTC action to prevent over voltage at one feeder might result in under voltage on another feeder.

Fluctuating voltages resulting from stochastic weather patterns can lead to an increased number of tap changes. Unnecessary tap changing causes arcing which damages the insulation and reduces the life of the transformer [25]. In feeders with significant DER installation OLTCs require more than just the local voltage information to improve upon its regulation capabilities. A number of researchers have suggested either installing additional voltage measurement devices or coordination control action with other devices capable of voltage regulation [26] [27]. Solid state tap changers are a recent development that uses thyristors for switching. The advantage of such a scheme is that arcing is prevented. One disadvantage is a limited tolerance to short-circuit currents which increases in presence of DERs as they themselves contribute to the short-circuit current [28].

1.3.4 Reverse power flows

Traditionally, radial networks have been designed for unidirectional power flow. In networks with significant DER presence if generation exceeds demand, power is exported from

the distribution network to the external grid. This phenomenon is known as reverse power flow. Many transformers are constructed in a way that the permissible reverse flow is lesser than the nameplate rating of the transformer [29]. In some districts of Germany where the average nameplate capacity of rooftop PV systems is over 5 kW reverse flow may exceed transformer rating resulting in equipment damage [30].

A report published by GE Global Research and National Renewable Energy Technology states that reverse power flows are associated with a number of potential problems in the distribution grid. They are responsible for over voltage in on the distribution feeder and reduction in voltage regulation capabilities of OLTC transformers. In certain scenarios they can increase short circuit current that can damage the installed equipment. They are also known to desensitize protection equipment that can in worst cases lead to equipment failure. Reverse power flows also have the potential to initiate incorrect control action from regulating devices installed on a network [31] [32]. IEEE standard 1547-2003 required a DER to have a protection capable of detecting reverse power flow and disconnecting from the grid if reverse power flow exceeds a certain threshold [24].

1.3.5 Reconfiguration of protection scheme settings

Protection systems installed in power system are responsible for isolating faults, protecting expensive equipment and maintaining power quality. Protections schemes used in DNs were developed considering unidirectional power flows. The settings of protection devices may need to be reconfigured and additional protection equipment might be required to ensure secure power supply and mitigate unintentional tripping. DERs connected in a DN contribute to the short circuit current and as input power of a DER changes due to the stochastic weather behavior so does its fault current contribution. This can lead to situations like sympathetic tripping or desensitization of a relay and failure in tripping. Power ratings of the installed protection equipment need to be reevaluated to ensure they are capable of withstanding larger short circuit currents and can perform in a number of different scenarios.

IEEE standard 1547-2003 required DERs to disconnect in case a fault occurs. However, standard 1547.2-2008 now requires inverters connect to the grid to have limited fault ride through capability. This requirement prevents against possible grid instability caused by a large number of PV systems disconnecting from a grid in case of a fault [33]. In recent years Japan (NEDO Std), Germany (VDE-AR-N 4105), Australia (AS4777), Italy (CEI 0-16-2012 and CEI 0-21-2014) and a number of other countries have revised grid codes and made it mandatory for grid connected inverters to have fault ride through capabilities [34]. In their work G, Antonova *et al.* have reviewed in great detail possible impacts of distributed generation on distribution networks [32].

In August 2012, a voltage fluctuation lasting only a few milliseconds triggered the protection system of Hydro Aluminum in Hamburg, Germany. The production stopped so abruptly that a part of the rolling mill was damaged and the repairs cost about € 10,000 [35].

1.3.6 Increased probability on unintentional islanding

A microgrid is part of the power system consisting of DERS, controllable loads and other resources etc. capable of operating with or without the main grid. Islanding refers to the control action when a microgrid is disconnected from the main power grid. Islanding can either be intentional (for example based on pricing strategy) or unintentional (for example caused by a fault).

Grid standards differ for US and Europe when it comes to islanding operation of grid connected inverters. Most European grid codes require the DER to be capable of operating in islanded mode. In the US however std. 1547 requires DERs to disconnect quickly incase an island is formed [24] [36]. Improper grounding, protection and a number of other issues can result in unstable islanding. Out of phase reconnection to the grid stresses it and can potentially cause faults [37, 38]. Detection and reconnection of islanding is an active research topic and has been the subject of a number of research papers that have been extensively reviewed by Li *et al.* in [39].

1.3.7 Increased error in state estimation

In real-time operation of the electrical grid state estimation plays a key role. It estimates the state of system based on available real time measurements, historical load profiles and equipment nameplate ratings (e.g. transformers). It is very useful in power systems as it provides the bases for contingency analysis, security enhancement, optimization applications and other applications necessary for reliable network operation.

Traditionally, most of the measurement devices had been installed in the HVN and the states within a distribution network were unobservable hence reliable estimation of a state within a DN was not possible. Historic profiles and pseudo measurements were used by DSOs to improve the quality of the estimation [40]. Increasing number of DERs in the DN has sensitized the power grid to the weather and as weather is a stochastic phenomenon, historic profiles are getting increasing inaccurate. This has led to increased error in state estimation [41].

For DERs to be able to participate in the energy market knowing the current state of the system is necessary. Also, demand response strategies and coordination based algorithms presented in a number of papers for efficient control of DERS require either a communication infrastructure which can be costly or an accurate state estimation [25]. These problems motivate to develop SE at the distribution level. A number of papers have suggested additional measurement devices at optimal locations within a DN to improve upon the estimation errors [42, 43, 44].

1.3.8 Voltage imbalance

In an ideal three phase power system the voltages in all three phases should be displaced from each other by a phase angle of 120° and should have the same magnitude. An increasing number of single phase PV systems are being installed in three phase low voltage networks. This can result in increased voltage imbalance within the LVNs if a significant number of DERs are

connected on the same phase are not uniformly distributed among the three phases. European standard on power quality EN 50160 stipulates that in distribution networks (both LV and MV) imbalance should be no more than 2% for 95% of the time in a week [45].

Voltage imbalance in a network results in lower power system efficiency and more dissipation losses. Higher dissipation losses may lead to higher temperatures stressing power system components and reducing their life. This translates to higher operation and maintenance costs. Voltage imbalance results in high zero-sequence current which can desensitize protection relays leading to incorrect control action [46]. Asymmetrical voltages in a three phase system produce asymmetrical flux inside a transformer's core. This asymmetrical flux cause excessive heating, which in a worst case scenario may exceed rated values resulting in equipment failure. Some types of measurement equipment are sensitive to imbalance in voltage or current and negative and zero-sequence components of voltages or currents can result in inaccurate measurements [47].

1.3.9 Over voltage

In residential feeders, load demand usually peaks in the evening while PV systems installed along the feeder generate maximum energy when the sun is shining the brightest which is usually midday. This results in excessive generation during the day. In a scenario where generation from DERs exceeds the energy demand, high active power injection from PV systems in distribution networks may cause the voltage at the PCC to rise. In feeders with high R/X ratio the situation is exacerbated by increased sensitivity of voltage to active power. This may lead to violation of voltage bands prescribed by standards such as EN 50160 in Europe and ANSI C84.1 in the US [45, 48].

Over voltage in distribution network is associated with a number of problems in power systems. It increases the stress on insulation of the electrical appliances connected to the grid by consumers. This can significantly reduce the life of a product. In worst case scenarios insulation failure can occur resulting in faults. A number of electrical appliances have built-in over voltage protection that shuts down the appliance in case of a severe over voltage [49, 50]. Over voltage can potentially trigger protection relays resulting in unintentional islanding of a feeder from the main grid [51].

1.4 Research objective

This chapter has presented the motivation for the work presented in this thesis. It has been shown that increasing DER penetration in distribution networks brings with it a number of challenges. These challenges need to be addressed within the limitations of distribution networks. In recent years autonomous local voltage control strategies have been successfully deployed in distribution network to good effect. These strategies however use local information. This leads to inefficient use of resources. Advancements in communication technology, mass rollout of smart meters and introduction of state estimator for distribution systems in the last decade brings with it

numerous new opportunities that previously were not available. Coordinated control of resources available within the network can be used to improve the power system efficiency and help reduce operational cost. The overall goal of this thesis is to,

Identify the limits of local autonomous voltage control schemes and find technical alternative for these short comings, by coordinating the control action of available resource in distribution networks in an optimal manner.

The thesis aims to answer the following questions

- What are the problems or limitations associated with local voltage support solutions
- How can these limitations be addressed?
- What is the impact of the proposed method on grid operation?
- Which strategy is mutually beneficial for all stake holders?
- What are the impacts of the studied voltage support strategies on grid operation and how these depend on control parameters?

1.5 Summary of methodology

This section gives a brief overview of methodology used in this work. Chapter 3 provides a much more detailed account of the methodology used in this work. The steps taken are as follows,

- i. Study of regulations pertaining to integration of DERs in distribution networks
- ii. Study of the state-of-art voltage support strategies implemented in pilot projects and discussed in literature
- iii. Comparison of the state-of-art using multiple criterion and selection of most promising voltage control strategy
- iv. Selection of the appropriate network for test case implementation,
 - v. Modeling and verification local and coordinating controllers
 - vi. Execution of a series of simulations (both steady state and RMS depending on the test case)
 - vii. Analysis of the results and comparison with the state-of-art
 - viii. Comparison of the studied strategies based on a set of predefined KPIs
 - ix. Draw conclusions based on the results obtain and present an outlook on future possibilities

1.6 Thesis Outline

This dissertation has been divided in seven chapters. Chapter 1 provides an overview of the current trends in distribution networks and the motivation for the thesis. Chapter 2 details state-of-art pertaining to voltage regulation in distribution networks. Towards the end of the chapter methods detailed in the chapter have been compared based of response time, type of service each provides, footprint and several other factors. Chapter 3 details the methodology used in this work. Chapter 4 presents a coordination based reactive power dispatch scheme for DERs connected with the DN. The results and conclusions drawn from these results have also been presented in the same chapter. Chapter 5 presents a coordinated active power curtailment based method for mitigation of unfairness in local APC schemes. The method has been tested on a real network. Results and conclusions drawn have been presented at the end of the chapter. In Chapter 6 a DSM scheme has been proposed for combined frequency and voltage support. Chapter 7 provides a review of the main conclusions drawn from this work and provides an outlook for future possibilities.

2. State of the Art

2.1 Review of concepts

2.1.1 Active and reactive power

In AC power systems both voltage and current oscillate sinusoidally. Parasitic inductance and capacitance caused by presence of parallel conductors in presence of oscillating magnetic field and shielded cables result in voltage and current to go out of phase. In such a scenario, power flow through lines consists of two components namely active and reactive power shown in Figure 2-1. Active power is the real component of the apparent power and does useful work at the load. Reactive power on the other hand is useless power and cannot be used to do useful work.

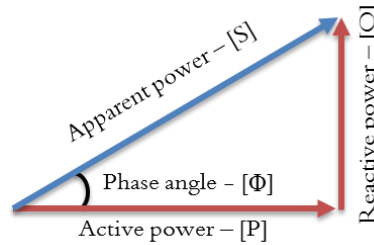


Figure 2-1 Active and reactive power components of apparent AC power

Power flow through a line can be calculated using the following equations. Where, $R + jX$ is the impedance of the line, u_1 and u_2 are source and line end voltage respectively and Φ is the phase angle between the two voltages [52].

$$P = \frac{u_1}{R^2 + X^2} [R(u_1 - u_2 \cos \Phi) + X u_2 \sin \Phi] \quad (1)$$

$$Q = \frac{u_1}{R^2 + X^2} [-R u_2 \sin \Phi + X (u_1 - u_2 \cos \Phi)] \quad (2)$$

As is evident from the equations, both active and reactive power impact the voltage level and the phase angle. The phase angle Φ is generally small and $\sin \Phi \approx \Phi$ and $\cos \Phi \approx 1$ are reasonable approximations. If these assumptions hold, voltage drop along a line becomes proportional to net active and reactive power demand at a node. Therefore, if the flow of reactive power is not controlled it can adversely impact voltage levels. In LV networks however, line resistance is either comparable to or much greater than reactance of the distribution line. If resistance of a line is greater than the reactance, active power has a more dominant impact on voltage level compared to reactive power.

2.1.2 Voltage drop in radial feeders

Conventionally power systems operated in a unidirectional mode. A voltage drop results from the impedance of the line between the substation and the load. When designing a DN, the feeder length and conductor type are chosen such that the voltage drop remains within limits prescribed by the international standards.

As detailed in the first chapter, the dynamics of distribution network have changed in the recent years. Power flow in this evolved DN is bidirectional. Periods of high PV production and low consumer consumption results in over voltages. As the electrical distance from the transformer along the feeder increases this phenomenon becomes more prominent. In some cases the voltage rise can be severe enough to damage electrical equipment [47, 53].

Voltage drop is defined as loss of voltage that occurs between the source and the load due to the impedance of the circuit. Figure 2-2 is a visual interpretation of the voltage drop using phasor diagram. The distribution system were built to ensure that the voltage drop at the end of the feeder did not exceed limits set by standards such as EN 50160 in Europe and ANSI C84.1 in the US [45, 48].

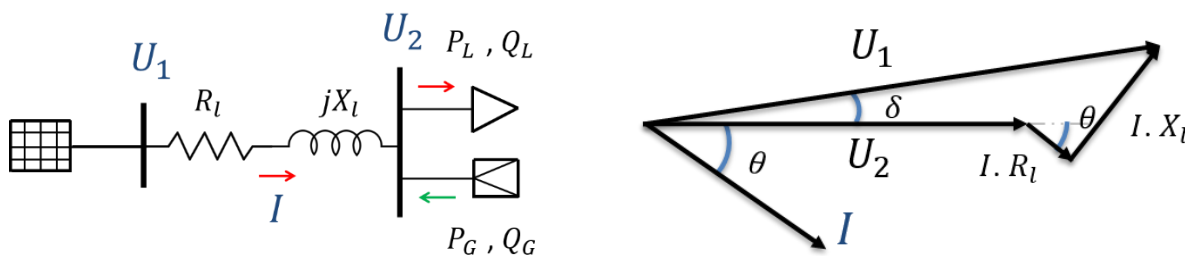


Figure 2-2 Single line and phasor diagram for voltage drop along a DL

Inherent intermittence of renewable generators such as PV systems connected at low voltage in a parallel to consumer load makes several power flow scenarios possible.

1. If P_G and Q_G are zero, the consumer load is served entirely by the grid and a voltage drop is observed between the transformer and the point of common coupling of the PV and the grid.
2. If the active and reactive power produced by the PV system is less than the consumer load at the time, a reduction in voltage drop and distribution system power losses is observed.
3. When the generation and demand are equal, the voltage drop along the feeder is zero resulting in zero power loss in the distribution network.
4. When the PV power generation exceeds the consumer load reverse power flow occurs. This results in voltage rise and an increase in distribution losses. If the difference between generation and consumption is large enough, thermal limits of distribution lines and MV/LV distribution transformer may be exceeded.

The power system has been designed to cope with scenario 1 and 2. Scenario is 3 the ideal case, but it is improbable the generation will equal to demand for any significant period of time. Scenario 4 is a new phenomenon which is why a detailed study is required to mitigate problems associated with reverse power flow and over voltage problems.

2.1.3 Reactive power compensation

Traditionally, both active and reactive power flow from source to load. Reactive power compensation or RPC is a technique used for reducing reactive power flow from the external grid by compensating reactive power locally. Shunt capacitors are a cheap source of reactive power that are widely used to compensate for inductive loads connected to the network. As reactive power is supplied locally, apparent power flowing transmission network to distribution network decreases. This reduces total current flow on the transmission lines allowing them to have smaller current ratings.

Inverter based distributed energy resources such PV systems can themselves take part in voltage control by either compensating reactive power, curtailing active power or by combining the DER with a storage. RPC is control schemes can be used to limit voltage in the distribution network. An added advantage of RPC is an increase in power carrying capacity of the distribution feeder as local reactive power compensation apparent power flowing through a line. Reactive power is also useful in smoothing fast changes in load and generation. The phasor diagrams in Figure 2-3 illustrate the impact of reactive power on voltage.

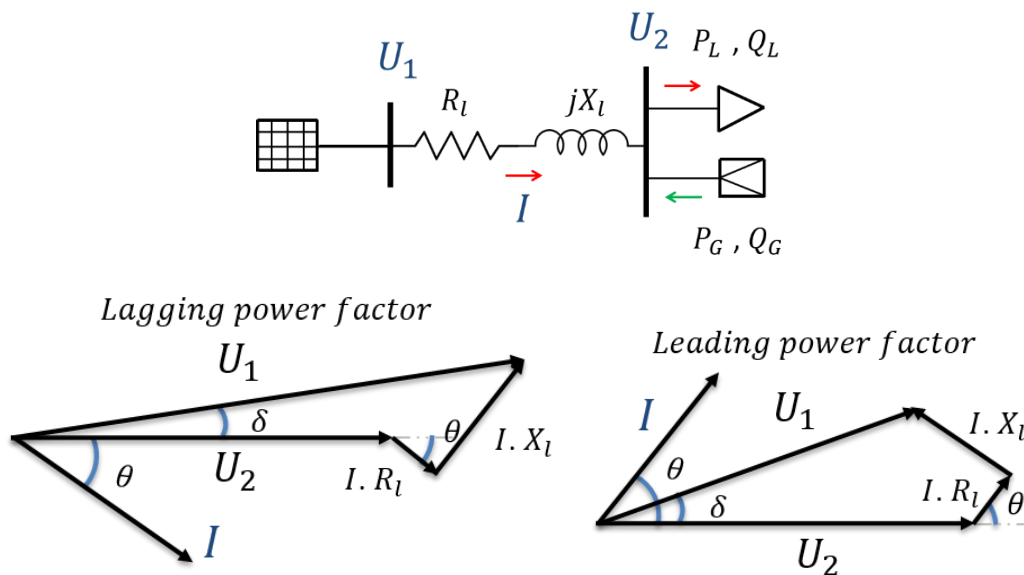


Figure 2-3 Impact of power factor on voltage drop

In the low voltage network R/X ratio is high (usually greater than 1) when compared to the medium or the high voltage network. Reactive power therefore has limited influence over the voltage [49]. It is therefore important to optimize reactive power resources in the LVN to maximize

the impact on voltage. Additionally, reactive power flow between two voltage levels reduces the power carrying capacity of the network and increases network losses. Hence there is a need for coordination among inverters to ensure optimized reactive power dispatch. Finally, reactive power compensation increases switching losses within an inverter. It is therefore imperative to supply reactive power only when overvoltage is an issue.

2.1.4 Active power curtailment

As already discussed, RPC can lead to higher current therefore higher network losses. Additionally, in feeders with R/X ratio greater than one voltage is more sensitive to active power rather than reactive power. Typical urban LVN feeders can have R/X ratio ranging between 0.8 and 2. Finally, RPC results in increased inverter switching losses and decreases the life of an inverter. In low voltage networks where voltage is more sensitive to active power rather than reactive power, active power curtailment becomes an attractive option for voltage control. In countries like India, Bangladesh and Canada where reactive power compensation is illegal, active power curtailment is only option for voltage control using DERs [54] [55] [56].

In first generation inverters, over voltages were handled by disconnecting the DER from the grid altogether [24]. This was achieved via local control and resulted in considerable loss of revenue for DER owner. New inverters have the capability of regulating the voltage at the PCC by reducing active power. Inverters installed in Germany after 2012 are required to have active power curtailment capabilities [57]. Similarly in the US revised grid codes require inverter to have APC capabilities [58]. Figure 2-4 shows a typical power-voltage characteristic diagram for droop based active power curtailment. The generation is only curtailed once the voltage at PCC exceeds the lower limit. This ensures that active power from the prosumer is not unnecessarily curtailed.

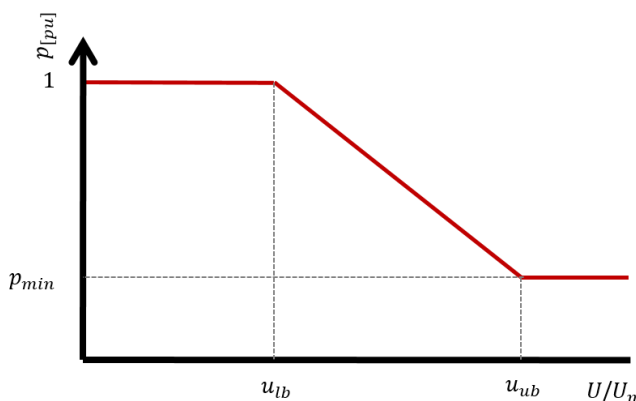


Figure 2-4 Typical characteristics for droop based active power curtailment

In Germany inverters rated greater than 30 KVA are required to have active power curtailment capability via remote signal from the DSO. DSO is permitted to curtail power in steps of 10 percent to ensure network reliability and security of supply. Large installations require additional communication interfaces to send live data to the central control center.

2.2 Voltage regulation methods in distribution networks

Number methods are currently employed to ensure the voltage at any point within a DN complies with the standards listed before. The most commonly used method of voltage control is using an OLTC at the substation transformer. Capacitors are a cheap source of reactive power and are used in feeders that face chronic under voltages. In certain instances devices like STATCOM can be employed to regulate voltage. These methods have been reviewed in a number of books and papers [59, 60, 25, 61, 62]. In this section a review of state of art voltage regulation methods in DNs will be provided. Merits, demerits and limitations of each technique will be discussed. Figure 2-5 lists various methods used of proposed for voltage control in DNs.

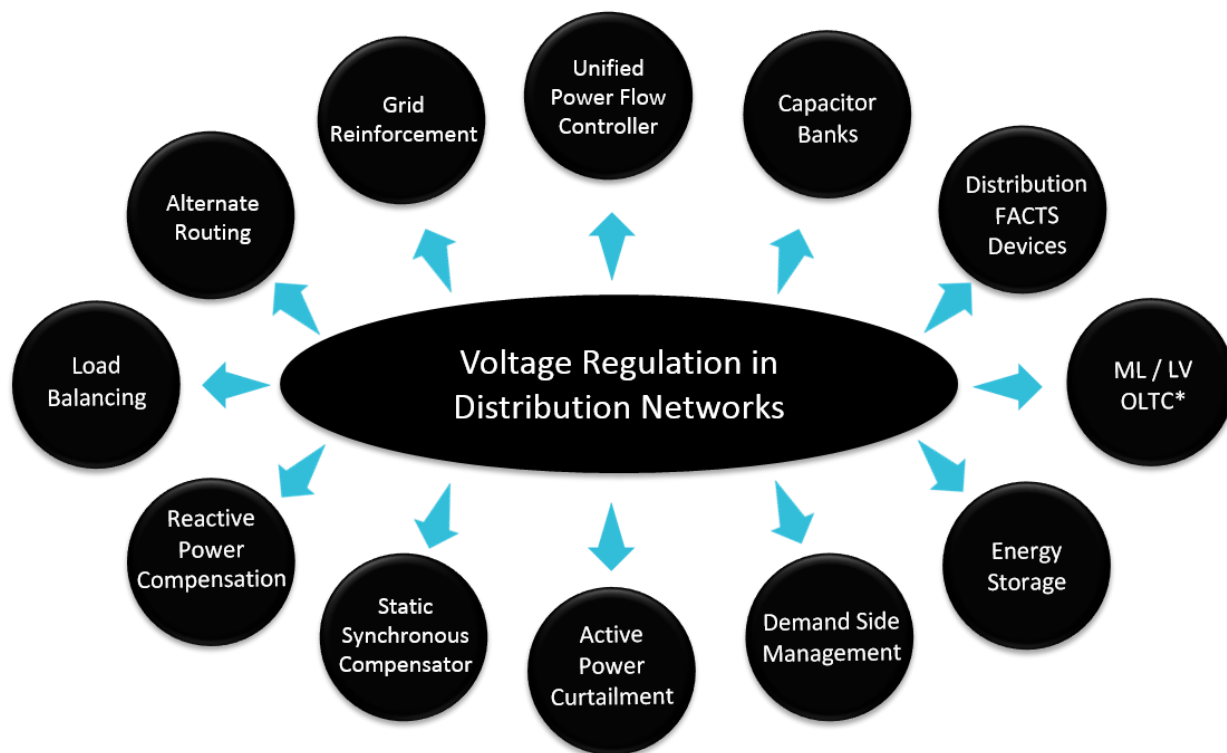


Figure 2-5 Voltage regulation methods in distribution networks

2.2.1 Grid reinforcement

The term grid reinforcement means physical upgrade of certain components of the DNs. In this method the electrical component responsible for the bottle neck in power delivery is upgraded to mitigate the problem. For example in case of transformer overloading due to reverse power flow the transformer will be replaced with a higher rated transformer.

Increasing the cross sectional area of a conductor reduces impedance. Voltage sensitivity to active or reactive power is function of the impedance matrix and as impedance decreases so does the deviation in voltage due to power injection. One advantage of grid reinforcement is that

it can cater natural load growth over a long time period. Replacing conductor can be very expensive and in many cases can make the solution economically infeasible [63].

Using meshed topology instead of radial topology for distribution networks has also been suggested in literature. This would incur costs related to additional infrastructure and equipment. In their work [64] have shown that meshed DN networks can significantly increase DER hosting capacity by reducing voltage rise. In cases where grid reinforcement is economically infeasible other voltage control methods can be used.

2.2.2 Alternate routing

Alternate routing is another option which can be used for voltage control. In this method power is delivered via an alternate path using sectionalizing and tie switches thus overcoming voltage violations at a specific location. An advantage of alternate routing is that topology of the network can be dynamically adapted according to varying conditions in the power system thus mitigating over voltages.

A large percentage of DERs are connected in the LVN and alternate paths for power delivery may not be present. In such cases, it is not possible to regulate voltage by delivering power via an alternate route and other options need to be explored. In literature a number of heuristic and deterministic optimal routing algorithms have been suggested for voltage regulation [65, 66, 67].

2.2.3 MV/LV on-load tap changing transformer

One method of regulating voltage in the DNs is by using on-load tap changing transformers. Tap changers regulate voltage by changing the turn ratio of primary side to the secondary side making use of the relation in Eqn. (3)

$$\frac{U_p}{U_s} = \frac{I_s}{I_p} = \frac{N_p}{N_s} \quad (3)$$

Automatic voltage control (AVC) relay installed at the secondary side of the transformer detect voltage violations and react to change the tap position of the OLTC accordingly. Line drop compensator (LDC) has traditionally been used to estimate the voltage at a remote point on the feeder that needs to be regulated using local voltage and current measurements and line impedance. Voltage calculated by the LDC is used as an input for the AVC [68].

Voltage control capability of an OLTC is limited by the number of taps and the difference between the minimum and maximum voltages seen in the feeders. In a DN with varied DER penetration in different feeders, a big difference in the maximum and minimum voltage can exist. This can drastically reduce voltage regulation capabilities of an OLTC transformer. Figure 2-6 presents a graphical illustration of such a scenario. In such a situation additional voltage control measures are required to ensure proper regulation.

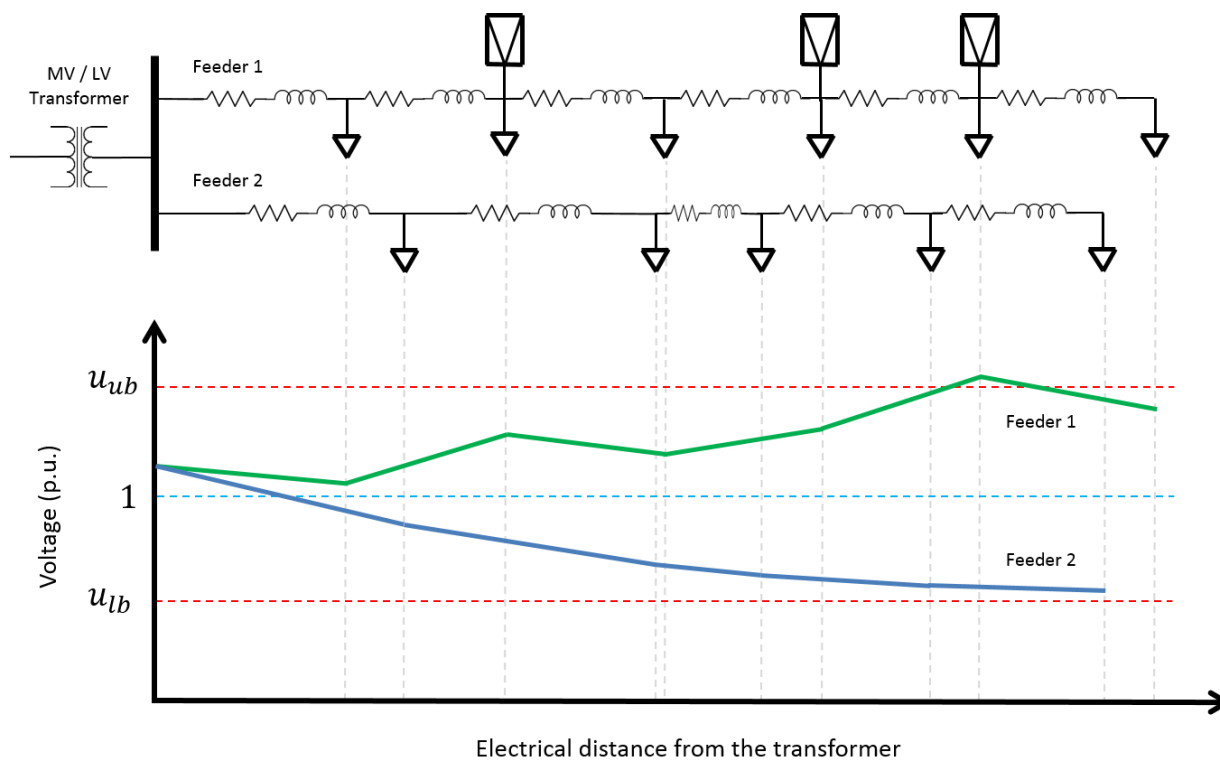


Figure 2-6 Typical voltage trends along feeders with and without PV systems

OLTC transformers are usually at the HV / MV substation though in recent years distribution transformers with OLTCs are becoming increasingly popular specially in countries with high penetration of DERs in the DN. Based on their work in Long and Ochoa have concluded that installing an OLTC on distribution transformer can improve voltage regulation and increase PV hosting capacity of a LVN up to 20% depending on network topology and PV distribution along the feeders [69]. There are a few drawbacks of using OLTC transformer for voltage control. Firstly intermittent nature of most DERs can cause excessive tap changes in an OLTC. In [70] authors have stated that integration of DERs in DN can lead to 30% increase in tap changes leading to premature aging of transformers. The taps should be changed only when absolutely necessary because tap changing causes arcing damaging the insulation and reducing the life of the transformer [25]. Solid state OLTCs using thyristor have overcome the menace of arcing but have limited fault tolerance. Other major drawbacks of using OLTC are its slow response time in the event of a voltage violation and its limited control capability. Finally, OLTCs provide stepped voltage regulation which deteriorates power quality [28].

2.2.4 Capacitor/ Reactor Banks

Capacitors are a cheap source of reactive power and are commonly used in DNs to improve voltage profile. Local provision of reactive power has the added advantage of mitigating line congestion and reducing active power losses. Fixed capacitor banks however can exacerbate voltage rise resulting from increasing number of DERs installed in the network. In some cases,

fixed capacitors may have to be replaced with switchable ones. Timed capacitors are switch based on the time of the day and not on the voltage at the PCC. In their report the IEEE power engineering society have suggested replacing these with capacitor banks capable of switching based on the voltage at the PCC [71].

Like the OLTC, intermittent nature of power injection from DERs can potentially lead to a large number of switching operations causing premature aging of the equipment. Switching transients resulting from excessive switching are also responsible for deteriorated power quality [72]. In networks facing excessive over voltage phenomenon, capacitors can be replaced with reactor banks. In LVNs capacitors can have lesser impact on voltage compared to MVNs due to high R/X ratio.

2.2.5 Inverter based voltage regulation

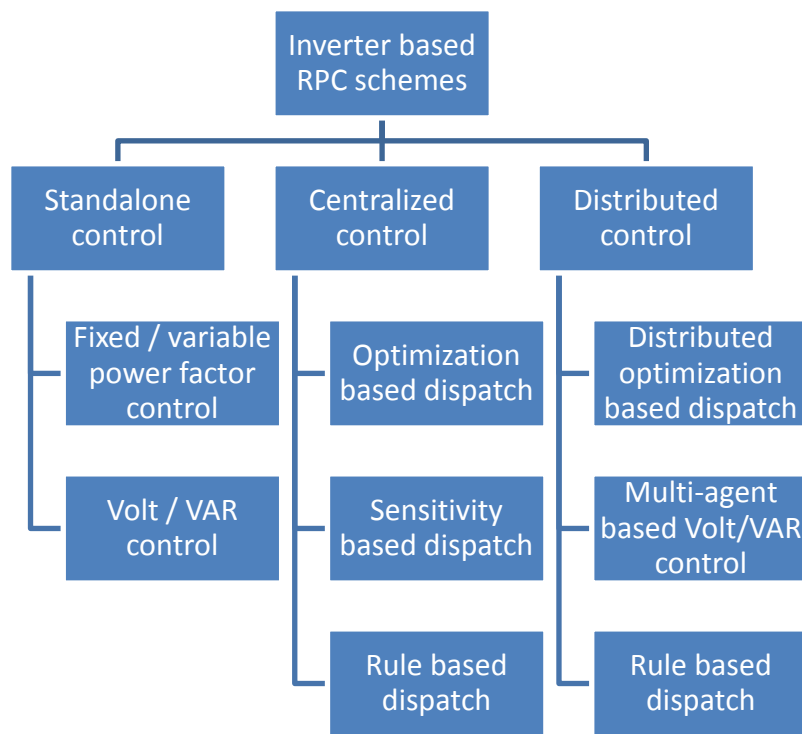


Figure 2-7 Typical characteristics for closed loop voltage control

In recent years, the possibility of DER’s participating in system stability and suppling auxiliary services like voltage support has been actively researched. Inverters are capable of regulating voltage by either reactive power compensation or by active power curtailment [73]. Additionally, inverters can be used to regulate voltage either in a standalone manner reacting only on local information or in a coordinated manner (this includes both centralized and distributed schemes), where a central controller gathers network data and generates a set point for every inverter based on a pre-defined objective function. This sub-section will provide a detailed literature review of inverter based voltage control schemes proposed in literature.

Reactive power compensation

Standalone VAR compensation: First generation inverters operated at unity power factor. Current generation of inverter, however, is capable of regulating voltage at the PCC using RPC. There are three main reactive power compensation techniques that have been reviewed in literature namely, constant power factor mode, variable power factor mode and voltage droop mode (a.k.a. Volt/VAR control) [74].

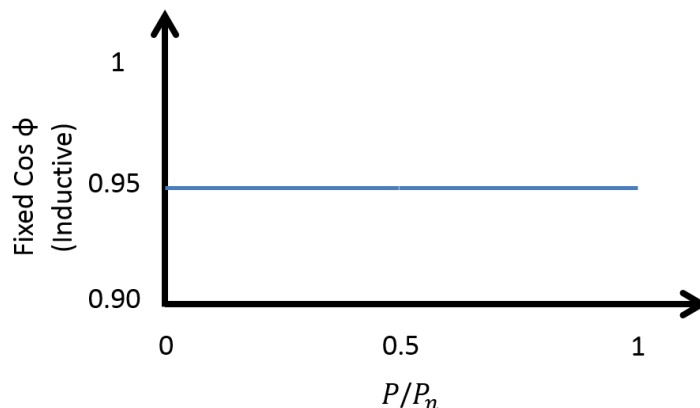


Figure 2-8 Constant power factor control

In [75] authors have proposed a closed loop feedback control scheme using a proportional integral (PI) controller. The control scheme requires inverters to have current and potential transformer installed at inverter output and makes use of local information such as current and voltage to calculate power factor. This is fed back to the controller and compared to the reference point. Any deviation from the set point is corrected using a PI controller. While operating in constant power factor mode, inverter reactive power follows its active power output, thus ensuring power factor remains constant. Constant power factor control mode is cost effective as no additional components are required and is simple to implement. However, constant power factor control is an inherently inefficient compensation technique as reactive power is supplied not taking into consideration the current state of the network. This unnecessary RPC can result in network congestion and increased inverter switching losses.

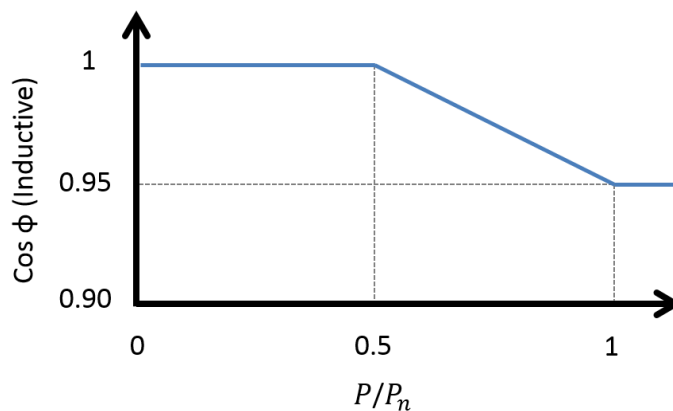


Figure 2-9 Variable power factor control

Variable power factor control is another reactive power compensation method that has been that has been the subject of research for a number of scholars. The idea is to operate the inverter at unity power factor while output power is less than a preset fraction of the rated power of the inverter. Once power generation exceeds the preset limit, power factor decreases linearly as a function of inverter power output. At times of peak generation, power factor is at a minimum hence the reactive power supply is maximum. This method is much more efficient when compared with constant power factor mode. An added advantage of using variable power factor control is that it does not require additional sensor, and has no voltage feedback loop hence is very stable [76]. For DERs rated less than 13.5 KVA the German standard for connecting distributed generation to the electrical grid, VDE-AR-N 4105, also recommends variable power factor control (Figure 2-9) [77]. However, as reactive power compensation is dependent on the input power of the inverter and not the voltage at the point of common coupling, this can lead to inaccurate RPC and result in inefficient use of resources. In a comparative economic study Stetz *et al.* implement four inverter based voltage control strategies. One important deduction from their work is that variable power factor control results in considerable economical savings when compared with constant power factor control [78].

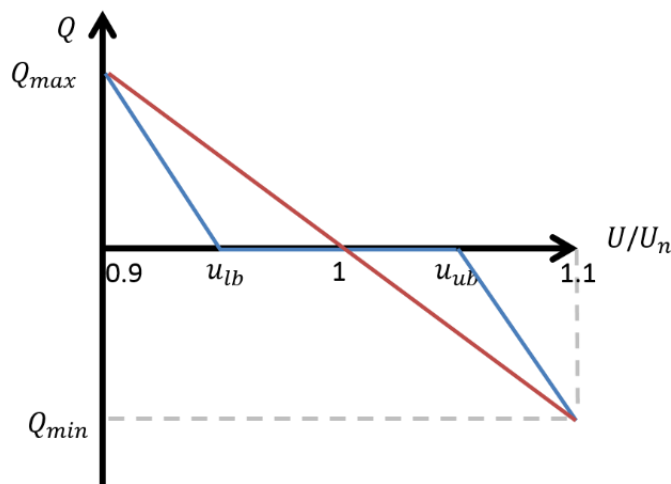


Figure 2-10 Typical characteristics for voltage feedback control

Droop based reactive power compensation also known as Volt/VAR control is another local reactive power compensation method that has been an active research topic in recent years. In this control method the amount of reactive power an inverter will absorb or inject is dependent upon the voltage at the PCC. Figure 2-10 shows a typical VQ characteristic diagram. In literature a researchers have experimented with a different droop curves including linear, piece-wise linear and non-linear curves. The advantage of having a dead band in Volt/VAR droop characteristics is that, it minimizes unnecessary compensation when voltage is within the prescribed bounds. In their work [76] Esslinger and Witzamn have shown that stability of Volt/VAR droop control is only an issue if control parameters are chosen poorly. Additionally, results show that Volt/VAR droop control is more efficient in voltage regulation compared to variable power factor control. Also, it

has the ability to reduce network losses if implemented efficiently. Agrawal *et al.* [79] carried out a detailed simulation based comparative study comparing performance of power factor controller with Volt/VAR controller. Simulations were carried out on the IEEE 123 node radial test feeder. Controller performances have been assessed comparing total reactive power drawn from the external grid and the maximum voltage deviation at consumer end during the entire simulation time period. While comparing the performance of the two controllers, authors have noted that Volt/VAR controller has superior voltage regulation capabilities; however, it results in larger power factor deviation within the system. If the primary aim to the DSO is to regulate network power factor and reactive power flow then power factor control is the better option. If however, the primary aim is voltage regulation at consumer end then Volt/VAR control will provide superior performance. Voltage deviation typically increases as the electrical distance from a transformer increases. Inverters connected close to end of a feeder and operating in Volt/VAR mode do bulk of RPC. Inverters further away from the transformer therefore typically have shorter equipment lifespan and incur greater economic losses [80].

Centralized VAR compensation: In the last few years, the focus of research has shifted from standalone reactive power compensation schemes to coordination based schemes. In standalone schemes inverter reacts only to local information. By coordinating reactive power compensation from the installed inverters resources can be utilized in an optimal manner.

A number of researchers have proposed using a secondary voltage controller in distribution network. In centralized control schemes reactive power set points are usually calculated by either solving an optimization problem or by using reactive power – voltage sensitivity matrix or by implementing a rule based algorithm. In [81] Robbins and Garcia have formulated the reactive power dispatch problem as an optimization problem for an unbalanced IEEE 123-node radial network. They have proposed formulating the objective function as weighted sum of voltage deviation at all DER connected nodes. Non-convexity resulting from nonlinearities in the constraints has been taken care of using a technique called convex relaxation. Simulation results presented in the paper validate the proposed method as voltage deviation reduces significantly. Similarly in [82] authors Guggilam *et al.* have proposed a number of optimization algorithms for optimal reactive power dispatch in distribution networks with high PV integration. Instead of relaxing constraints, authors have opted to linearize AC-OPF equations. This reduces the non-convex problem to a quadratic program. The authors have further proposed distributed algorithm to solve the problem as it improves scalability and reduces computation burden. Authors have also pointed out that distributed implementation facilitates integration with distribution network markets.

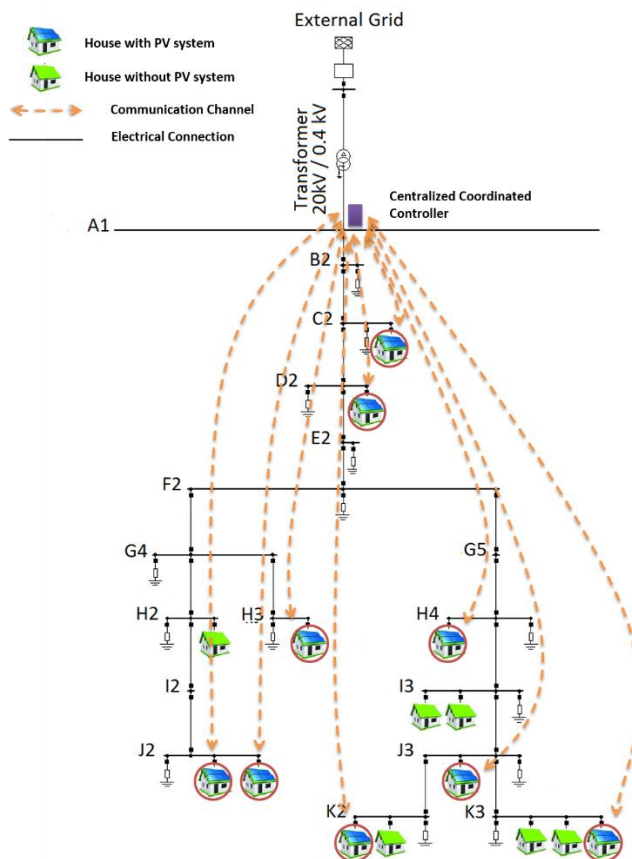


Figure 2-11 Typical centralized coordinated control implementation

A number of researchers have used heuristic optimization algorithms to solve the formulated optimization problem. In [83] authors have proposed a hybrid algorithm based on Delaunay triangulation and ant colony optimization for optimal reactive power resource planning in distribution networks. The purpose of hybridization is to improve algorithm’s search capabilities and enhance convergence. A rural German network has been chosen as a test case. The authors in their work formulated the objective function as the sum of voltage deviation at all DER connected nodes. Simulation results presented in the paper show that the proposed approach improves voltage regulation. Additionally, it reduces network operational costs by up to 2.5%. Chen *et al.* in their work [84] have proposed a fuzzy adaptive hybrid particle swarm optimization method. Fuzzy logic has been used for guided search minimizing chances of algorithm getting stuck in local optima. The objective function has been formulated as the sum of power loss cost, LTC operation cost and capacitor switching cost. Authors have opted to add voltage limits as a constraint unlike the previous paper where authors chose to use voltage deviation as an objective. The proposed method has been tested on the IEEE 33 node test feeder. As per the results presented in the paper the proposed algorithm shows the best performance when compared with a number of other heuristic optimization algorithms.

A major advantage heuristic techniques have over deterministic techniques is that they can be used for non-convex problems. Most heuristic algorithms are highly parallelizable hence can make use of parallel processors. Heuristic techniques however have a number of limitations. They suffer from premature convergence; also, there is no guarantee that the solution found is the globally optimum solution. Scalability is also a major issue as increase in the dimension of the problem results in an explosion of search space making heuristic infeasible in a many real world applications.

Rule based coordinated voltage control has also been proposed by a number of researchers. A fuzzy logic based coordinated voltage control has been presented by Hashim and Mohamed in [85]. The proposed algorithm makes use of three methods for voltage regulation namely DER power factor control, DER active power curtailment and use of on load tap changer. Node voltages and DER output are grouped into three categories called high, medium and low. Fuzzy logic based controller then decides which voltage regulation methods are to be used on which nodes. The centrally coordinated scheme shows good results with voltages at some nodes reducing by nearly 9% after the implementation of the algorithm. In [86] authors have proposed a two-step voltage regulation solution. In the first step, a multi objective optimization is solved using genetic algorithm and a Pareto front is formed. Next, a decision making function is used to make the best possible compromise and select a solution. Finally, fuzzy logic implementation is used to generate DERs' reactive power set points. Results presented in the paper show improved voltage regulation compared to other voltage regulation methods used for comparison in the paper. A priority based centralized coordinated voltage control for distribution networks with a high percentage of DERs has been presented in [87]. In this work, authors first minimize active power losses subject to voltage constraints, DER power injection constraints and power balance constraints. A priority based algorithm is then used to select the type of voltage regulation needed for a particular node. The results show improved voltage regulation compared to the base case.

Another centralized reactive power dispatch method employed by a number of researchers is sensitivity based reactive power dispatch. In [88] Abbott *et al.* have proposed sensitivity based reactive power dispatch. Output power is curtailed once reactive power resources have been exhausted and voltage limits are violated. The proposed method has been implemented on the IEEE 13 node test feeder. Results look very promising as the proposed method reduced reactive power losses by over 85% freeing conductor's current carrying capacity by 17%. Daroj and Limpananwadi in their work have derived a real power loss sensitivity factor (sensitivity of active power loss to reactive power injection) [89]. They have then formulated an objective function using the derived sensitivity factor. The proposed method has been tested on the IEEE 38 node radial test feeder and the results presented in the paper show a significant decrease in losses due to intelligent centralized reactive power dispatch.

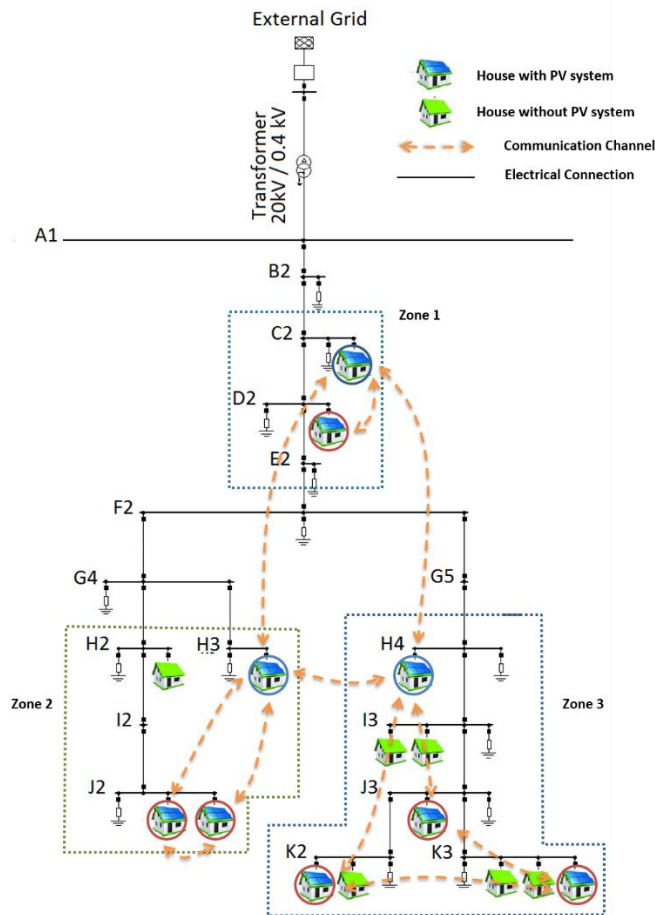


Figure 2-12 Distributed voltage control implementation

Distributed VAR compensation: Distributed approach in solving distribution network centric optimization problems has been the focus of research in a number of papers. Zhao *et al.* have proposed solving the optimal reactive power dispatch problem for an interconnected multi area power grid in a distributed manner [90]. The authors decompose the global optimization problem into an N number of optimization problems that can be run locally for each predefined zone. Primal dual interior point method has been used to solve the partial optimization problems. Exchange of boundary bus admittance matrix is necessary in the proposed scheme as convergence of phasor voltage at zone boundary require weighted sum of voltage magnitudes and phases. These weights are calculated using the admittance matrix. Simulation studies have been performed on a number of IEEE test cases and results presented in the paper show that the performance of the proposed method is comparable to that of a centralized scheme. In [91] Zheng *et al.* have also proposed a distributed reactive power optimization that is capable of converging to global optimum of non-convex problems in distribution networks. Second order conic relaxation has been used to convert a non-convex problem into a convex problem. Authors have also provided a proof on guaranteed convergence in reality however; rate of convergence is dependent on the tuning parameter. To overcome such a problem, authors have additionally proposed a distributed penalty parameter tuning technique. Simulations have been run on the IEEE 69 node test feeder and IEEE

123 node test feeder. Results show improved voltage regulation in every scenario simulated. In [92] Li *et al.* have also proposed network partitioning method for dividing a global optimization problem into a number of optimization problems than can be solved locally. Partitioning a network reduces the dimension of a problem hence require less time for computation. A decomposition algorithm has been used to cluster nodes and define zones based on electrical distance. The method has been tested on a real 234 nodes network. Results show considerably improved voltage regulation compared to the base case.

Agent based distributed Volt/VAR control has been the topic of research for a number of scientists. In [93] authors Chen *et al.* have proposed a multi-agent based Volt/VAR control scheme that aims at improving both voltage profile and power factor regulation within a distribution network. The proposed scheme is dependent on exchange of information within agents. The method proposes propagating voltage correction upstream from the affected node, while prorogating the power correction message downstream from the distribution transformer. The aim here is to ensure participation all DERs connected within the network, while keeping number of messages exchanged to a minimum. Authors have reported significant improvement in voltage profile compared base case results. In [94] the authors have proposed an iterative agent based distributed voltage regulation method for distribution networks with high penetration of DERs. In the proposed method, when a leader agent senses voltage violation requests neighboring agents to participate in reactive power compensation. This message is propagated via other agents connected within the network, allowing all DERs to contribute in reactive power compensation to alleviate voltage violation. Results show improved voltage regulation compared to base case simulation result. Similarly, in [95] Ren *et al.* have proposed an agent based distributed voltage regulation approach that aims at minimizing voltage violation while also minimizing reactive power injection. In [96] a fuzzy multi agent based voltage regulation control scheme has been proposed. Data from sensors is sent directly to control agent that make decision based on fuzzy logic. Simulations carried out for a period of 24 hours demonstrate the effectiveness of the proposed scheme. Ahmad *et al.* have proposed a multi agent system for reactive power dispatch [97]. The proposed algorithm has been tested on a co-simulation based test bed, where the agents have been implemented in Jade and the electrical grid has been implemented in PowerFactory. Matlab has been used to facilitate exchange of data from PowerFactory to Jade. The objective function formulated in this work is minimization of reactive power dispatch. This ensures optimal resource utilization. In this work, it has been assumed that each control agent has partial reactive power sensitivity matrix information. A leader-follower based distributed algorithm has been proposed where the leader requests its neighbors for reactive power support when voltage violation occurs.

Active power curtailment

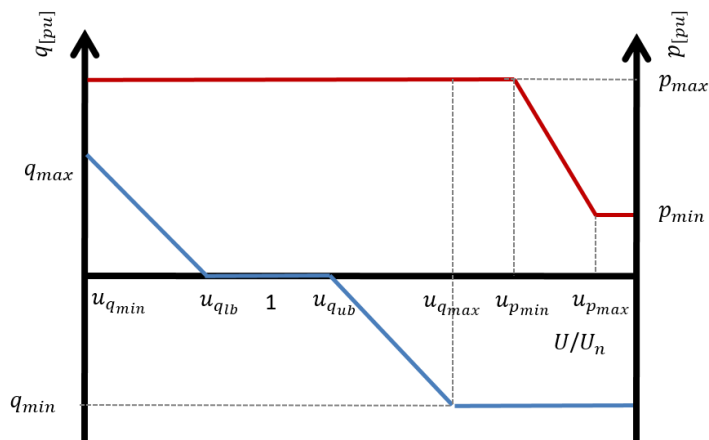


Figure 2-13 Combined RPC and APC control

A number of local and coordination based active power curtailment schemes have been presented in literature. Tonkoshi and Lopes proposed droop based active power curtailment of non-dispatchable DERs like PV systems for local voltage regulation [98]. The proposed scheme has been simulated using a hypothetical LV network with 12 houses serviced by a 75 kVA transformer. Simulation results showed a reduction in PV active power contribution reducing to 53kW from 84kW. An additional observation made in this work is that moving down stream along a PV saturated feeder, voltage tends to rise. This results in unfair curtailment of PV systems along a feeder as PV systems at close to the end of the feeder get a larger portion of the active power curtailed. Bozalakov *et al.* carried out research on a damping based local voltage strategy supported by EC-FP7 project ‘INCREASE’ [99]. In their work, authors have proposed a three phase damping control strategy with linear APC capabilities. A damping controller has been proposed whose damping conductance is the function of the voltage at PCC. The intention behind the use of the droop controller is to cater to over voltages, while damping controller has been proposed to cater to voltage imbalance at PCC. The proposed method has been tested on a hypothetical 10 node test feeder. The impact of the proposed scheme on over voltage, positive sequence and zero sequence voltage components has been studied and presented in the paper. Results show that using the proposed method, power curtailment reduces by more than 50% compared to positive sequence droop control. Additionally, voltage unbalance is significantly reduced. In [40] Ghosh *et al.* have experimented with combined local RPC and APC on the IEEE 34 node test feeders. In a series of experiments, the authors have implemented the proposed approach for uniform and non-uniform PV distribution scenarios. The results have compared using two KPIs namely, total number of tap changes required and PV hosting capacity. Simulation results show that combined RPC-APC scheme successfully regulated voltage in all simulated scenarios. Additional benefit of the proposed scheme is that it reduces the total number of tap changes, thereby increasing the life of the voltage regulator. Extending their work, in [100] Ghosh *et al.* have proposed a local voltage regulation scheme that adapts RPC and APC using PV generation forecast. Short term forecasts (15 seconds) are generated using current irradiance/ temperature measurements, historical profiles

and physical PV model. Using forecasted values, set points for active and reactive power are generated. An important feature of the proposed method is that it provides limits for curtailment even during times over voltage is not likely. This makes the proposed method resilient to instantaneous changes in inverter input power. The proposed method requires only local information hence no communication infrastructure is needed. The method has been tested on the IEEE 34 node test feeder. Simulation results show improved voltage profile, additionally, it has been shown that total curtailed power is related to power factor constraints of the inverter. Vandoorn *et al.* [101] in his work experimented with numerous droop strategies for RPC and APC.

Coordinated active power curtailment has been active research topic in recent years. X. Su *et al.* have formulated an objective function as a weighted sum of voltage imbalance, voltage deviation, network losses and PV curtailment cost [102]. The cost function has been solved using the sequential quadratic programming solver in Matlab. The proposed algorithm generates optimal set points for both active and reactive power of the connected inverters. 24 hour period simulations have been carried out for a number of scenarios. Simulation results show that the proposed method is capable of mitigating voltage imbalance and over voltages. In their work, Calderaro *et al.* proposed an algorithm to generate optimal active and reactive power set points for PV inverter and formed the objective function as a weighted sum of dispatch reactive power and network losses [103]. The resulting non-convex problem has been solved using the multi objective genetic algorithm as it is capable of avoiding local minima. The Pareto front obtained by changing objective weights represents optimal tradeoff between network losses and reactive power dispatch. In their work, Gabash and Li have proposed formulating the objective function as a yield maximization problem [104]. The cost function has been formulated as PV output minus power loss and net power demand. This aims at minimizing active power curtailment along with system losses and net power demand. Results presented in the paper show that optimal active and reactive power set points generated in this paper can increase yield by up to 25%.

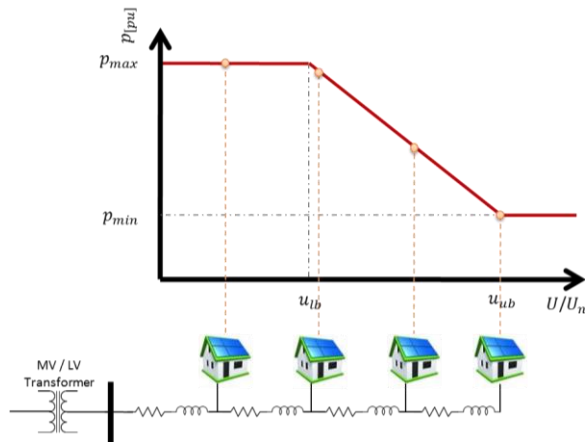


Figure 2-14 Curtailment typically increases as the electrical distance from the transformer increases

The Voltage at the PCC is a function of the active and reactive power being injected at that point and the grid impedance as seen by the inverter at PCC. As the electrical distance from a transformer increases, so does the voltage sensitivity (Figure 2-14). At times of high generation,

inverters connected at PCC with higher voltage sensitivity may violate voltage limits. As a result, the inverters that are violating voltage limits have their output curtailed. Essentially, PV owners located at the end of the feeder are more susceptible to voltage violations and getting their power curtailed resulting in loss of revenue. DSOs commonly calculate a feeders' hosting capacity using the worst case over voltage scenario which might further limit the size of PV that can be installed by the house owner connect near the end of the feeder. Worst case voltage is calculated using a scenario assuming no load and all single phase PV inverter units are connected on the same phase.

A number of different solutions have been presented in literature to mitigate this inherent unfairness in droop based APC schemes for voltage control. In Japan for example, as of 2012, if power from a PV inverter is curtailed for more than 30 days a year (8%), the owner has to be compensated by the DSO [105]. In [106], authors have suggested using batteries at times of low consumption and high distributed generator (DER) generation. An added advantage of using battery storage is that it minimizes fluctuations in DER output. Researchers have also suggested using demand side management and increasing self-consumption, thereby reducing power injection during the time power curtailment is an issue [107]. Tonkoski *et al.* [108] developed a coordinated algorithm to mitigate unfairness by experimenting with different droop curves for DER owners and achieved excellent results. Perera *et al.* [109] developed an iterative algorithm that improves fairness while keeping voltage within limits. Zhao *et al.* [110] have addressed unfair APC by formulating it as part of the objective function in an optimization problem. The proposed algorithm uses load and solar irradiance forecast profiles to calculate active power dispatch values for PVs while minimizing both unfairness in curtailment and total curtailment and satisfying voltage constraints. In [108, 111] researchers have exploited the voltage sensitivity matrix to calculate potential voltage rise and reduction in active power injection required to ensure that voltage remains within limits.

2.2.6 FACTS Devices

Flexible AC transmission system or FACTS are usually power electronic based devices used for regulating parameters like voltage, power factor etc. They enhance power transfer capability and critical power system parameters within prescribed bounds [112]. FACTS devices were originally conceived to regulate the transmission network; recently however, they are increasingly being used in the DN for improved regulation. In comparison to capacitor banks, FACTS devices are much more costly and require and much larger footprint for installation.

Static VAR Compensator

Static VAR compensators (SVC) are the most popular first generation shunt devices belonging to the FACTS family. They are the most commonly used FACTS device today. They regulate voltage by means of reactive power compensation. A SVC controls a shunt capacitor or inductor via a thyristor which improves voltage profile. In [113] the authors introduce a new D-SVC device that has three different modes of operation. The device is capable of short term voltage fluctuations, additionally; it can maintain the voltage within specified limits. One advantage SVC

has over D-STATCOM is that it is much more precise voltage regulating capability, even in scenarios where there is significant variation in load and generation in the DN [114]. In [115] a coordinated control scheme has been introduced that coordinates control actions of OLTC, shunt reactor, shunt capacitor and SVC. Coordinated control of step voltage regulator and SVC using Reactive Tabu search has been presented in [116] and was shown to be better than normal Tabu search algorithm for the proposed scheme.

Distribution Static Synchronous Compensator

D-STATCOM is a shunt connected voltage source converter based static compensator and belongs to the family of FACTS devices. They are commonly used for power factor correction; however, they can also be used for voltage regulation using reactive power compensation. A D-STATCOM is capable of both supplying and consuming reactive power to the network, and therefore, can cater to both under and over voltage in a radial network [117]. This makes it suitable candidate for voltage regulation in distribution networks with high PV penetration that are susceptible to both under and over voltages.

Aggarwal *et al.* investigated the possibility of using a distribution D-STATCOM in LVNs with high PV penetration. Results showed that the use of D-STATCOM improves voltage regulation; it also suppresses harmonic distortion [118]. A coordinated control strategy for OLTC and D-STATCOM has been presented in [119]. The authors have concluded that proposed scheme is capable of mitigating both over voltages and voltage imbalances via active and reactive power control respectively. D-STATCOMs typically have a faster response time than SVC. Additionally, they have lower harmonic emissions and exhibit constant current characteristic with varying voltage at PCC unlike SVC [112].

Distribution Unified Power Flow Controller

A UPFC consists of solid-state voltage source converters couple together through a DC link. Having both series and shunt compensation block, it has control over line parameters, voltage and phase angle. It is therefore capable of both controlling both power flow and voltage magnitude.

In [120] the authors investigated the impact of D-UPFC device on voltage regulation in IEEE 10 bus distribution system. Results showed that using D-UPFC in conjunction with OLTC on distribution transformer can significantly improve voltage regulation capabilities. P. Kumar *et al.*'s work in [121] shows that D-UPFC is capable of regulating voltage in presence of DERs. It can additionally damp oscillations associated with DER technologies. In [122] a novel control circuit has been developed to regulate voltage using D-UPFC in DN with high PV penetration. Simulations results presented in the paper show that D-UPFC is capable of handling both under and over voltages.

2.2.7 Energy Storage

The idea of using distributed energy storage for improving voltage profile in networks with high DER penetration has been gaining ground in recent years. The idea is to store excessive energy during times of high DER generation and use the stored energy when the demand is high and there is little or no generation from the DER systems installed. In literature a number of storage solutions such as chemical batteries, super capacitor, fly wheel, compressed air storages and thermal energy storages have been investigated [123]. Storage requires capital investment, which might deter consumer investment. Chemical batteries, most readily available and interfaceable energy storage devices, are expensive, bulky and have a limited lifespan compared to PV panels. Hence they incur a recurring cost. They are also susceptible to self-discharge and therefore increase system losses [124].

M. J. E. Alam *et al.* in their work used distributed chemical battery storages with non-linear charging and discharging behavior to improve voltage profile on a test network with high DER penetration. Simulation results showed that using storages not only improved the voltage profile, it also reduced voltage fluctuations resulting from stochastic PV generation. One important observation they made in their work is that for effective resource utilization, charging and discharging rates of a battery need to be optimized [125, 126]. In [127] authors have investigated a number of storage planning options and an iterative method based on voltage sensitivity has been proposed for optimal placement and sizing of distributed storages.

2.2.8 Demand Side Management

Traditionally, generation was regulated to follow the power demand. Demand side management (DSM) means actively modifying the consumer's power demand pattern so that demand is regulated to follow generation. Due to ever increasing demand for power, DSM has been an active research topic in the last decade. In recent years a number demand side management based voltage based schemes have been proposed. They aim to increase self-consumption and reducing export of power to the external grid at times of high DER generation. Reduction of net power export results in reduced voltage rise.

In [128] authors have simulated DSM based scheme on a real Czech-Republic network. The scheme optimizes electric water control in two stages. The first stage computes schedules for a day-ahead time horizon and the second stage caters to real time deviations. Experimental results show that the proposed scheme improves power balance, reduces energy losses and significantly improves voltage regulation. In [129] authors have presented working of a patented device that facilitates DSM and regulates customer voltage. The results reported show that a reduction of up to 15% in maximum voltage rise is possible with mass use of the device in the distribution network. The device can be remotely controlled, but requires a communication medium to facilitate that. In [130] authors have suggested use of smart metering devices and DSM based scheme to curtail power theft, reduce both demand and generation peaks and improve power reliability.

2.2.9 Power electronic voltage regulator

Technological breakthroughs and cost reduction in recent years have made use power electronic devices one possible solution to the distribution network voltage regulation problem. Several operational approaches of using PEVR in LVNs have been suggested in recent papers. This requires additional network components and thus additional capital. PERVs typically consist of two converters coupled via DC link and DC storage.

A major advantage of using this approach is that unlike OLTC transformer this provides step less voltage control. It has a faster response time than the OLTC transformer. Additionally, PEVRs can work in both centralized and distributed schemes. Studies have shown that it is possible to increase DER penetration levels in DN by using PEVR based control [131]. In [132] F. V. Lima *et al.* proposed PEVR installation on low voltage side of distribution transformers. This allows voltage regulation in DN. Added strength of the proposed scheme include power factor correction. Final simulation results show that the proposed control algorithm is capable of mitigating voltage rise and drop by 30%. In [133] a comparison of regulation capabilities of OLTC, PEVR, active power filters (APF) and UPFC has been presented based on simulation results. The results show that in networks with high PV penetration (> 60%). All voltage regulation devices except for APF were able to regulated voltage within prescribed limits.

2.3 A visual comparison of the state-of-art

	Grid reinforcement	Alternate routing	OLTC for MV/LV tr.	Capacitor banks	Energy storages	Demand side management
Service type	Static	Dynamic Discrete	Dynamic Discrete	Dynamic Discrete	Dynamic Continuous	Dynamic Discrete
Cost (Investment and operational)	High	High		Low	High	
Response time	High	High	Slow	Fast	Fast	Slow
Caters to both under and over voltage	Yes	Yes	Yes	Only under voltage	Yes	Yes
Voltage imbalance correction capability		No	Yes	Yes		Yes
Footprint				Large	Large	Small
Requires communication	No	Yes	No	No	No	Yes
	D-STATCOM	D-UPFC	D-SVC	PEVR	Inverter based RPC	Inverter based APC
Service type	Dynamic Continuous					
Cost (Initial and operational)				Same as OLTC	Low	High
Response time	Fast		Slow	Fast	Fast	Fast
Caters to both under and over voltage	Yes	Yes	Yes	Yes	Yes	Over voltage only
Voltage imbalance correction capability	Yes			Yes	Yes	
Footprint	Large	Large	Large	Mid-sized	Small	Small
Requires communication	No	No	No	No	No	No

Table 2-1 Comparison of the state-of-art voltage regulation techniques in distribution network

3. Methodology

This chapter provides a detailed account of the methodology used in the work presented in this thesis. The two simulation tools chosen for conducting simulations studies presented in this work are DIgSILENT PowerFactory and Python. The before mentioned tools have been chosen with due diligence by considering factors like domain usage, ease of use, external interfacing capabilities etc. DIgSILENT PowerFactory is a popular simulation tool for the power system domain. Python is a high level open source scripting language with a large active community.

The focus of this thesis is to identify limitations of local autonomous voltage regulations schemes in DNs and proposing methods to overcome these limitations. In this work three such limitations have been identified and subsequently solutions have been proposed to overcome these limitations.

In order to assess the limitations of inverter based local RPC schemes for voltage regulation three standalone voltage control schemes namely fixed power factor control, variable power factor control and Volt/VAR control have been implemented on the chosen test network. To compare the impact of each of these schemes a worst case scenario has been chosen as base case. The worst case scenario has been defined a day with high DER injection and low load consumption. Additionally, inverters connected to the network operate at unity power factor no voltage control mechanism has been employed. This allows us to investigate the impact of each the three state-of-art local RPC schemes on a number of network parameters like system losses, transformer loading, import of reactive power form the external grid etc. Simulation results from the first set of experiments provide and insight into the limitations of local autonomous RPC schemes. Local RPC schemes operate using local information. This can lead to inaccurate compensation leading to deteriorated system efficiency, increased system losses and reduced power factor. To improve these limitations of local RPC schemes, a coordination based RPC scheme has been proposed in the thesis. The problem has been formulated as a minimization problem. The derived objective function is a weighted sum of two individual objectives namely the voltage regulation objective and the active power loss objective. The constraints on the problem render the problem non-convex, which is why a population based meta-heuristic algorithm called Modified Bat Algorithm has been chosen to optimize the system and generate new set points for the inverters. In the first instance, the proposed method has been implemented in a centralized manner. The simulation results show that the proposed coordination based method is capable of regulating system voltage while also reducing system losses. Centralized methods scale poorly. To improve upon the scalability of the proposed method, clustering based method has been proposed that defines zones within the chosen electrical network. Each zone has its own coordinating controller that works independently and autonomously. Simulation results from decentralized implementation are

comparable to results obtained from centralized implementation which shows that the proposed method scales well.

Local APC is another local voltage control method for distribution networks with high DER penetration. In LVNs the R/X ratio is generally greater than 1. For this reason active power curtailment is a much more effective method of voltage control in LVNs. To understand the limitations of local APC schemes, a base case has been defined as a day with high generation from DERs and low demand. Additionally, all DERs connected to the network have been equipped with local APC controller that regulates the voltage the PCC using local voltage information. Base case simulation results show that the general trend is that as the electrical distance from the transformer increases, so does the value of the curtailed energy. This is because voltage sensitivity to active power injection is a function of the electrical distance. This means that local APC scheme is inherently unfair to house owners connected further along the LV feeder. To quantify this unfairness KPIs have been derived that have later been used for comparison of the control strategies. For mitigation of unfairness in curtailment plug and play coordination based control scheme has been proposed. Each inverter is equipped with a controller capable of estimating the sensitivity of voltage to active power and communicating it along with the value of the voltage at the PCC and the rated power to the coordinating controller. Assumptions made to simplify the network have been detailed and explained extensively. Impact of the assumptions on the control scheme has also been thoroughly studied. A coordinating controller has been proposed that uses the sensitivity matrix to generate new active power set points for the connected DERs. Results show that the proposed scheme can significantly mitigate the unfairness in local APC scheme by coordinating the control action however this fairness comes at the cost of increase in curtailed power. The impact of the control parameters on the performance of the proposed method has also been studied in detail and the results have been presented along with in-depth discussion. The impact of communication delay and failure on the proposed method has been presented towards the end of the chapter.

A significant number of loads like heaters, air conditions, refrigerators etc. connected to the DN are controlled using a thermostat that use difference between the reference and the current temperature to change the switch state of the load. The principal of thermal inertia allows the possibility of remotely altering the normal state of operation of such loads without compromising on consumer comfort. TCLs therefore are ideally suited to participate in DSM schemes and have the potential to help DSOs and TSOs achieve operational goals such as frequency and voltage regulation. In Chapter 6 a DSM scheme has been proposed for combined frequency and voltage regulation. The aggregation of TCLs has been modeled as a battery that can be charged and discharged depending upon the positive or negative deviation from the reference signal. In base case simulation, the modeled battery tracks the reference power deviation signal. The simulation results show good tracking performance. In the next step forced switching has been performed on TCLs experiencing voltage violation. The impact of forced switching on TCL availability and

tracking performance signal has been discussed in great detail. Figure 3-1 provides a graphical overview of the methodology used in this work.

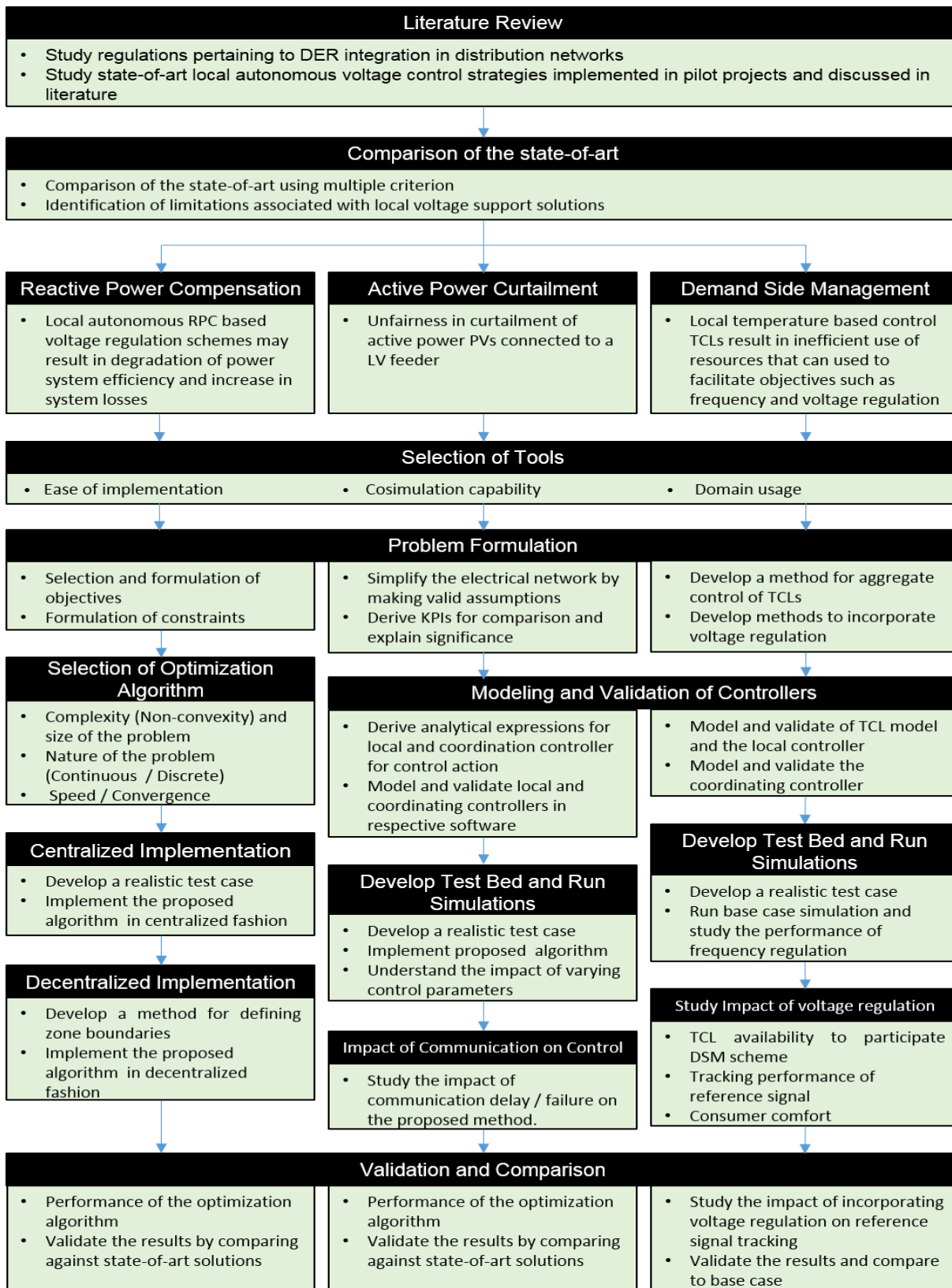


Figure 3-1 Methodology flowchart

4. Optimal reactive power in distribution networks

4.1 Introduction

Inverter based reactive power compensation is an effective voltage regulation method in distribution networks with high DER penetration as it is capable of providing dynamic regulation, is economically viable, has a smaller foot print and can be implemented in a distributed manner. Inefficient VAR compensation however can result in network congestion, increased inverter losses and reduction in inverter useful life. Coordinated Volt/VAR control of inverters has been suggested by a number of authors. The problem is inherently non-convex. A number of authors have opted to solve the problem using deterministic techniques by either using linear approximations of power flow equations or by relaxing constraints and reducing the problem to a convex approximation then solving the problem using a convex solver. Deterministic techniques are generally fast; however, usually require approximations or simplifications to the real model. Additionally, gradient based techniques are prone to getting stuck in local optima.

Heuristic optimization methods are a powerful alternative to deterministic optimization techniques. These methods are that are capable of handling non-convex problems unlike most deterministic techniques. Most heuristic optimization techniques are parallelizable and can make use of multi-processor technology. Additionally, these techniques may avoid local minima. Premature convergence is a major problem associated with heuristic techniques. Scalability is also a major issue as increase in the dimension of the problem results in an explosion of search space making heuristic infeasible in a many real world applications.

Secondary voltage control is an optimization problem. A suitable algorithm is needed to be able to solve the optimal reactive power dispatch problem close to real time due to varying network conditions resulting from the stochastic nature of DERs.

In this chapter, an optimal reactive power dispatch problem has been formulated subject to constraints relating to both the power systems capability and inverter capability. Next, a population based meta-heuristic technique has been introduced. To avoid premature convergence, improve exploration of search space and gain control over global and local search, two modifications to the optimization technique have been proposed. The first modification proposes adding a bad experience component to the velocity update equation, while the second modification proposes using a non-linear inertia weight component. The modified algorithm has been tested on benchmark equations like the Rastrigin function. The formulated problem has solving centralized and decentralized implementation of the algorithm. Test network, modifications and a detailed overview of the use case has been presented in section 4.4. The results have been compared and discussed in section 4.5.

4.2 The optimization algorithm

4.2.1 The Bat Algorithm

Nature has been the inspiration behind a number meta-heuristic algorithms proposed in literature. Bio inspired algorithms can be classified in two main categories, namely evolutionary algorithms based on Darwin's theory of survival of the fittest or swarm intelligence algorithms that try to model collective behavior of living organisms.

Bat algorithm (BA) is a nature inspired population based metaheuristic optimization algorithm proposed by Xin-She Yang in 2010 [134]. The algorithm models the echelon behavior bats use to navigate and compensate for poor eyesight. The bats emit loud pulses and listen to the echo to help them steer and hunt in dark caves. The frequency of the emitted pulses is in the range of 25 kHz and 100 kHz and they last only for a few milliseconds.

Each bat is initialized at a random position with a random velocity vector. Each iteration as bats move towards the best know position, their emitted frequency, velocity and position is updated using the equations.

$$f_i^t = f^l + (f^u - f^l) \cdot u(0,1) \quad (4)$$

$$v_i^t = v_i^{t-1} + (x_i^{t-1} - x_b^{t-1}) \cdot f_i^t \quad (5)$$

$$x_i^t = x_i^{t-1} + v_i^t \quad (6)$$

Where $i \in [1, N]$ and N is the population size. f_i^t is the frequency of the emitted pulse and f^l and f^u are the lower and upper limit for the frequency of the pulse. The symbol $u(0,1)$ donates a uniform random number between 0 and 1. v_i^t and x_i^t donate the velocity and the position of the i^{th} bat at t^{th} iteration. x_b^{t-1} denotes the best global position up to $t - 1^{th}$ iteration. In the original bat algorithm, Yang proposed using random walk near better solutions to improve upon local search capabilities of the algorithm.

$$x_i^t = x_b^t + \varphi A_i^t \cdot u(-1,1) \quad (7)$$

Where φ is a scaling factor that limits the step size of the random walk, A_i donates the amplitude of the pulse emitted by the i^{th} bat at t^{th} iteration. $N(0, \sigma)$ denotes random number sampled from a normal distribution with mean 0 and standard deviation σ . To avoid accidentally alerting its prey, bats tend to reduce the amplitude of the emitted pulse but increase the rate of emission. This phenomenon has been modeled by Yang using equations Eqn. (8) and (9).

$$A_i^{t+1} = \alpha A_i^t \quad (8)$$

$$r_i^t = r_i^0 [1 - e^{-\gamma t}] \quad (9)$$

Where α and γ are constants that control the rate of convergence of the algorithm. It should be noted that as $t \rightarrow \infty$, $A_i^t \rightarrow 0$ and $r_i^t \rightarrow r_i^0$.

For a number of benchmark tests random walk proposed by Yang performs poorly as it does not provide guided search. In [135] Fister et al. have proposed hybridizing bat algorithm (HBA) with differential evolution and replacing random walk with differential mutation, thus providing guided search rather than randomly search the search space. In DE two randomly selected chromosomes (solution) are subtracted scaled and added to a third randomly selected chromosome. This can mathematically be written in the form:

$$m_i^t = x_{r_0}^t + F \cdot (x_{r_1}^t - x_{r_2}^t), \quad (10)$$

Where F is a scaling constant. r_0 , r_1 and r_2 are random integers in the range 1 to N , where N is the population size. Next, the crossover is performed which is mathematically express as follows:

$$z_{ij}^t \begin{cases} m_{ij}^t & u_i(0,1) \leq \beta, \\ x_{ij}^t & otherwise, \end{cases} \quad (11)$$

Where $j \in [1, D]$ and D is the number of dimensions to the problem. $u_i(0,1)$ is a vector of uniformly sampled number between 0 and 1. β is a scaler that controls extent of crossover. In the final step, the fitter of the two chromosomes replaces the current one.

$$x_i^{t+1} \begin{cases} z_i^t & \text{if } f(z_i^t) \leq f(x_i^t), \\ x_i^t & otherwise, \end{cases} \quad (12)$$

4.2.2 Modifications

In this work, two modifications have been made to both BA and HBA to improve its exploration and local search capabilities.

Add bad experience component: In [136] Selvakumar and Thanushkodi proposed expanding the velocity update equation by adding bad experience component in particle swarm optimization. Using the same concept, velocity update equation has been modified so that the bats are attracted towards local and global best solutions and move away from local and global worst solutions. The purpose of this modification is to improve initial convergence and exploration capabilities so that the algorithm converges in smaller number of iterations. The modified velocity update equation is mathematically formulated as follows:

$$v_i^{t+1} = v_i^t + [c_1(x_i^t - x_b^t) + c_2(x_i^t - x_{b_i}^t) + c_3(x_w^t - x_i^t) + c_4(x_{w_i}^t - x_i^t)] \cdot f_i^t \quad (13)$$

where x_b^t and x_w^t are the global best and worst solutions. $x_{b_i}^t$ and $x_{w_i}^t$ are the personal best and worst positions. Parameters C_n where $n \in [1,4]$ govern the acceleration of the bat towards or away from a solution.

Nonlinear inertia weight: The second modification made to the algorithm is also on the velocity update equation. A nonlinear inertia weight has been used to weigh the impact previous velocity v_i^t and velocity update part of the equation has on the new velocity v_i^{t+1} . As bats close in on prey (number of iterations increase), weight of the previous velocity increases and the weight of update part decrease. Introduction of inertia weight serves two purposes. First, it aims at improving local search by reducing the weight of the update part. Second, it aims at providing control transition between global and local search to the used. The weight has been calculated using the following equations:

$$W^t = 1 - \frac{1}{1 + e^{\frac{b-t}{a}}} * (W^u - W^l) + W^l \quad (14)$$

Where W^u and $W^l \in [0,1]$ are maximum and minimum bounds of inertia weight coefficient. t_{max} is maximum allowed iterations. a and b are constants calculated using the following equations:

$$a = \frac{t_{max} - 1}{G} \quad (15)$$

$$b = \frac{t_{max} + 1}{(1 + 10^{(1 - \frac{2*H}{t_{max}})})} \quad (16)$$

Where $G \in [1,20]$ and $H \in [1, t_{max}]$

The constants G and H are tunable parameters that can be adjusted for a particular problem. The constant H controls the transition from global to local search. Constant G controls the rate of the transition. Figure 4-1a shows the effect of tuning variable G while H is kept constant at 250. Figure 4-1b shows the effect of tuning H while keeping G constant at 10. In both graphs the upper and lower bounds for inertia weight are 1 and 0 respectively.

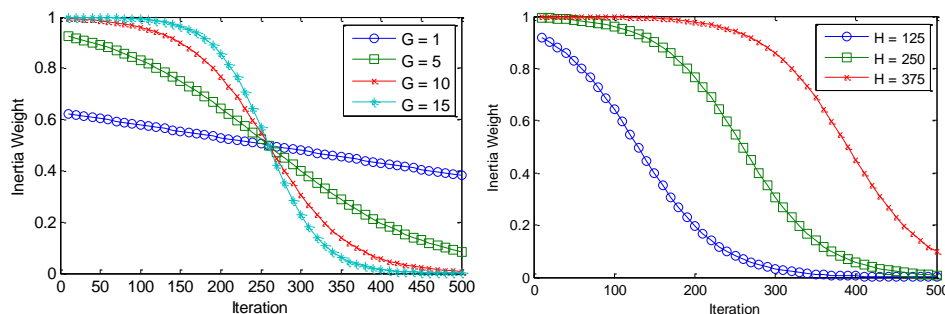


Figure 4-1 Effect of tuning parameters G and H

The final form of the modified velocity update equation is given below.

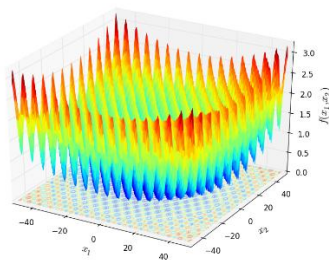
$$v_i^{t+1} = v_i^t W^t + (1 - W^t) \cdot f_i^t \cdot [C_1(x_i^t - x_b^t) + C_2(x_i^t - x_{b_i}^t) + C_3(x_w^t - x_i^t) + C_4(x_{w_i}^t - x_i^t)] \quad (17)$$

The pseudo code for the modified bat algorithm is illustrated in Algorithm 3-1.

Algorithm 4-1 Pseudo code for modified bat algorithm

- 1 Objective function formulation $f(\vec{X})$ where $\vec{X} = (x_1, \dots, x_d)^T$
 - 2 Initialize bat population at initial position x_i^0 with velocity v_i^0 where $i \in [1, N]$
 - 3 Set frequency of pulse f_i at position x_i^0
 - 4 Initialize pulse rates r_i and the loudness A_i and acceleration constants C_n where $n \in [1, 4]$
 - 5 **While** $t \leq t_{max}$ **Do**
 - 6 Adjust wavelengths λ_i for each bat and update their velocity v_i^t , position x_i^t and inertia weight W^t
 - 7 **If** $u(0,1) < r_i^t$ **Then**
 - 8 Select a solution among the best solutions x_i^t
 - 9 Walk randomly or Differential evolution
 - 10 Generate a new solution by flying randomly
 - 11 **If** $u(0,1) < r_i^t$ **and** $f(x_i^t) < f(x_b^t)$ **Then**
 - 12 Accept the new solutions
 - 13 Reduce pulse rate r_i^{t+1} and loudness A_i^{t+1} for the next iteration
 - 14 Rank bats according to fitness $f(x_b^t)$ and find the best global solution x_b^t
 - 15 Return optimal solution $x_b^{t_{max}}$ and its fitness $f(x_b^{t_{max}})$
-

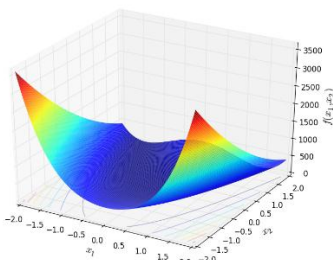
4.2.3 Comparison using benchmark equation



Griewangk's function

$$f(\vec{x}) = -\prod_{i=1}^D \cos\left(\frac{x_i}{\sqrt{i}}\right) + \sum_{i=1}^D \frac{x_i^2}{4000} + 1$$

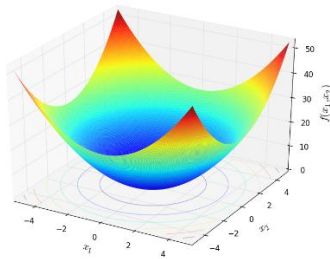
where, $-600 \leq x_i \leq 600$



Rosenbrock's function

$$f(x) = \sum_{i=1}^{D-1} 100(x_{i+1} - x_i^2)^2 + (x_i - 1)^2$$

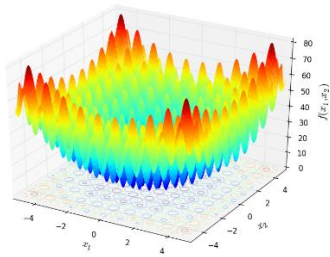
where, $-15 \leq x_i \leq 15$



Sphere function

$$f(x) = \sum_{i=1}^D x_i^2$$

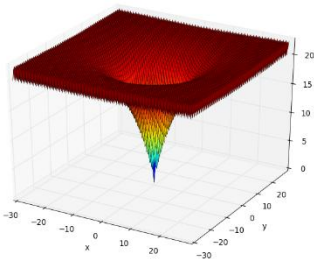
where, $-15 \leq x_i \leq 15$



Rastrigin's function

$$f(x) = 10n + \sum_{i=1}^D (x_i^2 - 10\cos(2\pi x_i))$$

where, $-15 \leq x_i \leq 15$



Ackley Function

$$f(x) = \sum_{i=1}^{D-1} [20 + e - 20e^{-0.2\sqrt{0.5(x_{i+1}^2 + x_i^2)}} - e^{0.5(\cos(2\pi x_{i+1}) + \cos(2\pi x_i))}]$$

where, $-32 \leq x_i \leq 32$

Figure 4-2 Benchmark equations used for testing the optimization algorithms

To study the impact of the modifications, the benchmark equation listed above have been optimized by using BA, MBA, HBA and MHBA a hundred times. Best, worst, mean and median fitness for the hundred run along with the standard deviation have been listed in Table 4-2. Table 4-1 provides the parameter setting used for the experiment.

Parameter	f^l	f^u	φ	C_n	A_i^0, r_i^0	F, β	G	H	N	t_{max}	D
Value	0	2	0.1	1	0.5	0.5	5	500	40	1000	10

Table 4-1 Values of parameters used for benchmarking test

OBJECTIVE FUNCTION	BAT ALGORITHM	MODIFIED BAT ALGORITHM	HYBRIB BAT ALGORITHM	MODIFIED HYBRID BAT ALGORITHM
GRIEWANGK	worst = 19.603 best = 1.858 Mean = 8.922 median = 8.144 stdev = 4.678	worst = 25.609 best = 1.549 Mean = 8.537 median = 7.147 stdev = 6.349	worst = 0.0188 best = 4.714e-04 Mean = 0.00490 median = 0.00277 stdev = 0.00524	worst = 0.0254 best = 1.618e-05 Mean = 0.00444 median = 0.00248 stdev = 0.00595
SPHERE	worst = 1.116 best = 0.538 Mean = 0.855 median = 0.893 stdev = 0.165	worst = 1.109 best = 0.476 Mean = 0.803 median = 0.785 stdev = 0.108	worst = 1.229e-11 best = 8.553e-13 Mean = 4.353-12 median = 2.792e-12 stdev = 3.285e-12	worst = 7.628e-12 best = 9.438e-13 Mean = 2.460e-12 median = 1.811e-12 stdev = 1.907e-12
RASTRIGIN	worst = 64.130 best = 26.616 Mean = 41.170 median = 40.430 stdev = 7.818	worst = 62.270 best = 26.582 Mean = 41.113 median = 38.955 stdev = 10.335	worst = 1.552e-06 best = 6.213-08 Mean = 4.348e-07 median = 3.085e-07 stdev = 4.007e-07	worst = 9.042e-07 best = 8.249e-09 Mean = 1.547e-07 median = 1.008e-07 stdev = 1.958e-07
ACKLEY	worst = 0.055 best = 0.0025 Mean = 0.0252 median = 0.0235 stdev = 0.0128	worst = 0.060 best = 0.0073 Mean = 0.0250 median = 0.0213 stdev = 0.0136	worst = 8.100e-10 best = 1.490e-11 Mean = 1.871e-10 median = 1.570e-10 stdev = 1.840e-10	worst = 1.908e-09 best = 6.480e-12 Mean = 2.68e-10 median = 1.335e-10 stdev = 4.450e-10
ROSENBROCK	worst = 963.40 best = 47.538 Mean = 188.436 median = 97.159 stdev = 214.161	worst = 849.38 best = 29.022 Mean = 169.47 median = 93.757 stdev = 195.241	worst = 19.621 best = 1.655 Mean = 7.138 median = 6.346 stdev = 4.663	worst = 16.886 best = 0.725 Mean = 6.149 median = 5.352 stdev = 3.867

Table 4-2 Results of optimization benchmark equations with multiple local minima

MBA algorithm found the best solution for 4 of the 5 functions when compared with BA. The average and median fitness obtained by MBA was better than BA for all 5 functions. The standard deviation however was lower for BA on 3 occasions showing tighter clustering of the results obtained by BA when compared with MBA. MHBA also consistently outperformed HBA finding the best solution and better average solution 4 out of 5 time. Median fitness of the solutions obtained by MHBA is better than HBA all five times.

4.3 Problem formulation

4.3.1 Assumptions

- The DERs have been modeled as an ideal negative load. This means that switching losses of individual inverter and the internal controls have not been modeled.
- The chosen network has been modified to from an unbalanced network to a balanced network. MV networks in EU are balanced hence, the assumption is valid.

4.3.2 Formulation of objectives and constraints

Power loss in power networks has a real and imaginary component called active and reactive power loss respectively. Line resistance is responsible for active power loss, while reactive is responsible for reactive power loss. Inflow of active power from the external grid is typically much higher than reactive power inflow in distribution networks. Consequently, active power losses are also much higher than reactive power losses. For DSOs the reduction of active power losses is an important objective, as it improves system efficiency and reduces operational cost.

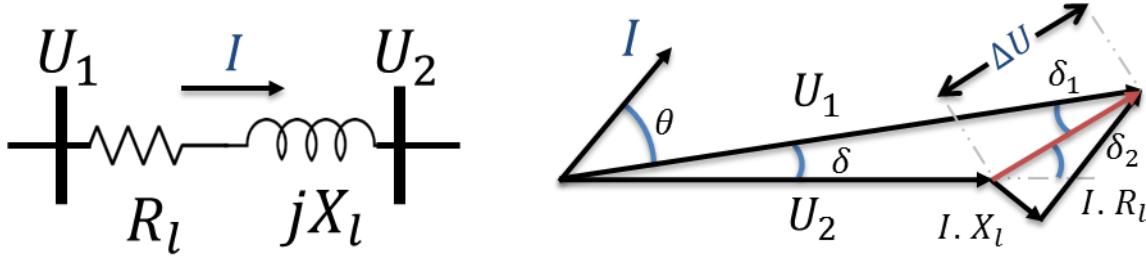


Figure 4-3 Voltage drop phasor diagram for 2 bus system

In a simple two bus network, the current through a line can be calculated using the potential difference and line impedance using the equation.

$$I = \frac{U_1 \angle \delta_1 - U_2 \angle \delta_2}{R_l + jX_l}, \quad (18)$$

Where $R_l + jX_l$ is line impedance, U_1, U_2 are the line voltages at either ends of the line and δ is angle between the two voltage phasors. Active power loss through a branch is a function of the magnitude of current I and the resistance R and can be calculated using the equation.

$$P_{loss} = |I|^2 R_l, \quad (19)$$

Expanding Eqn. (18) the current I can be written in complex form

$$I = \frac{R_l C_1 + X_l C_2}{R_l^2 + X_l^2} + j \frac{R_l C_2 + X_l C_1}{R_l^2 + X_l^2}, \quad (20)$$

Where

$$C_1 = U_1 \cos \delta_1 - U_2 \cos \delta_2 \quad (21)$$

$$C_2 = U_1 \sin \delta_1 - U_2 \sin \delta_2 \quad (22)$$

The magnitude of the current is square root of the sum of squares of the real and imaginary component and can be calculated using $|I| = (Re\{I\}^2 + Im\{I\}^2)^{1/2}$. By calculating the magnitude

of current using Eqn. (20) and substituting it in Eqn. (19), active power losses can be written in the form, where $\delta = \delta_2 - \delta_1$

$$P_{loss} = \frac{R}{(R^2 + X^2)} (U_1^2 + U_2^2 - 2U_1U_2 \cos \delta), \tag{23}$$

Total active power loss within a network can therefore be written as a summation of losses in all the branches in the network and can be calculated using Eqn. (24).

$$P_{loss} = \sum g_k (U_k^2 + U_l^2 - 2U_kU_l \cos \delta_{kl}), \tag{24}$$

Where g_k is branch conductance, δ_{kl} is the angle between U_k and U_l ; voltage at k^{th} and l^{th} bus respectively. Using reactive power dispatch for active power loss in distribution network can negatively impact network voltage. Local supply of reactive power translates to reduction of reactive power import from the external grid. This reduction results in increased power carrying capacity in distribution lines and reduction in peak current. As active power losses are a function of magnitude of the current flowing through the line, reduction in line current results in reduction active power losses. Suppling local reactive power requires DERs to operate in capacitive mode, which causes the voltage at the PCC to rise. The phasor diagram in Figure 4-4 explains the phenomenon

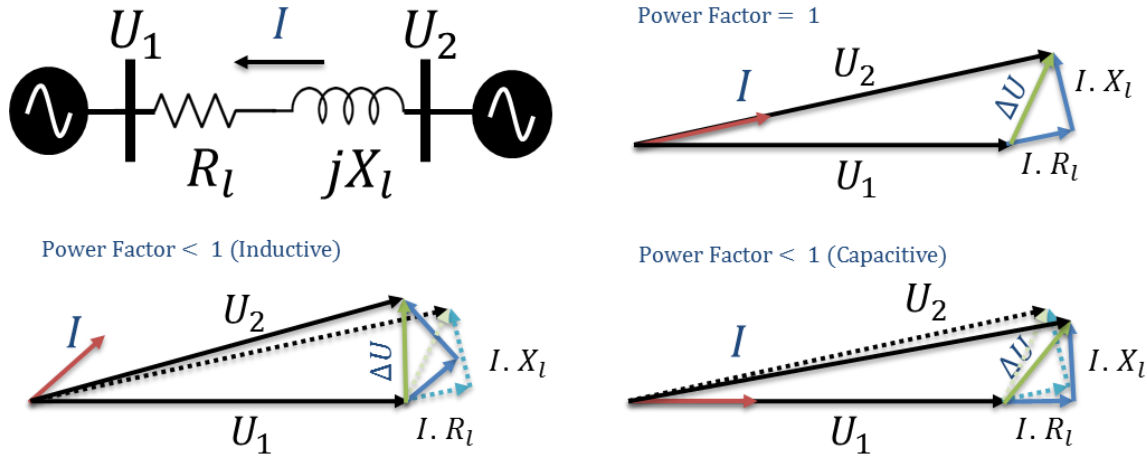


Figure 4-4 Phasor diagrams explaining the impact of reactive power in voltage

Consumer voltage is an important power quality parameter and should not exceed limits prescribed by standards such as EN 50160 [45] or ANSI C84.1 [48]. Here in Austria, the voltage in distribution system should not exceed $\pm 10\%$ of the nominal voltage. This range is shared between the MV and the LV network. DSOs regulate voltage $\pm 5\%$ of the nominal voltage at the MV level. By consuming reactive power and behaving as an inductor, DERs connect to the distribution network can mitigate over voltage. Consumption of reactive power increases net reactive power infeed from the external grid, increases network congestion and increases network losses. In this study case, the upper u^u and lower u^l voltage limits have been at 1.05 and 0.95 p.u. respectively for the MV network. To ensure voltage limits are not violated, they can be made part

of the optimization problem by either adding them as an inequality constraint or as part of the objective function. In this work, voltage violation has been made part of the objective function.

$$u^{uv} = \begin{cases} u^{max} - u^u & \text{if } u^{max} > u^u \\ 0 & \text{else} \end{cases}, \quad (25)$$

$$u^{lv} = \begin{cases} u^l - u^{min} & \text{if } u^{min} < u^l \\ 0 & \text{else} \end{cases}, \quad (26)$$

Where u^{min} and u^{max} are the minimum and maximum voltage seen in the network respectively. This formulation ensures that both u^{uv} and u^{lv} , the upper limit and lower limit violation indices are non-negative and have a positive value only if a voltage limit has been violated. These formulations helps adding the voltage violation to the objective function and solving it as a minimization problem. The final objective function can be formulated as a weighted summation of the two objectives, namely, active power loss minimization and voltage limit violation minimization.

In most optimization problems with multiple objectives, each objective is weighted. The weights are updated iteratively and the optimization is run again. Pareto front is obtained using non-dominant solutions. A decision making function is then used to make the best possible compromise between contradicting objectives and select a solution. This iterative process increases computational complexity. As voltage regulation in DN with high penetration is a real time problem, there is a need for a fast optimization technique. Most multi objective heuristic optimization techniques have computational complexity of either $O(MN^3)$ e.g. NSGA or $O(MN^2)$ e.g. NSGA II. Where M is the number of objectives and N is the number of variables. In this work, the objective function has been formulated as the sum of active power loss objective derived in Eqn. (24) and the voltage violation objective derived in Eqns. (25) and (26).

$$\text{Minimize } F(Q_{g_i}) = P_{loss} + e^{\zeta(u^{uv} + u^{lv})} \quad (27)$$

Where ζ is the amplification constant and Q_{g_i} is the reactive power set point of the i^{th} DER. The voltage violation indices derived in Eqns. (25) and (26) have been weighted by an exponential function. In case of a voltage violation, objective increases exponentially, resulting in $e^{\zeta(u^{uv} + u^{lv})} \gg P_{loss}$, essentially reducing the objective function to $F(Q_{g_i}) = e^{\zeta(u^{uv} + u^{lv})}$. At times during which voltage violation is not an issue both u^{uv} and u^{lv} are zero and the overall objective function is reduced to $F(Q_{g_i}) = P_{loss} + 1$. The formulation does not require outer iteration to update objective weights or decision making function thus reducing calculation complexity.

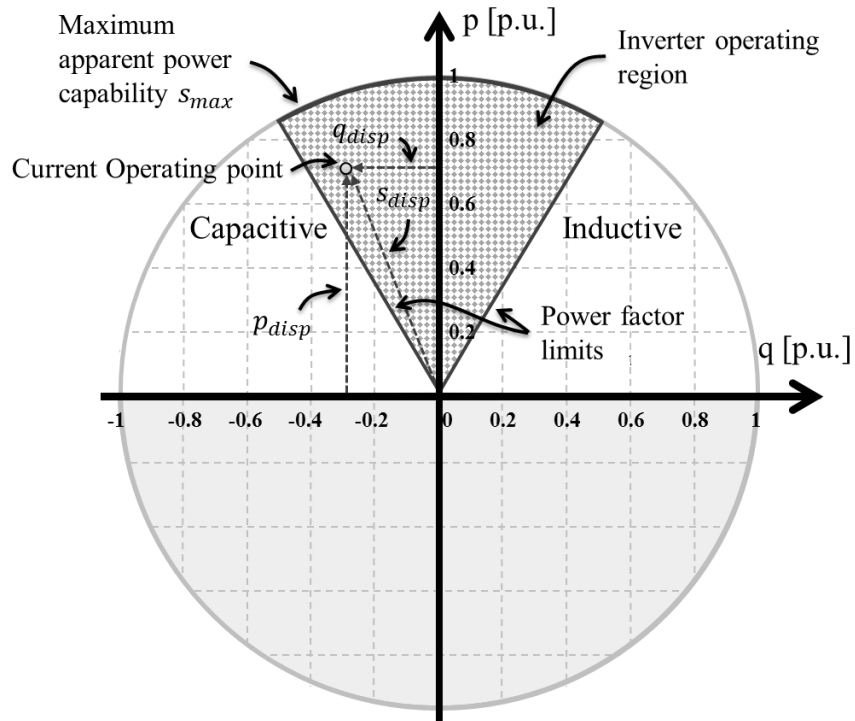


Figure 4-5 Capability curve for third generation inverters

The formulated optimization problem is subject to constraints relating to grid operation, DER capability and standards like VDE-AR-N 4105 [57] and IEEE STD 1547 [58]. Power balance constraint ensures that sum of power generated is equal to the sum power consumed plus the sum of losses in each branch. Inverter apparent output power is limited by its design and rating. This can be added as an inequality constraint so that inverter output power does not exceed its rated apparent power. The German grid integration standard requires DERs to support power factors of 0.9 in MV and LV networks [57]. This power factor requirement visually shown in Figure 4-5 can be added as a constraint to the overall optimization problem. Power factor constraint can be translated into reactive power constraint using the equation $\pm \sin[\cos^{-1}(PF)] \cdot S_{G_i}$, where PF is the power factor limit and S_{G_i} is the current apparent power output of the i^{th} inverter. Thermal ratings of lines and equipment such as transformers should not be exceeded as it adversely affect their performance and lifespan. This is formulated as the final inequality constraint in Eqn. (29). The overall problem can be formulated in the form

$$\text{Minimize } F(Q_{g_i}) = P_{loss} + e^{\zeta(u^{uv} + u^{lv})} \quad (28)$$

Subject to constraints

$$\sum_{i=1}^K S_{G_i} = \sum_{i=1}^L S_{D_i} + \sum_{i=1}^M S_{loss_i} \quad (29)$$

$$Q_{G_i}^l \leq Q_{G_i} \leq Q_{G_i}^u$$

$$PF \geq PF_{min}$$

$$S_{tr.} \geq S_{tr.}^u.$$

Where K is the number of DERs in the network, L is the number of loads connected in the network and M is the total number of branches. S_{G_i} is the complex power generated by i^{th} DER. S_{D_i} is the complex power demand by i^{th} load and S_{loss_i} are the losses in the i^{th} branch. $Q_{G_i}^l$ and $Q_{G_i}^u$ are the lower and upper limits for reactive power dispatch respectively. PF_{min} is the minimum permissible power factor. $S_{tr.}$ is transformer load, while $S_{tr.}^u$ is the maximum permissible transformer loading.

4.4 Study case 1: Optimal reactive power compensation

4.4.1 Test case over view

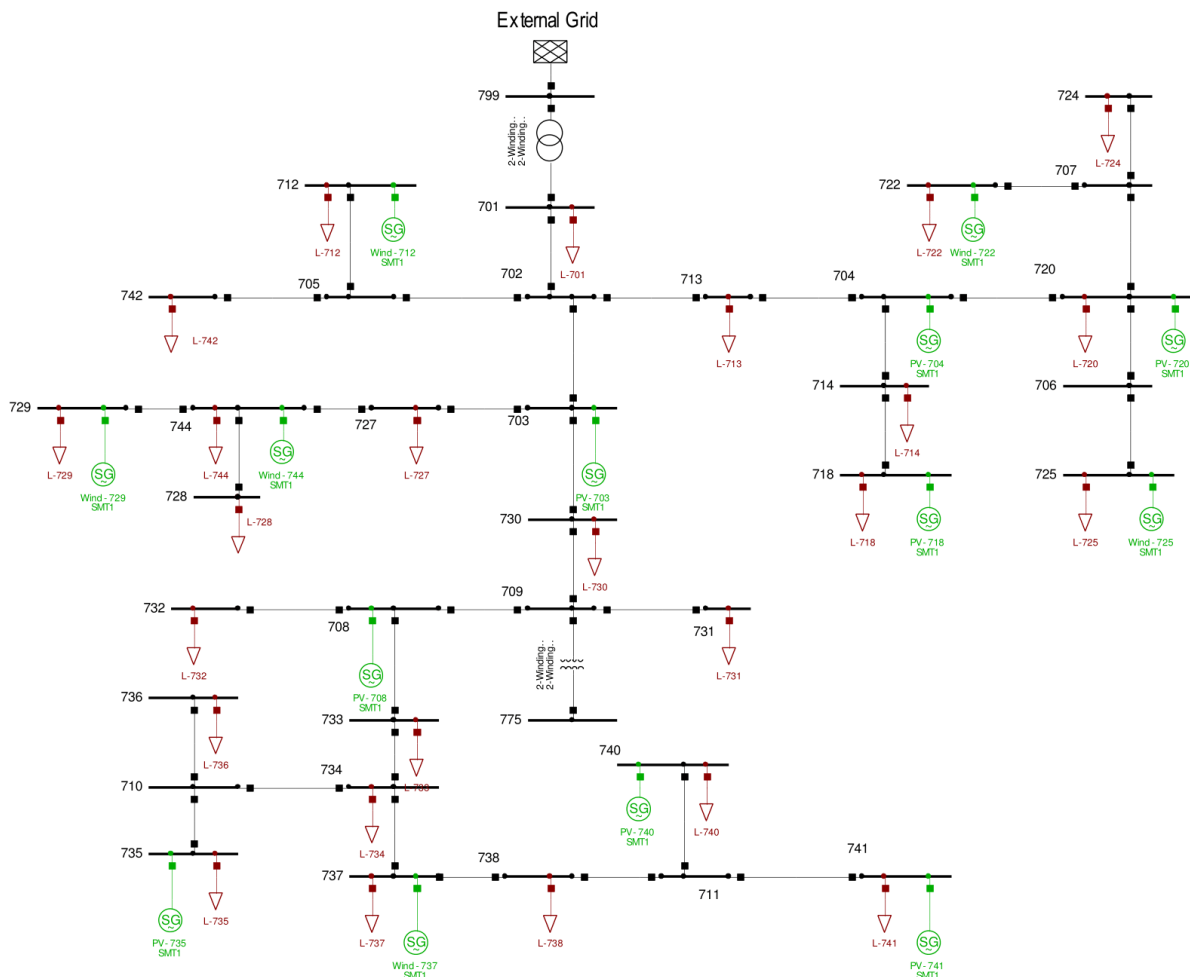


Figure 4-6 The modified IEEE 37 node test feeder

The test case chosen for conducting the simulations for the proposed method is the IEEE 37 node MV test network. In the original network, a 2.5 MVA transformer services 25 loads. Fourteen DERs consisting of eight PV systems and six wind generators have been connected at randomly selected nodes. Node ID, active power rating and DER type have been listed in Table 4-3. Figure 4-6 is a graphical representation of the modified IEEE 37 node test feeder.

Rating MW	Node ID	Type	Rating MW	Node ID	Type
0.40	703	PV	0.60	741	PV
0.51	704	PV	0.39	712	Wind
0.67	708	PV	0.40	722	Wind
0.68	718	PV	0.34	725	Wind
0.59	720	PV	0.44	729	Wind
0.52	735	PV	0.30	737	Wind
0.63	740	PV	0.37	744	Wind

Table 4-3 Rated power, Node ID and type of the distributed generator

For the purpose of simulation normalized real 15 minute average load, PV generation and wind generation profiles have been used [137] [138]. Each load has randomly been assigned either a residential or a commercial load profile. Simulations have been run for a sunny day with significant wind generation only in the second half of the day. Table 4-4 provides the parameter values used for the simulation results obtained in Section 4.5.

Parameter	f^l	f^u	A^0	r^0	N	t_{max}
Value	-0.1	0.1	10	0.3	30	30

Parameter	G	H	α	Υ	Z	$C_{1,2,3,4}$
Value	5	15	0.9	0.9	10	[2,1,1,1]

Table 4-4 Values of parameters used for the simulations

The proposed method has been implemented by coupling Python [139], a powerful open source scripting language with a large number of multi domain libraries, and DIgSILENT PowerFactory [140], a domain specific tool for power systems simulation. An instance of PowerFactory is created from a Python script using the Python API provided by DIgSILENT. The IEEE 37 node test feeder has been implemented in PowerFactory, while the MHBA has been implemented in Python. PowerFactory is additionally used as a load flow engine to calculate the fitness value of a solution generated by MHBA.

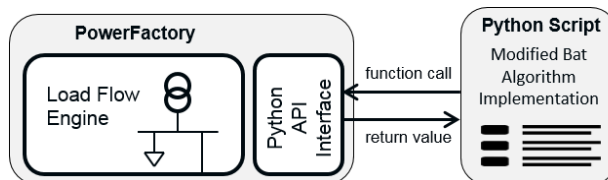


Figure 4-7 Graphical illustration of PowerFactory and Python coupling scheme

4.4.2 Control Implementation

For purpose of comparison, simulations have been conducted for five different inverter based reactive power facilitated voltage control schemes. Three of the simulated voltage control scheme namely, fixed power factor, variable power factor and Volt/VAR control, are local control schemes. These rely on local information like and voltage at the PCC, and do not require an external control loop or exchange of information.

For fixed power factor simulation, all inverters connected to the network operate at a fixed power factor of 0.9 lagging (inductive). In the variable power factor experiment, inverters operate at unity power factor up to 50% of the of the inverters rated power. The power factor then decreases linearly and at maximum inverter output the power factor reduces to minimum permissible value of 0.9 (lagging). For final local control implementation, Volt/VAR control has been simulated with 10% droop gradient with no voltage dead band.

In the next experiment, the proposed reactive power dispatch method has been implemented in a centralized and decentralized manner. In the centralized implementation of the proposed method, one controller gathers information from all the inverters connected in the network. The optimization algorithm is then run, after which, new set points for reactive power are dispatched to the inverters. It is important to note that the proposed method runs load flow repeatedly during the optimization process which means, it is assumed that network topology and location of the inverters is known.

For the final experiment, the network has been divided into zones using the reactive power / voltage sensitivity matrix and the distance matrix. Each zone has a controller responsible for coordination of reactive power dispatch via inverters connected within the zone. Each controller has access to information relayed by inverters connected within the zone. This means each zone controller works independently from one another and do not exchange information.

Decentralized implementation has several advantages over centralized implementation.

- **Resilient to single point failure** – Centralized systems are prone to single point failure, that is, if the central controller fails the entire system fails. Traditionally, redundant communication channels, sensors and other auxiliary equipment have been used by TSOs at the HV level. Decentralized control is much more robust against single point failure as part of the systems keeps working even if one zone controller stops working.
- **Supports deregulation** – In recent years, many countries in the world have been moving from regulated towards deregulated energy markets. It is therefore important that any new technology introduced should be able to support deregulation. Unlike centralized control, decentralized control implementation fully supports deregulation as each controller is responsible for its own zone and runs independently.
- **Scalable** – Increasing the size of the distribution network increases the complexity of centralized implementation. This is because in centralized implementation, the controller

is required to communicate with all the inverters connected within the network. This makes scalability an issue for centralized control schemes. Decentralized implementation of voltage control scheme are highly scalable as large networks can be divided into zones each with its own dedicated controller responsible for coordinating the action of local resources.

- **Improved algorithm convergence** – As already discussed, population based meta-heuristic algorithms suffer from the ‘curse of dimensionality’, that is, increase in the dimension of the problem results in an explosion of search space. For very large networks, centralized implementation using meta-heuristic based optimization algorithm might not even be feasible. Decentralized implementation reduces the dimension of the problem by dividing a global objective into a number of zonal objectives resulting in reduced search space and improved convergence.
- **Local resolution of a local problem** – Unlike the power loss objective, voltage violation is a local phenomenon and should ideally be catered to using local resources. A color plot of the du/dQ matrix in Figure 4-8 shows that reactive power absorption only at nodes in close proximity to the node experiencing voltage violation have a significant impact its voltage. Decentralized voltage control scheme therefore allows local resolution of a local problem.
- **Requires less information exchange** – As coordination based control schemes require communication, large amount of data exchange in real time can result in delays resulting in control action lagging behind current state of the network. Decentralized implementation requires communication with inverters installed within a zone instead of the entire distribution network, hence information exchange is reduced.

There are two drawback of the decentralized over centralized implementation that require a mention.

- **Conflicting objectives** – First, as each zone controller has knowledge of zonal information, a scenario might occur where neighboring zones might be optimizing conflicting objectives and inadvertently deteriorate the performance of the coordinating control scheme.
- **Convergence to local optimum** – Secondly, each zone controller converges to a local optimum as it only has zone’s information. For a convex problem, local optimum is also the global optimum. For non-convex problems however the local optimum might differ from global optimum resulting in reduced performance when compared with results obtained from centralized implementation.

4.4.3 Zone creation using visual approximation

To overcome the problems associated with centralized control paradigm discussed in the previous subsection, decentralized implementation of the proposed method has been carried out. Moving from a centralized control paradigm to decentralized control paradigm requires dividing the network into autonomous self-governing regions referred to as zones in this work. The simplest way of dividing the network into zones is by developing a visual representation of the normalized distance matrix using the du/dQ matrix and grouping the nodes using visual inference. For large networks, visual inference can be tedious and error prone. In such a case, clustering techniques can be used for automated zone creation. A number of researchers have worked on the development such algorithms. In [141] Satsangi et al. have proposed using K-means clustering based approach to define voltage control regions for efficient reactive power management. Similarly in [142], Bahramipناه et al. have proposed two clustering based zoning algorithms that have been tested on the IEEE 13 node test feeder and the IEEE 123 node test feeder. In this work clustering based zoning has been used to define zones within the chosen network.

The Jacobean matrix is a set of linear equations that provides a linear approximation of the system. Load flow algorithms like Newton-Raphson algorithm use the Jacobean matrix to calculate the state of the system. In power system, the Jacobean matrix consists of four sub matrices. The fourth submatrix commonly referred to as J_4 is real and unsymmetrical. The inverse of J_4 is used to calculate the sensitivity matrix, which is also real and asymmetrical. The sensitivity matrix reflects the sensitivity of a node's voltage to change in reactive power in any node in the network. The extent of voltage coupling between any two nodes in a network can be quantified by the maximum change in voltage variation between two nodes. Electrical distance is a symmetric matrix and to obtain a symmetric matrix from the asymmetrical attenuation matrix mirror elements of the attenuation matrix are multiplied before the logarithmic operation is performed. In the final step, the distance matrix is normalized [143]. The process is as follows.

1. Calculate the Jacobian matrix and use it to obtain the $\partial Q/\partial u$ matrix.

$$\begin{bmatrix} \Delta P \\ \Delta Q \end{bmatrix} = \begin{bmatrix} \frac{\partial P}{\partial \delta} & \frac{\partial P}{\partial u} \\ \frac{\partial Q}{\partial \delta} & \frac{\partial Q}{\partial u} \end{bmatrix} \begin{bmatrix} \Delta \delta \\ \Delta u \end{bmatrix} \quad (30)$$

$$J_4 = \frac{\partial Q}{\partial u} \quad (31)$$

2. Calculate the sensitivity matrix B by calculating the inverse of J_4 .

$$B = J_4^{-1} = \frac{\partial u}{\partial Q} \text{ where } b_{ij} = \frac{\partial u_i}{\partial Q_j} \quad (32)$$

3. Calculate the attenuation matrix α by dividing the non-diagonal elements by the diagonal elements using the following equation.

$$\alpha_{ij} = b_{ij} / b_{jj} \quad (33)$$

4. Calculate the electrical distance using Eqn. (34) and obtain the normalized distance matrix using Eqn. (35).

$$D_{ij} = - \log(\alpha_{ij} \cdot \alpha_{ji}) \quad (34)$$

$$D_{ij}^{norm} = D_{ij} / \max(D_i) \quad (35)$$

The figure below shows the color map of the sensitivity matrix $(\partial u / \partial Q)$ for the IEEE 37 node test feeder. Figure 4-9 shows the color map of the normalized distance matrix. Nodes with tight voltage coupling are clearly visibly.

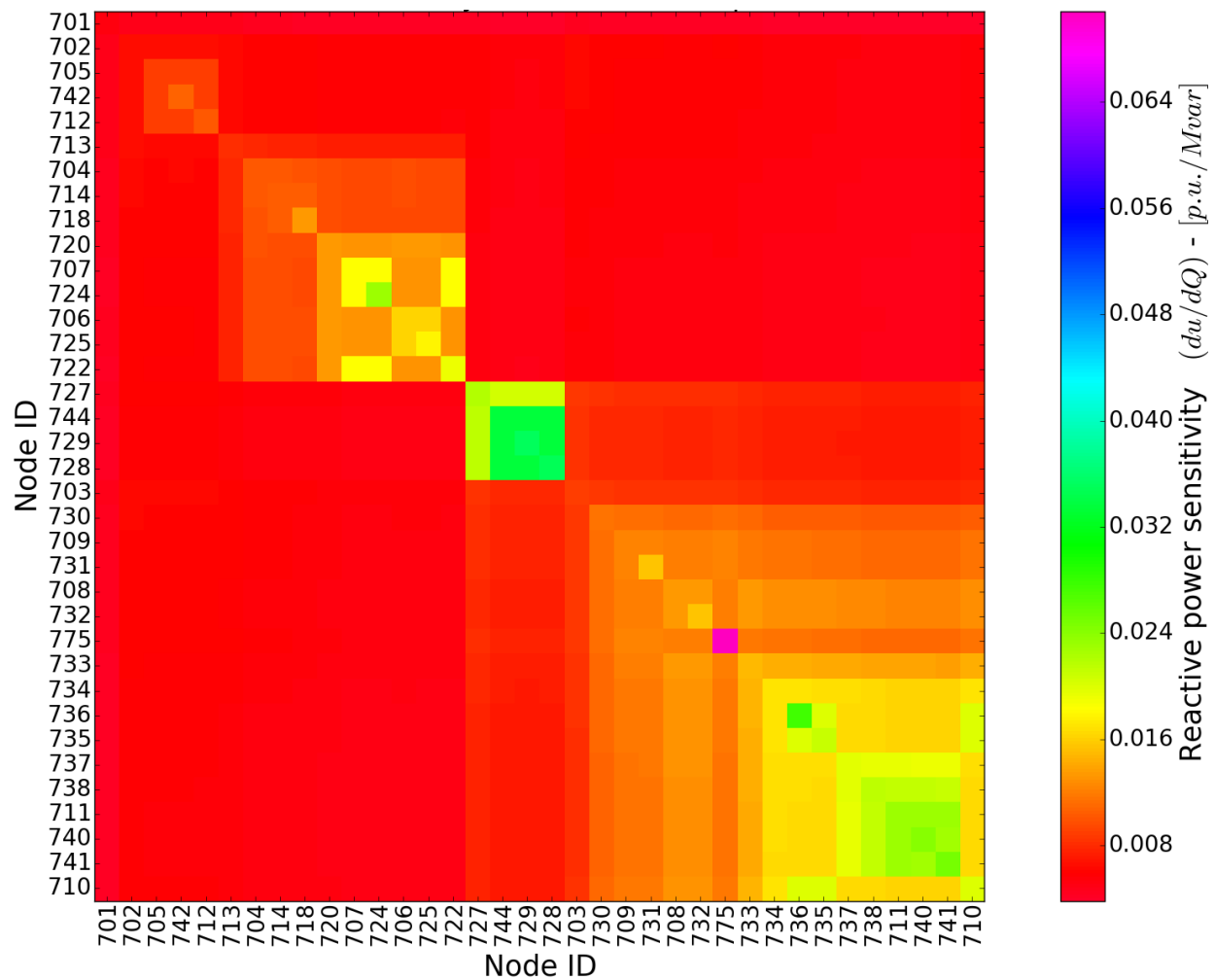


Figure 4-8 Color plot of the reactive power sensitivity matrix for the IEEE 37 node test feeder

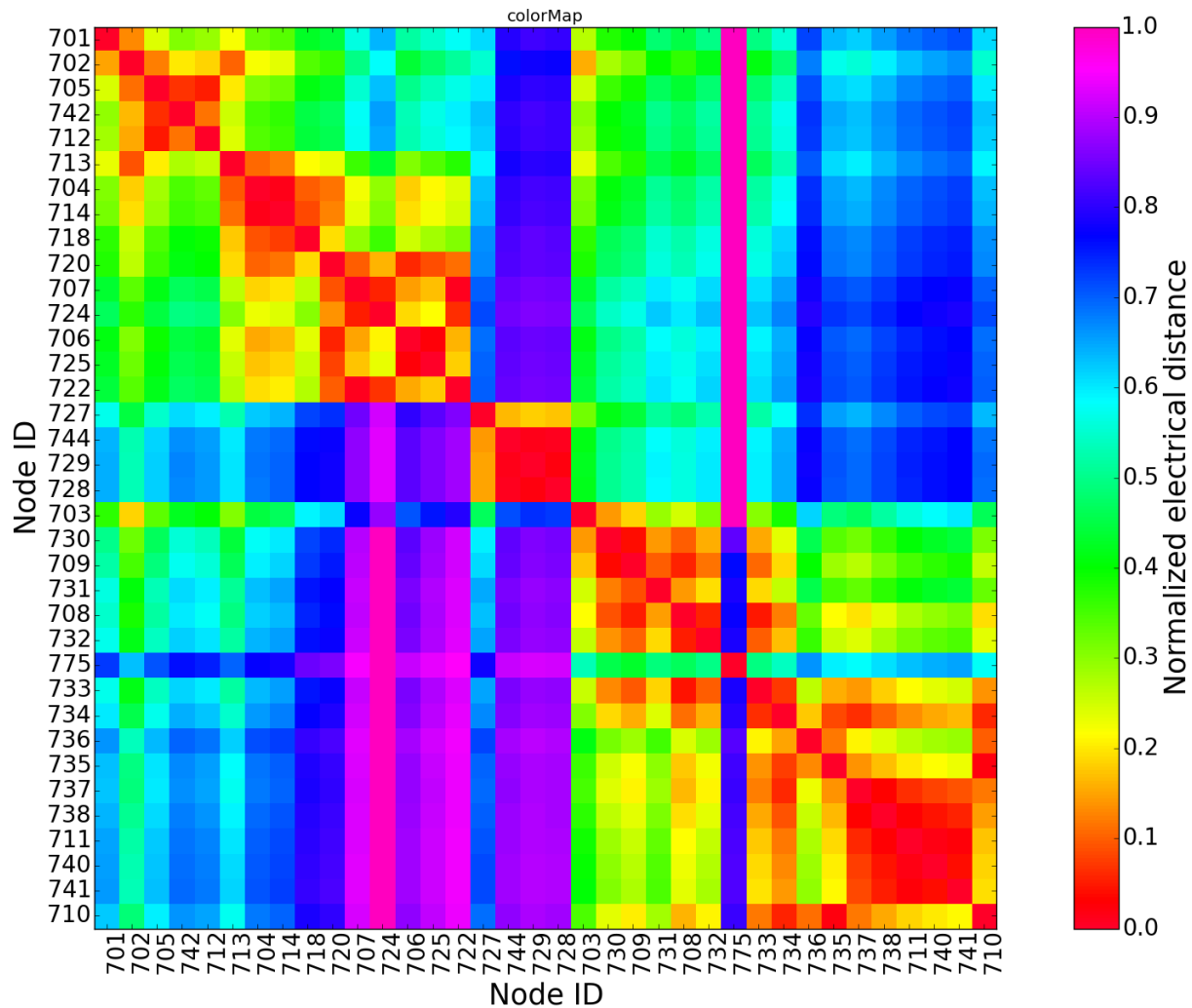


Figure 4-9 Color plot of the normalized electrical distance matrix for the IEEE 37 node test feeder

Once the normalized distance matrix has been calculated, either visual inference or a clustering method can be employed to create autonomous, independent zones within a network. As already mentioned, for large networks, zone allocation using visual inference can be tedious and error prone. In this work, ward linkage based hierarchical agglomerative clustering method has been employed for zone creation.

Hierarchical agglomerative clustering is an iterative clustering algorithm that creates a hierarchy of clusters following a bottom-up approach. Initially n clusters are created, (where n is the number of elements that need to be clustered) each containing only one element. Clusters are then iteratively combined until finally only one cluster remains containing all elements. In order to decide which two clusters should combine each iteration, a measure of dissimilarity is used. Of the remaining clusters, two the least dissimilar to one another are combined at each step. The dissimilarity measure can be calculated by choosing a linkage method most suit for the problem.

In this work ward linkage has been used. Other commonly used linkage methods are single linkage, complete linkage, average linkage and centroid linkage.

Ward minimum variance method aims at minimizing variance within clusters. The variance is calculated by adding the sum of squares over all variables belonging to the two clusters. The two clusters with least variance are selected each iteration. The distance between the two clusters is defined by,

$$d(C_x, C_y) = \|C_x - C_y\|^2 \quad (36)$$

Where C_x, C_y are two predefined clusters. Algorithm 4-2 presents the pseudo code for hierarchical agglomerative clustering with ward linkage.

Algorithm 4-2 Pseudo code for hierarchical agglomerative clustering with ward linkage

```

1  Input: An  $n \times n$  distance matrix  $D$  (also known as proximity matrix)
2  Begin with  $n$  clusters, each with only one object having both sequence number  $k$  and level
    $L(k)$  equal to zero
3  While Number of clusters  $\neq 1$  do
4      Find the least dissimilar pair of cluster  $C_a, C_b$  where  $a, b \in [1, \dots, n]$  according to
       ward linkage criterion
5      Increment the sequence number  $k = k + 1$ . Merge clusters  $C_a, C_b$  into a single
       cluster. Set the level of clustering  $L(k) = d(C_a, C_b)$ 
6      Update the normalized distance matrix
7      Delete the rows and columns corresponding to  $C_a, C_b$ 
8      Add row and column corresponding to newly formed cluster  $C_{a+b}$ , calculated
       using the equation  $d[C_o, C_{a+b}] = \min(d(C_o, C_a), d(C_o, C_b))$ 
9  Output: dendrogram and scree plot

```

In this work, a python script has been used to export network sensitivity matrix to Python using the API provided by DIgSILENT PowerFactory. Distance matrix has been obtained using the four steps listed in this section. Finally, Scipy's hierarchical clustering library for Python has been used to obtain the dendrogram presented in Figure 4-10. Ward linkage has been chosen so that clusters created have tight coupling and voltage dependency. The aim is to form clusters with high voltage interdependency for efficient use of reactive power resources.

It should be noted that hierarchical agglomerative clustering produces a hierarchy of clusters and there is no exact method to decide upon the best number of clusters. Ideally, a scree plot (Figure 4-11) starts off with steep curve, followed by a bend (aka. knee point) and finally a straight line. In literature it has been suggested to use the knee point as the reference for ideal number of cluster. Using only knee point information might not be enough and system knowledge and experience might be required to choose ideal number of zones.

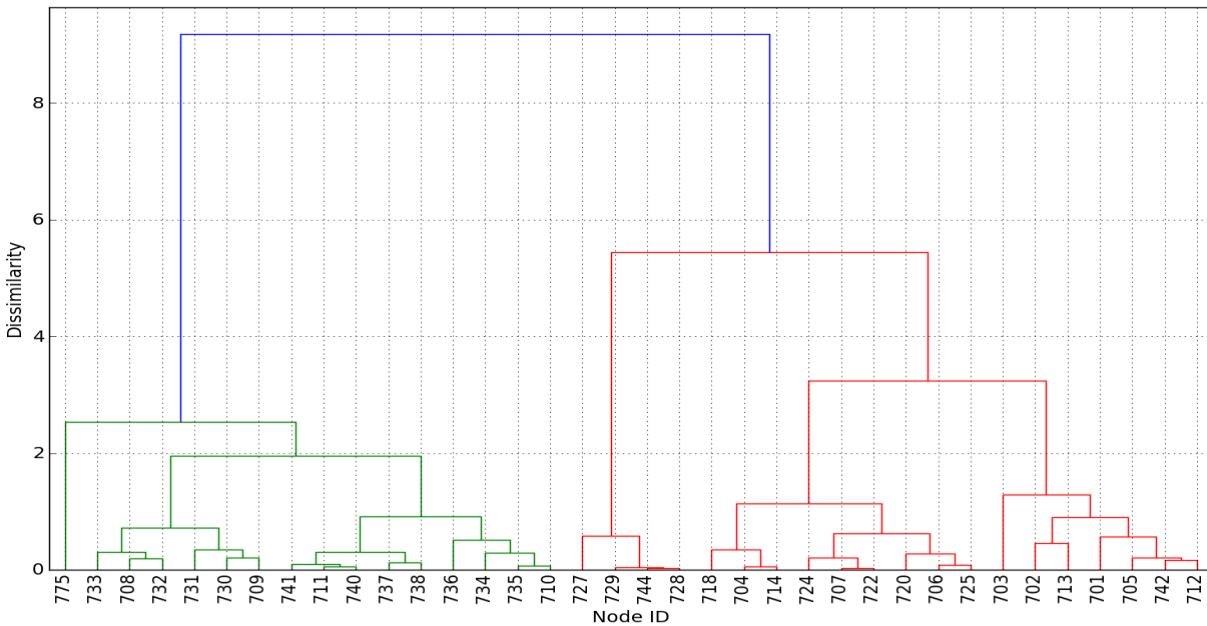


Figure 4-10 Dendrogram for clusters produced using ward linkage based agglomerative hierarchical clustering

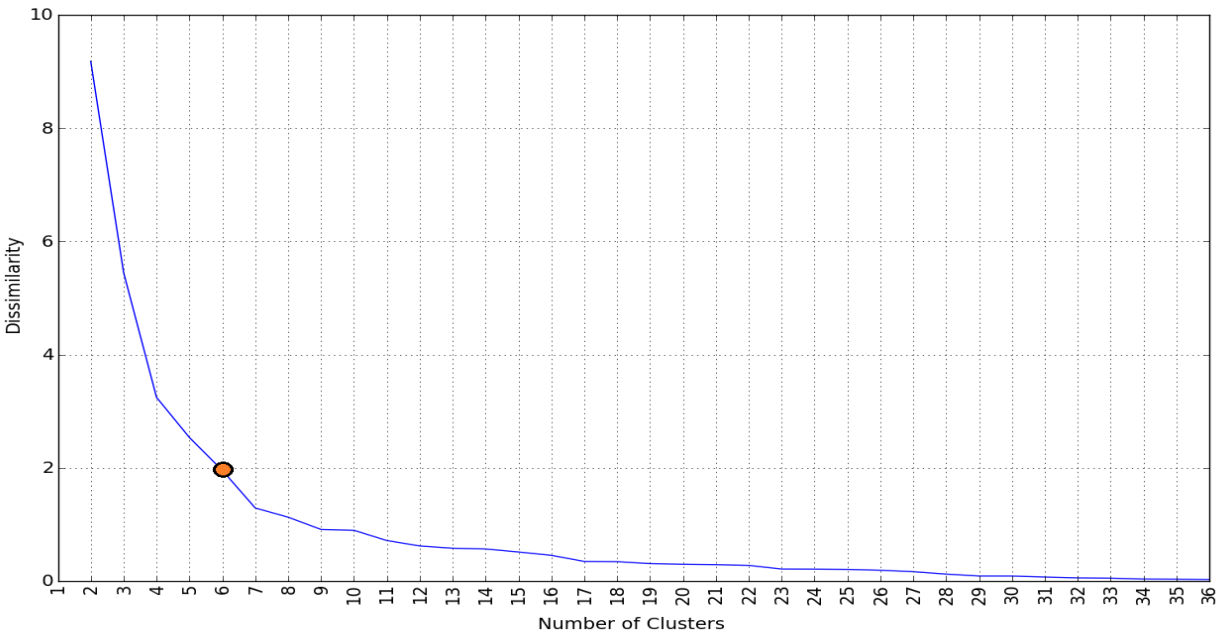


Figure 4-11 Scree plot for the dendrogram

From the dendrogram above, at dissimilarity equal to 2, six tight clusters are clearly visible. The knee point in the Scree plot also occurs at $k = 6$, which makes six clusters a good choice for the number of clusters. Node 775 however has been identified as a cluster containing a single element. One criterion for an acceptable zone is that it should contain at least one node connected to a DER; otherwise, parts of the network would be unregulated due to lack of controllable devices.

Optimal reactive power in distribution networks

For this reason in this work node 775 has been grouped with the neighboring zone. Table 4-5 shows the nodes clustered in each zone.

Zone 0	Zone 1	Zone 2	Zone 3	Zone 4
708	710	727	704	701
709	711	728	706	702
730	734	729	707	703
731	735	744	714	705
732	736		718	712
733	737		720	713
775	738		722	742
	740		724	
	741		725	

Table 4-5 List of nodes grouped in a cluster using hierarchical clustering

Figure 4-12 gives a graphical overview of the zones created for the IEEE 37 node MV test feeder.

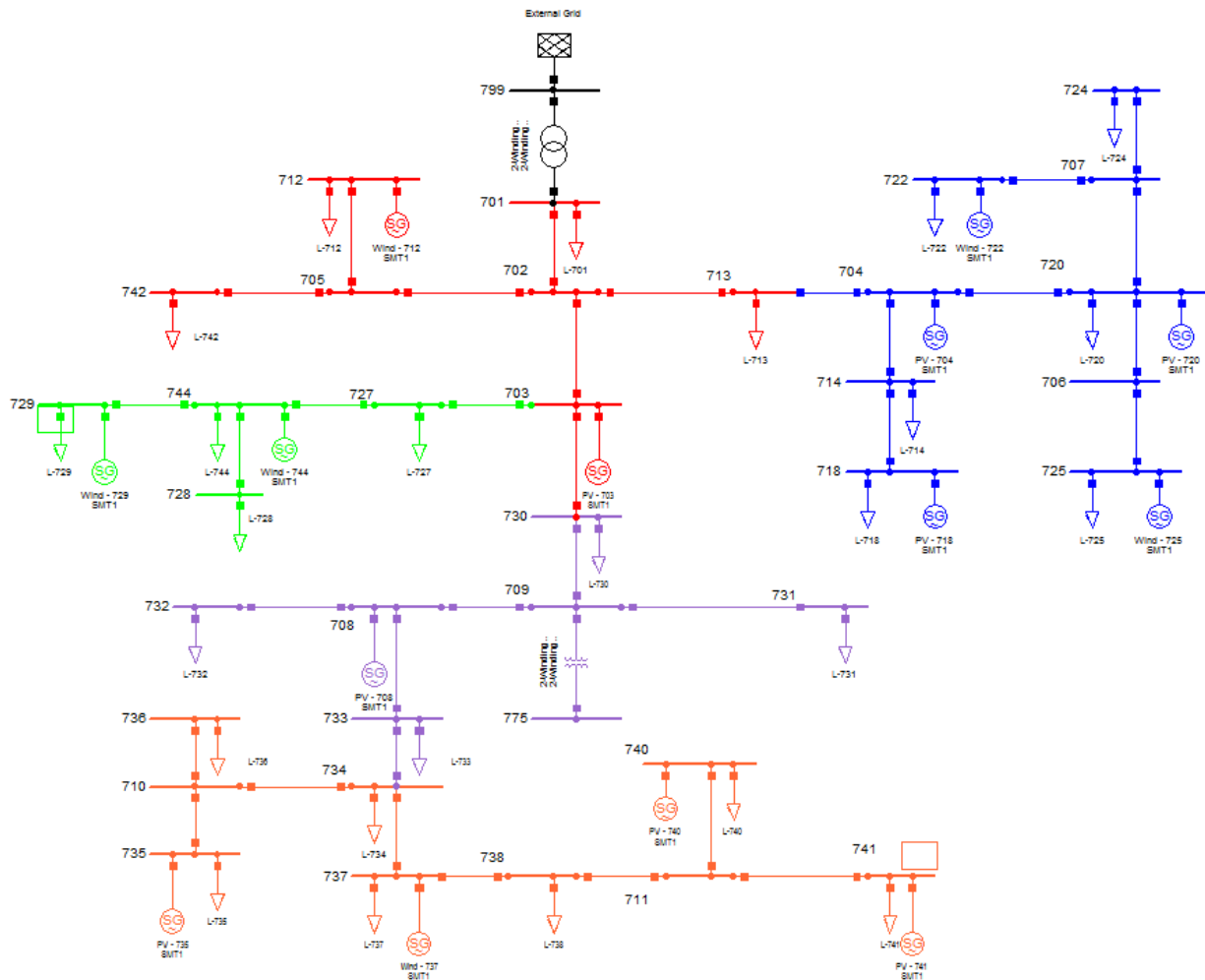


Figure 4-12 Graphical illustration of the zones created using agglomerative hierarchical clustering

4.4.4 Flowchart for the proposed method

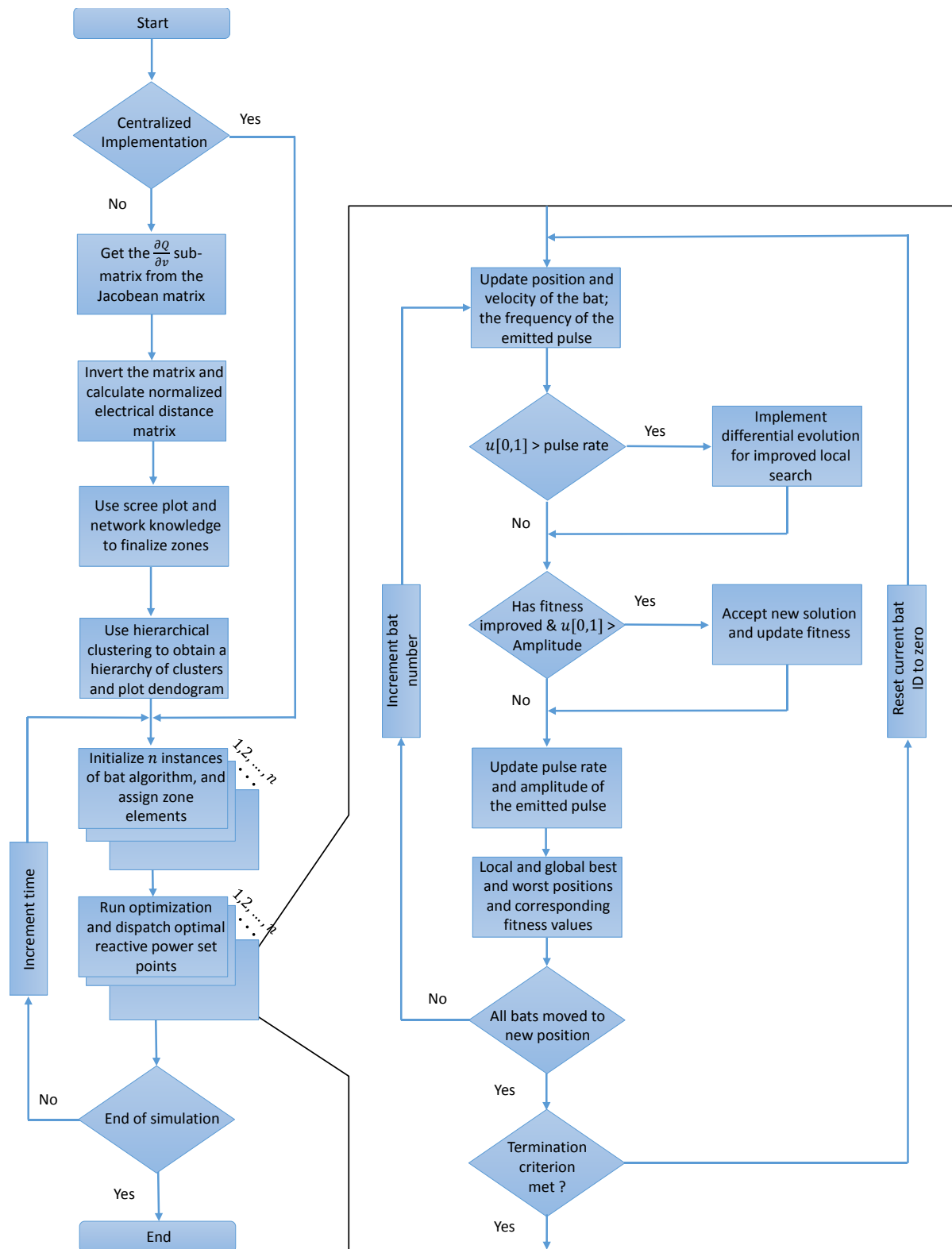


Figure 4-13 Flow chart for the proposed coordinated RPC method

4.5 Results and discussion

In this section simulation results for five methods of reactive power compensation covered in Section 4.4.2 have been presented and discussed in detail.

4.5.1 Constant power factor

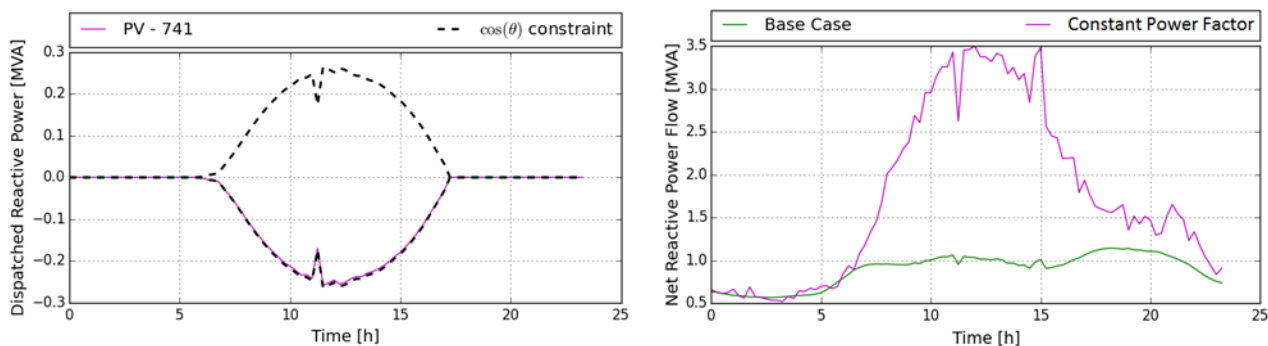


Figure 4-14 Dispatched reactive power set points for PV 741; and net reactive power flow from the external grid

In a constant power factor based reactive power compensation scheme, the reactive power follows the active power output of the inverter. In Figure 4-14-a the dashed black lines represent power factor limit of 0.9 leading and lagging. Each DER installed in the network is operating at a fixed power factor of 0.9 lagging (inductive). Figure 4-14-b shows that during mid-day as PV active power output increases, so does reactive power consumption. This results in increase (over 300%) in net reactive power flowing from the external grid. As reactive power is the function of active power output, lack of PV generation during nighttime results in comparable net reactive power flow during this time.

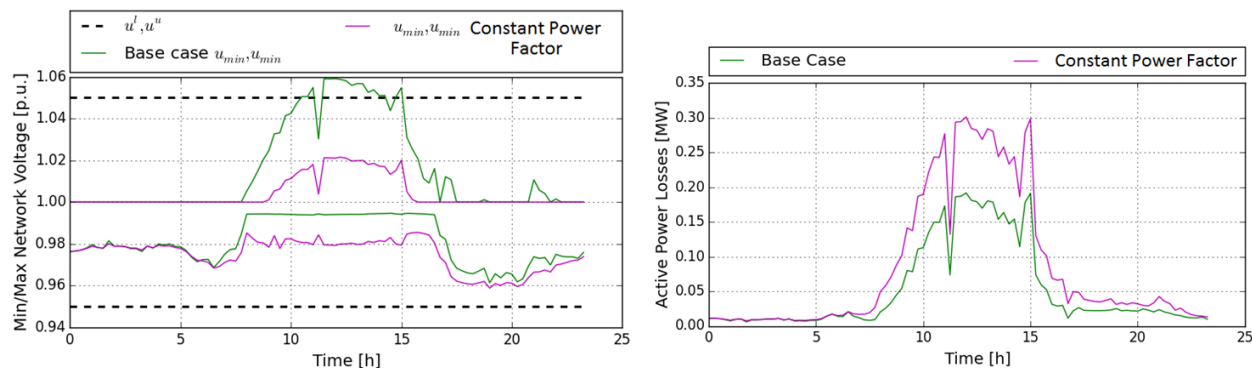


Figure 4-15 Minimum and maximum voltage seen in the network; and active power losses profiles

Increase in local reactive power consumption during times of peak generation results in a significant decrease (0.04 p.u.) in maximum network voltage, as is visible in Figure 4-15-a. Fixed power factor control however, is an inefficient RPC method as it does not take into account the current state of the network. Increased inflow of reactive power from the external grid causes line congestion resulting in increase in current magnitude. As both active and reactive power losses are

a function of the magnitude of current, they both increase. Figure 4-15-b shows that active power losses can increase as much as 65% for the chosen test case, compared to the base case.

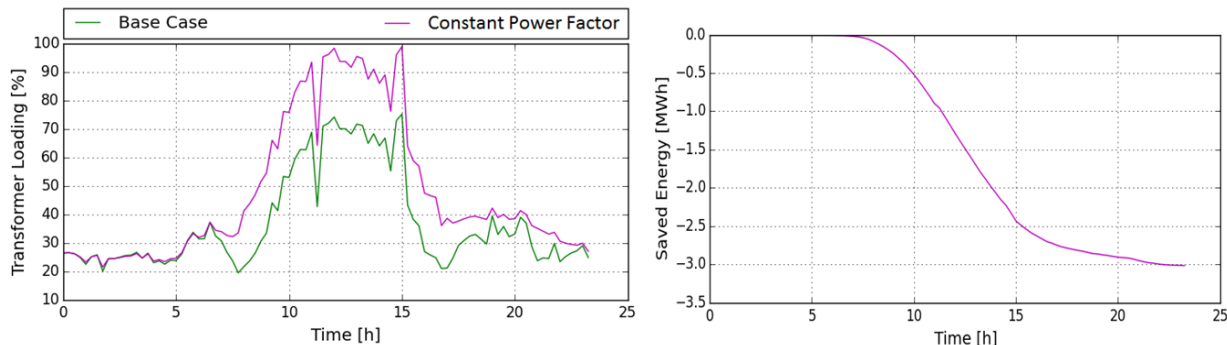


Figure 4-16 Transformer loading profiles; and saved energy profile

Increase in the magnitude of current resulting inefficient reactive power compensation can also lead to increase in transformer loading (Figure 4-16-a). Increase in transformer loading leads added stress on the insulation of the winding, reducing the useful life of the transformer. In worst case scenario this can lead to insulation failure and local blackout. In this test case, maximum transformer loading increase of about 25% was observed. Finally, inefficient RPC leads to increases system losses and reduced efficiency. For fixed power factor method, it was observed that total additional energy lost compared to base case during the days was about 3 MWh.

4.5.2 Variable power factor

In a constant power factor based reactive power compensation scheme, inverter output maintains unity power factor as long as inverter output is less than a predefined percentage of its rated output. Once inverter output exceeds the predefined value, power factor decreases linearly until it reaches the minimum permissible value (in this case 0.9 lagging). Each DER installed in the network is operating variable power factor. Comparing Figure 4-17-a with Figure 4-14-a it can be seen that minimum reactive power is reached only when inverter output is maximum. This method of RPC is much more efficient compared to the fixed power factor method. Using variable power factor based RPC reduced average reactive power inflow during the day, however, peak reactive power inflow remains the same.

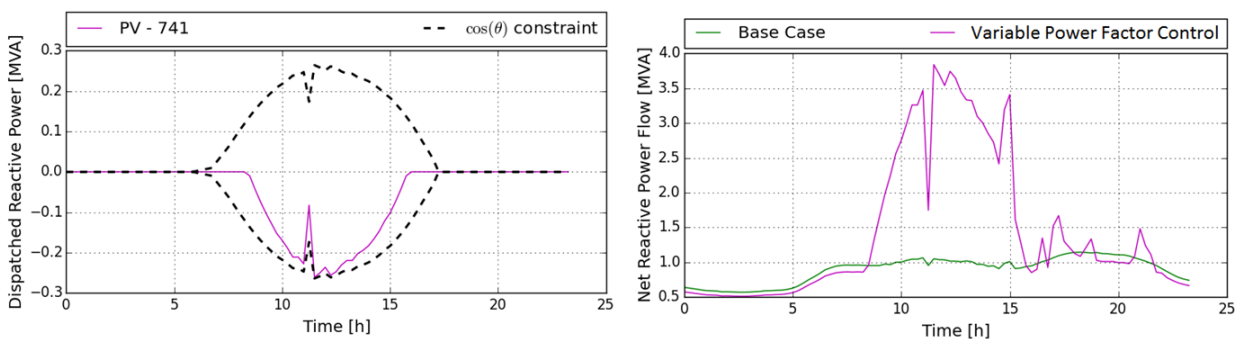


Figure 4-17 Dispatched reactive power for PV 741; and net reactive power flow from the external grid

The impact of variable power factor on voltage regulation is comparable to the fixed power factor method of RPC. Increase in local reactive power consumption during times of peak generation results in a significant decrease (0.04 p.u.) in maximum network voltage, as is visible in Figure 4-18-a. Variable power factor does not make use of local voltage information and can therefore perform inaccurate compensation. During the time of peak generation, the results for fixed and variable power factor control are the same as both operate at 0.9 PF lagging. For most of the day, inverter output is less than its rated values resulting in reduced reactive power consumption. This results in reduction in average active power losses, even though the peak power loss is the same as the first scenario.

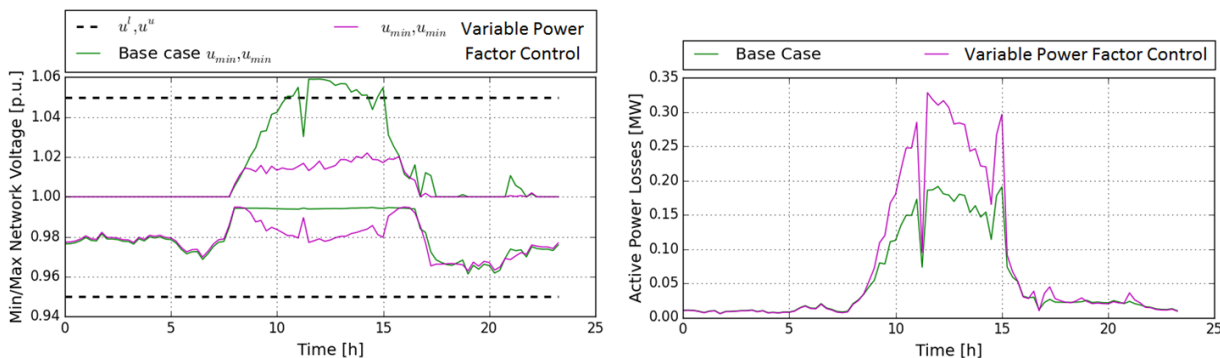


Figure 4-18 Minimum and maximum voltage seen in the network; and active power losses profiles

Peak transformer loading for this case is also approximately 100%. This is an increase of about 25% compared to the base case. For the variable power factor method, it was observed that total additional energy lost compared to base case during the days was about 2.25 MWh. This is reduction of 25% compared to the fixed power factor method. Transformers thermal constraint is the DER hosting limiting factor for the given network if either FPF or VPF method of RPC is used.

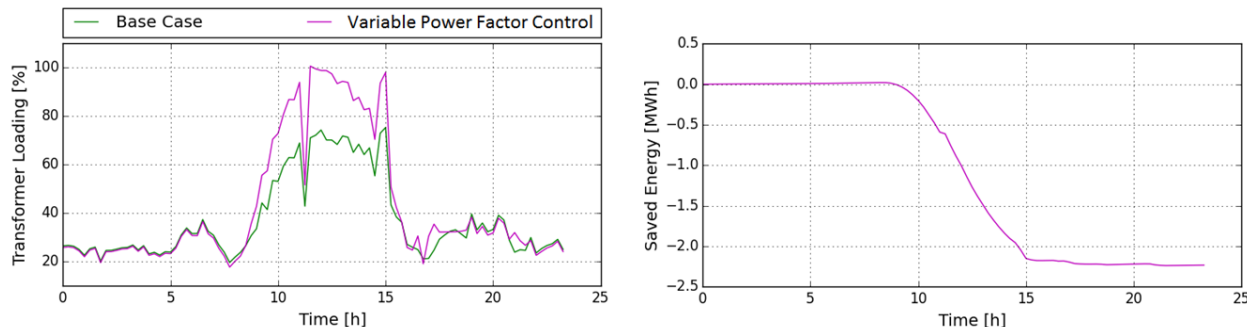


Figure 4-19 Transformer loading profiles; and saved energy profile

4.5.3 Volt/VAR control

In Volt/VAR control (VVC), inverters reactive power is a function of the voltage at the point of common coupling and not the active power output. This can lead to violation of the power factor constraint as can be seen from Figure 4-20-a. In this experiment, the reactive power output has a linear relation to the voltage and no voltage dead band has been used. Before

7 am, voltage at all nodes is less than 1 p.u. this causes inverters to supply reactive power locally resulting in reduction in net reactive power import from the external grid. During times of peak generation (between 7 am and 5 pm when both wind and PV generators are supplying local power) the voltage at most nodes in the network exceeds 1 p.u. causing inverters to absorb reactive power. This causes net reactive power inflow from the external grid to increase (Figure 4-20-b).

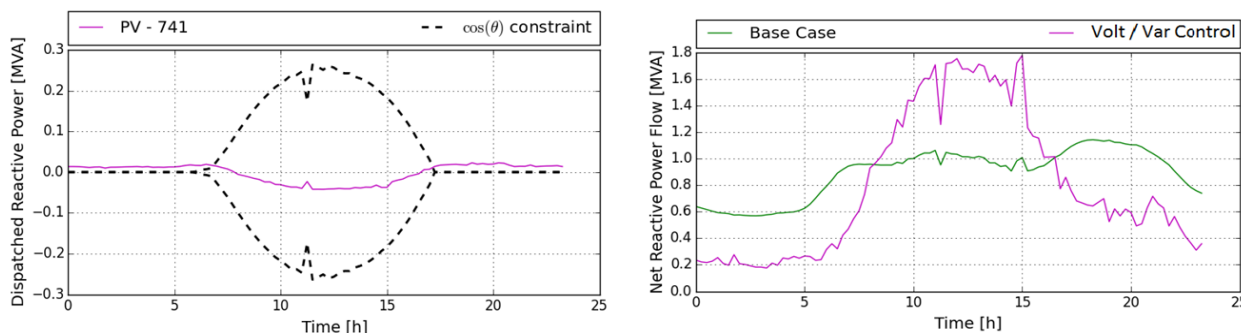


Figure 4-20 Dispatched reactive power for PV 741; and net reactive power flow from the external grid

The impact of VVC on voltage regulation is can be seen in Figure 4-21-a. Injection of reactive power before 7 am and after 5 pm causes the voltage to rise, however during times of peak generation; VVC was able to regulate voltage within prescribed limits reducing the voltage by 0.013 p.u. at time of peak generation. Injection of local reactive power resulted in net reactive power inflow leading to reduction in the magnitude of the current resulting in reduction in losses. At times of peak generation however, lagging power factor causes the losses to increase (Figure 4-21-b). The increase in active power loss however, is much lesser compared to both FPF and VPF compensation methods. The VVC method makes use of the voltage band unlike the previous two methods.

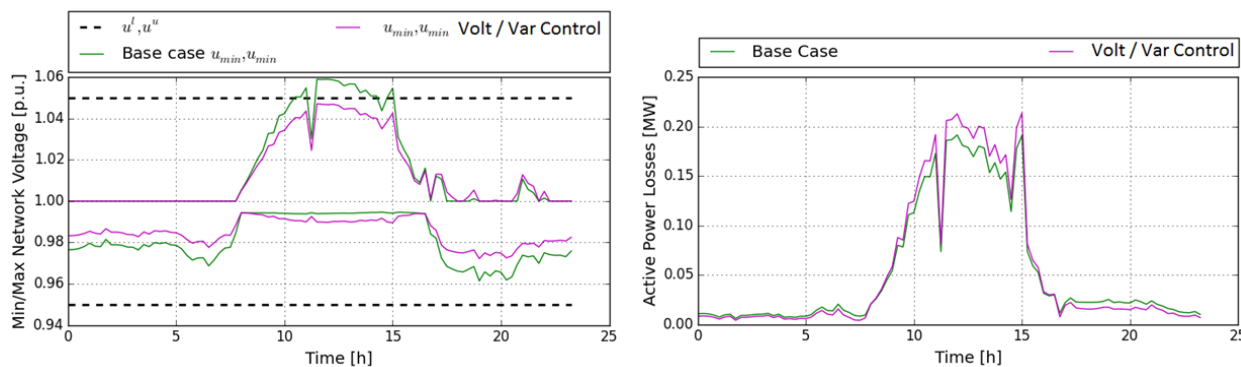


Figure 4-21 Minimum and maximum voltage seen in the network; and active power losses profiles

Reduction in magnitude of the current at morning at evening times leads to reduction in transformer loading. Even during the time of peak generation, increase in transformer loading is about 6% about 20% less either FPF or VPF. This means that using VVC can potentially reduce transformer loading thereby increasing the DER hosting capacity of the network. Although energy

is lost increases compared to base case, it is considerably lower than previously simulated RPC schemes.

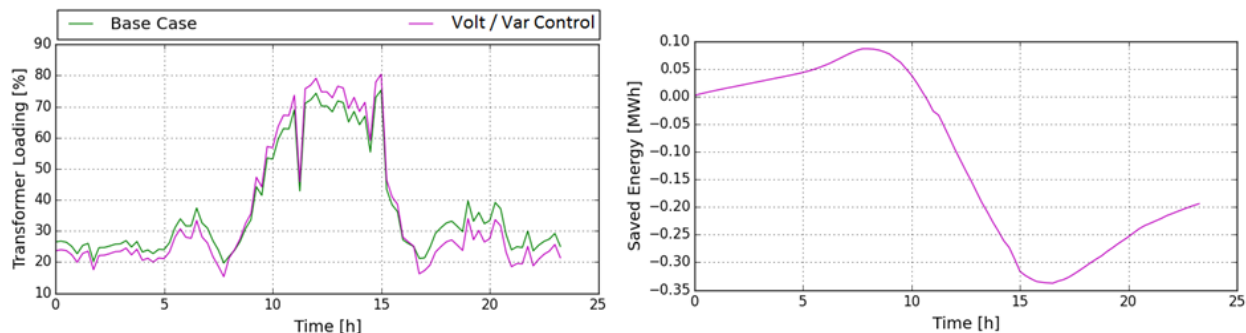


Figure 4-22 Transformer loading profiles; and saved energy profile

4.5.4 Centralized implementation

In this subsection, results for centralized implementation of the proposed method have been discussed. Figure 4-23-a shows that the power factor limits of the inverter are not violated. Instead of regulating using only local voltage information, maximum and minimum voltage seen in the network have been used for the coordination based scheme. The idea here is to efficiently use the complete voltage band.

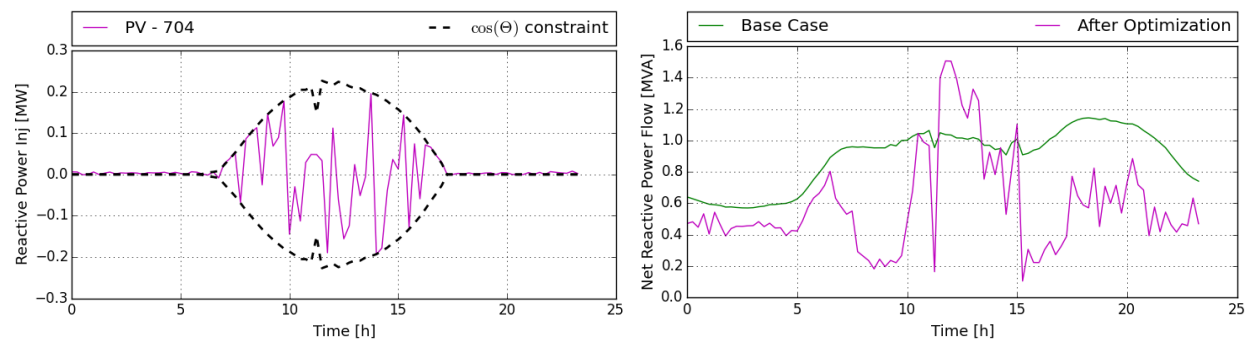


Figure 4-23 Dispatched reactive power for PV 704; and net reactive power flow from the external grid

Local supply of reactive power improves voltage. It has the added advantage of reducing net inflow of reactive power from the external grid by up to 80%. Figure 4-23-b shows this phenomenon. Reduced reactive power inflow reduces line congestion and power losses. It also leads to significant reduction in transformer loading as can be seen in Fig. 4-25-a. Before 7 am limited wind generation and no PV generation means limited reactive power dispatch capability as DERs need to operate at power factors greater than 0.9. After 3 pm increase in wind generation results in increased reactive power dispatch capability, resulting in larger reduction in active power losses and a larger voltage rise (Figures 4-24 a and b). The graph shows reduction in active power losses before, 10 am and after 3 pm. During this time there is no voltage violation hence $u^{uv}, u^{lv} = 0$ and objective function reduces to $F(Q_{g_i}) = P_{loss}$. During the same time a rise in voltage compared

to base case can be seen in Figure 4-24-a. This is due to inverters supplying reactive power acting as a capacitor, thereby, improving network power factor.

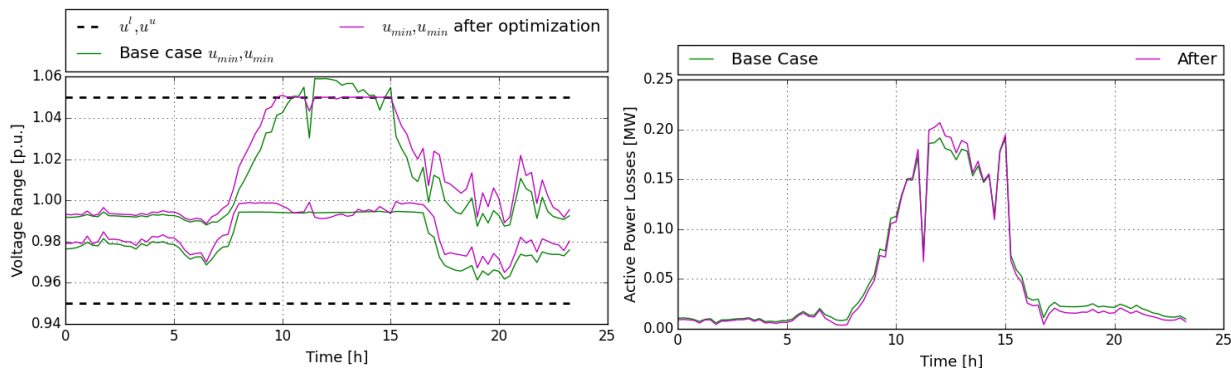


Figure 4-24 Minimum and maximum voltage seen in the network; and active power losses profiles

Increased injection of active power results in voltage violation. As the objective function is exponentially related to voltage violation functions u^{uv} and u^{lv} , even a small violation causes $e^{\zeta(u^{uv} + u^{lv})}$ to increase rapidly. As $e^{\zeta(u^{uv} + u^{lv})} \gg P_{loss}$ even for a small voltage violation, the objective function approximately reduces to $F(Q_{g_i}) = e^{\zeta(u^{uv} + u^{lv})}$.

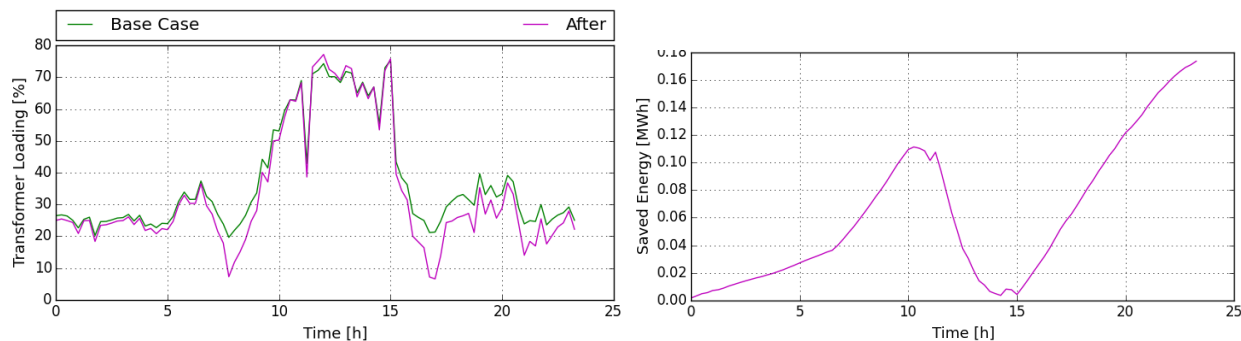


Figure 4-25 Transformer loading profiles; and saved energy profile

The proposed method is capable of regulating voltage while also improving system efficiency by reducing network losses and saving energy during a day’s operation. Unlike previous simulated RPC methods, saved energy is positive when compared to base case results. The saved energy graph dips between time 10 am and 1 pm then voltage violation objective is the dominant one.

4.5.5 Decentralized implementation

Population based meta-heuristic algorithm suffer from the ‘curse of dimensionality’. Scalability is therefore an issue and for large distribution networks with high DER penetration using meta-heuristic based optimization is not feasible. In this experiment therefore, the chosen MV distribution network node test feeder has been divided into five zones each completely autonomous and independent. The clusters have been defined on the bases of normalized electrical

distance matrix. As the zone controllers have no knowledge of the network outside zone boundary, each controller minimizes part of the global objective function. The figure below shows two PV systems located in two different zones. PV 704 is placed within a zone where over voltage is not an issue hence, it continues to operate with a leading power factor even during times over voltage is an issue within the network. PV 741 however is in zone 4 that experiences over voltage during peak generation hours. This causes the inverter to switch from leading to lagging power factor between 10 am and 3 pm.

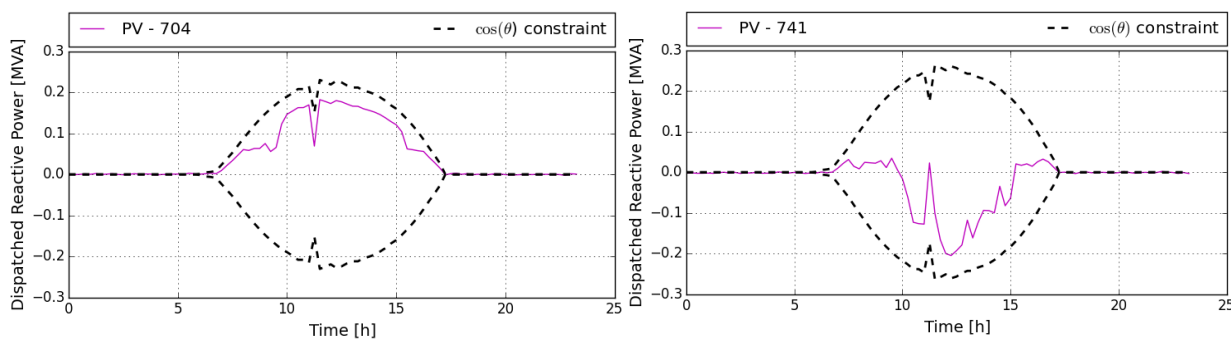


Figure 4-26 Dispatched reactive power for PV 704 and PV 741

The impact of decentralized implementation of the proposed method on net reactive power inflow from the external grid is significantly different from centralized implementation. The color plot in Figure 4-9 shows that if the electrical distance between two nodes is large change in reactive power on one node will not have a significant change in the voltage of the other node. Clusters formed using ward linkage based hierarchical clustering have high voltage dependencies hence voltage regulation using reactive power dispatch is more effective. Four of the five zones do not experience voltage violation hence, for these zones; active power loss minimization is the dominant objective. This causes DERs installed within these zones to operate at leading power factor. Zone 4 is the only zone that experiences over voltage causing DERs to operate at a lagging power factor. As most inverters are operating at leading power factor and supplying reactive power, peak reactive power inflow from the external grid is significantly less.

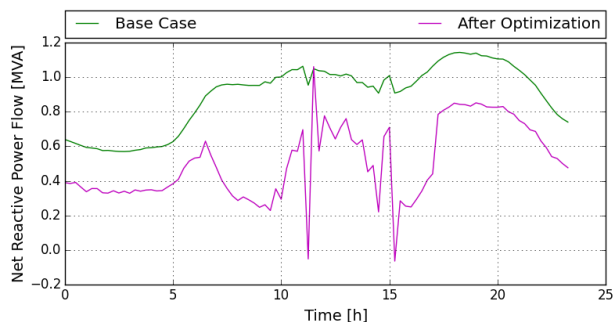


Figure 4-27 Net reactive power flow from the external grid

The decentralized implementation of coordination based RPC approach successfully maintains voltage within the prescribed limits except for a slight over voltage at noon. Probable

cause of the over voltage can be premature convergence of the heuristic algorithm. The distributed approach like the centralized approach makes efficient use of the complete voltage band. Active power losses follow a similar pattern with losses decreasing during times of low DER generation and increasing during times of high DER generation.

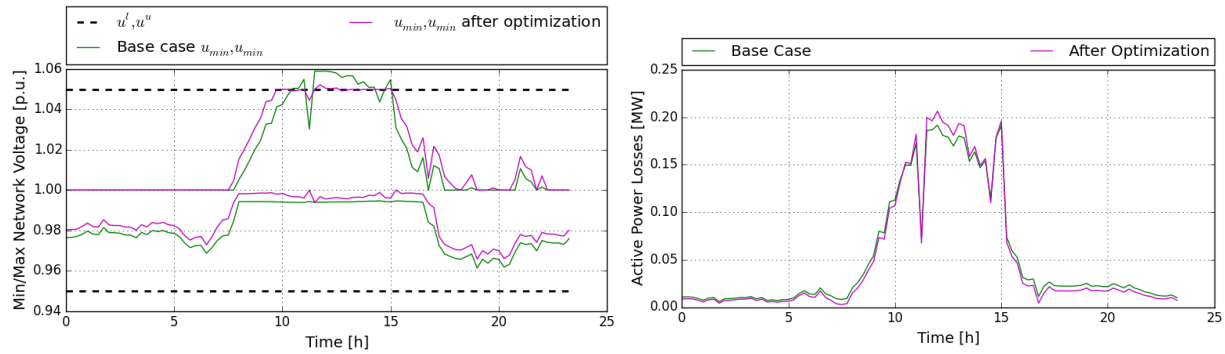


Figure 4-28 Minimum and maximum voltage seen in the network; and active power losses profiles

Decentralized implementation of the proposed method results in improved power system efficiency and lesser energy is lost compared to base case simulation results. This results in lower operational cost and monetary savings.

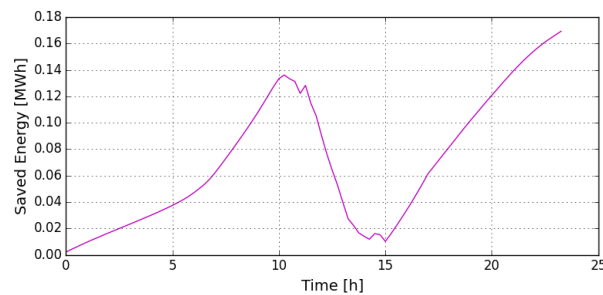


Figure 4-29 Energy saved compared to base case

4.5.6 Comparison of results

In this work, five reactive power based voltage regulation schemes have been implemented on the IEEE 37 node test feeder. Comparative results show that fixed power factor control has a significant impact on peak voltage seen in the network causing the peak voltage to drop by 0.039 p.u. Similarly, variable power factor results in a drop of 0.035 p.u. in the peak voltage appearing within the network. The VVC is a much more efficient method of local voltage control. It significantly reduces unnecessary RPC thereby reducing losses and improving system efficiency. Peak voltage experienced by centralized and decentralized implementations of coordinated control schemes is very similar.

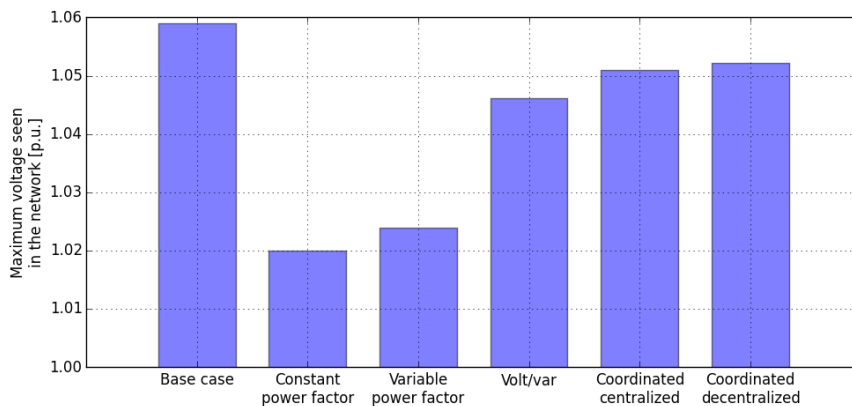


Figure 4-30 Comparison of maximum voltage seen in the network

Figure 4-31 is the plot of the energy saved compared to base case implementation. As can be seen, both FPF and VPF control result in a significant increase in active power losses. VVC scheme is a more efficient RPC scheme that in this case results in considerable reduction in losses. It should be noted that for both centralized and decentralized implementations of coordinated control net energy saved is positive and equal. With intelligent zoning and decentralized implementation, it is possible to achieve results comparable to centralized implementation for the proposed optimization method.

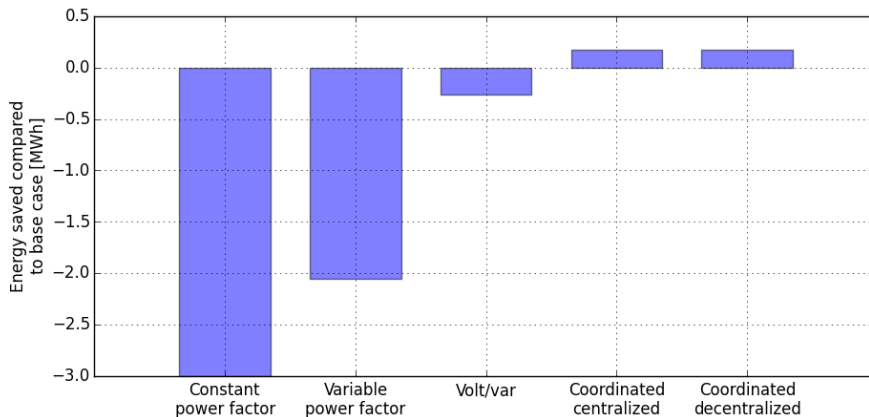


Figure 4-31 Comparison of energy saved compared to base case

4.6 Conclusion

In this chapter, the possibility of coordinating reactive power for achieving multiple power system objectives has been discussed. In the context of this analysis, a multi-objective cost function has been formulated along with constraints pertaining to inverter capability and security of supply. The objective of the work presented in this chapter is to,

- Investigate the possibility of improving power system efficiency using coordinated reactive power dispatch.
- Analyze the performance of the proposed method under multiple scenarios.
- Compare the performance of the proposed method against the state-of-art.
- Investigate the possibility of using meta-heuristic algorithms for distribution system optimization

The formulated multi-objective cost function has been constructed as a weighted sum of two separate objectives namely, power loss minimization and voltage regulation. Ensuring voltage limits are not violated has greater priority than power loss savings for the DSO. Keeping this in mind, the voltage regulation violation objective has been weighed exponentially thus ensuring that even a small voltage violation results in voltage violation objective dominating the final multi-objective cost function.

To solve the formulated non-convex multi-objective problem a population based meta-heuristic algorithm, namely the Bat Algorithm, has been chosen. To improve upon the performance of the algorithm two modifications has been suggested to the original Bat Algorithm. These include adding a bad experience component to the velocity update equation and adding an inertia weight. The modifications aim to the exploration capability of the algorithm and provide control over the transition between global and local search. The performance improvement of modified algorithm has been validated using five benchmark equations.

The proposed method has been implemented in centralized and decentralized manner on the modified IEEE 37 MV test feeder. For the centralized implementation the coordinating controller requires voltage information from the entire network. Although the result obtained using simulation studies show that it is indeed possible to improve network efficiency which also ensuring voltage regulation, requiring voltage information from all DERs connected to the network results poor scalability of the proposed method.

To improve upon the scalability the proposed method has also been implemented in a decentralized manner. Zones have been created using the reactive power/voltage sensitivity matrix and the normalized electrical distance matrix. Hierarchical agglomerative algorithm has been used to automate the zone creation process. Ward linkage criterion has been used to define zones with tight voltage coupling. This ensures efficient use to local reactive power resources. Finally, each zone has its own coordinating controller that has access to information within the zone.

Both centralized and decentralized implementations have favorable results when compared to state-of-art local RPC schemes, namely fixed power factor control, variable power factor control and Volt/VAR control. The coordination based scheme makes use of the complete voltage band. One interesting insight gained from the results is that even though zones created within the electrical network optimized conflicting objectives the degradation performance (in terms of calculated KPIs) when compared to centralized implementation is insignificant. This shows that by intelligently defining zones the results from decentralized implementation are comparable to centralized optimization for the formulated problem. This is exciting news as decentralized implementation is scalable and can accommodate future reactive power markets.

5. Coordinated Active Power Curtailment in LVN

5.1 Introduction

Commercial and residential PV installed in LV distribution networks amount to significant portion of total installed PV capacity in a number of energy markets around the world. The share is influenced by the country's policy regarding PV integration. With high levels of PV penetration in distribution networks built for unidirectional power flow, reverse power flow is a possibility. Voltage regulation in these networks is therefore a challenge. Although inverter based reactive power compensation is possible in many cases using RPC for voltage regulation might ineffective or downright not possible. In many countries where grid codes lag behind the state-of-art, voltage regulation is the sole responsibility of the DSO and reactive power compensation is not permitted by PV owners connected to the LVN. In such scenario active power curtailment is the only possible method for inverters to regulate voltage at the PCC. Additionally, In MV and HV networks, R/X ratio is low and the voltage at the PCC is more sensitive to changes in reactive power than in active power. In LVN however, R/X ratio is typically high. For networks with R/X ratio higher than unity, active power has a larger influence on voltage rather than reactive power making it a more suitable candidate for voltage regulation. Although APC might be a more suitable method of voltage regulation in some network, curtailment of active power means loss of revenue for the PV owner and loss of green energy and associated subsidies for the DSO.

Voltage sensitivity to active power is a function of the electrical distance from the transformer. As the electrical distance increases, so does this sensitivity. This means that nodes further away from the transformer are more susceptible to over voltages due to active power injection from distributed generators. As local active power curtailment method uses only local voltage information, PV owners connected towards the end of the feeder are susceptible to excessive curtailment while PV owner connected close to the distribution transformer are least susceptible to active power curtailment. This is unfairness to PV owners connected lower down feeder as their return on invest would be significantly lower than some PV owner connected in the same feeder even though the initial invest was the same. A number of solutions have already been proposed by researchers to mitigate this inherent unfairness in APC. These have been covered in the literature review section. The proposed solutions can be broadly grouped into four categories, namely, policy based solution, use of storage, increasing self-consumption during times of excessive power injection using DSM and coordinated control of PV inverters with a feeder.

The scope of the work presented in this chapter is twofold. The first goal is to derive mathematical expressions to quantitatively express the unfairness in active power curtailment. The second step is to introduce a coordination based APC scheme that can mitigate this inherent unfairness by ensuring every PV owner participates equally in the voltage regulation process.

5.2 Problem Formulation

Equations for net power flowing through a line can be derived using the two bus system introduced in the previous chapter.

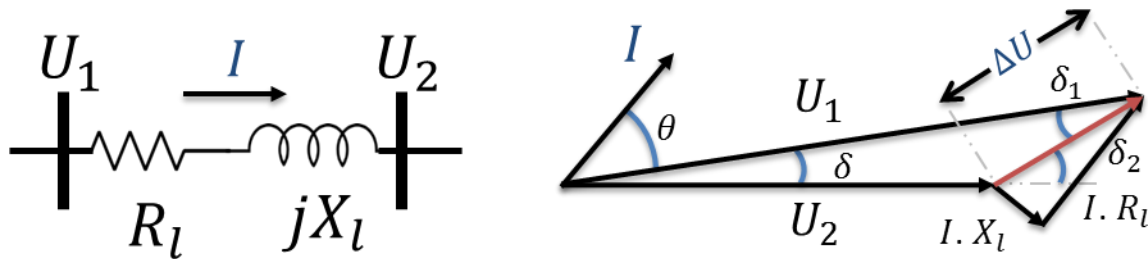


Figure 5-1 Phasor diagram explaining the voltage drop phenomenon in radial networks using a 2 bus system

In a simple two bus network, the current through a line can be calculated using the potential difference and line impedance using the equation.

$$I = \frac{U_1 \angle \delta_1 - U_2 \angle \delta_2}{R_l + jX_l}, \quad (37)$$

Active and reactive power flowing through a line can be calculated using the equations

$$P = U_2 I \cos(\theta + \delta), \quad (38)$$

$$Q = U_2 I \sin(\theta + \delta), \quad (39)$$

By expanding the equations (38) and (39) using trigonometric identities and substituting I from Eqn. (37) in these equations, they can be reduced to the form

$$P = \frac{U_1}{R_l^2 + X_l^2} [R_l(U_1 - U_2 \cos \delta) + X_l U_1 \sin \delta], \quad (40)$$

$$Q = \frac{U_1}{R_l^2 + X_l^2} [-R_l U_2 \sin \delta + X_l (U_1 - U_2 \cos \delta)], \quad (41)$$

As bulk of the load in LVN is resistive, phase angle between any two nodes is generally small. By assuming that the angle between any two connected nodes is small, the Eqn. (40) and (41) can be reduced to the form by approximating $\cos \delta \approx 1$ and $\sin \delta \approx \delta$.

$$P \approx \frac{U_1}{R_l^2 + X_l^2} [R_l(U_1 - U_2) + X_l U_2 \delta], \quad (42)$$

$$Q \approx \frac{U_1}{R_l^2 + X_l^2} [-R_l U_2 \delta + X_l (U_1 - U_2)], \quad (43)$$

Solving for δ Eqn. (42) can be rewritten in the form

$$\delta \approx \frac{P(R_l^2 + X_l^2)}{R_l U_1 U_2} - \frac{R_l (U_1 - U_2)}{X_l U_2}, \quad (44)$$

It should be noted that $U_1 - U_2$ is the change in voltage magnitude ΔU . By substituting Eqn. (44) in Eqn. (43) and eliminating δ from the system of equation, the equation reduces to

$$\Delta U \approx \frac{P R_l + Q X_l}{U_1}, \quad (45)$$

As the net power flowing through a node in difference between the power generated at the node and the demand at the load the equation for change in voltage can be rewritten in the form.

$$\Delta U \approx \frac{(P_G - P_D) R_l + (Q_G - Q_D) X_l}{U_1}, \quad (46)$$

For a PV inverter operating at unity power factor Q_G is zero. Typically residential load is restive meaning $Q_D \ll P_D$. Additionally, if the network in question has a high R/X ratio, $R_l > X_l$. Under these conditions the expression for voltage drop can be reduced to the form

$$\Delta U \approx \frac{(P_G - P_D) R_l}{U_1}, \quad (47)$$

The expression shows that for LVN with high R/X ratio, change in voltage is proportional to the net power flowing through the node. As P_D is uncontrollable and R_l is a constant, inverter generation P_G can be controlled to ensure that the change in node voltage ΔU is restricted to ensure voltage remains within prescribed bounds.

5.3 Controller modeling

5.3.1 Implementation of local voltage controller

For local voltage control, a voltage droop based APC controller has been implemented in PowerFactory. Below a critical the voltage u_{cri} , P^{cal} follows maximum power point tracking (mppt). Once the voltage at the bus exceeds the critical voltage the active power of the inverter is curtailed linearly until the maximum permissible reduction is active power is achieve. If an inverter in operating at P_{min} additional curtailment is not possible. For the purpose of comparison,

simulation results for local voltage regulation have been chosen as base case results. The following equations provide a mathematical representation of implemented droop based controller.

$$\begin{cases} p^{cal} = p^{mpppt} & u < u^{cri} \\ p^{cal} = p^{mpppt} - m(u^u - u) & u^{cri} \leq u \leq u^u \\ p^{cal} = p^{min} & u^u \leq u \end{cases} \quad (48)$$

Approximation of the sensitivity matrix – A node's voltage is a function of active power flowing in all nodes within the system.

$$U_i = f(P_{1,\dots,N}, Q_{1,\dots,N}), \quad (49)$$

Where N is the total number of nodes within the network. The impact of varying active and reactive power flow in the network voltage can be written in the form of a set of partial differential equations. For a resistive network with a high R/X ratio and the bulk portion of the power demand resistive, the impact of reactive power can be neglected. These interdependencies can be mathematically written in the form

$$\begin{bmatrix} \Delta P_1 \\ \vdots \\ \Delta P_N \end{bmatrix} = \begin{bmatrix} \frac{\partial P_1}{\partial U_1} & \cdots & \frac{\partial P_1}{\partial U_N} \\ \vdots & \ddots & \vdots \\ \frac{\partial P_N}{\partial U_1} & \cdots & \frac{\partial P_N}{\partial U_N} \end{bmatrix} \begin{bmatrix} \Delta U_1 \\ \vdots \\ \Delta U_N \end{bmatrix}, \quad (50)$$

By taking the inverse of the sensitivity matrix, the change in voltage at the i^{th} node can be written in the form

$$dU_i = \sum_{j=1}^N \left(\frac{\partial U_i}{\partial P_j} \cdot dP_j \right), \quad (51)$$

By replacing ΔU with $U_1 - U_2$, Eqn. (47) can be rewritten in the form. This equation can be generalized for any two nodes within the system by writing it in the form

$$U_2 \approx U_1 - \frac{(P_G - P_D)R_l}{U_1}, \quad (52)$$

$$U_i \approx U_0 - \frac{\sum(R_{ij} \cdot P_j)}{U_{nom}}, \quad (53)$$

Where R is the real part of the impedance matrix, R_{ij} is the resistance between the i^{th} and the j^{th} node and U_{nom} is the nominal voltage of the network. Finally, by comparing Eqn. (52) and (53) it can be shown that the sensitivity coefficients can be computed using the following equation

$$\frac{\partial U_i}{\partial P_j} = - \frac{R_{ij}}{U_{nom}}, \quad (54)$$

The resistance of a line is a function of conductor resistivity ρ , length of the line L and conductor's cross sectional area A and can be computed by the formula $R = \frac{\rho L}{A}$ or $R = rL$, where r is the parameter dependent on resistivity and cross sectional area. The resistance matrix can therefore be rewritten in the form

$$R_{ij} = r_{ij}L_{ij}, \quad (55)$$

By assuming that conductor type and cross sectional area is uniform for the entire low voltage network, r_{ij} can be reduced to a scalar multiplier r and the resistivity matrix can be reduced to

$$R_{ij} \approx rL_{ij}, \quad (56)$$

The expression above shows that the resistance between any two nodes within a radial low voltage network is a function of the electrical distance between them. Therefore by substituting Eqn. (56) in Eqn. (54), the expression for sensitivity coefficient can be written in the form

$$\frac{\partial U_i}{\partial P_j} \approx - \frac{rL_{ij}}{U_{nom}}, \quad (57)$$

This expression shows that the impact of varying active power on node j on the voltage of node i is proportional to the electrical distance between the two nodes and that longer the feeder length more susceptible it is to over voltages. The value L_{ij} of the electrical distance between any two nodes can be calculated following these two rules [144].

- a. For $i = j$, L_{ij} is the minimum electrical distance from the transformer to the i^{th} node.
- b. In case $i \neq j$, L_{ij} is the maximum overlap of the paths formed from the transformer to the i^{th} and j^{th} node.

Where r is the average resistance per kilometer of the branches belonging to L_{ij} . Figure 5-2 explains the calculation of method using a simple radial network. The self-sensitivity coefficients (diagonal elements of the sensitivity coefficient matrix) of any node the electrical distance as can be seen in scenario A (without branching) and B (with branching). The electrical distance between

node i and j , however is not the distance between the two node, but the maximum common path between the nodes and the distribution transformer.

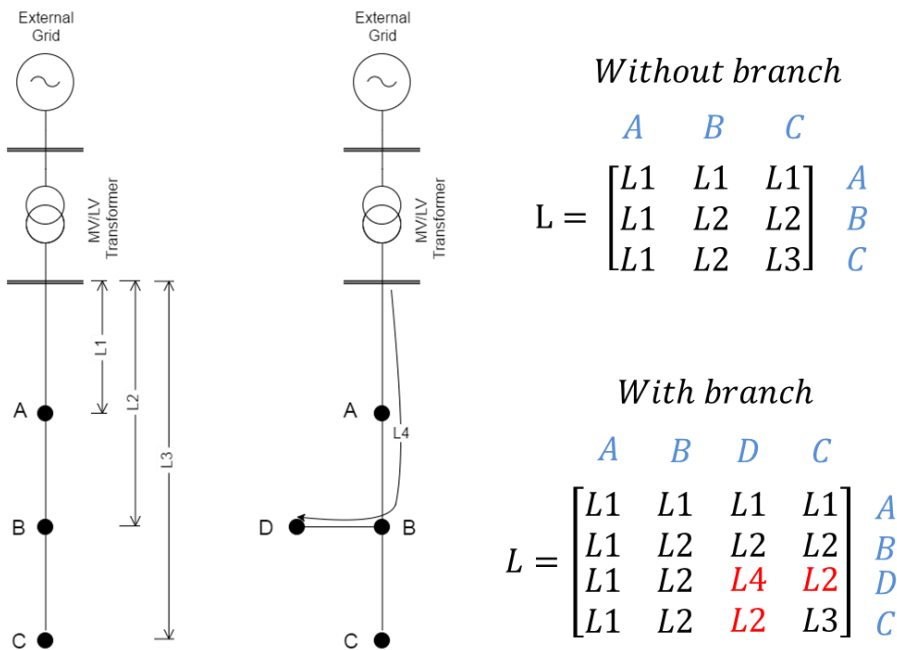


Figure 5-2 Graphical illustration of the method for calculating electrical distance

From Figure 5-2 it can be shown that if, the branch length $L_4 - L_2$ is much smaller than the common path L_2 then, the approximation of common path $L_4 \approx L_2$ is reasonable. By applying the assumption to all nodes and rewriting the sensitivity coefficient equation in increasing electrical distance such that

$$\frac{\partial P_1}{\partial U_1} < \frac{\partial P_2}{\partial U_2} < \dots < \frac{\partial P_N}{\partial U_N}, \tag{58}$$

An approximation of the electrical sensitivity coefficient matrix S can be written in the form

$$S \approx \begin{bmatrix} \frac{\partial P_1}{\partial U_1} & \frac{\partial P_1}{\partial U_1} & \dots & \frac{\partial P_1}{\partial U_1} \\ \frac{\partial P_1}{\partial U_1} & \frac{\partial P_2}{\partial U_2} & \dots & \frac{\partial P_2}{\partial U_2} \\ \vdots & \vdots & \ddots & \vdots \\ \frac{\partial P_1}{\partial U_1} & \frac{\partial P_2}{\partial U_2} & \dots & \frac{\partial P_N}{\partial U_N} \end{bmatrix}, \tag{59}$$

Observing Eqn. (59) it should be noted that an approximation of the sensitivity coefficient matrix S can be constructed knowing only the self-sensitivity coefficients (diagonal elements of

the sensitivity coefficient matrix). This shows that if each inverter installed within the LVN were able to calculate sensitivity coefficient at the point of common coupling and communicate that information to a central controller, an approximation of the sensitivity matrix could be made to help coordinate and improve fairness in active power curtailment. It is important to note that to create the approximation of the sensitivity matrix, the topological information is not needed additionally, for a static topology, the matrix S is also static. If however, the topology of the network changes, the matrix S would need to be recalculated.

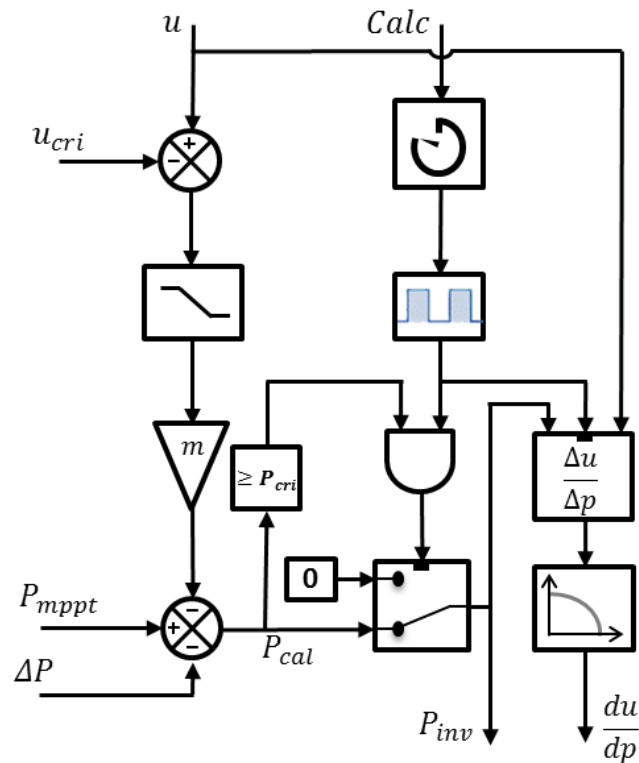


Figure 5-3 Droop based APC controller with du/dp estimation logic

In this work, additional logic has been implemented to estimate the voltage sensitivity at the PCC to active power (du/dp). When the Calc signal is set high, a pulse generator generates pulses for a predefined time interval. If P_{cal} is greater than a critical value P_{cri} , the inverter set point is switched to zero temporarily. The change in voltage is then recorded and du/dp is estimated using finite difference. The process is repeated to and the results are filtered to minimize estimation errors. For this work, P_{cri} has been set to 70% of the rated power. P_{cri} is intentionally set high so that a significant change in the voltage can be recorded and the impact of other inverters and the load present in the system can be neglected. The main thought process behind estimation of voltage sensitivity is to provide a truly plug and play solution for voltage control.

5.3.2 Implementation of the coordinating controller

Each node in the feeder is assigned a unique ID referred to as ‘Node ID’ in the rest of the chapter. At initial run, the coordinating controller sequentially requests inverters to estimate local sensitivity coefficients. It is important that estimation to be done sequentially (one PV inverter at a time) as large active power injection change in a nodes in close proximity can lead to large errors in estimation of sensitivity coefficient at a node. Once sensitivity coefficient estimation at nodes connect to a PV inverter is complete, the coordinating controller requests for and receives rated powers, estimated sensitivity coefficients and Node IDs from inverters connected to the feeder. Rated output power of the PV systems are stored in a $k \times l$ matrix P^{rated} where k is the number of unique nodes in a feeder with a PV connection and l is the maximum number of PVs connected to a single node. As the sensitivity coefficients of only the nodes connected to a PV are known, the resulting matrix is $k \times k$ matrix rather than a $N \times N$ matrix. The sensitivities arranged in an ascending order form the diagonal part of the sensitivity coefficient matrix S . Non-diagonal elements of the sensitivity matrix are populated using Eqn. (59). Traditionally, the MV/LV transformer has an of load tap changer to cater to seasonal variations in load. By assuming that on the primary side of the transformer is fixed at u^{nom} p.u. the voltage at the secondary side can be calculated using the equation,

$$u^{trlv} = u^{nom} - \Delta u^{tap} \cdot x^{tap} \quad (60)$$

Where u^{trlv} is the voltage at the secondary side of the distribution transformer, Δu^{tap} is the p.u. change in voltage per tap and x^{tap} is the current tap position. Maximum possible voltage rise at a node can be calculated multiplying the elements of sensitivity matrix S with the inverter rated power matrix P^{rated} .

$$\Delta u_i^{max} = \sum_{j=1}^k \sum_{m=1}^l P_{mj}^{rated} \cdot S_{ij} \quad (61)$$

With $i = 1, 2, \dots, k$

The voltages at PCC of each inverter are continuously monitored and sent to the coordinating controller after a fixed time interval. At the time maximum voltage in the feeder u^{max} exceeds the low bound u^{lb} the value of critical voltage u_i^{cri} for the i^{th} inverter (starting point for APC) is set to the current value of the voltage u_i at the PCC. Otherwise, u_i^{cri} is set to the upper limit for voltage u^{ub} , thus ensuring power is not curtailed. This process can be mathematically formulated using the following equations.

$$u^{max} = \max(u_{1,2,\dots,k}) \quad (62)$$

$$u_i^{cri} = \begin{cases} u_i & | u^{max} = u^{lb} \\ u^{ub} & \text{otherwise} \end{cases} \quad u^{max} \geq u^{lb} \quad (63)$$

If $I \in [1, \dots, k]$ is the index of the node with the maximum measured voltage u^{max} , reduction in voltage required (Δu) to ensure no over voltage occurs can be calculated using Eqn. (64).

$$\Delta u = u^{trlv} + \Delta u_I^{max} - u^{ub} \quad (64)$$

Once reduction voltage required to comply with LVN power quality standards has been calculated, one of two methods can be used to calculate the set points for active power curtailment for individual inverters.

Equal loss of revenue for each PV owner – The first perspective being every PV owner connected to the grid participated equally in the voltage regulation process. Curtailment in output power is the same for all PV systems irrespective of system's rated power. The method was first proposed by Tonkoski in [108]. Maximum permissible reduction in active power injection can be calculated using the equation

$$\Delta P^{max} = \frac{\Delta u}{\sum_{i=1}^k m_i \cdot S_{il}} \quad (65)$$

Where m_i is number of non-zero elements in the i^{th} row of P^{rated} matrix (number of PV connected to a node). It should be noted that ΔP^{max} is a scaler value hence the same for every inverter irrespective of its power rating.

Equal percentage reduction in revenue – In this work, an alternate perspective of fairness has been presented and consequently, an alternate method for calculated of maximum permissible reduction in active power injection for inverters has been proposed. In this work it has been proposed that curtailment in active power be proportional to the rating of the system. This would mean that each PV owner has an equal percentage reduction in revenue.

$$z = \frac{\Delta u}{\sum_{i=1}^k \sum_{j=1}^l P_{ij}^{rated} \cdot S_{il}} \quad (66)$$

$$\Delta P^{max} = z \cdot P^{rated} \quad (67)$$

Where z is scaler value representing the percentage reduction in active power required from each inverter to ensure no over voltage. In this case, ΔP^{max} is $k \times l$ matrix. In the final step, S function is used to reduce excessive curtailment.

$$\Delta P_{ij} = \frac{\Delta P_{ij}^{max}}{1 + e^{\frac{B - u^{max}}{A}}} \quad (68)$$

Where

$$B = \frac{u^{ub} - u^{lb}}{2} \quad (69)$$

Where A is a constant that controls the rate at which ΔP_{ij} increases from zero to ΔP_{ij}^{max} . This ensures that maximum possible curtailment occurs only when necessary. Algorithm 5-1 presents the pseudo code for the proposed coordinating algorithm.

Algorithm 5-1 Pseudo code for the coordinating controller

```

1  Input:  $\overrightarrow{RP}$  (Inverter rated power vector) and the corresponding  $\overrightarrow{Node\ ID}$ ,
2  Construct the  $P^{rated}$  matrix using inputs
3  For  $i = 1$  to  $k$  (Number of unique nodes connected to a PV system)
4      |   Set  $Calc_i = 1$ 
5      |   Get estimated sensitivity coefficient for node  $i$ 
6      |   Set  $Calc_i = 0$ 
7  Construct the sensitivity matrix  $S$ 
8  While End of simulation time not reached do
9      |   Calculate the secondary side of the transformer  $u^{trlv}$ 
10     |   Calculate maximum voltage rise at each node  $\Delta u_i^{max}$ 
11     |   Use the maximum voltage in the network to calculate the critical voltage  $u_i^{cri}$  for
12     |   each inverter
13     |   Calculate  $\Delta u$  reduction in voltage required at the node experiencing over voltage
14     |   Calculate the maximum permissible power that can be curtailed from each inverter
15     |   using either of the two methods
16     |   Use the  $S$  function calculate the final set points  $\Delta P_{ij}$  for active power curtailment
17     |   for each inverter
18 Calculate KPIs and compare results
    
```

5.4 Formulation of key performance indices (KPIs)

Three performance indices have been formulated to evaluate and compare the performance of the proposed algorithm against the state-of-art solutions. Formulation and relevance of each of these KPIs, namely, total curtailed energy (TCE), curtailment unfairness index 1 (CUI1) and curtailment unfairness index 2 (CUI2) is discussed in detail in this sub-section.

5.4.1 Total Curtailed Energy

Total energy curtailed is a meaningful measure for comparison against the state-of art as any proposed coordination based control scheme for fair APC should not significantly increase total curtailed energy as it would lead to loss of green energy for DSO and loss of additional revenue for PV owners.

$$P_i^{cur} = P_i^{inv} - P_i^{mppt}, \quad (70)$$

$$E_i^{cur} = \int P_i^{cur} dt, \quad (71)$$

$$TCE = \sum_1^N E_i^{cur}, \quad (72)$$

for $i = 1, \dots, N$

Where N is the number of PV systems installed on a particular feeder. P_i^{mpp} , P_i^{inv} , E_i^{cur} are the maximum possible active power output, actual active power output and the curtailed energy of the i^{th} inverter. TCE is therefore total energy curtailed from all inverters present in the feeder participating in voltage regulation.

5.4.2 Unfairness in active power curtailment

As already discussed, unfairness in APC can be viewed from two different perspectives. The first perspective being, the loss of revenue for all PV system owners should be equal irrespective of the nominal rating of the PV system. CUI1 index formulated in Eqn. (73) has been used in this work to quantify the fairness from this perspective and compare different control strategies.

$$CUI1 = \sqrt{\frac{\sum (E_i^{cur} - \overline{E^{cur}})^2}{N - 1}}, \quad (73)$$

Where $\overline{E^{cur}}$ is the average energy curtailed during a 24 hour period from all PV systems connected to a feeder. The calculated index CUI1 is the standard deviation of curtailed energies, hence, a measure of spread of total energy curtailed during the day from the installed PV systems. If equal energy is curtailed from each PV system CUI1 will be zero implying fair curtailment. If however the installed PV systems differ in rating a PV system with a smaller rating would incur higher percentage reduction in revenue. Another way to accommodate the unfairness is to ensure that percentage reduction in revenue for every PV system owner is the same. Curtailed power can be normalized by dividing instantaneous curtailed power P_i^{cur} by the rated output of the inverter P_i^{rated} . Integrating normalized curtailed power gives normalized curtailed energy and as P_i^{rated} is a constant it can be calculated using Eqn. (75).

$$e_i^{cur} = E_i^{cur} / P_i^{rated}, \quad (74)$$

$$CUI2 = \sqrt{\frac{\sum (e_i^{cur} - \overline{e^{cur}})^2}{N - 1}}, \quad (75)$$

Where P_i^{rated} is the rated power for the i^{th} inverter and $\overline{e^{cur}}$ is average of the normalized curtailed energies of all PV systems present in a feeder. The second index formulated in this work (CUI2) is a measure of spread of percentage of the energy curtailed from each PV rather than total energy curtailed from the PVs. Low values of CUI1 and CUI2 indicate small spread hence higher fairness and vice versa.

5.5 Simulation setup and study case implementation details

5.5.1 Simulation setup

The distribution network and the local voltage controller detailed in Section 5.3.1 have been implemented in PowerFactory [140] a popular power network simulation tool. The secondary voltage controller, detailed in Section 5.3.2, has been implemented in Python [145] because of PowerFactory's limitations while dealing with matrices. Direct communication between the coordinating controller developed in Python and the local controller developed using DSL (DIgSILENT simulation language) blocks within PowerFactory is not possible due to the limitations of PowerFactory. However, during RMS simulation it is possible for controllers modelled in DSL blocks to call functions from an external C++ library. In [146] a C++ library has been used to implement socket communication that uses an XML file to assign sockets to individual DSL blocks. This enables controllers modeled using DSL blocks to connect to external software and simulators. In this work this library has been used to establish communication between PowerFactory and Python during RMS simulation. Socket based communication is both flexible and extendable. For example, with socket based communication, it is easy to incorporate a network simulator such as OMNET++ to study the impact of communication on the proposed voltage control scheme. Figure 5-4 is a graphical illustration of coupling scheme used.

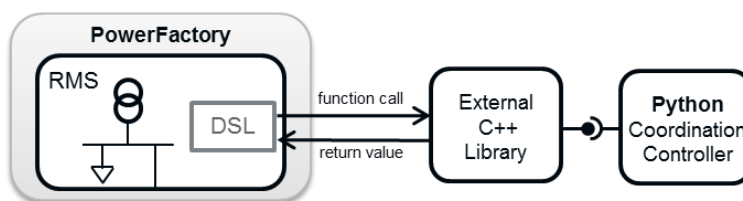


Figure 5-4 PowerFactory and Python coupling via sockets using external DLL

5.5.2 Study case 1: Impact of assumptions on sensitivity matrix estimation

In this subsection, a simplistic LV network (Figure 5-5) presented in [147] has been used to study the impact of the assumptions taken to estimate the sensitivity matrix. Three set of simulation studies have been conducted to understand how each of the three identified parameter namely, length of a branch, position of a branch and the number of branches, affects the quality of the estimated sensitivity matrix S .

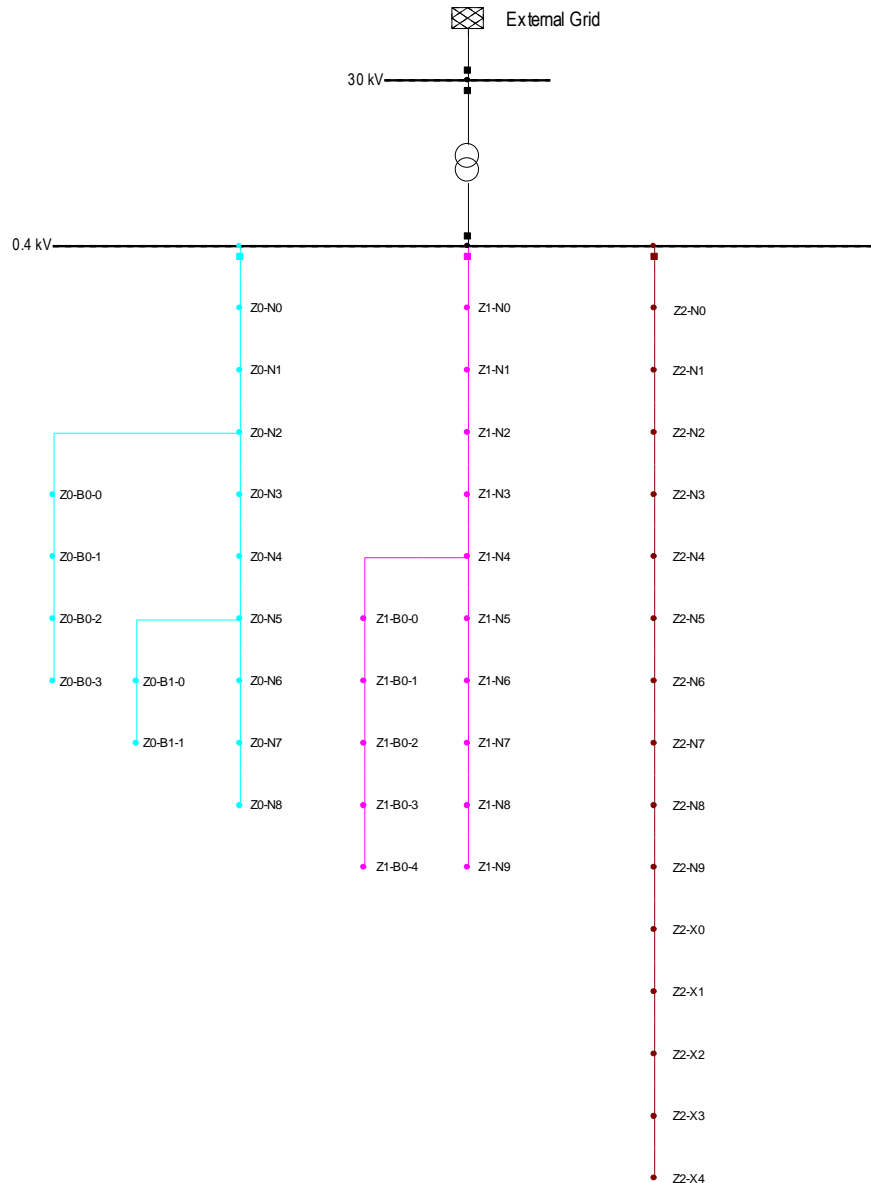


Figure 5-5 A simplistic hypothetical radial LV network

Each node in the selected simplistic LV network is connected to a dynamic load with peak demand rated uniformly between 5 and 8 kW. Additionally, PV systems have been connected at each node rated at 5 kW. PV systems have been equipped with local voltage controller with sensitivity estimation capability modeled in Section 5.3.1. For each of the three experiments, the estimated sensitivity matrix has been compared with the actual sensitivity matrix calculated by PowerFactory. The line length connecting any two nodes is 40m. The conductor used for this experiment is NAYY 4x120SE, which is commonly used in LV networks. The error in estimation has been calculated using the formula,

$$\varepsilon_{ij} = (S_{ij}^{PF} - S_{ij}) / S_{ij}^{PF} \times 100 \quad (76)$$

for $i, j = 1 \rightarrow k$

In the first simulation the impact of branch length on sensitivity matrix estimation error has been studied. In the said study, Feeder 2 (one branch) has been chosen. The length of lines connecting all nodes have been increased linearly from 4m to 40m. Figure 5-6 below is a plot for the estimation error verses the maximum and average estimation error. The results show that the estimation error has a linear dependence on the length of the branch and the estimation error increases from 6% to almost 90%. The maximum estimation error is always at the node located at the end of the branch (in this case node Z1-B0-4 and Z1-N9). The average estimation error (calculated for all nodes) also shows strong linear dependence to the length of the line. In section 5.3.1 it was shown that the approximation holds if $L_4 - L_2 \ll L_2$, where the length of the branch is $L_B = L_4 - L_2$. Increase in average estimation error is more than 15 fold increasing from about 2.5% to 53%.

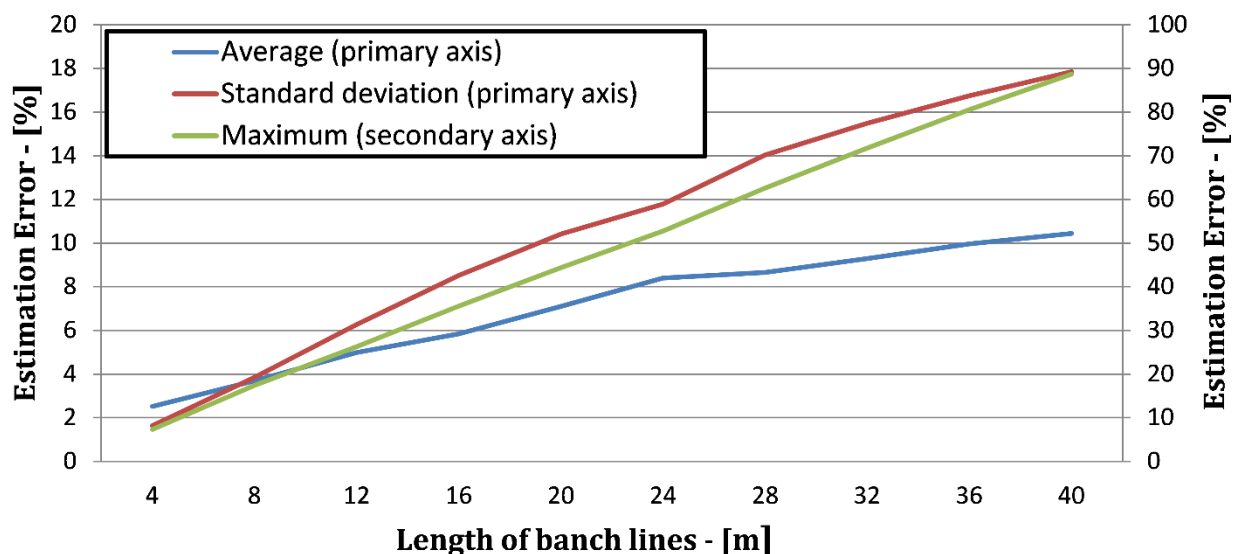


Figure 5-6 Impact of branch length on estimation error

In the second experiment, the position of the branch was changed starting from the node closest to the transformer (Z1-N0) and ending at node Z1-N9, while the length of lines connecting branch nodes was fixed at 8m. The results plotted in Figure 5-7 show that the maximum estimation error is highly sensitive to the distance branching line from the distribution transformer. In Section 5.3.1 it was shown that approximation of the sensitivity matrix holds only if the expression $L_4 - L_2 \ll L_2$ holds. In this experiment changing the branching position changes L_2 and for small values of L_2 the approximation does not hold. Connecting the branch at node Z1-N9 results in a radial network with no branches. The results from the first two experiments show that the estimated sensitivity matrix is sensitive to both the position and the length of branches within a LV network. The average error in estimation is lower than 10% for all nodes except for the node Z1-N0 and less than 5% for nodes after Z1-N4.

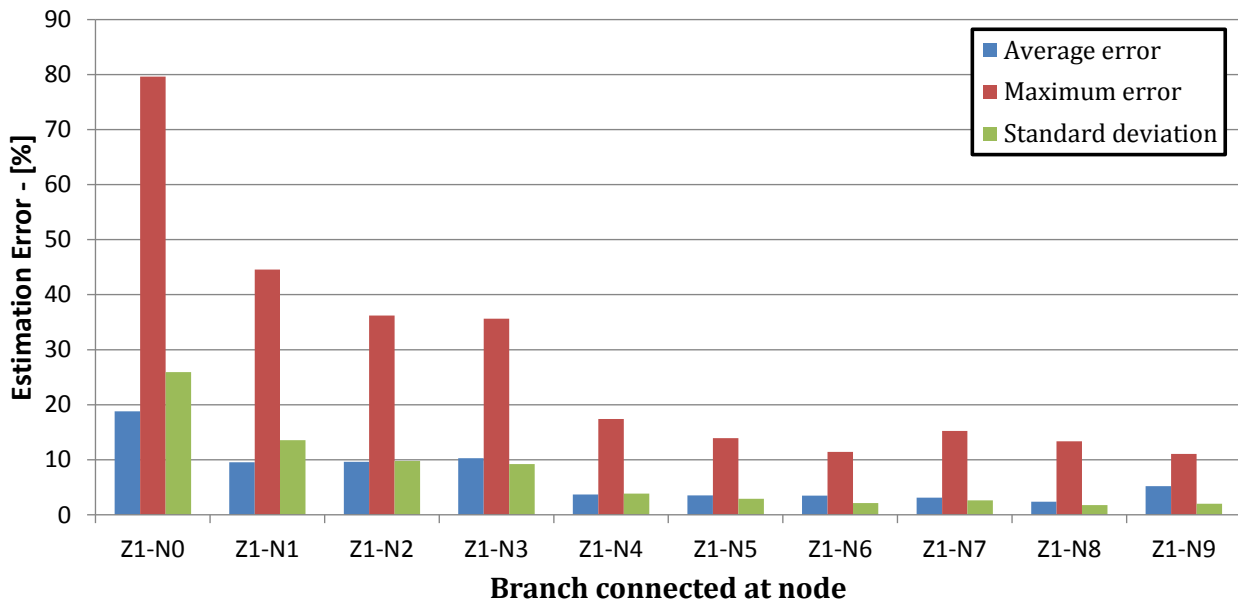
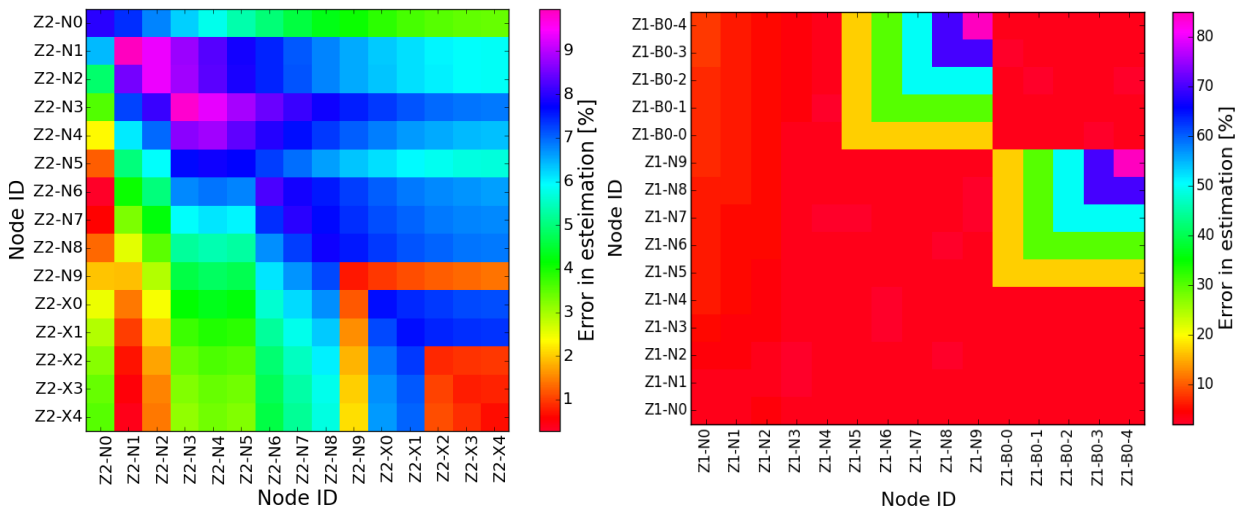


Figure 5-7 Impact of the branch position in estimation error

In the final experiment the error in sensitivity matrix estimation has been calculated for the three feeders in Figure 5-5. The error matrices for each of the three feeders have been presented in form of a color map. The color map for feeder 2 (no branching) shows that for feeder with no branching the error in estimation of the sensitivity matrix is low (less than 10%). An important insight gained from the color plot is that the percentage error in estimation of self-sensitivity is highest at nodes closest to the transformer. The reason is that the values self-sensitivity coefficients (diagonal elements of the matrix) are proportional to the electrical distance between the node and the distribution transformer. For nodes closer to the transformer, the coefficients have small values. Dynamic network conditions results in error in sensitivity coefficient estimation. Same absolute error at two different nodes results in a much larger percentage deviation for the node closer to the transformer.



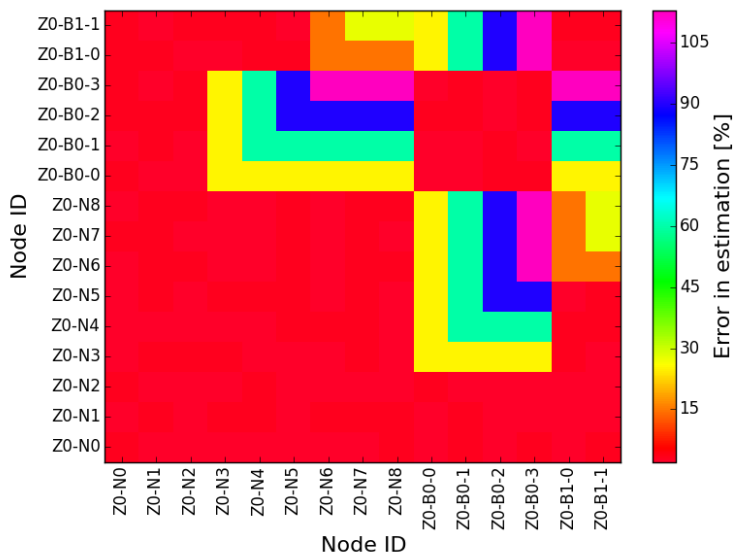


Figure 5-8 Impact of the increasing the number of branches on estimation error

Finally, an important observation information that can be made from the color plots for the three feeders is that error in sensitivity matrix estimation is also sensitive to increasing the number of branches. The maximum error for a coefficient increases 10% for feeder with no branching to 120% for a feeder with two branches.

The results from the study case show that good estimation of the sensitivity matrix is only possible in networks with a few branches with small line lengths. Additionally, the branching should ideally be closer to the end of the feeder.

5.5.3 Study case 2: Implementation of the proposed method on a real LV network

The test case chosen for this work is the real low voltage distribution network. It consists of a two feeder network connected to medium voltage network through a 100 KVA transformer. The low voltage network consists of two feeders connecting 27 consumers. For the purpose of the test case, 16 photo voltaic systems have been placed randomly within the network. The PV systems have been randomly sized between 4 and 9 KVA. PV inverters provide voltage support using active power curtailment. For the purpose of simulation one minute average load and generation profiles have been used. Network data is listed in Tables 5-1 to 5-4. The topology of residential test feeder used for this work is presented in Figure 5-9.

Table 5-1 Line Parameters

	Resistance	Reactance	Capacitance
+ SEQ	0.3211 OHM/KM	0.069 OHM/KM	0.5900 UF/KM
0 SEQ	1.0844 OHM/KM	0.276 OHM/KM	0.3308 UF/KM

Table 5-2 Line Lengths

Line	Length	Line	Length	Line	Length
A1-B1	69 m	H1-I1	46 m	F4-G3	53 m
B1-C1	67 m	I1-J1	36 m	G2-H2	44 m
C1-D1	67 m			H2-I2	40 m
D1-E1	85 m	A2-B2	88 m	E2-F5	67 m
E1-F1	55 m	B2-C2	74 m	F5-G4	66 m
E1-F2	46 m	C2-D2	90 m	G4-H3	42 m
E1-F3	77 m	D2-E2	67 m	H3-I3	44 m
F2-G1	76 m	E2-F4	105 m	I3-J2	38 m
G1-H1	54 m	F4-G2	61 m	I3-J3	61 m

Table 5-3 Transformer data

Voltage Rating	Rated Power	Type	Tap Changer	Voltage/Tap
20 kV / 0.4 kV	80 kVA	Dyn11	-4 : +4	1.25 %

Table 5-4 Generator operational limits

Inverter ID	Rating [kVA]	Inverter ID	Rating [kVA]
PV B1	4	PV C2	5
PV C1	5	PV G3	6
PV F1	9	PV G4	4
PV G1	7	PV I2-1	8
PV H1-1	6	PV I2-2	5
PV H1-2	5	PV I3	8
PV J1	7	PV J2	8
PV B2	5	PV J3	7

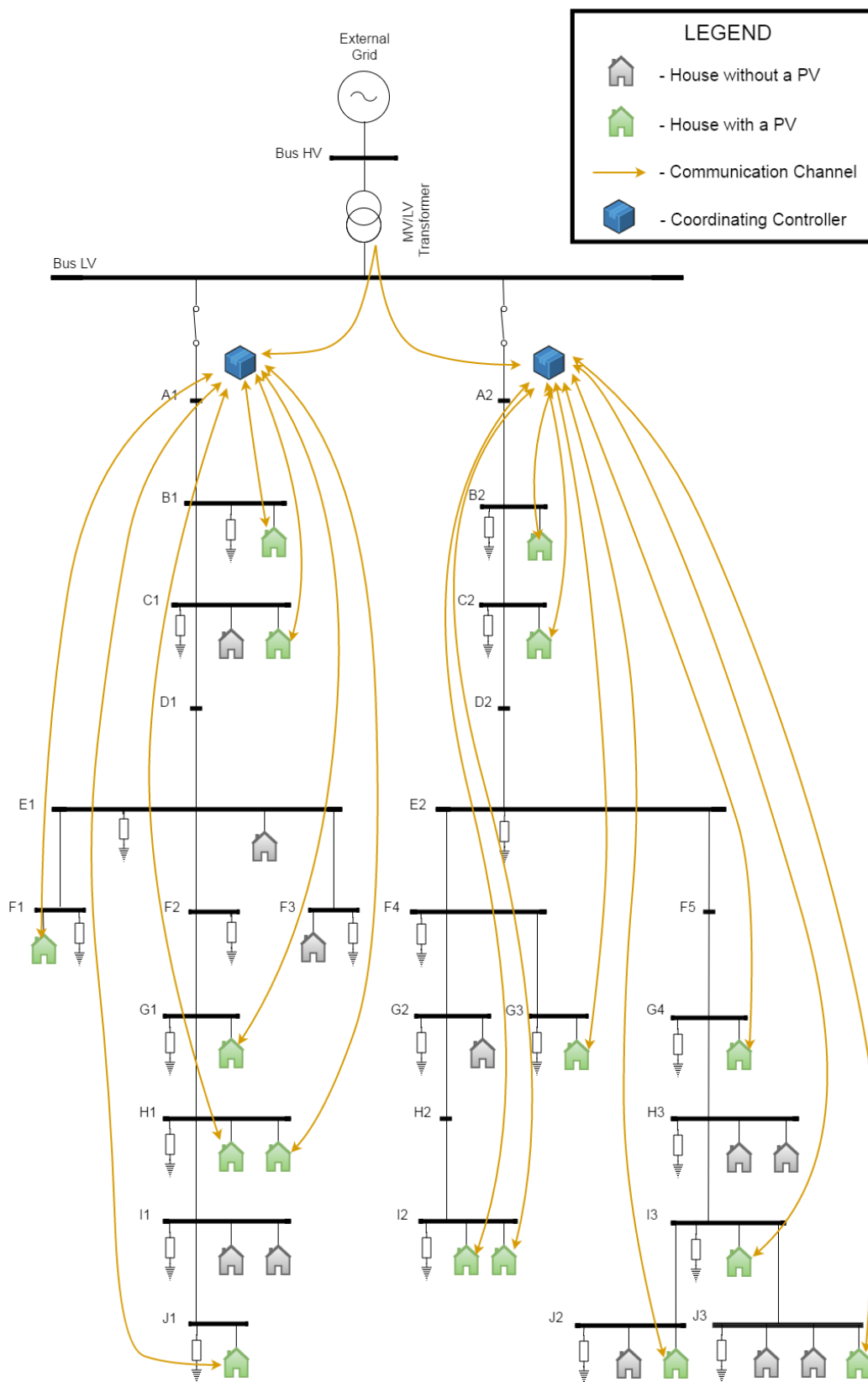


Figure 5-9 A real low voltage distribution network

5.6 Results and discussion

5.6.1 Estimation of the sensitivity matrix

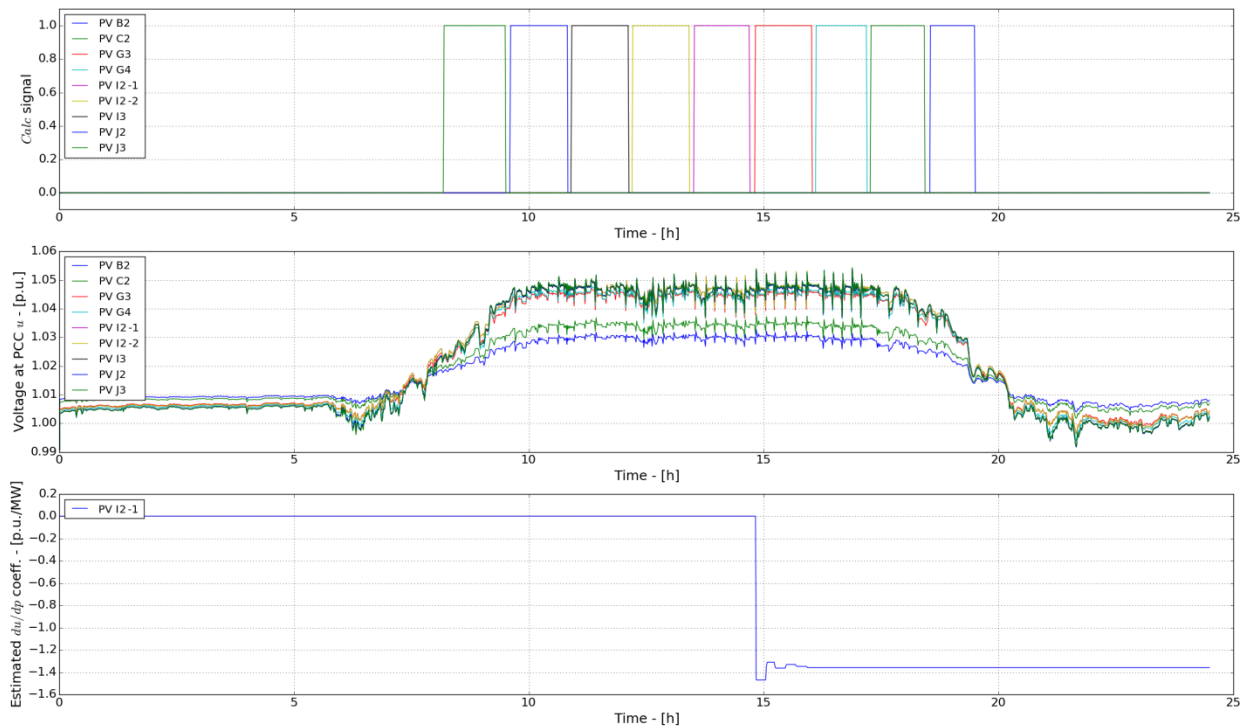


Figure 5-10 Calc control signal from the coordinating controller; Voltage at PV connected nodes; du/dp estimation results for PV I2-1

The estimation of the self-sensitivity coefficients of the matrix S is performed using logic proposed in Section 4.3.1. The $Calc$ signal is set high by the coordinating controller, thereby ensuring that no two inverters are estimating the coefficient at the same time. The coefficient is calculated using finite difference and the process is repeated numerous times to mitigate the error in estimation originating to dynamic network condition (varying load and DER generation at other nodes in the network). It is important to note that the estimated matrix S is constant for a network with a static topology. If however, the topology of the network changes, resulting from network extension or alternate routing, the matrix would require recalculation. It should also be noted that estimation requires significant change in active power injection to cause a significant change the voltage at the PCC. This results in spikes in voltage of the PCC resulting in deteriorated power quality. However, as the estimation of the coefficients is a one-time process this is a tolerable side effect. Figure 5-10-c shows the value of the coefficient estimated for PV I2-1. In similar fashion, the coefficients for the rest PV connected nodes have been estimated.

The estimated sensitivity matrix is compared with the actual sensitivity matrix calculated using PowerFactory. The percentage error in estimation of the sensitivity matrices for feeder 1 and 2 have been presented in Figure 5-11-a and Figure 5-11-b respectively. A number of observations

can be made from the two color plot. First, the error in estimation of the diagonal elements is much less than the error is smaller compared to non-diagonal elements of the matrix. Second, the error in estimation is highest for branch nodes. This to be expected reasons for which have been explained in great detail in study case 1. Additionally, the maximum percentage error in estimation is significantly smaller for feeder 1 due to simpler network topology with comparatively fewer branches. Finally, from Figure 5-2 it can be seen that L_2 is always less than L_4 and approximating $L_2 \approx L_4$ for the non-diagonal elements (marked in red in Figure 5-2) will always result in an over approximation. Over approximation results in increased active power curtailed resulting in lower voltage at the PCC.

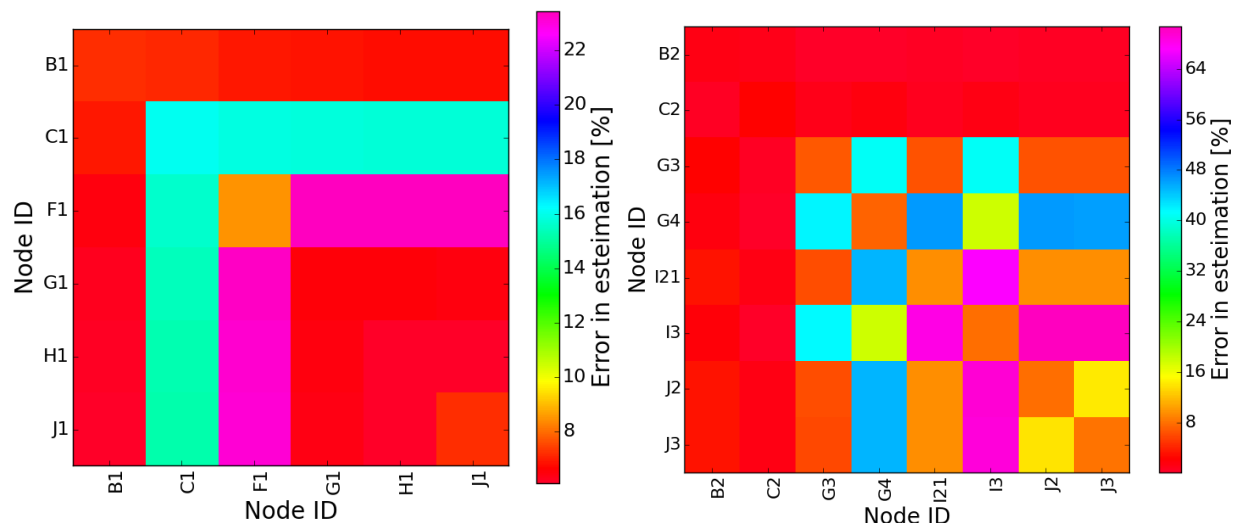


Figure 5-11 du/dp estimation error for Feeder 1 and Feeder 2

5.6.2 Results for voltage control schemes

Base Case Results

In this subsection, simulation results for base case along with local APC scheme and the proposed method have been presented. The voltage profile for the PCC of each PV system has been presented in Figure 5-12. For the purpose of simulation, real one minute average profiles have been used. In a scenario, where demand is low and generation is high, the voltage at the PCC tends to rise. In base case scenario PV are operating at unity power factor and do not have voltage regulation capability. This results in violation upper limit of the assigned voltage band. For base case the maximum voltage seen in the network is 1.067 p.u.

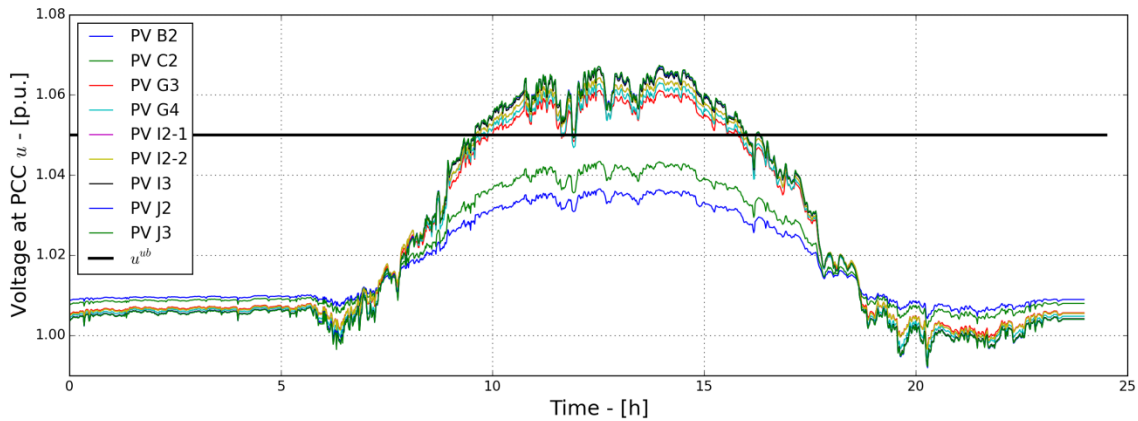


Figure 5-12 Voltage profiles at PCC of each inverter with no voltage control function

In this section three methods for voltage regulation have been simulated and the results for each of these methods have been discussed in great detail.

Results for local voltage control

For the local voltage control scheme, each PV inverter is equipped with a local APC controller for regulating voltage at the PCC. The local APC scheme requires only local information hence does not need a communication infrastructure. Additionally, due to the nature of the voltage control scheme it is a scalable solution. Once the voltage at the PCC exceeds the critical voltage u^{cri} the output power of the PV inverter is linearly curtailed until active power output reached P^{min} , at which point no more power can be curtailed. In this experiment, P_{min} has been set at 50% of the rated power of the PV inverter. Additionally, the critical voltage u^{cri} and threshold voltages u^{thr} have been set at 1.02 p.u. and 1.05 p.u. respectively for every inverter on the residential feeder. Simulation results for the voltage at the PCC of each inverter are presented in Figure 5-13.

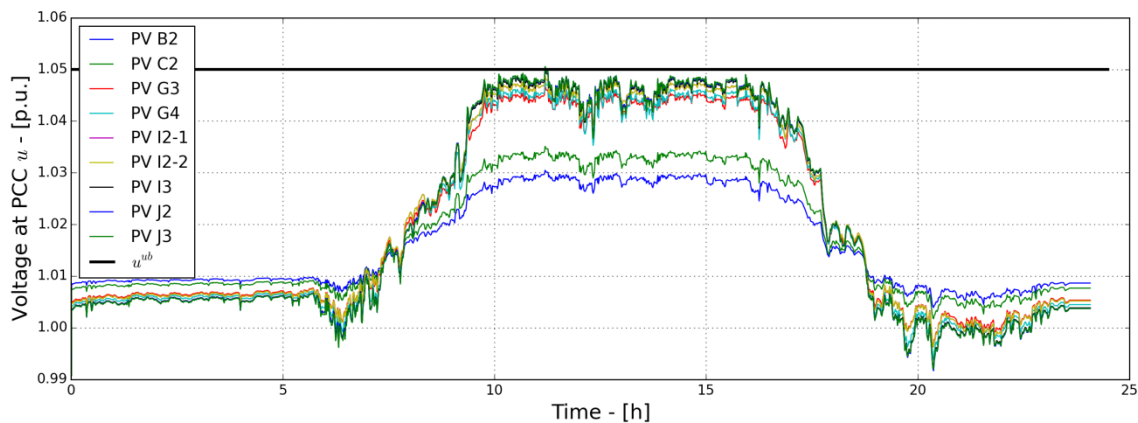


Figure 5-13 Voltage profiles at PCC of each inverter with local voltage controller

As explained earlier, a node’s voltage sensitivity to active power at the PCC is a function of the electrical distance from the transformer. This means that the PV systems installed further away from the transformer are more susceptible to over voltage problems. Figures 5-14 and 5-15 illustrate this phenomenon. The local active power based voltage regulation is inherently unfair to PV owner connected to further away from the transformer.

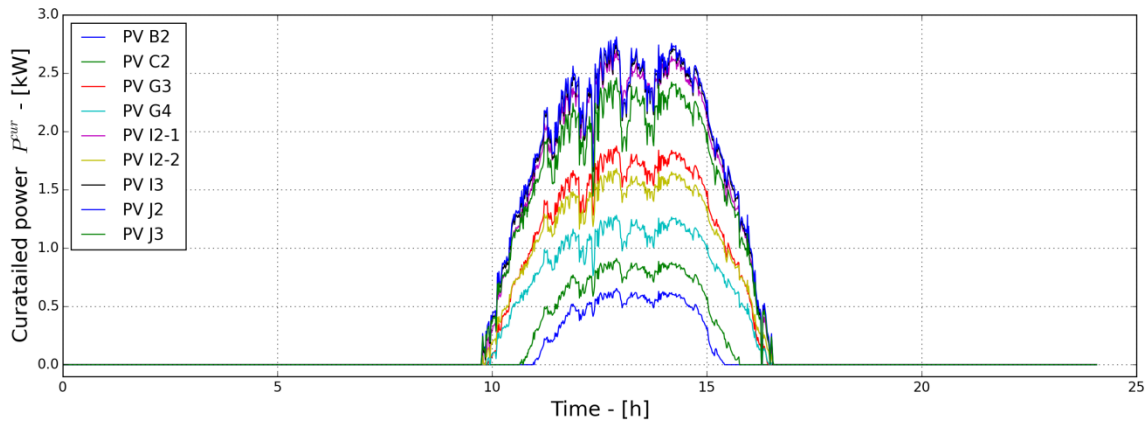


Figure 5-14 Curtailed power form each inverter using local droop based voltage curtailment

The plot for curtailed power highlights this inherent unfairness. At the time of peak PV generation, active power curtailed from PV installed at node B2 is 0.6 kW while the power curtailed from PV installed at node J3 is 2.7 kW. This is an increase of about 450%. It should also be noted that over voltage first appears at nodes further away from the transformers. From Fig XX it can be seen that curtailment for PV at node J3 starts a little before 10 am while curtailment for PV connected at node B2 starts a little after 11 am. This further exacerbates the unfairness in curtailed power. The plot in figure 5-15 shows the total energy curtailed during the day’s simulation.

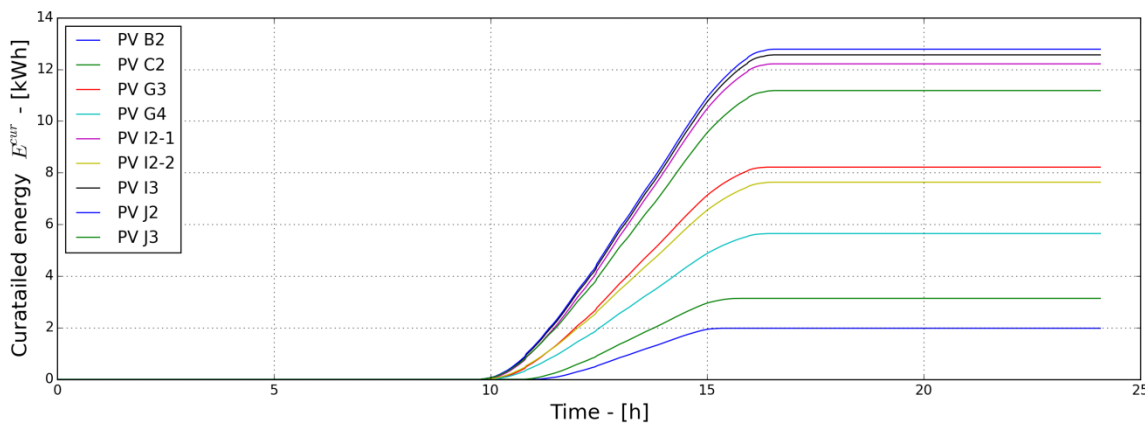


Figure 5-15 Curtailed energy form each inverter using local droop based voltage curtailment

Results for coordinated control (CC1) - First perspective of fairness

The first perspective of fairness aims at ensuring that each PV system installed on the feeder participates equally in voltage regulation using APC. This would result in equal loss of revenue for each PV owner at times of high generation and low demand. The proposed scheme requires real time voltage information from all the PV connected nodes. Thus for real world implementation, a communication infrastructure would be required to implement the coordination based scheme. In this section, an ideal communication channel has been presumed (no information loss and no delay). The lower voltage limit u^{lb} , after which coordinated curtailment starts, is set at 1.02 p.u. for this experiment. The upper voltage limit u^{ub} , which should not be exceeded, has been set at 1.05 p.u. for all experiments.

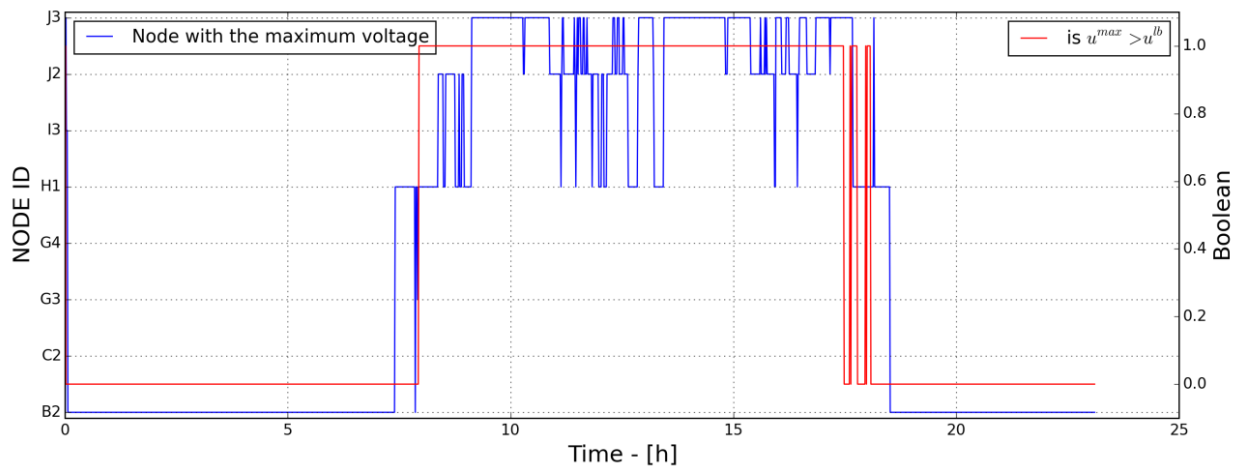


Figure 5-16 Node currently experiencing the maximum voltage within the network; Signal for starting active power curtailment

Although the node furthest away from the transformer is most susceptible to over voltage, dynamically varying loads may cause the node experiencing the highest voltage in the network to change. Figure 5-16 is a plot of the node with highest voltage as a function of time. The proposed algorithm takes into account the node at which the highest voltage is currently being experienced while calculating the active power curtailment value. This ensures that excessive power by only using worst case scenario (sensitivity coefficients corresponding to node J3). The coordinating controller generates curtailment set points ΔP and critical voltages set points u^{cri} for each PV system only if the maximum voltage seen in the network u^{max} exceeds the lower voltage bound u^{lb} . The $u^{max} > u^{lb}$ is a Boolean condition that has been plotted in Figure 5-16. The plot shows times during which coordinating controller is active.

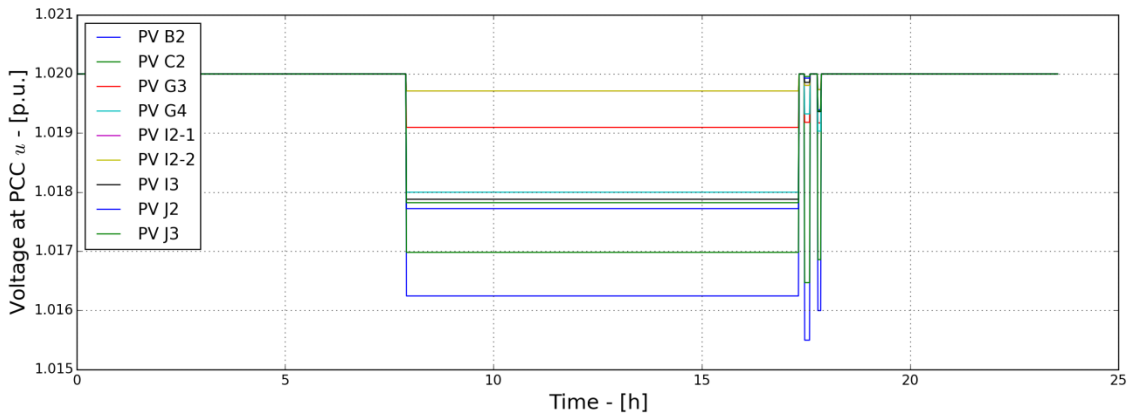


Figure 5-17 Critical voltage set points calculated for each inverter connect to feeder 2

Once the coordinating controller is active, critical voltages for each inverter are calculated using Eqn. (63). It should be noted that the voltage first tend to rise at nodes with the largest electrical distance from the transformer. For this reason, critical voltage is smallest for PV system connected to node closest to the transformer (Node B2) and increases for the rest of the systems as the electrical distance from the transformer increases.

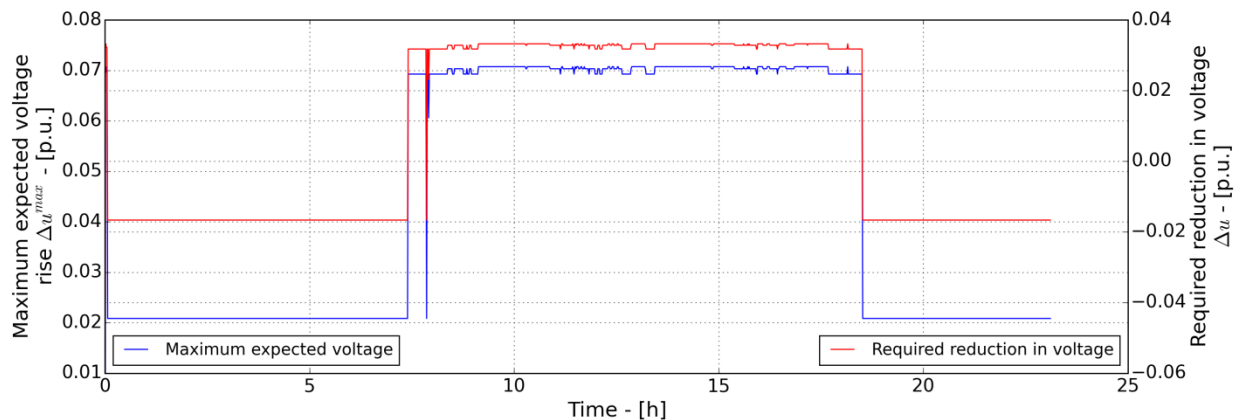


Figure 5-18 Maximum expected voltage in the network; reduction in voltage required to ensure no voltage violation occurs

Next, the maximum expected voltage rise is calculated for each node using the sensitivity matrix S and the rated active power matrix P^{rated} . The index of the node with the maximum voltage and the maximum expected voltage rise values are used to calculate reduction in voltage required at any given time. It should be noted that the maximum expected voltage rise is a function of the index of the node currently experiencing the maximum voltage in the feeder. From Figure 5-18 it can be seen that the maximum expected voltage rise in the network is around 0.07 p.u. and the expected reduction in voltage required to ensure that feeder voltage does not violate the prescribed band is about 0.032 p.u.

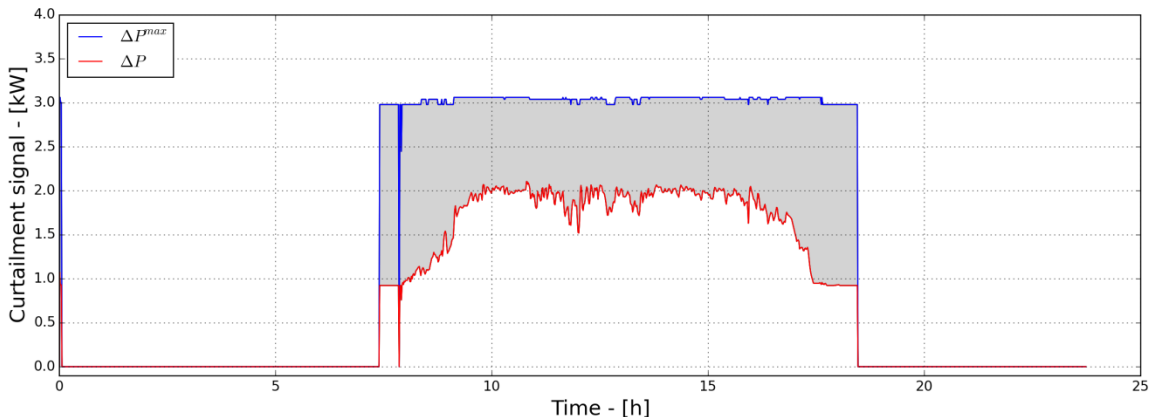


Figure 5-19 Power curtailment signal before and after the use of the S function

Reduction in active power injection required (ΔP^{max}) to ensure that voltage is reduced to the maximum permissible level is calculated using the estimated sensitivity matrix. As already discussed estimation of sensitivity matrix results in excessive curtailment. It should be noted that maximum permissible reduction ΔP^{max} is a function of the sensitivity matrix, the inverter rated power matrix P^{rated} and I the index of the node experiencing maximum voltage and not the voltage in the network. To reduce excessive curtailment, the S function has been used to make the active power curtailment set point ΔP a function of the maximum voltage in the network. The parameter A in Eqn (68) can be tuned by the DSO to achieve best results. In this experiment the value of A has been set to 2.5. The shaded area in Figure 5-19 shows the energy saved from potential curtailment during the course of the day’s simulation. The use of S function reduces curtailment set point for PVs and reduces E^{cur} from 31 kWh to 21 kWh (theoretical maximum curtailment) a reduction of 32.2%.

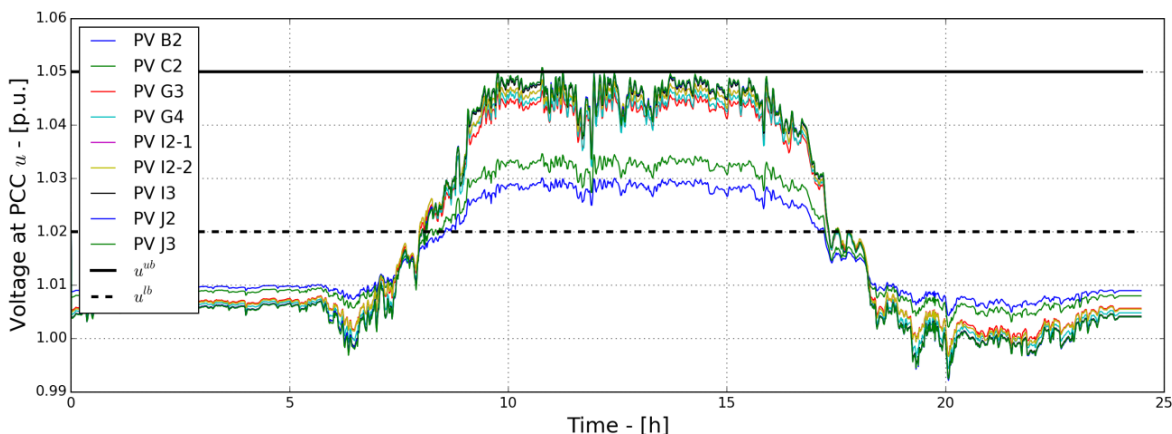


Figure 5-20 Voltage profiles at PCC of each inverter with CC1 control scheme

Figure 5-20 presents the voltage profiles at the PCC of each PV system. As can be seen from the graph, the coordination based methods is capable of regulating voltage and keeping it within the prescribed bounds. Figure is a plot of the power curtailed from each PV inverter. Comparing Figure 5-21 with Figure 5-14 mitigation of unfairness is evident. The difference in

time at which curtailment starts for each PV system is the consequence of dynamically varying loads.

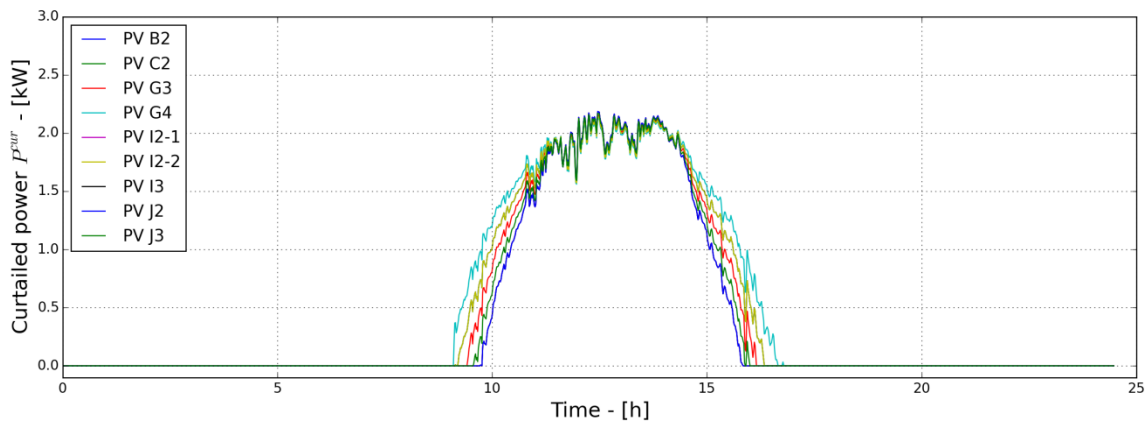


Figure 5-21 Curtailed power form each inverter using CC1 control scheme

CC1 control scheme tries to ensure that every PV system connected to the feeder participates equally in the voltage regulation process irrespective of the individual rating. This means that time of peak curtailment 2.2 kW is curtailed from PV B2 and PV J2 rated at 5 kW and 8 kW respectively. Curtailment of 2.2 kW results in 44% reduction in revenue for the owner of PV B2, while the owner of PV J2 suffers a reduction of 27.5%. To ensure that each PV owner participates fairly in the voltage regulation scheme a modification to the method has been proposed and the results have been presented in the next sub section.

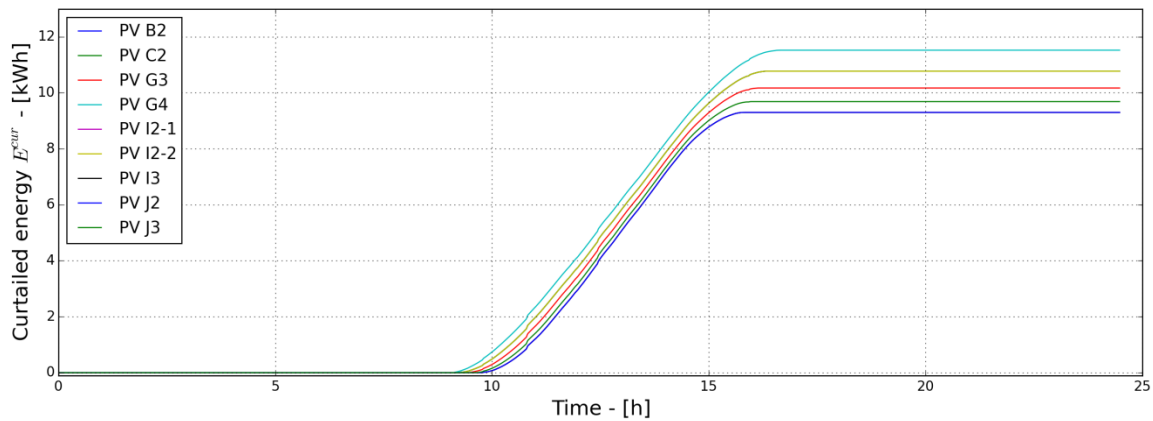


Figure 5-22 Curtailed energy form each inverter using CC1 control scheme

Results for coordinated control (CC2) - Second perspective of fairness

The second perspective of fairness aims at ensuring that each PV system installed on the feeder participates in voltage regulation depending on the rating of installed PV system. This

would result in equal percentage loss of revenue for each PV owner. The initial steps for the two variants of the coordination based APC scheme are the same. Initially, critical voltages u^{cri} for each of the inverter are calculated once the maximum voltage u^{max} in the network exceeds the lower voltage limit u^{ul} . Next, I the index of the node experiencing the maximum voltage is used to calculate the maximum expected voltage Δu^{max} in the network, which is further used to calculate the reduction in voltage Δu required to ensure over voltage does not occur. The next steps differ for the two coordinated controllers.

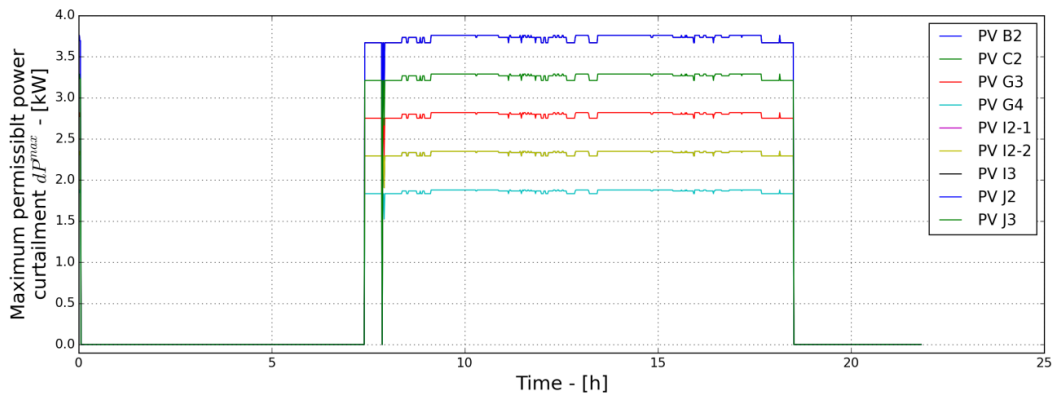


Figure 5-23 Power curtailment signals calculated for each inverter

For CC1 the reduction in active power curtailment required (ΔP^{max}) to ensure no over voltage is a single value for all PV inverters connected to the feeder. For CC2 however, ΔP^{max} is also the function the inverter rated power matrix P^{rated} thus ensuring that each PV owner contributed fairly in the voltage regulation process. As a result like P^{rated} , ΔP^{max} is also a $k \times l$ matrix for the CC2 control scheme. Figure 5-23 presents the reduction in active power injection required at each node to ensure over voltage does not occur. In the final step, the S function is used to ensure that excessive curtailment does not occur.

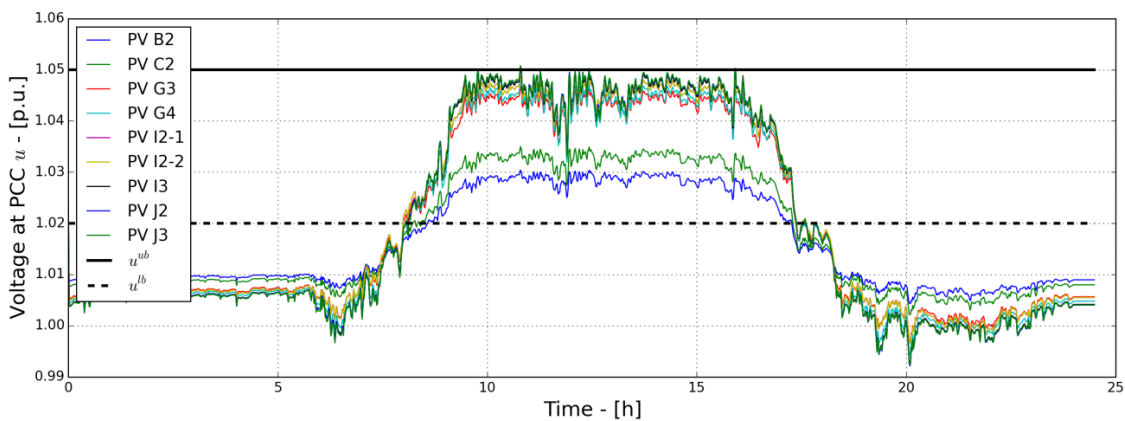


Figure 5-24 Voltage profiles at PCC of each inverter with CC2 control scheme

Figure 5-24 presents the voltage profiles at the PCC of each PV system. The plot shows that similar to the local APC solution and the first coordination based APC solution, CC2 is also capable of regulating the voltage within the prescribed voltage limits.

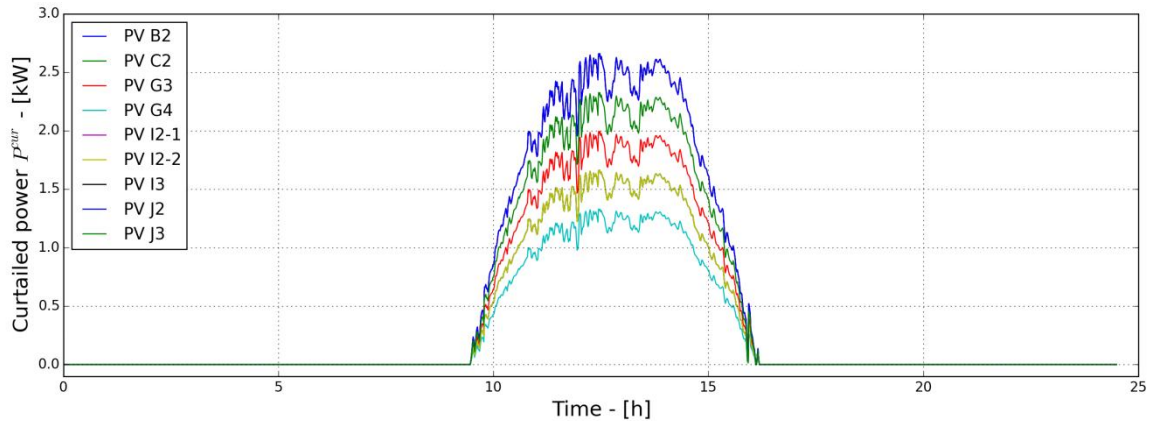


Figure 5-25 Curtailed power form each inverter using CC2 control scheme

The plot for the curtailed active power for each PV in Figure 5-25 shows that unlike CC1, the power curtailed from each PV is different. At time of peak generation, the active power curtailed from PV G4 rated at 4 kW is about 1.3 kW; however, active power curtailed from PV J2 rated at 8 kW is about 2.6 kW an increase of 100%. The per unit curtailment calculated by dividing the curtailed power by the rated active power output of the PV for the two PV systems is the same. Figure 5-26 is the plot for the total energy curtailed during the course of the day.

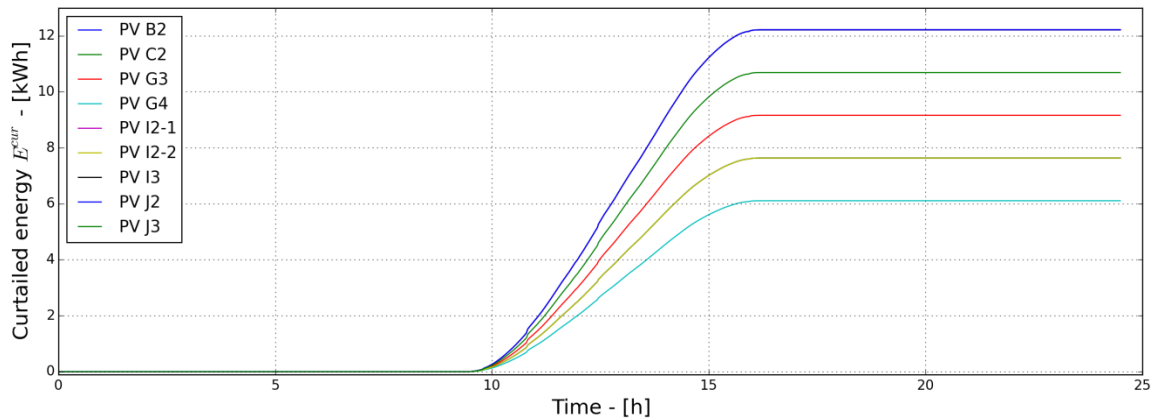


Figure 5-26 Curtailed energy form each inverter using CC2 control scheme

5.6.3 A comparison of results

From figure 5-27 it can be seen that for the local APC scheme for voltage control the curtailed energy varies between 1.97 kWh and 12.78 kWh almost a six fold difference. It should be noted that the energy curtailed tends to increase as the electrical distance from the transformer increases. The total energy curtailed from all PVs is 75.34 kWh. The energy curtailed from the first four PV systems amounts to 18.97 kWh or 25% of the total curtailed energy. The rest of the five PV systems therefore suffer the bulk of curtailed.

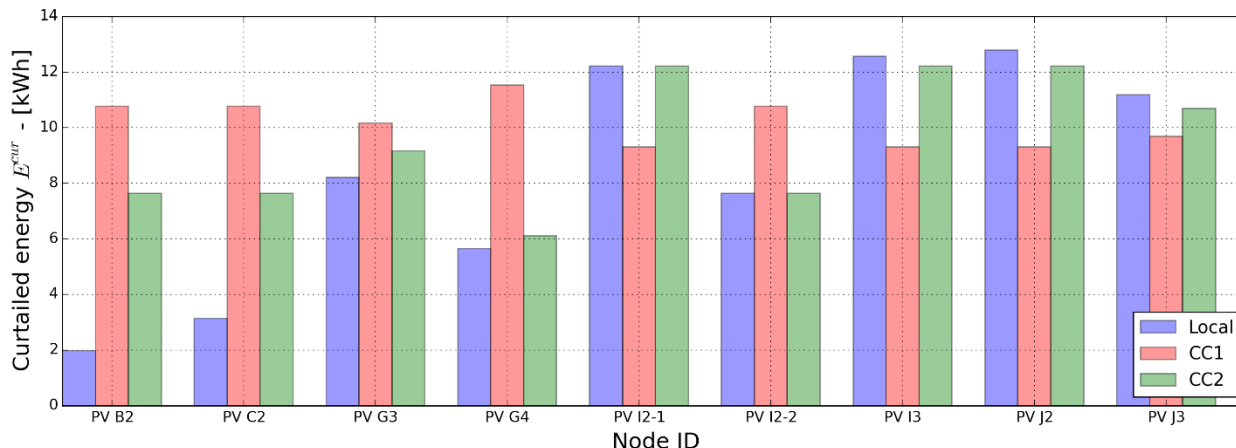


Figure 5-27 Energy curtailed from each inverter for the three APC control schemes implemented

In the first coordination based scheme (CC1), energy curtailed from each PV ranges from 9.30 kW – 11.52kW. Compared to local APC schemes mitigation in unfairness is quite evident. The coordinating controller ensures that the curtailment for every PV systems is approximately the same. One drawback of this scheme however, is that those PV owners with smaller ratings incur a bigger percentage decrease in revenue generated by the PV. At times of peak curtailment PV B2 rated at 5 kW gets 10.77 kWh curtailed, while PV J2 rated at 8 kW gets 9.3 kWh curtailed. Equal curtailment in active power results in a larger percentage decrease in revenue for PV owners with smaller rated outputs. From figure 5-27 it can be seen that using CC1 scheme results in significant increase in curtailment of some PV systems (PV B2, PV C2, PV G4) while results in a significant decrease in curtailment for other PV systems (PV I2-1, PV I3, PV J2).

In the variation of the coordinated control scheme (CC2), the curtailed energy from the PVs connected to the feeder ranges from 7.14 kWh to 14.2 kWh. The aim of the second variation of the coordinating controller is to generate curtailment set point based on the rated output of the PV system, thus enabling fair participation in voltage regulation scheme.

Table 5-5 Calculated KPI for the implemented control schemes.

	Local	CC1	CC2
TCE - kWh	75.34	91.61	85.52
CUI1 – kWh	4.12	0.82	2.39
CUI2 – h	0.453	0.606	1.61E-5

The use of the first variant of the coordinating controller (CC1) results in 21.5% increase in curtailed energy compared to the local APC scheme. This would mean additional loss of revenue for PV owners. For the second variant coordinating based APC scheme (CC2) the increase in energy curtailment in 11.3% compared to the local APC scheme. There is therefore a tradeoff between increasing fairness in curtailment and loss of green energy. For the chosen network using CC2 scheme results in significantly less curtailment compared to the CC1 scheme. Curtailment

unfairness index 1 (CUI1) reduces by 80% for CC1 and by 33% for CC2. CC1 has negligible impact on the second unfairness index (CUI2), while, CC2 reduces CUI2 to almost zero meaning every PV owner participates fairly in the APC scheme. The results show that CC2 is more efficient in achieving its objective reducing CUI2 by 99.99% compared to CC1 that reduced CUI by 80%.

5.6.4 Impact of control parameters

In the last sub section results for three APC schemes have been presented and discussed in detail. In this sub section the impact of varying two control parameters on voltage and total energy curtailment have been presented. As already discussed the S function used in Eqn. (68) is used to mitigate excessive curtailment by making the APC signal a function of the maximum voltage in the network. This ensures that maximum power is curtailed once voltage reaches the maximum permissible voltage limit. In mathematical terms $\Delta P \rightarrow \Delta P^{max}$ as $u^{max} \rightarrow u^{ub}$ and $\Delta P \rightarrow Zero$ as $u^{max} \rightarrow u^{lb}$. The parameter A in Eqn. (68) control the shape of S function’s curve. Figure 5-28 shows the impact of changing parameter A on total curtailed energy and the total duration of the over voltage seen in the network. Increasing A increases the slope of the S function resulting in an increase in total curtailed energy from 70 kWh to 107 kWh. This is an increase of 53 %. This shows that increasing the value of parameter A can significantly increase curtailment hence small values are preferable. Values of A smaller than 2 lead to insufficient curtailment and results in sharp increases in the duration of the over voltages experienced by the network. In this work there a tradeoff has been made and the value of A has been set at 2.5 for all simulations performed in the previous subsection.

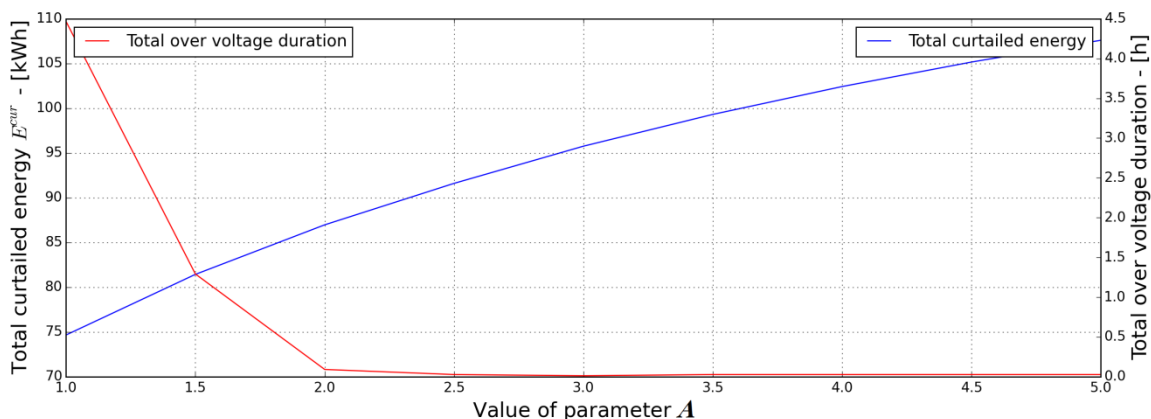


Figure 5-28 Impact of control variable A on energy curtailed and over voltage duration

The second parameter of importance in the selection of the voltage lower bound limit. Increasing the value u^{lb} reduces total curtailed energy. The reason is evident, increasing the value of u^{lb} reduces the voltage band during which curtailment is performed this results in reduced total energy curtailment. Increasing u^{lb} from 1.02 p.u. to 1.04 p.u. results in reduction in total curtailed energy of 8 kWh or 8.7%. Reducing the difference between u^{ub} and u^{lb} can adversely affect system stability as even small changes in the voltage at the PCC will lead large changes in active

power injection in the feeder. Rapidly changing active power injection and voltage lead to deteriorated power quality. Figure 5-29 shows that increasing u^{lb} increases both the peak voltage seen in the feeder and total duration of the overvoltage. Therefore, although increasing the value of u^{lb} decreases the total curtailed energy it should not be increased to an extent that it leads to system instability.

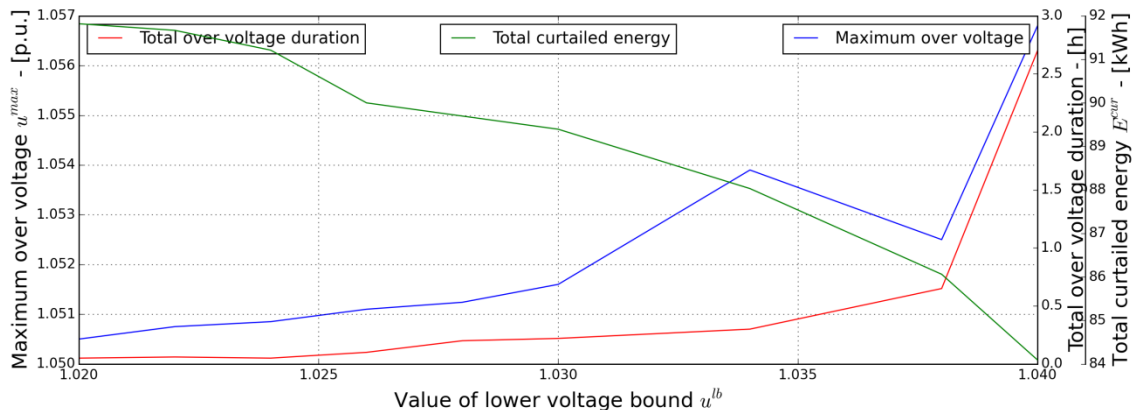


Figure 5-29 Impact of control varying the lower voltage bound on energy curtailed, over voltage duration and the peak voltage experiences by the network

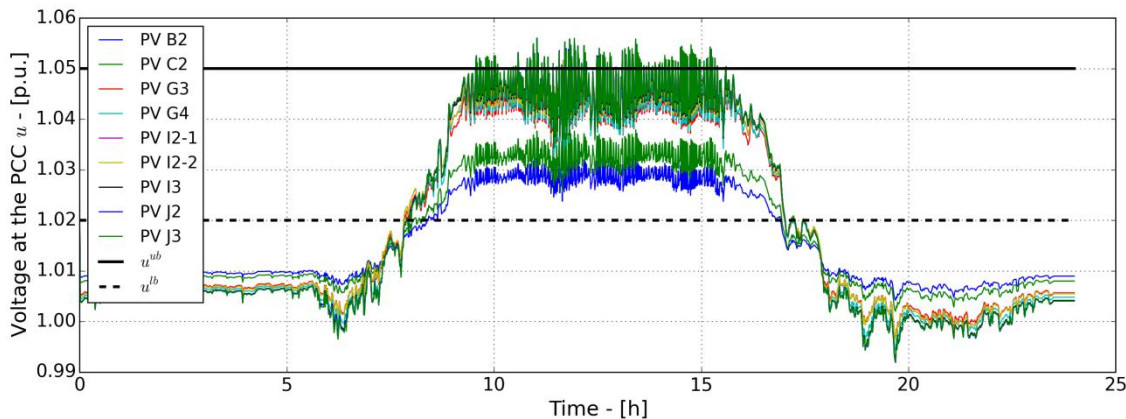


Figure 5-30 Impact of a high value of lower voltage bound on voltage fluctuations

5.6.5 Impact of communication delay and failure on the proposed scheme

As has already been discussed, the coordination based schemes require information from the entire network. Real world implementation of the proposed method therefore requires communication infrastructure. Up until now, an ideal communication channel has been assumed. In reality however, packet loss, network congestion and limited channel bandwidth leads to delays in communication. It is therefore important to understand the impact of communication delays on the proposed coordination based scheme.

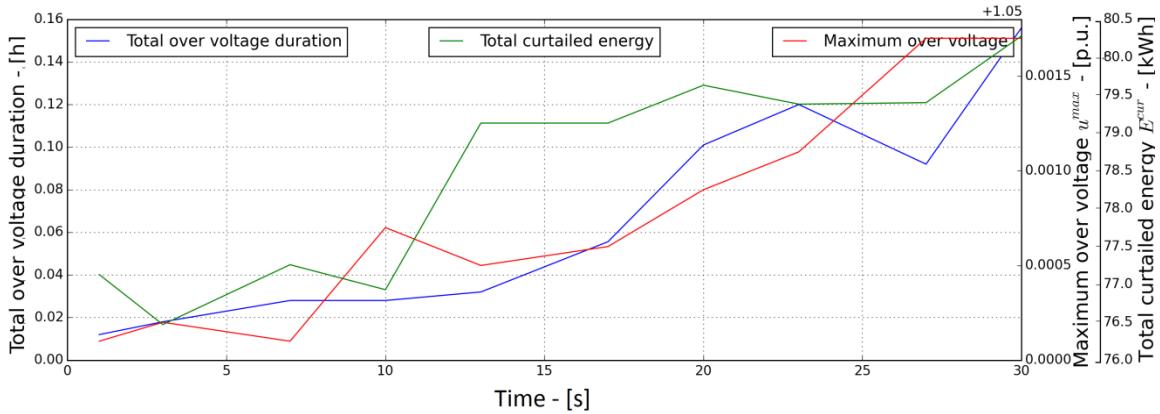


Figure 5-31 Impact of communication delay on over voltage duration and peak network voltage on a sunny day

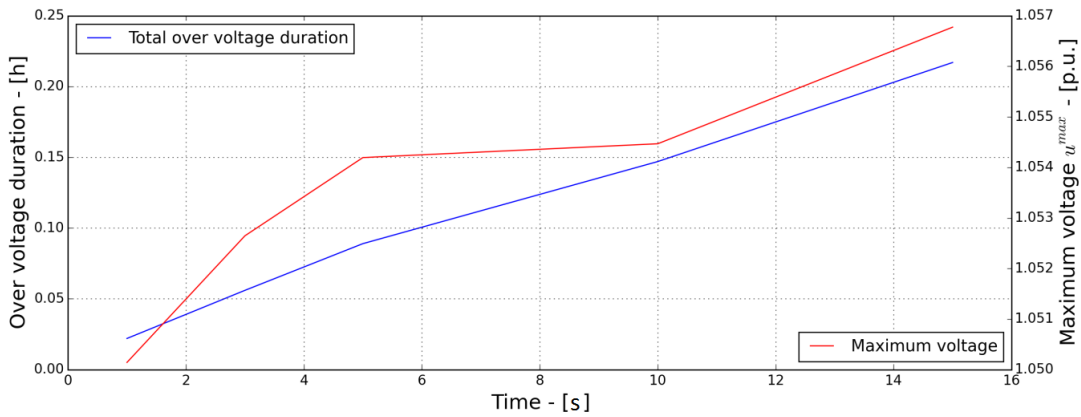


Figure 5-32 Impact of communication delay on over voltage duration and peak network voltage on a cloudy day

Delay in communication results in coordinating controller lagging behind the current state of the network. Comparing results in Figure 5-31 and 5-32 it can be seen that network voltage is much more sensitive to communication delays on days with intermittent cloud cover. Stochastic weather pattern can result in large deviations in active power injection and consequently the network voltage. Even a small delay in communication can result in large errors in the set points calculated by the coordinating controller.

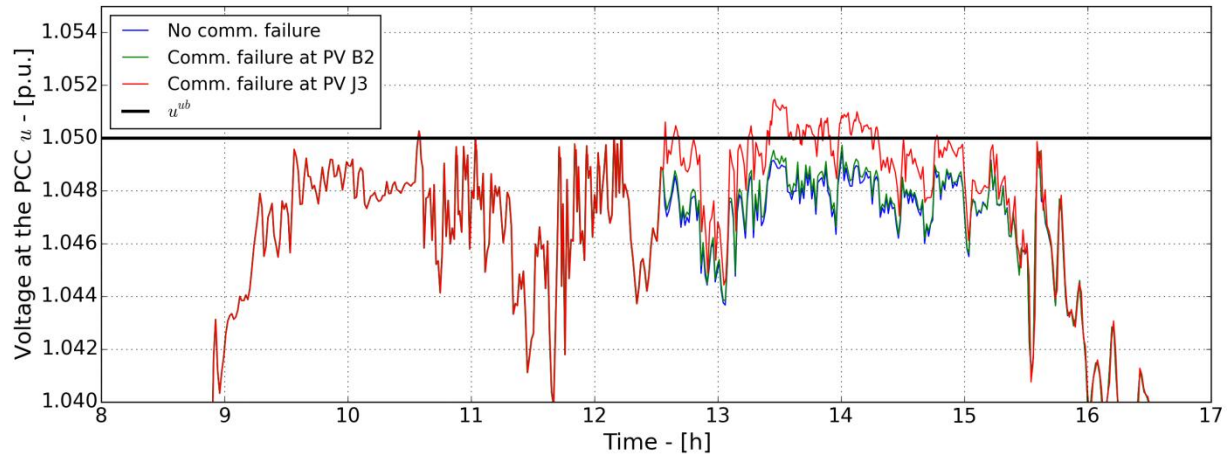


Figure 5-33 Impact of communication failure on peak voltage

Figure 5-33 presents the results for maximum over voltage in the network for three scenarios. The first scenario is for an ideal communication channel with no communication failure. In a scenario when there is no communication failure, the state of the voltage at PCC of PV systems is known. In such a scenario, controller does well to ensure that no over voltage occurs. In the second scenario at 1 pm the communication link between PV B2 and the coordinating controller fails. In such a scenario, state of part of the network is not known this causes a slight rise in the maximum voltage seen in the network. In the final scenario, the communication link between PV J3 and the coordinating controller is severed at 1 pm causing the voltage to rise significantly and resulting in multiple over voltage instances. Voltage rise due to communication failure is sensitive to the electrical distance of PV with the severed communication link. Communication failure for PVs further away from the transformer increase the likelihood of over voltage occurring.

5.7 Conclusion

Increasing the penetration of distributed energy resources in LVN can result in voltage limits being violated. Reactive power compensation is one method of voltage regulation. In LVNs however, high R/X ratio reduce the effectiveness of RPC based voltage control schemes. Additionally, in a number of countries grid codes do not permit individual PV owners to compensate reactive power. In such a scenario, active power curtailment is alternate approach for regulating the voltage at the PCC. Voltage sensitivity is the function of the electrical distance between the transformer at the PCC of the PV and the grid. Local APC scheme is inherently unfair as PV systems connected further along the LV feeder are more susceptible to voltage violation and getting the power from the PV system curtailed.

In this chapter a sensitivity based plug and play control strategy has been introduced to mitigate this unfairness in curtailment and ensuring all PV owners participate in the voltage regulation process. In the context of this analysis, the following technical aspects were considered to be of special interest:

- Understanding the impact of parameters like branch line length and branch position on sensitivity matrix estimation error.
- Analyzing the coordinating controller's performance regarding mitigation of unfairness in APC and impact on the total energy curtailed.
- Analyzing the performance of the coordination based voltage control strategies against variations in control parameters.
- Analyzing the robustness of the coordination based voltage control against communication delays and failures

As a basis for this investigation, PV has been modeled as a negative load. The local APC controller has been implemented in using DIgSILENT simulation language (DSL) in PowerFactory. The coordination controller has been implemented in Python and the communication between the two controllers has been achieved via sockets.

Approximation of the sensitivity matrix results in excessive curtailment. To avoid this, an S function has been used to mitigate excessive curtailment by making the curtailment set point a function of the maximum voltage in the network and not only the sensitivity matrix and the rated inverter power. The G can DSOs control over the extent of curtailment

KPIs used for comparison have been derived in Section 5.4. Two variations of the coordination controller have been simulated each mitigating unfairness from a different perspective. The results show that although the mitigation of unfairness is possible, it comes at the cost of total curtailment. This results in loss of revenue for PV owner.

Results obtained by varying control parameters show that voltage regulation is much sensitive to both the value chosen for voltage lower bound and the value of the parameter A . From DSO's perspective, small value for voltage lower bound is advisable as it smooths out the transients; however, it results in a higher curtailed energy although the increase is not very significant. Similarly, choosing the right value for parameter A is critical as total curtailed energy has a strong correlation to the value of A and even a small change in the value of A results in a significant change in total curtailed energy.

Finally, simulations results show that impact of communication delays on the proposed method on a sunny day is insignificant. On an intermittently cloudy day however, delays in communication can lead to significant over voltages within the network. DSOs have the option of tuning the parameter A depending on the weather forecast to mitigate overvoltage resulting from communication delays. Finally, results for simulated communication failure show that failure of PVs further away from the transformer increase the likelihood of over voltage occurring.

6. Combined frequency and voltage regulation using DSM

6.1 Introduction

Maintaining balance between generation and demand close to real time is the primary objective of AC electrical grid. Balancing generation and demand is not trivial. In case the demand exceeds generation, the difference is compensated by conversion of kinetic energy of the rotors to electrical energy. Loss of kinetic energy causes in the rotor's speed to decrease resulting in depressed frequency. A governor is typically uses the error signal (difference between the actual frequency and the set point) to recover and maintain set point frequency [148].

Long term load variation is a result of factors such as seasonal load patterns or dynamic weather patterns. These factors can be predicted with reasonable accuracy and can be accounted for when calculating day a head generation schedules for the dispatchable generation resources. Real time load fluctuations however are a result of millions of individual loads stochastically turning on and off during the day. These patterns are unpredictable thus to ensure system stability and reliability of supply frequency regulation is necessary. Ever increasing share of renewable energy in the total energy mix has increased uncertainty in generation thereby increasing probability of power imbalance within the electrical grid [149]. Conventional methods for frequency regulation require generators to maintain a reserve to cater to these power imbalances. Increase in generation uncertainty has increased the cost of keeping a minimum frequency reserve. In such scenarios alternate methods for frequency support need to be explored. Demand side management is a promising candidate for providing frequency support. International Energy Agency estimates that every \$ 1 investment in DSM is equivalent to \$ 2 investment in upgrading generation capabilities [150].

Traditionally, frequency regulation has been the TSO's responsibility. DSM based frequency support has been an active research topic in recent years. Appliances such as refrigerators, heaters and air conditioners are characterized as thermostatically controlled loads (TCLs). Principal of thermal inertia allows control of TCLs without compromising on the comfort of the end customer. The aggregation of TCLs can be viewed as distributed energy storage with dynamic flexibility. In [151] and [152] a stochastic battery model for aggregated TCL control has been proposed. The proposed method allows DSO to provide ancillary services like frequency support. This chapter builds upon the work presented in the above mentioned papers and explores the possibility of providing an additional ancillary service (voltage support).

Voltage violation is a local problem and should ideally be solved using local resources. In radial networks, change in voltage at any node of a function of the line parameters and the net active and reactive power injection at the node. By changing the switch status of TCLs connected within a network, the voltage profile can be altered. In this chapter a DSM based frequency and voltage regulation method is being proposed.

6.2 Control modeling

6.2.1 TCL controller modeling

Principals of thermal inertia allows interruption of load without affecting the comfort of the end consumer. A bang bang contoller is used with most heating and cooling devices to ensure that the temperatue is regulated in a predefined deadband around the set temperature (Figure 6-1). The dyanmics of a TCL can be modelled using a the difference equation.

$$\theta^i[k+1] = g^i\theta^i[k] + (1 - g^i)(\theta_a[k] - \delta^i[k]\theta_g^i) + \epsilon^i[k], \quad (77)$$

Where,

$$g^i = e^{-h/(R^iC^i)} \quad (78)$$

$$\theta_g^i = R^iP^i\eta^i \quad (79)$$

Where, h is the sampling time, R^iC^i is the time constant of the TCL, $\theta_a[k]$ is the ambient temperature at time k and P^i is the rated power of the TCL. The difference equation defines the dynamics of the system by calculating the impact of the state of the TCL on the temperature at the previous time step. The final term $\epsilon^i[k]$ is the error in temperature measurement and has been sampled from a normal distribution with mean 0°C and a standard deviation of 0.5°C .

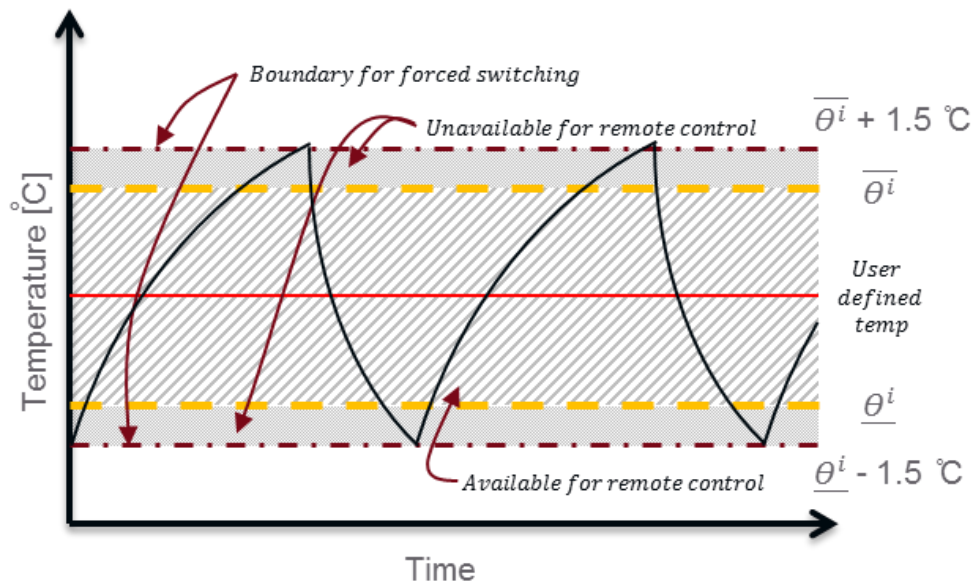


Figure 6-1 Illustration explaining the dynamics of a TCL and the proposed local control scheme

Once the temperature reaches the upper or the lower boundary a hard switch overrides the current switching state of the TCL and the TCL is switch on or off depending on which temperature boundary has been reached. To avoid excessive hard switching, a temperature region has been defined within the hard upper and lower temperature limits (shown in Figure 6-1 as slanted lines).

A TCL is available for DSM participation only if the internal temperature lies within this region. The equations for hard switching are as follows.

$$\delta^i[k+1] = \begin{cases} 1 & \theta^i[k+1] > \bar{\theta}^i + 1.5 \\ 0 & \theta^i[k+1] < \underline{\theta}^i - 1.5 \\ \delta^i[k] & \text{otherwise} \end{cases} \quad (80)$$

Each TCL takes remote control signal $\beta^i[k]$ as inputs, it updates its on switching state $\delta^i[k]$ using the control algorithm detailed in Algorithm 6-1. The parameters such as TCL availability $\lambda^i[k]$ and the relative temperature distance from the switching boundary $\pi^i[k]$ are calculated by the local controller and sent to the coordinating controller, which uses these values for the decision making process.

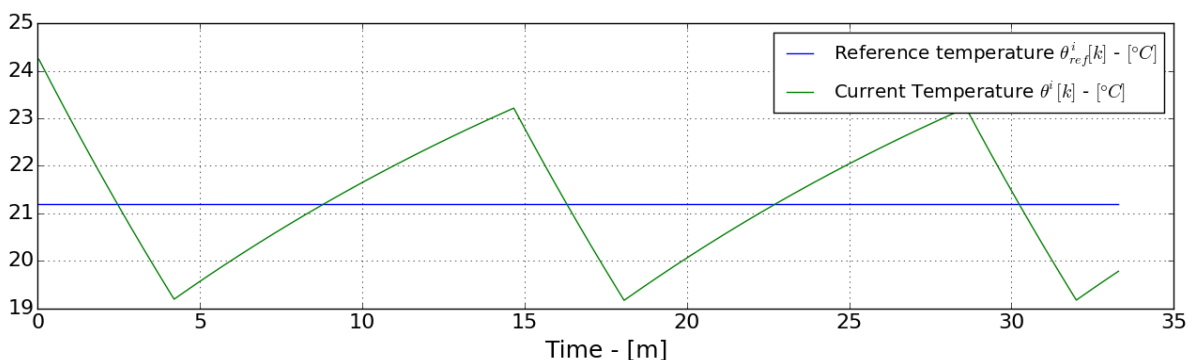


Figure 6-2 Current and reference temperature profiles for the TCL connect at node 118

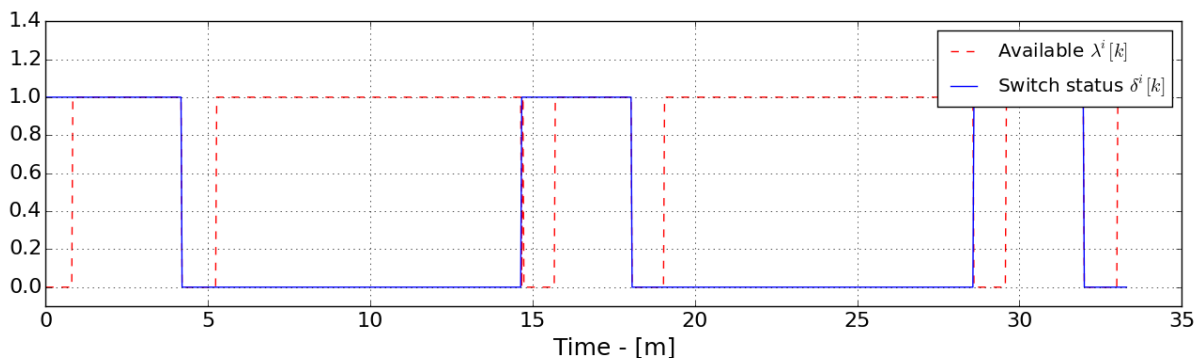


Figure 6-3 Time profile for the switch status and the availability of the TCL connect at node 118

In addition to the temperature constraint, a cyclic constraint has also been implemented in for the local controller. Once the switching status of the TCL changes, it is unavailable for participation in DSM for a predetermined period of time. This ensures that TCLs are protected from excessive switching. Hard switching at temperature boundaries also resets the cycling constrain. A TCL is available only if the cyclic constraint is satisfied and the temperature is with the soft switching range.

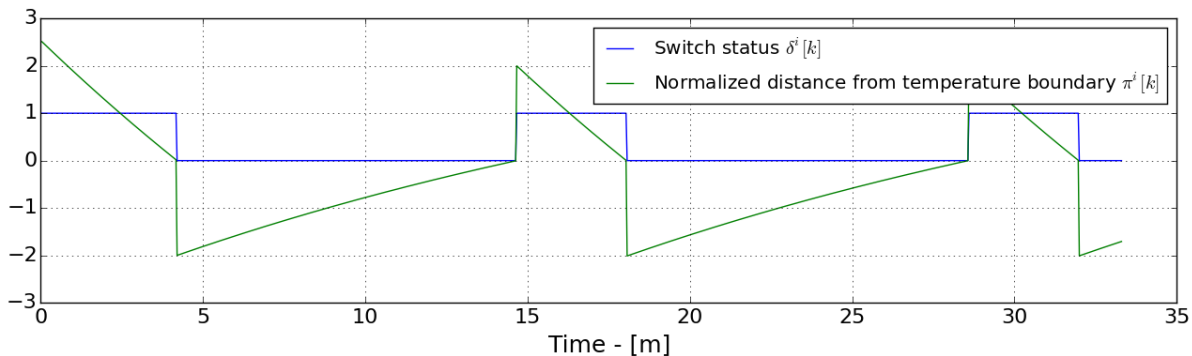


Figure 6-4 Time profile for the switch status and normalized distance from the temperature boundary for the TCL connect at node 118

At time of steady state operation, the temperature θ^i is equal to the set reference temperature θ_{ref}^i . In such a scenario, average power consumption can be calculated using the equation [153],

$$P_O^i[k] = \frac{\theta_a^i[k] - \theta_{ref}^i[k]}{R^i \eta^i} \quad (81)$$

Therefore, the aggregate average power consumption of all TCLs can be calculated using the equation.

$$P_{base}[k] = \sum_{i=1}^N P_O^i[k] \quad (82)$$

Where N is the total number of TCLs. Actual power consumption at any time k can be calculated by adding the rated powers of the TCL on at the time. Mathematically, this can be expressed using the equation,

$$P_{agg}[k] = \sum_{i=1}^N \delta^i[k] \cdot P^i \quad (83)$$

The power deviation signal can be calculated by calculating the difference between actual and average power consumption using the equation

$$\psi[k] = P_{agg}[k] - P_{base}[k] \quad (84)$$

The aggregation of TCLs has been modeled as a battery that can be charged or discharged depending on the input reference signal $r[k]$. In case $r[k] > \psi[k]$, the battery charges and TCLs are turned on. In case $r[k] < \psi[k]$ the battery is in the state of discharge and TCLs are turned off. TCLs can be used for frequency regulation if the reference power imbalance signal can be followed in real time. The parameters for the stochastic battery limits have been presented in [151].

Algorithm 6-1 Algorithm for local TCL controller

Input: control signal $\beta^i[k]$, voltage at PCC $u^i[k]$,

Output: status $\beta^i[k+1]$, availability $\lambda^i[k+1]$, normalized temp. distance $\pi^i[k+1]$

$$1 \quad \theta^i[k+1] = g^i \theta^i[k] + (1 - g^i)(\theta_a^i[k] - \delta^i[k] \theta_g^i) + \epsilon^i[k]$$

$$2 \quad \text{if } \rho^i[k] > \overline{\rho^i} \text{ then}$$

$$3 \quad \quad \text{if } \underline{\theta^i} \leq \theta^i[k+1] \leq \overline{\theta^i} \text{ then}$$

$$4 \quad \quad \quad \lambda^i[k+1] = 1$$

$$5 \quad \quad \quad \text{if } \beta^i[k] = 1 \text{ then}$$

$$6 \quad \quad \quad \quad \delta^i[k+1] = 1; \rho^i[k+1] = 0$$

$$7 \quad \quad \quad \text{else if } \beta^i[k] = -1 \text{ then}$$

$$8 \quad \quad \quad \quad \delta^i[k+1] = 0; \rho^i[k+1] = 1$$

$$9 \quad \quad \quad \text{Else}$$

$$10 \quad \quad \quad \quad \delta^i[k+1] = \delta^i[k]$$

$$11 \quad \quad \text{else if}$$

$$12 \quad \quad \quad \lambda^i[k+1] = 0; \delta^i[k+1] = 0; \rho^i[k+1] = 0$$

$$13 \quad \quad \quad \text{Else}$$

$$14 \quad \quad \quad \lambda^i[k+1] = 0; \delta^i[k+1] = 1; \rho^i[k+1] = 0$$

$$15 \quad \quad \text{Else}$$

$$16 \quad \quad \quad \lambda^i[k+1] = 0$$

$$17 \quad \quad \quad \text{if } \theta^i[k+1] < \underline{\theta^i} - 1.5 \text{ then}$$

$$18 \quad \quad \quad \quad \theta^i[k+1] = 0; \rho^i[k+1] = 0$$

$$19 \quad \quad \quad \text{else if } \theta^i[k+1] < \overline{\theta^i} + 1.5 \text{ then}$$

$$20 \quad \quad \quad \quad \theta^i[k+1] = 1; \rho^i[k+1] = 0$$

$$21 \quad \quad \quad \text{Else}$$

$$22 \quad \quad \quad \quad \delta^i[k+1] = \delta^i[k]$$

$$23 \quad \rho^i[k+1] = \rho^i[k] + 1$$

$$24 \quad \text{if } \delta^i[k+1] = 1 \text{ then}$$

$$25 \quad \quad \pi^i[k+1] = (\theta^i[k+1] - \underline{\theta^i}) / \Delta^i$$

$$26 \quad \text{if } \delta^i[k+1] = 0 \text{ then}$$

$$27 \quad \quad \pi^i[k+1] = (\overline{\theta^i} - \theta^i[k+1]) / \Delta^i$$
6.2.2 Coordinating controller

Each TCL participating in DSM uses Algorithm 6-1 to calculate its availability, current switching status and temperature distance from the switching boundary to and communicate it to the coordinating controller. It has been assumed that the coordinating controller has knowledge of each TCL's rated power. Finally, for the TCLs available for participation in DSM two priority stacks are created one for TCLs that are currently on and the second one for the TCLs that are currently off. TCLs list is in increasing temperature distance. The reference power deviation signal is tracked by switching the state of the TCLs, with TCLs with smallest distance to switching boundary having higher switching priority. Figure 6-5 gives a graphical overview of the simulation setup. The pseudo code for the coordinating controller has been presented in Algorithm 6-2.

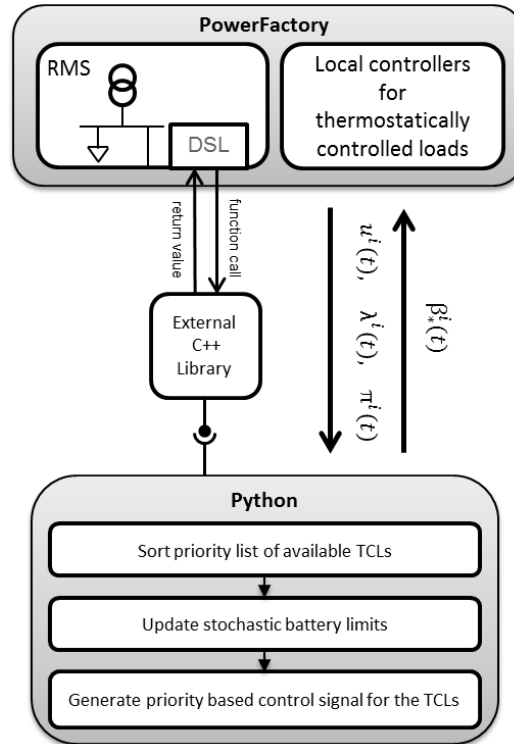


Figure 6-5 Graphical overview of the simulation setup

Algorithm 6-2 Algorithm for the coordinating controller

Input: status $\beta^i[k + 1]$, availability $\lambda^i[k + 1]$, normalized temp. distance $\pi^i[k + 1]$

Output: Forced state of the TCL β_*^i

- 1 Calculate battery parameters (C, n_+, n_-)
- 2 **for** $t := 1 \dots T$ **do**
- 3 Sample input frequency regulation signal $r[k]$
- 4 **for** $i := 1 \dots N$ **do** (*TCL iteration loop*)
- 5 Sort priority list of available TCLs
- 6 Update stochastic battery limits (C', n'_+, n'_-)
- 7 **if** ($R'_+ \leq r[k] \leq R'_-$) **then**
- 8 $\xi = r[k] - \psi[k]$
- 9 **if** $r[k] < \psi[k]$ **then** (*Priority list based control*)
- 10 Turn Off available TCLs till $\delta P < \xi$
- 11 **else**
- 12 Turn On available TCLs till $\delta P < -\xi$
- 13 **if** $\delta^i[k + 1] = 1$ **then**
- 14 *Regulation not possible*

6.3 Simulation setup

6.3.1 Network model

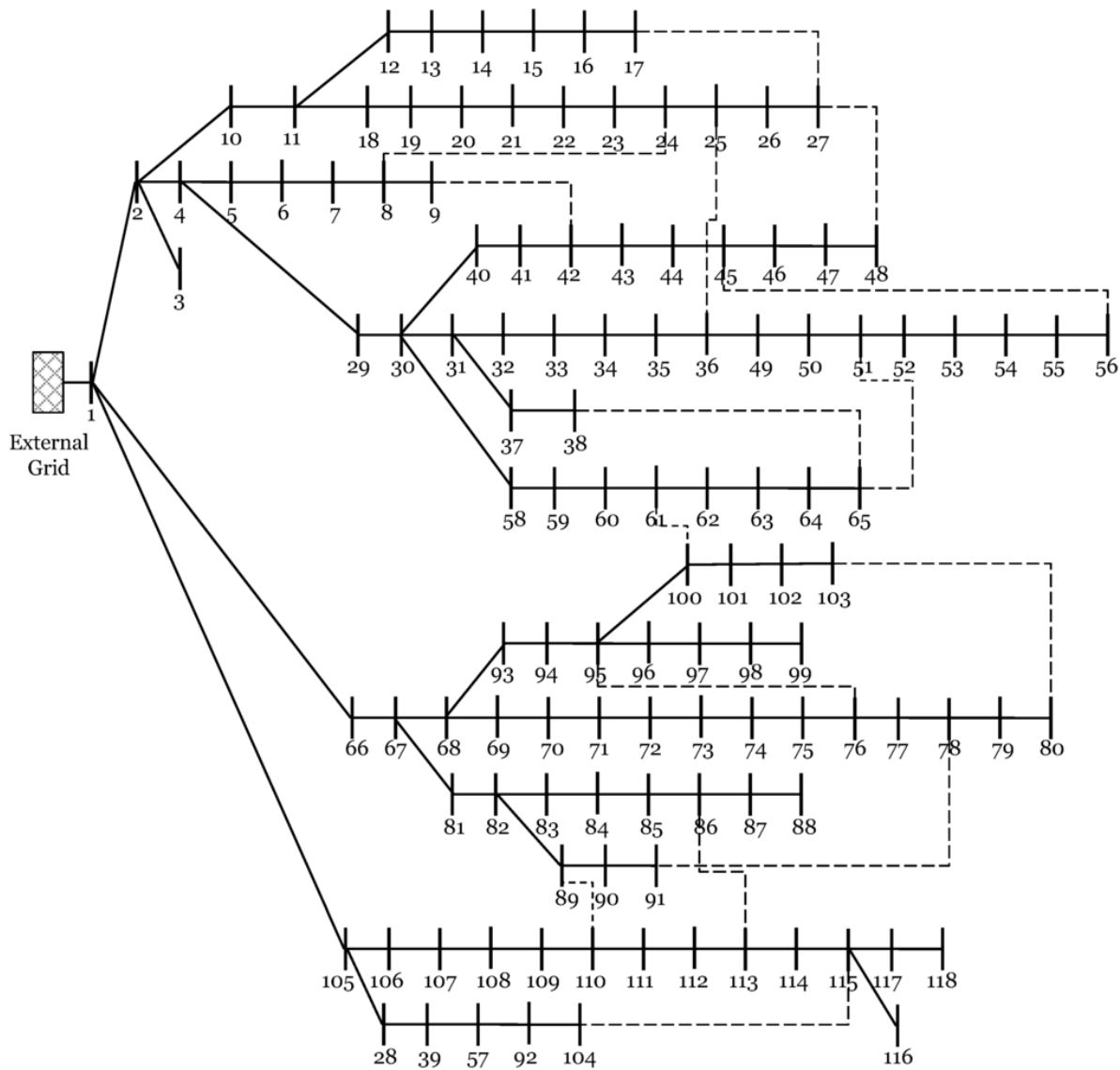


Figure 6-6 The 119 node test feeder

The proposed method has been implemented and tested in a hypothetical 119 node MV test feeder [154] (Figure 5-6). TCLs have been randomly sized between 15% and 25% percent of the total load connected at the node. For the experiment, the short cycling constraint has been set at one minute. The power deviation reference signal has been sampled at 2 sec interval. Finally, the thermal dynamics of the building have been modeled as equivalent RC model.

6.3.2 Co-simulation setup

TCL dynamics and the local controller responsible to calculating availability, switching status and the distance from the temperature boundary have been implemented in PowerFactory using DSL blocks. The biggest advantage of implementing the local controller in PowerFactory is that changing the local models automatically updates all local controllers. One limitation of PowerFactory however is the inability to perform matrix calculations required to create priority stacks. To overcome this shortcoming, the coordinating controller has been implemented in Python, a high level scripting language capable of performing complex matrix manipulations. The coupling between the two has been achieved using a C library that enables DSL models to communicate information via sockets. Figure 6-5 gives a graphical overview of the coupling scheme used in this simulation setup.

6.4 Results and discussion

6.4.1 Base case: no voltage consideration

Figure 6-7 shows the tracking performance of the algorithm proposed in [152] on the hypothetical 119 node test feeder. A number of important observations can be made from the plot. First, the tracking signal follows the reference power deviation signal fairly accurately. This shows that an aggregate of TCLs can be used for frequency regulation without compromising on consumer comfort. This can potentially, reduce frequency reserve required from the online generator and can potentially save revenue.

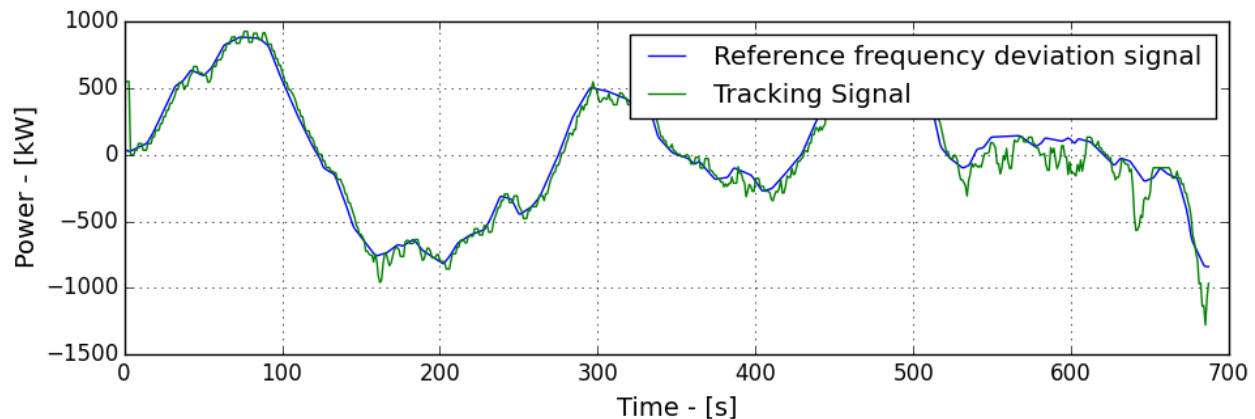


Figure 6-7 Base case reference signal tracking performance

Deviations in tracking occur due to several reasons

- **Discrete nature of a TCL load** – A TCL switching event is discrete in nature and results in an abrupt change in the tracking signal. Additionally, the ratings of TCLs vary and changing the switch state of a TCL with a high rating results in a larger deviation.

- **Limited resources** – Large deviations in tracking occur when resources are depleted (availability of TCLs in low) due to the cyclic constraint placed on remote switching.
- **Forced switching at temperature boundary** – If the internal temp of the reaches either the minimum or maximum permissible temperature, the switch status of the TCL is changed forcefully. This can also results in deviation in tracking.

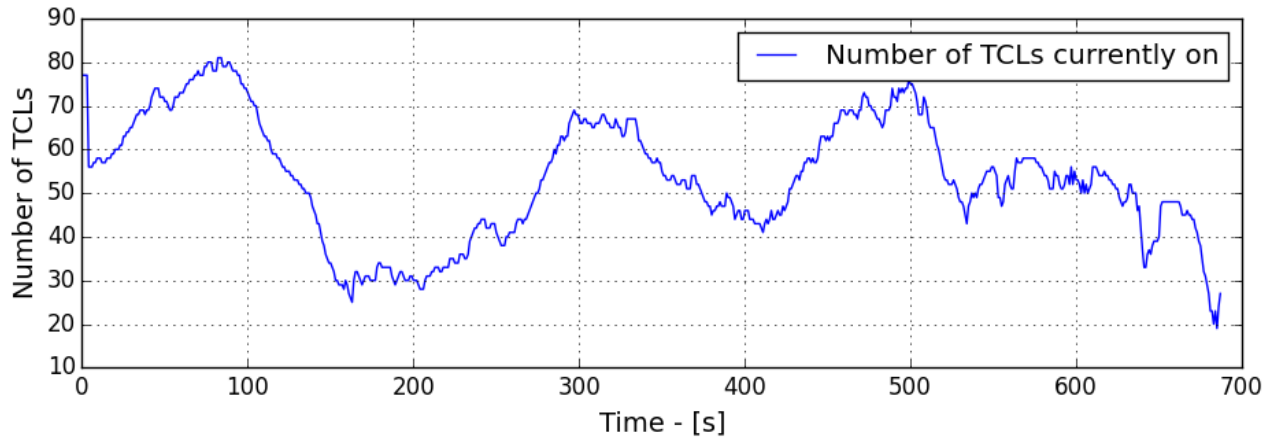


Figure 6-8 Time profile for the number of TCLs on at any given time

As already discussed, in case the reference signal $>$ the tracking signal, the aggregate battery model is in the state of charging and available TCLS are turned on. From Figure 6-7 it can be seen that for the time period between 0 *sec* and 80 *sec*, the tracking signal lags the reference signal. This causes the coordinating controller to turn on available TCLs that are currently off. Similarly, between the time 90 *sec* and 140 *sec* the tracking signal exceeds the reference signal. This causes the aggregate battery model to discharge and turn off TCLs that are currently on and available. This phenomenon is clear from the plot in Figure 6-8. For the first 80 *sec* the number of TCLs currently on rises as the battery charges and turns on available TCLs. After the 90 *sec* mark, the number of on TCLs decreased as the aggregate battery model discharges.

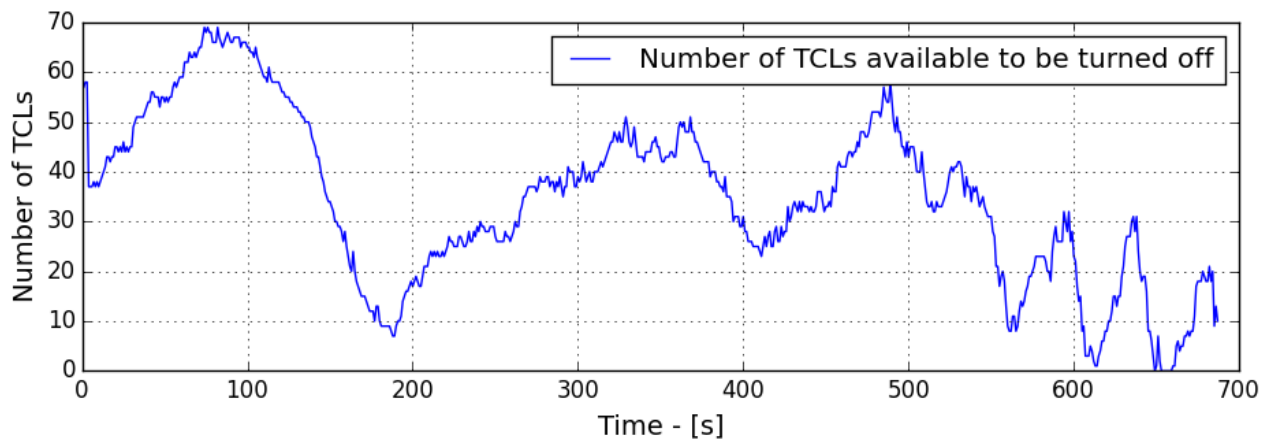


Figure 6-9 Time profile for the number of TCLs available to be turned off

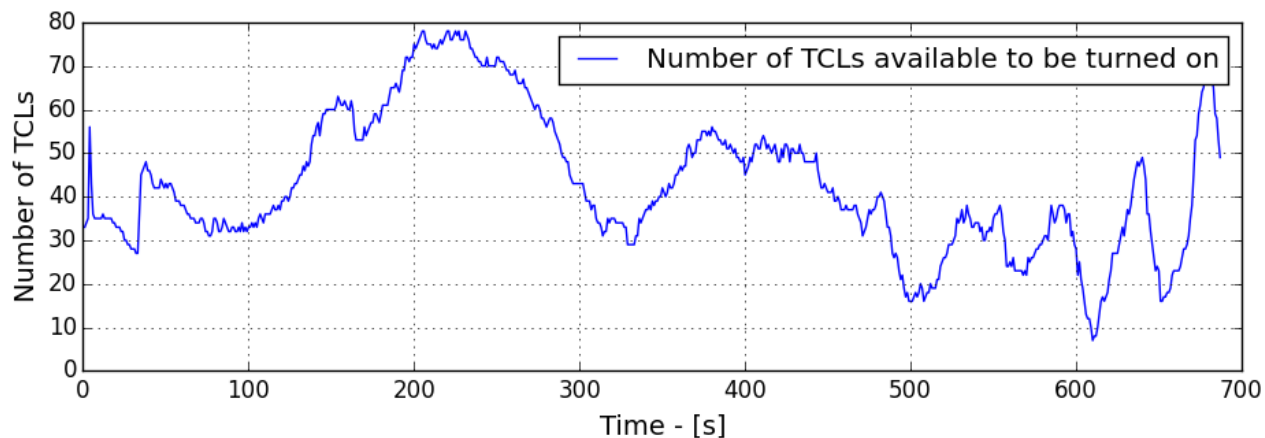


Figure 6-10 Time profile for the number of TCLs available to be turned on

Charging and discharging cycle of the aggregated TCL battery model impacts the availability of TCLs for participation DSM. Between 0 *sec* and 80 *sec* the number of TCLs available to be turned off increase as the coordinating controller turns on more are more TCLs as can be seen from Figure 6-9 and 6-10. It is important to note that availability of TCLs in dependent on the value of the cyclic constraints time constant. Longs periods of unavailability will reduce the number of switching operations but will lead to unavailability of TCL resources and poorer tracking performance.

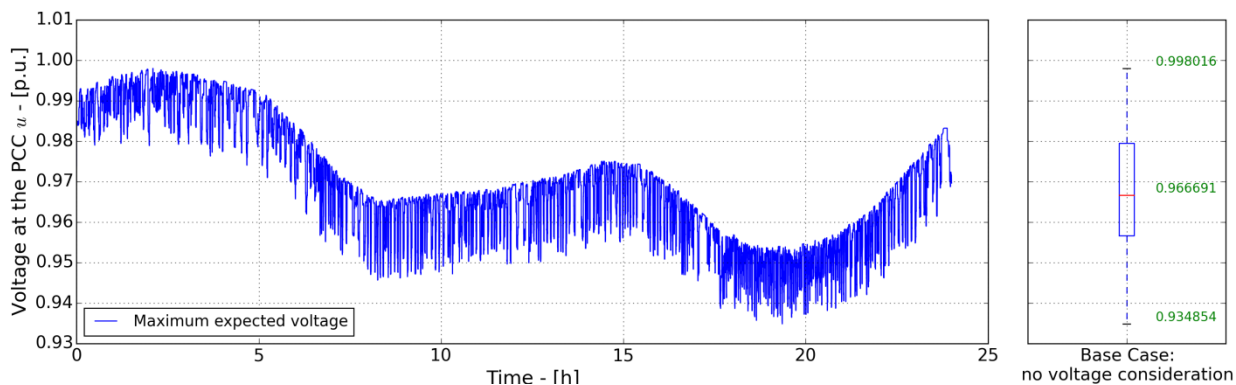


Figure 6-11 Base case voltage profile; box plot for the voltage profile

In radial networks the change in voltage at the PCC is also a function of the net active power consumption at the node. TCL based DSM schemes require switching of individual loads. Switching being a discrete event leads to fluctuations in the voltage and deterioration in power quality. In certain scenarios, the voltage may also violate the bounds prescribed by international standards. As voltage sensitivity is a function of the electrical distance from the transformer, consumers connected at the end of a radial are most prone to voltage violation. Figure 6-11 is the base case voltage profile for node 118. The plot shows voltage violates the lower permissible voltage limit on multiple occasions. The box plot shows the maximum and the minimum voltage seen at node 118 during the day’s simulation.

6.4.2 Study case 1: Penalizing voltage violation by forced switching

In the study case, TCLs connected to nodes experiencing voltage violation are forcefully turned on or off depending on whether the upper or lower voltage boundary has been violated. In this simulation study TCLs with voltage at the PCC below 0.955 p.u. are forcefully turned off until the time voltage violation is no more. As can be expected, forcefully turning off TCL results in deteriorated tracking performance during times of voltage violation. The figure below is the plot for the reference signal tracking performance.

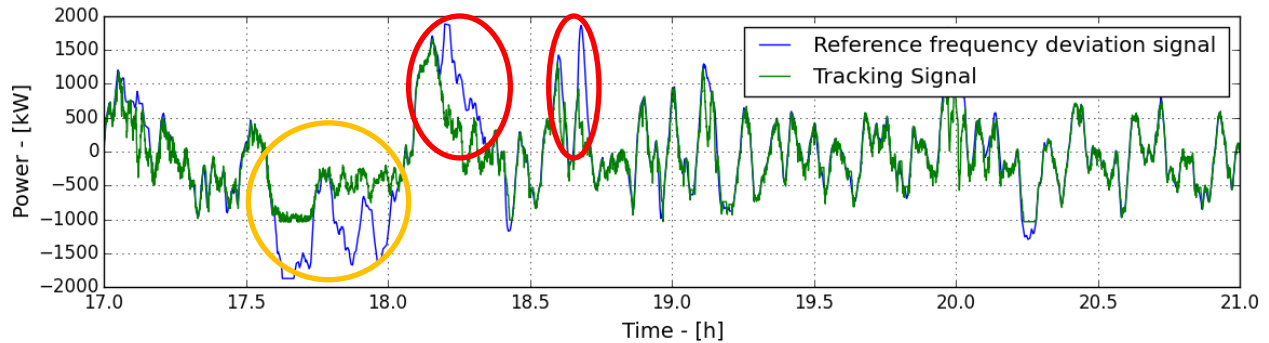


Figure 6-12 Impact of forced switching on reference signal tracking

Forcefully turning off TCLs experiencing voltage violation drastically reduced the number of TCLs that are available to be turned off. This results in a large deviation depicted by the yellow circle. When tracking signal exceeds the reference signal the battery in operating in discharging mode. To be able to track the reference signal it requires to turn off TCLs that are available and currently on. Unavailability of TCLs in such a state results in large deviations in tracking. The voltage violation ends at time 20.3 *hour* resulting in increase in the availability of TCLs that are on.

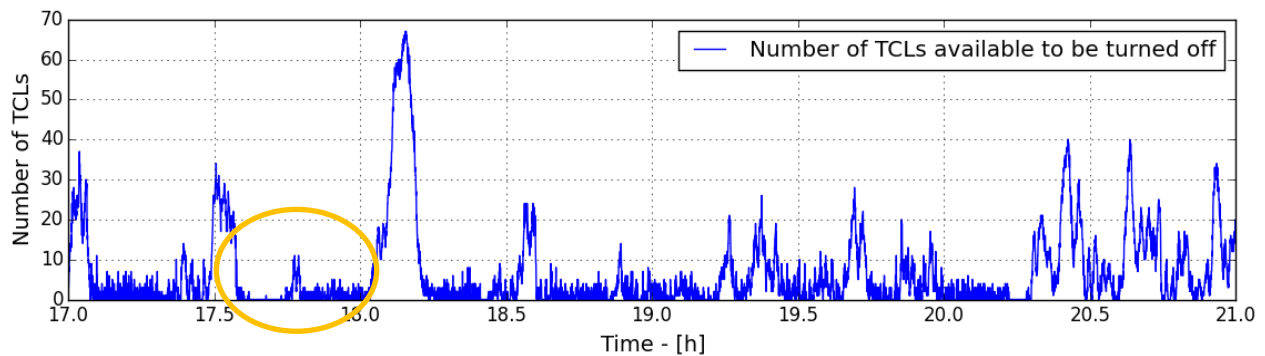


Figure 6-13 Impact of forced switching on the availability of TCLs that can be turned off

Similarly, when tracking signal < the reference signal the battery in operating in charging mode tracking the reference signal requires to turn on TCLs that are available and currently off. Unavailability of TCLs in such a state results in large deviations in tracking and are marked using red circles in Figure 6-12 and 6-14.

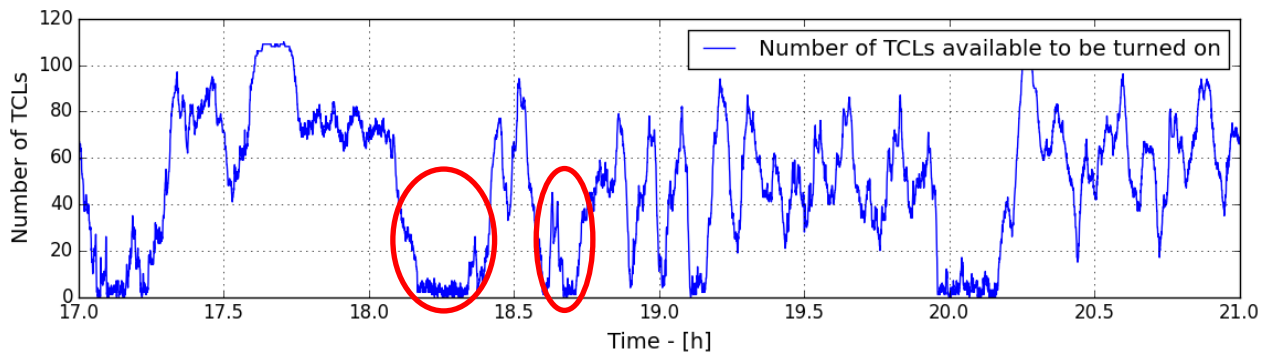


Figure 6-14 Impact of forced switching on the availability of TCLs that can be turned on

Forcing a switch state on TCL during times of voltage violation results in interruption of service and leads to violation of the temperature boundary set by the consumer. This approach therefore is only applicable for non-critical loads. It is also important to note that as consumers connect at the end of the feeder are most susceptible to voltage violations, they are therefore also most susceptible to getting their service interrupted. Figure 6-15 shows temperature regulation of three TCLS connected at the start middle and the end of the feeder.

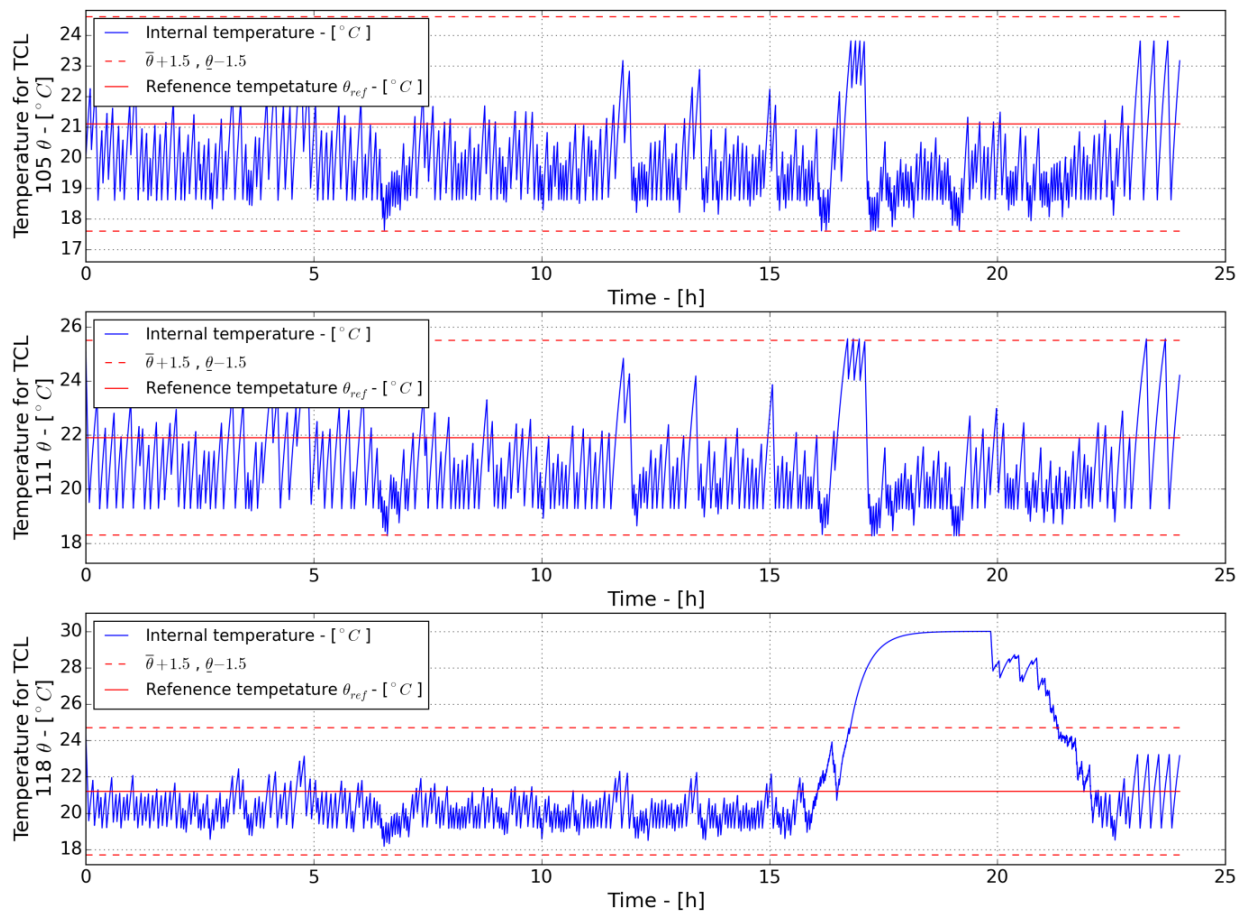


Figure 6-15 Impact of forced switching on temperature regulation

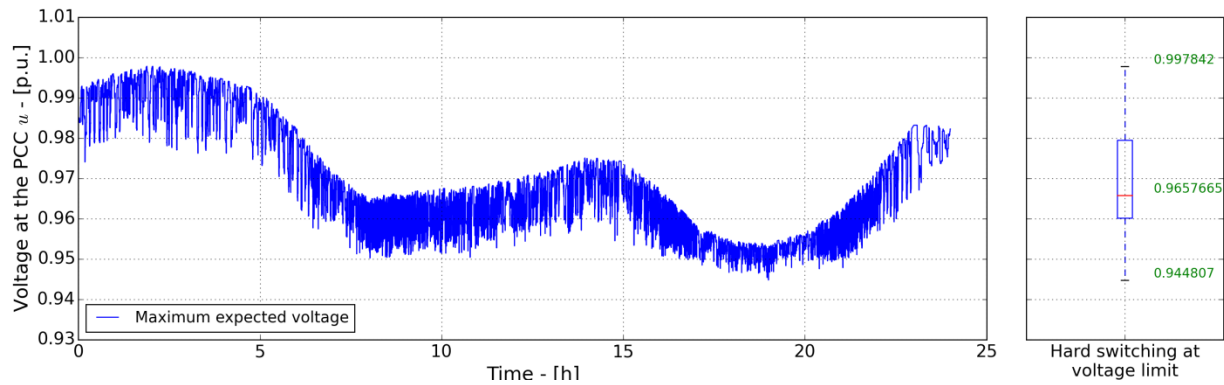


Figure 6-16 Impact of forced switching on voltage profile; box plot for the voltage profile

Penalizing voltage violation by forced switching has a considerable impact on the voltage profile. Even though the node still experiences voltage violation, the both amplitude and the duration of the violation is significantly reduced. Figure 6-16 is the voltage profile for node 118.

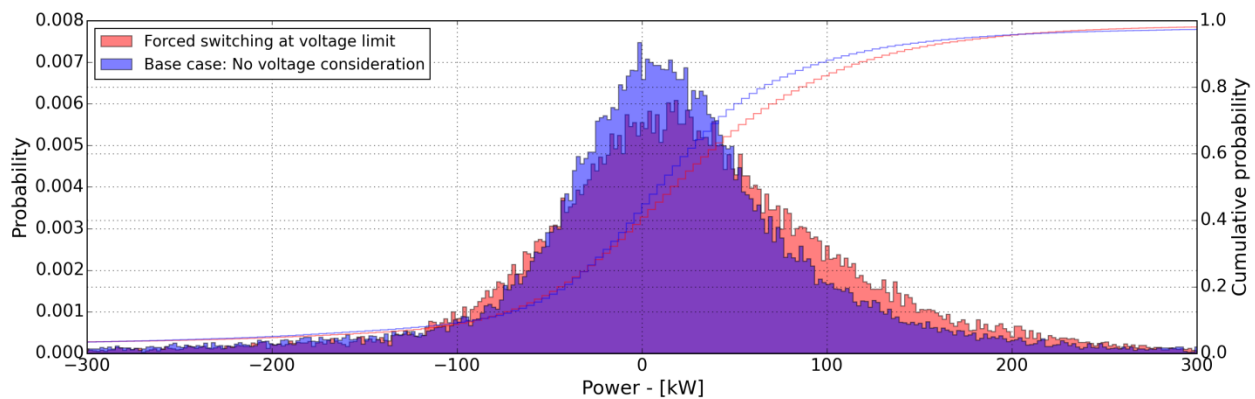


Figure 6-17 Comparison of base case and study case 1 tracking error

Finally, the impact of voltage regulation on tracking error has been compared to base case tracking error. PDF and CDF plots in Figure 6-17 show that forced switching negatively impacts the tracking performance. For the base case the probability of tracking error being less than ± 50 kW is about 0.5. For the forced switching case this probability goes down to about 0.4. The probability of error being less ± 200 kW is about 0.85 for both cases. There is a reduction in performance however it is not severe and therefore it is possible to regulate both frequency and voltage using the proposed method.

As already mentioned the proposed method leads to interruption of service and therefore can only be used for non-critical loads. Alternate solutions need to be explored to regulate voltage using DSM that without compromising on consumer comfort.

6.5 Conclusion

Balancing demand and supply of power is critical for the power system operation. Traditionally, frequency regulation has been the responsibilities of the TSOs who coordinated dispatchable resources to maintain this balance by following the demand curve. Real time frequency regulation requires fast online generators to maintain a reserve that can be used to maintain balance between generation and demand. This cost money leads to inefficient use of resources. Increasing number of non-dispatchable DERs in the network has led to increased unpredictability in generation. This has resulted in increased frequency reserve requirement thus, increase in associated cost. Thermostatically controlled loads are suited for demand side management schemes as they can switch without compromising on consumer comfort.

In this chapter a DSM based combined frequency and voltage regulation scheme has been introduced. In the context of this analysis, the following technical aspects were considered to be of special interest:

- Investigate the possibility of providing an additional ancillary service, namely voltage support along with frequency regulation using the proposed DSM scheme.
- Analyzing and understanding the impact of providing voltage support on the availability of TCLs for DSM participation and frequency signal tracking performance
- Understanding the pros and cons of each method proposed for voltage support regulation

The dynamics TCLs have been modeled using a difference equation and the local controller responsible for controlling the TCL switch state and calculating control parameters has been model in PowerFactory using DIgSILENT simulation language (DSL). The aggregate battery model for the TCLs and the priority based coordination algorithm has been modeled in Python.

Simulations results show that continuous switching of loads results in deterioration in voltage quality. Forced switching at voltage boundary does improve the voltage, however, it results in reduction in the number of TCLs available in to participate in the DSM. This can result in deteriorated frequency regulation performance. Forced switching results in service interruption and as TCLs connected near the end of a feeder are most susceptible to voltage limit violation; they are also most susceptible to interruption in service. This means that forced switching of loads is only possible non critical loads. Finally, forced switching at voltage boundary leads to deterioration in frequency regulation performance, however, the increase in deviation is acceptable.

7. Conclusion and outlook

Over voltage is one of many problems associated with high penetration of DERs in the distribution networks. Maintaining voltage in prescribed limits is critical for DSOs as over voltages can lead to equipment overheating, reduction in equipment life and insulation failure. In recent years a number of local autonomous voltage regulation schemes have been proposed. Although these schemes have been shown to regulate the voltage well, they only use local information. This results in inefficient use of resources. The focus of this thesis has been to develop coordination based strategies to improve upon the problems or limitations of local voltage support solutions.

Keeping in view the first research question '*What are the problems or limitations associated with local voltage support solutions?*' presented in Section 1.4, three limitations of local voltage support have been identified list below,

- Local autonomous RPC based voltage regulation schemes may result in degradation of power system efficiency and increase in system losses
- Local autonomous APC based are inherently unfair to PV owners connected near the end of the feeder. This result in unfairness in curtailment of active power PVs connected to a LV feeder.
- Local temperature based control TCLs result in inefficient use of resources that can used to facilitate both DSO and TSO objectives such as frequency regulation and voltage regulation, without compromising consumer comfort.

7.1 An overview of the contributions of this thesis

Considering these limitations three coordination based schemes have been proposed in this thesis that forms its core. In Chapter 4 a coordinating based RPC scheme has been proposed that aims to improve system efficiency by minimizing system losses while ensuring voltage remains within the prescribed bounds. In the proposed method, the problem has been modeled as an optimization problem. The objective function has been formulated as the weighted sum of two individual objectives namely, the voltage violation objective and the system active power loss objective. From DSO's perspective, voltage regulation is much more critical compared to loss minimization. For this reason, the voltage violation objective has been weighted exponentially. A heuristic optimization algorithm called Modified Bat Algorithm has been used to minimize the overall objective function. The proposed method has been implemented in centralized and decentralized manner on the chosen test case. Hierarchical Agglomerative Clustering has been used to define zones within a radial distribution network with high voltage interdependency. The decentralized implementation reduces the dimensions of the optimization problem and as voltage is a local phenomenon local resources are utilized to overcome overvoltage. This aids in efficient

utilization of local reactive power resources. By far the most important advantage of decentralized implementation is that unlike centralized implementation it is scalable. Additionally, the performance in terms of selected KPIs is comparable to centralized implementation. In this paper the proposed method has been presented using inverter based DERs, however, the method can easily be extended to other emerging technologies such as electric vehicles or battery storages.

In Chapter 5 a plug and play solution has been proposed to mitigate the inherent unfairness in local autonomous active power curtailment schemes. In low voltage networks, high R/X ratio means that change in voltage is more sensitive to active power rather than reactive power. This results in reduced voltage control capabilities of reactive power based schemes. Sensitivity of voltage change to active power at any point in a feeder is a function of the electrical distance from the distribution transformer. This means that PV owners connects close to the end of the feeder are more likely to experience voltage violation therefore, are also most susceptible to active power curtailment. The method proposed in this chapter uses certain assumptions detailed in the chapter to simplify the network. The sensitivity matrix is then used to calculate the maximum expected voltage at any given time. This information is used to calculate the reduction in active power injection required to comply with voltage standards. The KPIs derived in chapter give a measure of unfairness in curtailment in a feeder. From a DSO's perspective, a threshold can be set and the solution can be implemented on feeders that exceed a predefined threshold for unfairness in local APC schemes. Simulation results show that although improvement in fairness is possible using coordinated control it results in increase in overall curtailment. Therefore, the proposed should only be used on feeders with high curtailment unfairness index.

Thermostatically controlled loads are loads that operate within a predefined temperature range using a bang bang controller. TCLs have tremendous potential to facilitate power system operations like frequency regulation, demand peak mitigation and voltage regulation. EPRI estimates that each dollar invested in DSM schemes is equivalent to two dollars invested in network reinforcement. The principle of thermal inertia allows the operational status of the load to be changed for a limited period without having an impact on consumer comfort. In Chapter 6 a combined frequency and voltage regulation method has been proposed. The proposed method requires the TCLs to communicate availability and distance from the switching boundary to the coordinating controller. The coordinating controller uses priority tables based on operational status, switch status and distance from the temperature boundary to change the operational status of the TCLs and follow the reference power deviation signal (frequency regulation). Simulation results show that forced switching at the voltage boundary does improve the voltage profile of the network, however, it may result in violation of the temperature boundary resulting in temporary degradation in consumer comfort. As consumers connected towards the end of a feeder are most susceptible to voltage violation, they are also most likely to experience forced switching. Forced switching results in slight degradation in frequency regulation.

7.2 Evaluation from a stakeholder's perspective

In the distribution network three entities namely the end customers, the distribution system operators and the serving transmission system operator are the main stakeholders in distribution network operation. It is important that any new proposed method be beneficial for at least one of the main stakeholders without compromising the interests of other stakeholders; the method being beneficial for multiple stakeholders is a definite plus.

From an end customer's perspective, improved voltage regulation is of utmost importance as voltage violations may result in increased stress on appliance insulation, reduction in useful life, appliance malfunction and in some cases equipment failure altogether. This results in additional costs incurred by end consumers. Industrial customers are even more susceptible to voltage violations. Over voltage may trigger protection equipment resulting in an abrupt halt of normal production operations. The three methods proposed in this thesis aim to improve voltage regulation, thus improving power quality and DN operation. In chapter 4 a reactive power dispatch based voltage regulation scheme has been proposed. The method has been shown to regulate voltage with the prescribed limits while also improving upon power system efficiency. Costs incurred due to line losses are passed down to the end customer by the DSO, hence reduction in line losses can potentially be economically beneficial for end users. Inherent unfairness in local active power curtailment scheme in LV networks has been discussed in chapter 5. Essentially, residential customers with a DER connected at the end of the feeder bear the brunt of curtailment and economic losses. A coordination based method has been proposed that aims at mitigate this unfairness by ensuring that every customer with an installed DER participates fairly in the voltage regulation process. Simulation results show that the proposed method does well to mitigate this unfairness. The proposed method is therefore for beneficial residential customers connected at the end of feeder susceptible to over voltage. In chapter 6 a DSM based method has been proposed that aims to utilize TCLs connected with the DN as frequency reserve the method additionally penalizes customers that violate voltage boundary. This results in possible loss of service to TCL loads connected at the end of the feeder

The DSOs are responsible the operation of the DNs. They are therefore a major stakeholder in DN operation. Evaluating the proposed methods from a DSOs perspective is therefore imperative. The optimal reactive power dispatch based method proposed in chapter 4 is mutually beneficial for both the network operator and the end consumers as it improve system efficiency while ensuring voltage limits are not violated. Additionally, efficient use of local resources can potentially lead to reduction in costs associated with importing reactive power from the external grid. Reduction in current magnitude can additionally have a positive impact on the life time of equipment such as transformers. Simulation results show the algorithm for mitigation of unfairness proposed in chapter 5 does well to alleviate unfairness in curtailment, however, the decrease in unfairness come at the cost of increased total curtailment. From a DSO's perspective increase in curtailment means loss of green energy. If contract obligations are not met due to excessive

curtailment the proposed method could mean additional costs incurred on the DSO in form of penalties. It has therefore been suggested that the proposed method be implemented on feeders with high unfairness index.

Finally, TSOs are responsible for maintaining the balance between the supply of power and its demand. They are therefore responsible for regulating system voltage. The method proposed in chapter 6 (using TCLs for frequency regulation using priority based DSM) provides benefits to both TSOs and DSOs. Real time frequency regulation requires fast online generators to maintain a reserve that can be used to maintain balance between generation and demand. This cost money leads to inefficient use of resources. Using TCLs for frequency regulating can be used by TSOs to reduce this reserve requirement thereby reducing the associated costs.

7.3 Outlook

The methods proposed in this work aim at utilization local resources in an efficient manner to regulate network voltage while also schemes need to be test additional experiments while also providing additional benefits like reduction in network losses, mitigation of unfair curtailment and complementing network operation to ensure improved power quality. The methods have been implemented on standard test cases and show improvement compared to the state-of-art solutions, however, the methods need to be implemented on many networks to investigate their sensitivity to network topology and distribution of the DER units in the network. The method proposed for defining zones in chapter 4 for example needs to be tested using large distribution networks. Similarly, the impact of DER distribution on mitigation of unfairness and additional curtailed resulting from the proposed method need to be investigated further.

Coordination based schemes like the ones proposed in this work require a communication channel and delays in communication may cause the coordinating controller to lag the current state of the electrical network resulting in incorrect calculations of new set points. Advances in communication technology in recent years have tremendously reduced the communication overhead. Additionally, mass roll out of smart meters has made it possible to observe the state of the DN that has previously been unobservable. This has made it possible for resources available within a distribution network work in a coordinated manner. This ensures improved resources utilization, defers large investments in grid reinforcements and opens additional revenue generations options for regulators and consumers. Decentralized coordinated control has several advantages over centralized implementation like improved resilience to single point failure, support for deregulation, scalability and reduced communication overhead.

Although use of state estimator in transmission networks is a common practice it is currently not used in distribution networks. The main reason is the lack of available measurements rendering the DN unobservable. Distribution system state estimation is currently an active research topic. The current research focuses on three main areas namely development of a DSSE solver suitable for distribution networks, modelling of pseudo measurements and optimal

placement of measurement devices such than a small number of measurement devices can be used to estimate the state of the entire network. Further developments in the field will also facilitate implementation of coordination based schemes like the ones proposed in the thesis. As the penetration of DERs in DN is expected to increase in the future proposed methods can be useful for efficient utilization of resources available with DNs.

References

- [1] H. Farhangi, "The path of the smart grid," *Power and energy magazine, IEEE*, vol. 8, no. 1, pp. 18-28, 2010.
- [2] Green, Martin A, "Silicon photovoltaic modules: a brief history of the first 50 years," *Progress in Photovoltaics: Research and applications*, vol. 13, no. 5, pp. 447-455, 2005.
- [3] E. P. I. Association and others, "Global market outlook for photovoltaics until 2014," See http://www.epia.org/fileadmin/EPIA_docs/public/Global_Market_Outlook_for_Photovoltaics_until_2014.pdf, 2010.
- [4] Delta-ee, "The benefits of micro-CHP," COGEN Europe, Avenue des Arts 3-5, 1210 Bruxelles, 2015.
- [5] L. C. Fatih Birol, "World Energy Outlook," International Energy Agency (IEA), 2015.
- [6] R. Passey, T. Spooner, I. MacGill, M. Watt and K. Syngellakis, "The potential impacts of grid-connected distributed generation and how to address them: A review of technical and non-technical factors," *Energy Policy*, vol. 39, no. 10, pp. 6280-6290, 2011.
- [7] T. Ehara, "Overcoming PV grid issues in urban areas," *International Energy Agency, Photovoltaic Power Systems Program, Rep. IEA-PVPS T10-06-2009*, 2009.
- [8] T. Jamasb and M. Pollitt, "Electricity market reform in the European Union: review of progress toward liberalization & integration," *The Energy Journal*, pp. 11-41, 2005.
- [9] S. Borenstein, and J. Bushnell, "The us electricity industry after 20 years of restructuring," National Bureau of Economic Research, 2015.
- [10] da Gracca and M. Carvalho, "EU energy and climate change strategy," *Energy*, vol. 40, no. 1, pp. 19-22, 2012.
- [11] K. Solangi, M. Islam, R. Saidur, N. Rahim and H. Fayaz, "A review on global solar energy policy," *Renewable and sustainable energy reviews*, vol. 15, no. 4, pp. 2149-2163, 2011.
- [12] G. Andersson, P. Donalek, R. Farmer, N. Hatziargyriou, I. Kamwa, P. Kundur, N. Martins, J. Paserba, P. Pourbeik, J. Sanchez-Gasca and others, "Causes of the 2003 major grid blackouts in North America and Europe, and recommended means to improve system dynamic performance," *Power Systems, IEEE Transactions on*, vol. 20, no. 4, pp. 1922-1928, 2005.
- [13] E. SmartGrids, "Strategic Deployment Document for Europe's Electricity Networks of the Future," *European Technology Platform SmartGrids. Brussels*, 2008.

- [14] G. Masson, M. Latour, M. Reking, I.-T. Theologitis and M. Papoutsi, "Global market outlook for photovoltaics 2013-2017," *European Photovoltaic Industry Association*, pp. 12-32, 2013.
- [15] V. M. Quezada, J. R. Abbad and T. G. S. Roman, "Assessment of energy distribution losses for increasing penetration of distributed generation," *IEEE TRANSACTIONS ON POWER SYSTEMS PWRS*, vol. 21, no. 2, p. 533, 2006.
- [16] A. Picciariello, K. Alvehag and L. Soder, "State-of-art review on regulation for distributed generation integration in distribution systems," in *European Energy Market (EEM), 2012 9th International Conference on the*, 2012.
- [17] S. Ali, N. Pearsall and G. Putrus, "Impact of high penetration level of grid-connected photovoltaic systems on the UK low voltage distribution network," in *International Conference on Renewable Energies and Power Quality*, 2012.
- [18] "IEEE Recommended Practice for the Analysis of Fluctuating Installations on Power Systems," *IEEE Std 1453-2015 (Revision of IEEE Std 1453-2011)*, pp. 1-74, Oct 2015.
- [19] M. Ammar, "Flicker Emission of distributed wind power: A review of impacts, modeling, grid codes and mitigation techniques," in *Power and Energy Society General Meeting, 2012 IEEE*, 2012.
- [20] L. Peretto, L. Rovati, G. Salvatori, R. Tinarelli and A. E. Emanuel, "Investigation on the response of the human eye to the light flicker produced by different lamps," in *Instrumentation and Measurement Technology Conference, 2006. IMTC 2006. Proceedings of the IEEE*, 2006.
- [21] A. De Moura and A. De Moura, "Analysis of injected apparent power and flicker in a distribution network after wind power plant connection," *Renewable Power Generation, IET*, vol. 2, no. 2, pp. 113-122, 2008.
- [22] S. Hong and M. Zuercher-Martinson, "Harmonics and noise in photovoltaic (pv) inverter and the mitigation strategies," 2010.
- [23] M. Garcia-Gracia, A. Alonso, M. P. Comech and N. El Halabi, *Harmonic Distortion in Renewable Energy Systems: Capacitive Couplings*, INTECH Open Access Publisher, 2011.
- [24] T. S. Basso and R. DeBlasio, "IEEE 1547 series of standards: interconnection issues," *Power Electronics, IEEE Transactions on*, vol. 19, no. 5, pp. 1159-1162, 2004.
- [25] T. T. Hashim, A. Mohamed and H. Shareef, "A review on voltage control methods for active distribution networks," *Prz. Elektrotech*, vol. 88, pp. 304-312, 2012.
- [26] P. Esslinger and R. Witzmann, "Regulated distribution transformers in low-voltage networks with a high degree of distributed generation," in *Innovative Smart Grid Technologies (ISGT Europe), 2012 3rd IEEE PES International Conference and Exhibition on*, 2012.

- [27] X. Liu, A. Aichhorn, L. Liu and H. Li, "Coordinated Control of Distributed Energy Storage System With Tap Changer Transformers for Voltage Rise Mitigation Under High Photovoltaic Penetration," *IEEE Transactions on Smart Grid*, vol. 3, no. 2, pp. 897-906, June 2012.
- [28] N. Patel, "Design Of Solid-state On Load Tap-changing For Transformer," 2012.
- [29] L. Cipcigan and P. Taylor, "Investigation of the reverse power flow requirements of high penetrations of small-scale embedded generation," *Renewable Power Generation, IET*, vol. 1, no. 3, pp. 160-166, 2007.
- [30] M. Hasheminamin, V. G. Agelidis, V. Salehi, R. Teodorescu and B. Hredzak, "Index-Based Assessment of Voltage Rise and Reverse Power Flow Phenomena in a Distribution Feeder Under High PV Penetration," *Photovoltaics, IEEE Journal of*, vol. 5, no. 4, pp. 1158-1168, 2015.
- [31] Y. Liu, J. Bebic, B. Kroposki, J. De Bedout and W. Ren, "Distribution system voltage performance analysis for high-penetration PV," in *Energy 2030 Conference, 2008. ENERGY 2008. IEEE*, 2008.
- [32] G. Antonova, M. Nardi, A. Scott and M. Pesin, "Distributed generation and its impact on power grids and microgrids protection," in *Protective Relay Engineers, 2012 65th Annual Conference for*, 2012.
- [33] "IEEE Application Guide for IEEE Std 1547(TM), IEEE Standard for Interconnecting Distributed Resources with Electric Power Systems," *IEEE Std 1547.2-2008*, pp. 1-217, April 2009.
- [34] N. Roy and H. R. Pota, "Distribution grid codes: opportunities and challenges," in *PowerTech (POWERTECH), 2013 IEEE Grenoble*, 2013.
- [35] C. Schroder, "Energy Revolution Hiccups: Grid Instability Has Industry Scrambling for Solutions," *Der Spiegel*, 2012.
- [36] A. Q. Al-Shetwi, M. Z. Sujod and N. L. Ramli, "A REVIEW OF THE FAULT RIDE THROUGH REQUIREMENTS IN DIFFERENT GRID CODES CONCERNING PENETRATION OF PV SYSTEM TO THE ELECTRIC POWER NETWORK," 2015.
- [37] S.-I. Jang and K.-H. Kim, "An islanding detection method for distributed generations using voltage unbalance and total harmonic distortion of current," *Power Delivery, IEEE Transactions on*, vol. 19, no. 2, pp. 745-752, 2004.
- [38] M. G. M. Abdolrasol and S. Mekhilef, "Three phase grid connected anti-islanding controller based on distributed generation interconnection," in *Power and Energy (PECon), 2010 IEEE International Conference on*, 2010.
- [39] C. Li, C. Cao, Y. Cao, Y. Kuang, L. Zeng, and B. Fang , "A review of islanding detection methods for microgrid," *Renewable and Sustainable Energy Reviews*, vol. 35, pp. 211-220, 2014.

- [40] S. Ghosh, S. Rahman and M. Pipattanasomporn, "Local distribution voltage control by reactive power injection from PV inverters enhanced with active power curtailment," in *PES General Meeting/ Conference & Exposition, 2014 IEEE*, 2014.
- [41] A. Alimardani, S. Zadkhast, F. Therrien, J. Jatskevich and E. Vaahedi, "Impact of employing state estimation of distribution networks on state estimation of transmission networks," in *PES General Meeting / Conference Exposition, 2014 IEEE*, 2014.
- [42] M. Baran and T. McDermott, "Distribution system state estimation using AMI data," in *Power Systems Conference and Exposition, 2009. PSCE'09. IEEE/PES*, 2009.
- [43] R. F. Arritt, R. C. Dugan, R. W. Uluski and T. F. Weaver, "Investigation load estimation methods with the use of AMI metering for distribution system analysis," in *2012 Rural Electric Power Conference*, 2012.
- [44] J. Fan and S. Borlase, "The evolution of distribution," *Power and Energy Magazine, IEEE*, vol. 7, no. 2, pp. 63-68, 2009.
- [45] E. Standard, "50160," *Voltage characteristics of public distribution systems*, 2010.
- [46] P. Mitra, G. T. Heydt and V. Vittal, "The impact of distributed photovoltaic generation on residential distribution systems," in *North American Power Symposium (NAPS), 2012*, 2012.
- [47] T.-H. Chen, C. Yang, T. Hsieh and S. Chen, "Case studies of the impact of voltage imbalance on power distribution systems and equipment," in *WSEAS International Conference. Proceedings. Mathematics and Computers in Science and Engineering*, 2009.
- [48] A. Std, "C84. 1-2006," *For Electric Power Systems and Equipment-Voltage Ratings (60 Hz)*, 2006.
- [49] R. Tonkoski, D. Turcotte and T. H. El-Fouly, "Impact of high PV penetration on voltage profiles in residential neighborhoods," *Sustainable Energy, IEEE Transactions on*, vol. 3, no. 3, pp. 518-527, 2012.
- [50] J. Descheemaeker, M. Van Lumig and J. Desmet, "Influence of the supply voltage on the performance of household appliances," in *23rd International Conference on Electricity Distribution*, 2015.
- [51] J. Kennedy, P. Ciuffo and A. Agalgaonkar, "Over-voltage mitigation within distribution networks with a high renewable distributed generation penetration," in *Energy Conference (ENERGYCON), 2014 IEEE International*, 2014.
- [52] M. L. S. Kalyan K. Sen, "Introduction," in *Introduction to FACTS controllers: theory, modeling, and applications*, John Wiley & Sons, 2009, pp. 413-418.
- [53] R. Schainker, "Effects of Temporary Overvoltage on Residential Products," *Electric Power Research Institute, California, USA, Final Report*, pp. 6-11, 2005.

- [54] F. Olivier, P. Aristidou, D. Ernst, and T. V. Cutsem, "Active Management of Low-Voltage Networks for Mitigating Overvoltages Due to Photovoltaic Units," *IEEE Transactions on Smart Grid*, vol. 7, no. 2, pp. 926-936, 2016.
- [55] Mojumdar, Md R. Rejwanur, A. Bhuiyan, Md Waliullah, H. Kadir, and Md N.H. Shakil, "Design and analysis of an optimized Grid-Tied PV system: Perspective Bangladesh," *International Journal of Engineering and Technology*, vol. 3, no. 4, p. 435, 2011.
- [56] A. Magal, A. Gambhir, A. Kulkarni, G.B. Fernandes and R. Deshmukh, "Grid integration of distributed solar photovoltaics (PV) in India--A review of technical aspects, best practices and the way forward," Prayas (Energy Group) Report, 2014.
- [57] Informationstechnik, VDE Verband der Elektrotechnik Elektronik, "eV: VDE-AR-N 4105: 2011-08: Power generation systems connected to the low-voltage distribution network Technical minimum requirements for the connection to and parallel operation with low-voltage distribution networks," *English translation of the VDE application rule VDEAR-N-4105*.
- [58] "IEEE Standard for Interconnecting Distributed Resources with Electric Power Systems - Amendment 1," *IEEE Std 1547a-2014 (Amendment to IEEE Std 1547-2003)*, pp. 1-16, 2014.
- [59] S. Sivanagaraju, Power system operation and control, Pearson Education India, 2009.
- [60] T. Xu and P. Taylor, "Voltage control techniques for electrical distribution networks including distributed generation," in *Proceedings of the 17th World Congress The International Federation of Automatic Control, Seoul*, 2008.
- [61] P. N. Vovos, A. E. Kiprakis, G. P. Harrison and others, "Centralized and distributed voltage control: Impact on distributed generation penetration," *Power Systems, IEEE Transactions on*, vol. 22, no. 1, pp. 476-483, 2007.
- [62] J. Guisado, P. Carvalho, L. Ferreira, J. J. Santana and G. Marques, "Voltage control challenges and potential solutions for large-scale integration of PV resources in LV networks," in *Integration of Renewables into the Distribution Grid, CIRED 2012 Workshop*, 2012.
- [63] T. Stetz, M. Kraiczy, M. Braun and S. Schmidt, "Technical and economical assessment of voltage control strategies in distribution grids," *Progress in Photovoltaics: Research and Applications*, vol. 21, no. 6, pp. 1292-1307, 2013.
- [64] J. M. Bloemink and T. C. Green, "Increasing distributed generation penetration using soft normally-open points," in *Power and Energy Society General Meeting, 2010 IEEE*, 2010.
- [65] N. G. Boulaxis and M. P. Papadopoulos, "Optimal feeder routing in distribution system planning using dynamic programming technique and GIS facilities," *IEEE Transactions on Power Delivery*, vol. 17, no. 1, pp. 242-247, Jan 2002.

- [66] E. Diaz-Dorado, J. Cidras and E. Miguez, "Application of evolutionary algorithms for the planning of urban distribution networks of medium voltage," *IEEE Transactions on Power Systems*, vol. 17, no. 3, pp. 879-884, Aug 2002.
- [67] J. R. Shin, B. S. Kim, J. B. Park and K. Y. Lee, "A New Optimal Routing Algorithm for Loss Minimization and Voltage Stability Improvement in Radial Power Systems," *IEEE Transactions on Power Systems*, vol. 22, no. 2, pp. 648-657, May 2007.
- [68] A. Hagehaugen, "Voltage Control in Distribution Network with Local Generation," 2014.
- [69] C. Long and L. F. Ochoa, "Voltage Control of PV-Rich LV Networks: OLTC-Fitted Transformer and Capacitor Banks," *IEEE Transactions on Power Systems*, vol. PP, no. 99, pp. 1-10, 2015.
- [70] M. Cohen, P. Kauzmann and D. Callaway, "Economic Effects of Distributed PV Generation on California's Distribution System," 2015.
- [71] IEEE Power System Relay Committee and others, *Impact of distributed resources on distribution relay protection*, August, 2004.
- [72] P. Brady, C. Dai and Y. Baghzouz, "Need to revise switched capacitor controls on feeders with distributed generation," in *Transmission and Distribution Conference and Exposition, 2003 IEEE PES*, 2003.
- [73] T. Stetz, *Autonomous Voltage Control Strategies in Distribution Grids with Photovoltaic Systems: Technical and Economic Assessment*, vol. 1, kassel university press GmbH, 2014.
- [74] K. Turitsyn, S. Backhaus, M. Chertkov and others, "Options for control of reactive power by distributed photovoltaic generators," *Proceedings of the IEEE*, vol. 99, no. 6, pp. 1063-1073, 2011.
- [75] D. Taggart, K. Hao, R. Jenkins, and R. VanHatten, "Power factor control for grid-tied photovoltaic solar farms," in *proceedings of the 14th Annual Western Power Delivery Automation Conference, Spokane, WA*, 2012.
- [76] P. Esslinger and R. Witzmann, "EVALUATION OF REACTIVE POWER CONTROL CONCEPTS FOR PV INVERTERS IN LOW-VOLTAGE GRIDS," in *CIGRE Workshop*, Lisbon, 2012.
- [77] B. I. Cruaciun, T. Kerekes, D. Sera, and R. Teodorescu, "Overview of Recent Grid Codes for PV Power," in *Optimization of Electrical and Electronic Equipment (OPTIM), 2012 13th International Conference on*, 2012.
- [78] T. Stetz, F. Marten, and M. Braun, "Improved Low Voltage Grid-Integration of Photovoltaic Systems in Germany," *IEEE TRANSACTIONS ON SUSTAINABLE ENERGY*, vol. 4, no. 2, pp. 534-542, 2013.
- [79] A. Agrawal, K. Rahimi, R. P. Broadwater and J. Bank, "Performance of PV Generation Feedback Controllers: Power Factor versus Volt-VAR Control Strategies," in *North American Power Symposium (NAPS)*, 2015.

- [80] E. A. Man, "Control of grid connected PV systems with grid support functions", GlobeEdit, 2014.
- [81] B. A. Robbins, and A. D. Dominguez-Garcia, "Optimal Reactive Power Dispatch for Voltage Regulation in Unbalanced Distribution Systems," *IEEE Transactions on Power Systems*, vol. 31, no. 4, pp. 2903-2913, 2016.
- [82] S. S. Guggilam, E. Dall'Anese, Y. C. Chen, S. V. Dhople and G. B. Giannakis, "Scalable Optimization Methods for Distribution Networks With High PV Integration," *IEEE Transactions on Smart Grid*, vol. PP, no. 99, pp. 1-10, 2016.
- [83] N. Roterling, C. Schrodgers, J. Kellermann and A. Moser, "Medium-voltage network planning with optimized power factor control of distributed generators," in *IEEE Power and Energy Society General Meeting*, 2011.
- [84] S. Chen, W. Hu, C. Su, X. Zhang and Z. Chen, "Optimal reactive power and voltage control in distribution networks with distributed generators by fuzzy adaptive hybrid particle swarm optimisation method," *IET Generation, Transmission & Distribution*, vol. 9, no. 11, pp. 1096-1103, 2015.
- [85] T. J. Hashim and A. Mohamed, "Fuzzy Logic Based Coordinated Voltage Control for Distribution Network with Distributed Generations," *International Journal of Electrical, Computer, Energetic, Electronic and Communication Engineering*, vol. 7, no. 7, pp. 806-8011, 2013.
- [86] J. R. Castro, M. Saad, S. Lefebvre, D. Asber and L. Lenoir, "Coordinated Voltage Control in Distribution Network with the Presence of DERs and Variable Loads Using Pareto and Fuzzy Logic," *MDPI Energies*, vol. 9, no. 107, pp. 1-16, 2016.
- [87] R. Chidanandappa, T. Ananthapadmanabha and S. Vishwanath, "Priority Algorithm Based Coordinated Voltage Control for Distribution System with Distributed Wind Generators," *Procedia Technology*, vol. 21, pp. 368 - 375, 2015.
- [88] S.R. Abbott, B. Fox and D.J. Morrow, "Distribution network voltage support using sensitivity-based dispatch of Distributed Generation," in *2013 IEEE Power Energy Society General Meeting*, 2013.
- [89] K. Daroj and W. Limpananwadi, "Reactive Power Dispatch scheme evaluation for synchronous based distributed generators to reduce real power loss in distribution systems," in *IEEE International Conference on Sustainable Energy Technologies*, 2008.
- [90] Y. J. Z. D. Jinqun Zhao, "A Distributed Reactive Power Optimization," in *IEEE Innovative Smart Grid Technologies - Asia (ISGT ASIA)*, 2014.
- [91] "A Fully Distributed Reactive Power Optimization and Control Method for Active Distribution Networks," *IEEE TRANSACTIONS ON SMART GRID*, vol. 7, no. 2, pp. 1021-1033, 2016.
- [92] Z. Li, Y. Liu, R. Liu and X. Niu, "Network Partition for Distributed Reactive Power Optimization in Power Systems," 2008.

- [93] X. Chen, C. Zhang, W. Zhang and J. Zhou, "Study of multi-agent based distributed control for distribution system with integration of distributed generations," in *Power Engineering and Optimization Conference (PEOCO), IEEE*, 2014.
- [94] B. A. Robbins, A. D. Dominguez-Garcia and C. N. Hadjicostis, "Control of distributed energy resources for reactive power support," in *North American Power Symposium (NAPS)*, 2011.
- [95] F. Ren, M. Zhang and D. Sutanto, "A Multi-Agent Approach for Decentralized Voltage Regulation in Power Distribution Networks within Distributed Generators," in *International Foundation for Autonomous Agents and Multiagent Systems*, 2013.
- [96] A. Sajadi, H. E. Farag, P. Biczal and E. F. El-Saadany, "Voltage regulation based on fuzzy multi-agent control scheme in smart grids," in *Energytech, 2012 IEEE*, 2012.
- [97] I. Ahmad, P. Palensky and W. Gawlik, "Multi-Agent System based voltage support by distributed generation in smart distribution network," in *Smart Electric Distribution Systems and Technologies (EDST), 2015 International Symposium on*, 2015.
- [98] R. Tonkoski and A.C.L. Lopes, "Impact of active power curtailment on overvoltage prevention and energy production of PV inverters connected to low voltage residential feeders," *Renewable Energy*, vol. 36, no. 12, pp. 3566-3574, 2011.
- [99] D. Bozalakov, T. Vandoorn, B. Meersman, G. Papagiannis, A. Chrysochos and L. Vandeveldel, "Damping-Based Droop Control Strategy Allowing an Increased Penetration of Renewable Energy Resources in Low Voltage Grids," *IEEE Transactions on Power Delivery*, vol. PP, no. 99, pp. 1-1, 2016.
- [100] M. P. S. Ghosh and S. Rahman, "Distribution Voltage Regulation through Active Power Curtailment with PV Inverters and Solar Generation Forecasts," *IEEE Transactions on Sustainable Energy*, vol. PP, no. 99, pp. 1-10, 2016.
- [101] T. Vandoorn, J. De Kooning, B. Meersman and L. Vandeveldel, "Soft curtailment for voltage limiting in low-voltage networks through reactive or active power droops," in *Energy Conference and Exhibition (ENERGYCON), 2012 IEEE International*, 2012.
- [102] X. Su, M.A.S. Masoum and P.J. Wolfs, "Optimal PV Inverter Reactive Power Control and Real Power Curtailment to Improve Performance of Unbalanced Four-Wire LV Distribution Networks," *IEEE TRANSACTIONS ON SUSTAINABLE ENERGY*, vol. 5, no. 3, pp. 967-977, 2014.
- [103] V. Calderaro, G. Conio, V. Galdi, G. Massa and A. Piccolo, "Optimal Decentralized Voltage Control for Distribution Systems With Inverter-Based Distributed Generators," *IEEE TRANSACTIONS ON POWER SYSTEMS*, vol. 29, no. 1, pp. 230-238, 2014.

- [104] A. Gabash and P. Li, "ACTIVE-REACTIVE OPTIMAL POWER FLOW FOR LOW-VOLTAGE NETWORKS WITH PHOTOVOLTAIC DISTRIBUTED GENERATION," in *IEEE ENERGYCON Conference and Exhibition*, 2012.
- [105] D. Lew, L. Bird, M. Milligan, B. Speer, X. Wang, E. M. Carlini, A. Estanqueiro, D. Flynn, E. Gomez-Lazaro, N. Menemenlis and others, "Wind and solar curtailment," in *Int. Workshop on Large-Scale Integration of Wind Power Into Power Systems*, 2013.
- [106] V. M. Mansoor, P. H. Nguyen, W. Kling and others, "An integrated control for overvoltage mitigation in the distribution network," in *Innovative Smart Grid Technologies Conference Europe (ISGT-Europe), 2014 IEEE PES*, 2014.
- [107] M. Castillo-Cagigal, A. Gutierrez, F. Monasterio-Huelin, E. Caamano-Martin, D. Masa and J. Jimenez-Leube, "A semi-distributed electric demand-side management system with PV generation for self-consumption enhancement," *Energy Conversion and Management*, vol. 52, no. 7, pp. 2659-2666, 2011.
- [108] R. Tonkoski, L. A. Lopes and T. H. El-Fouly, "Coordinated active power curtailment of grid connected PV inverters for overvoltage prevention," *Sustainable Energy, IEEE Transactions on*, vol. 2, no. 2, pp. 139-147, 2011.
- [109] B. K. Perera, P. Ciufo and S. Perera, "Power sharing among multiple solar photovoltaic (PV) systems in a radial distribution feeder," in *Power Engineering Conference (AUPEC), 2013 Australasian Universities*, 2013.
- [110] J. Zhao, A. Golbazi, C. Wang, Y. Wang, L. Xu and A. Lu, "Optimal and Fair Real Power Capping Method for," in *IEEE PES General Meeting*, Denver, 2015.
- [111] M. Viyathukattuva Mohamed Ali, P. Nguyen, W. Kling, A. Chrysochos and T. Papadopoulos, "Fair Power Curtailment of Distributed Renewable Energy Sources to Mitigate Overvoltages," in *IEEE Eindhoven PowerTech*, Eindhoven, 2015.
- [112] X. Zhang, C. Rehtanz and B. Pal, "Flexible AC transmission systems: modelling and control," in *Springer Science & Business Media*, 2012.
- [113] K. Tsunedomi, Y. Imazu, S. Tamura, T. Sodeyama, T. Omori, D. Cheung, M. Parr and S. Gough, "Effectiveness of D-SVC on rural networks," in *22nd International Conference and Exhibition on Electricity Distribution*, 2013.
- [114] R. O'Gorman and M.A. Redfern, "Voltage control problems on modern distribution systems," in *Power Engineering Society General Meeting, 2004. IEEE*, 2004.
- [115] T. Senjyu, Y. Miyazato, A. Yona, N. Urasaki, Naomitsu and T. Funabashi, "Optimal distribution voltage control and coordination with distributed generation," *Power Delivery, IEEE Transactions on*, vol. 23, no. 2, pp. 1236--1242, 2008.

- [116] J. Sugimoto, R. Yokoyama, Y. Fukuyama, V.V.R. Silva and H. Sasaki, "Coordinated allocation and control of voltage regulators based on reactive tabu search," in *Power Tech, 2005 IEEE Russia*, 2005.
- [117] A. R. Gupta and A. Kumar, "Energy savings using D-STATCOM placement in radial distribution," in *4th International Conference on Eco-friendly Computing and Communication Systems, ICECCS*, 2015.
- [118] M. Aggarwal, S. K. Gupta, Madhusudan and G. Kasal, "D-STATCOM Control in Low Voltage Distribution System with Distributed Generation," in *Emerging Trends in Engineering and Technology (ICETET), 2010 3rd International Conference on*, 2010.
- [119] N. Efkarpidis, T. Wijnhoven, C. Gonzalez, T. De Rybel and J. Driesen, "Coordinated voltage control scheme for Flemish LV distribution grids utilizing OLTC transformers and D-STATCOM's," in *Developments in Power System Protection (DPSP 2014), 12th IET International Conference on*, 2014.
- [120] B. Youcef, and A. Allali, "Using D-UPFC in Voltage Regulation of Future," *INTERNATIONAL JOURNAL of RENEWABLE ENERGY RESEARCH*, vol. 5, no. 2, pp. 581-585, 2015.
- [121] P. Kumar, A. Rahul and S. Subha, "Prospects of the Applying of UPFC in Modern Distribution Network," *Middle-East Journal of Scientific Research*, vol. 20, no. 8, pp. 929-933, 2014.
- [122] K. Lee, H. Koizumi and K. Kurokawa, "Voltage Control of D-UPFC between a Clustered PV System and Distribution System," in *Power Electronics Specialists Conference, 2006. PESC '06. 37th IEEE*, 2006.
- [123] J. P. Barton and D.G. Infield, "Energy storage and its use with intermittent renewable energy," *IEEE Transactions on Energy Conversion*, vol. 19, no. 2, pp. 441-448, 2004.
- [124] K.C. Divya and J. Ostergaard, "Battery energy storage technology for power systems—An overview," *Electric Power Systems Research*, vol. 79, no. 4, pp. 511--520, 2009.
- [125] M. Alam, K. Muttaqi and D. Sutanto, "Distributed energy storage for mitigation of voltage-rise impact caused by rooftop solar PV," in *Power and Energy Society General Meeting, 2012 IEEE*, 2012.
- [126] M. Alam, K. M. Muttaqi and D. Sutanto, "Mitigation of rooftop solar PV impacts and evening peak support by managing available capacity of distributed energy storage systems," *Power Systems, IEEE Transactions on*, vol. 28, no. 4, pp. 3874-3884, 2013.
- [127] F. Marra, Y.T. Fawzy, T. Buló, and B. Blavzic, "Energy Storage Options for Voltage Support in Low-Voltage Grids with High Penetration of Photovoltaic," in *Proceedings of IEEE PES Innovative Smart Grid Technologies (ISGT)*, 2012.
- [128] O. Malik and P. Havel, "Active Demand-Side Management System to Facilitate Integration of RES in Low-Voltage Distribution Networks," *IEEE Transactions on Sustainable Energy*, vol. 5, no. 2, pp. 673-681, 2014.

- [129] D.A. Klavsuts, I.L. Klavsuts and T.V. Avdeenko, "Providing the quality of electric power by means of regulating customers' voltage," in *Power Engineering Conference (UPEC), 2014 49th International Universities*, 2014.
- [130] M. Gupta, S. Gupta and T. Thakur, "A strategic perspective of development of advanced metering infrastructure based Demand Side Management (DSM) model for residential end user," in *Power Electronics, Drives and Energy Systems (PEDES), 2014 IEEE International Conference on*, 2014.
- [131] F.V. Lima, S.F. Pinto and J.F. Silva, "Power electronics voltage regulators for distribution transformers," in *Power Engineering, Energy and Electrical Drives (POWERENG), 2013 Fourth International Conference on*, 2013.
- [132] F.V. Lima, S.F. Pinto and J.F. Silva, "Power electronics voltage regulators for distribution transformers," in *Power Engineering, Energy and Electrical Drives (POWERENG), 2013 Fourth International Conference on*, 2013.
- [133] T. Frost, P. D. Mitcheson and Green, Timothy C, "Power electronic voltage regulation in LV distribution networks," in *2015 IEEE 6th International Symposium on Power Electronics for Distributed Generation Systems (PEDER)*, 2015.
- [134] X.-S. Yang, "A new metaheuristic bat-inspired algorithm," *Science*, vol. 284, no. arXiv: 1004.4170, pp. 65--74, 2010.
- [135] I. Fister Jr, D. Fister, and X. Yang, "A hybrid bat algorithm," *ELEKTROTEHNIŠKI VESTNIK*, vol. 80, no. 1-2, pp. 1--7, 2013.
- [136] A. I. Selvakumar and K. Thanushkodi, "Anti-predatory particle swarm optimization: solution to nonconvex economic dispatch problems," *Electric Power Systems Research*, vol. 78, no. 1, pp. 2--10, 2008.
- [137] "Dolantechcenter.com," Dolan Technology Center, [Online]. Available: <http://www.dolantechcenter.com/Focus/DistributedEnergy/PowerGraph.aspx>. [Accessed 04 07 2016].
- [138] "Latest Outputs," PVOutput, [Online]. Available: <http://pvoutput.org/outputs.jsp>. [Accessed 07 04 2016].
- [139] G. V. Rossum and F. L. Drake, "The python language reference manual," in *The python language reference manual*, Network Theory Ltd., 2011.
- [140] D. Powerfactory, "PowerFactory User's Manual," *DIgSILENT, GmbH*, 2011.
- [141] S. Satsangi, A. Saini and A. Saraswat, "Voltage control areas for reactive power management using clustering approach in deregulated power system," in *Sustainable Energy and Intelligent Systems (SEISCON 2011), International Conference on*, 2011.

- [142] M. Bahramipanah, R. Cherkaoui and M. Paolone, "Decentralized voltage control of clustered active distribution network by means of energy storage systems," *Electric Power Systems Research*, vol. 136, pp. 370 - 382, 2016.
- [143] J. Zhong, E. Nobile, A. Bose, Anjan and K. Bhattacharya, "Localized reactive power markets using the concept of voltage control areas," *IEEE Transactions on Power Systems*, vol. 19, no. 3, pp. 1555-1561, 2004.
- [144] S. Conti, A. Greco and S. Raiti, "Voltage Sensitivity Analysis in MV Distribution Networks," in *Proceedings of the 6th WSEAS/IASME International Conference on Electric Power Systems, High Voltages, Electric Machines*, 2007.
- [145] M. F. Sanner and others, "Python: a programming language for software integration and development," *J Mol Graph Model*, vol. 17, no. 1, pp. 57-61, 1999.
- [146] F. Gonzalez-Longatt, J.L. Rueda, "PowerFactory applications for power system analysis", Springer, 2014.
- [147] J. Dickert, M. Domagk and P. Schegner, "Benchmark low voltage distribution networks based on cluster analysis of actual grid properties," in *PowerTech (POWERTECH), 2013 IEEE Grenoble*, 2013.
- [148] B. J. Kirby, "Frequency regulation basics and trends", United States. Department of Energy, 2005.
- [149] D.E. Newman, B.A. Carreras, M. Kirchner and I. Dobson, "The impact of distributed generation on power transmission grid dynamics," in *System Sciences (HICSS), 2011 44th Hawaii International Conference on*, Hawaii, 2011.
- [150] F. Birol and others, "World energy outlook," International Energy Agency, Paris, 2008.
- [151] S. Khan, M. Shahzad, U. Habib, W. Gawlik and P. Palensky, "Stochastic Battery Model for Aggregation of Thermostatically Controlled Loads," in *2016 IEEE International Conference on Industrial Technology (ICIT)*, Taipei, Taiwan, 2016.
- [152] A. Latif, S. Khan, P. Palensky and W. Gawlik, "Co-simulation based platform for thermostatically controlled loads as a frequency reserve," in *2016 Workshop on Modeling and Simulation of Cyber-Physical Energy Systems (MSCPES)*, Vienna, Austria, 2016.
- [153] J.L. Mathieu, M. Kamgarpour, J. Lygeros and D.S. Callaway, "Energy arbitrage with thermostatically controlled loads," in *Control Conference (ECC), 2013 European*, 2013.
- [154] A.Y. Abdelaziz, F.M. Mohamed, S.F. Mekhamer and M.A.L. Badr, "Distribution system reconfiguration using a modified Tabu Search algorithm," *Electric Power Systems Research*, vol. 80, no. 8, pp. 943 - 953, 2010.

AADIL LATIF

Deublergasse 18/34, 1210, Vienna, Austria | +4368860065124 | aadil.latif@gmail.com

RESEARCH INTERESTS

Smart Grids; Power System Modeling and Simulation; Demand Side Management; Optimal Resource Utilization in Distribution Networks; Operational Research

EDUCATION

DOCTOR OF PHILOSOPHY | NOVEMBER 2016 (EXPECTED) | VIENNA TECHNICAL UNIVERSITY, AUSTRIA

Major: Electrical Engineering

Dissertation Title: *Optimal Resource Utilization for Improved Voltage Regulation in Distribution Networks with High Distributed Generation Penetration*

CERTIFIED ASSOCIATE OF PLC AND SCADA | DECEMBER 2010 | NATIONAL UNIVERSITY OF SCIENCES AND TECHNOLOGY, PAKISTAN

MASTERS OF SCIENCE | NOVEMBER 2009 | THE UNIVERSITY OF SHEFFIELD, UNITED KINGDOM

Major: Electronics Engineering

Dissertation Title: *Modeling, Control System Design and HIL Implementation of a Brushless AC Drive*

BACHELORS OF SCIENCE | JUNE 2007 | GIK INSTITUTE OF ENGINEERING AND TECHNOLOGY, PAKISTAN

Major: Electronics Engineering

Dissertation Title: *Sensor Less Solar Tracking for a Solar Heliostat*

EMPLOYMENT HISTORY

RESEARCH FELLOW | COMPLEX ENERGY SYSTEMS, ENERGY DEPARTMENT, AUSTRIAN INSTITUTE OF TECHNOLOGY GmbH, AUSTRIA | JUNE 2013 – TO DATE

RESPONSIBILITIES

Conducting research work on the topic of my doctoral thesis.

Participating in national and international projects underway at AIT. Collaborating with the colleagues at AIT and external partners working on the project. Completing assigned tasks in a timely manner.

Development of software tools for coupling domain specific simulation software for modeling and simulating interdependencies in complex cyber physical energy systems.

Development of use cases for distribution networks to study the impact of implementing proposed smart grid solutions on real electrical networks.

Presenting the research work in reputed conferences and publishing in high impact factor journals.

ACHIEVEMENTS

Part of project iGreenGrid a European Commission FP7 collaboration focusing on increasing hosting capacity of distributed energy resources (DERs). I was responsible for studying the impact of DERs on state estimation error and finding methods of reducing said errors.

Developed a software tool used for coupling DigSILENT PowerFactory and MATLAB. The tool has been used in the DG-EV-HIL for automated scenario generation and analysis of results.

Developed a model for continuous control of aggregated thermostatically controlled loads [TCLs], thus enabling TCLs to participate in the frequency regulation process using demand response. The work was extended to provide additional ancillary services like voltage regulation.

Proposed a multi objective optimal reactive power dispatch scheme focusing on reducing network losses while also improving the voltage profile of the distribution network.

Proposed a method for quantifying unfairness in active power curtailment of rooftop PV systems. Developed a sensitivity based coordination based algorithm for active power curtailment in low voltage residential network.

ELECTRICAL ENGINEER | PAKISTAN ENGINEERING SERVICES | NOV 2011 – JUNE 2013

RESPONSIBILITIES

Working in conjunction with the electrical team on Dasu, a 4320MW run-of-river hydro power project and preparing detailed schematic drawings, technical reports, bill of quantities and bid documents.

Calculating critical parameters for the generators, transformers, circuit breakers and other auxiliary equipment and performing various technical studies for power requirement for the lighting of power house, transformer cavern, GIS cavern, GIL tunnel, Access Tunnel, Control room, Intake and the proposed worker colony.

Selection of substation equipment and operation scheme.

Periodically presenting the work to the World Banks officials, the financier of the project.

ACHIEVEMENTS

Performed cable sizing calculations and prepared routing diagrams on AutoCAD.

Performed calculations and designed a complex earthing mesh for highly resistive soil at Dasu site.

Executed load flow, short circuit calculations for several contingencies.

Conducted simulation studies for traveling waves originating lightning and circuit breaker switching. Used said studies to find the optimal size and location for surge arrester,

Designed the 11/0.4 kV distribution system for the power house complex and the proposed workers colony.

Calculated touch, step voltages and safety distances for the entire power house.

Prepared Single line diagrams, bill of quantities and bid Documents.

Performed calculations and prepared schematic drawings for internal and external electrification of the power house, main control building, roads, switchyard and the colony areas.

Control Building, Roads, Switchyard and Colony Areas Including Resettlement/Model Villages.

INSTRUMENTATION AND CONTROL ENGINEER (INTERN) | ALBARIO, PAKISTAN | JULY 2011 – OCTOBER 2011

Gained an in depth understanding of all the components of a Combined Cycle Power Plant e.g. Gas Turbine, Steam Turbine, Heat Recovery Systems, Generators, Condensers and other auxiliary equipment.

Worked with the operations department and was able to witness and understand plant startup and stop sequences.

ELECTRICAL SITE ENGINEER | UNI SERVE, LAHORE, PAKISTAN | JANUARY 2010 – JUNE 2011

RESPONSIBILITIES

Constant site supervision and ensuring quality and safety standards are met.

Submission of weekly reports entailing progress made, problems faced if any and possible ways to mitigate potential issues.

Interpretation and implementation of engineering drawings developed in the design phase.

Resources allocation such as manpower, materials, equipment tools and consumables.

ACHIEVEMENTS

The projects I worked on include extension of Punjab assembly, tax house building and Lahore College for Women University.

ELECTRONIC ENGINEER | DATA COMMUNICATION AND CONTROL, KARACHI, PAKISTAN | JUNE 2007 – AUGUST 2008

RESPONSIBILITIES

Liaising with clients, understanding their requirements and expectations and providing periodical updates on the progress.

Designing and implementing custom hardware/software based solutions for the clients.

ACHIEVEMENTS

Developed an AVR microcontroller based control system for a gas generator and its associated HMI using a touch screen LCD module.

Designed a PABX system with 64 digital and 64 analog inputs and outputs for a small, privately owned telephone exchange.

Designed a Vehicle Simulator to replicate the driving conditions to be used for training purposes.

Developed a six degree of freedom platform for a vehicle simulator. Developed the control algorithm for the DC brushless DC motors used for actuation.

KEY COMPETENCIES

POWER SIMULATION TOOLS – DIgSILENT PowerFactory, EMTP-RV, ETAP 7.1, OpenDSS, Simulink, MATPOWER

SCRIPTING LANGUAGES – Matlab, Python, Batch Scripting

PROGRAMMING LANGUAGES – Visual Basic, C++, Visual C#, Java

CAD SOFTWARES – ORCAD, AutoCAD

OTHER SIMULATION TOOLS - DIALux, Proteous, Electronic Workbench, Modelica

MICROCONTROLLER PROGRAMMING: AVR studio, MIKROBASIC, KEIL C

OTHER COMPETENCIES – LATEX, Technical report writing, Coupling of existing simulation tools

RESEARCH PROJECTS

iGREENGrid - iGREENGrid project is a collaborative project co-founded by the European Commission under the 7th Framework Program. The project focuses on increasing the hosting capacity for Distributed Renewable Energy Sources (DRES) in power distribution grids without compromising the reliability or jeopardizing the quality of supply.

DG-EV-HIL - DG-EV-HIL is project funded by the government of Austria. The aim of the project is fivefold.

These include; Facilitation integration of new technologies in future Smart Grids; Optimal resource utilization; Improving reliability and security of supply which includes data handling; Enhancing the flexibility of the current setup enabling market participation; and providing smart services.

AWARDS AND ACHIEVEMENTS

PhD fellowship award (2013) - The PhD fellowship award from AIT Austrian Institute of Technology, Austria, is intended to give the most accomplished PhD candidates at TU Vienna an opportunity to complete the dissertation. The research work focus broadly around the area combined simulation in complex energy systems with emphasis on Smart Grid operations.

Winner robotics competition (2006) - My team won the annual robotics competition held at National University of Science and Technology (NUST).

MEMBERSHIPS

Student member IEEE and IEEE Power and Energy Society

Member Pakistan Engineering Counsel